This is to certify that the

dissertation entitled

Computer-Assisted Optimization of Separations

in Capillary Zone Electrophoresis

presented by

Marina Franco Maggi Tavares

has been accepted towards fulfillment
of the requirements for

Ph.D. degree in Analytical Chemistry

Victoria McGuffin
Major professor

Date September 9, 1993

COM

COMPUTER-ASSISTED OPTIMIZATION OF SEPARATIONS IN CAPILLARY ZONE ELECTROPHORESIS

By

Marina Franco Maggi Tavares

A DISSERTATION

Submitted to
Michigan State University
in partial fulfillment of the requirements
for the degree of

DOCTOR OF PHILOSOPHY

Department of Chemistry

1993

In t

for capilla

optimizatio

electroosm

zone dispe

and buffe

instrument

routine.

optimizatio

overall qua

computer p

for optimal

The

response o

electrode.

singly charg

$NaClO_4$), as

potential, ar

the solution

classical eq

constants ar

ABSTRACT

COMPUTER-ASSISTED OPTIMIZATION OF SEPARATIONS IN CAPILLARY ZONE ELECTROPHORESIS

By

Marina Franco Maggi Tavares

In this work, a systematic approach to separations has been established for capillary zone electrophoresis with the development of a computer-assisted optimization routine. This program incorporates theoretical models for both electroosmotic and electrophoretic migration as well as a simple rationale for zone dispersion. Variables related to the buffer composition (pH, ionic strength and buffer concentration), capillary dimensions (diameter and length) and instrumental parameters (applied voltage or current) are input to the optimization routine. Resolution between adjacent zones is the primary criterion for optimization. By methodically varying the input parameters and evaluating the overall quality of the separation with an appropriate response function, this computer program can be used to predict the experimental conditions required for optimal separation of the solutes under consideration.

The mathematical model for electroosmotic migration describes the response of the fused-silica capillary surface in analogy to an ion-selective electrode. By studying the electroosmotic flow characteristics of solutions of singly charged, strong electrolytes (NaCl, LiCl, KCl, NaBr, NaI, $NaNO_3$, and $NaClO_4$), as well as the phosphate buffer system, an equation that relates zeta potential, and ultimately electroosmotic mobility, to the composition and pH of the solution was derived. The model for electrophoretic migration is based on classical equilibrium calculations and requires knowledge of the dissociation constants and electrophoretic mobilities of the solutes under investigation. In

the mode

from con

injection a

The

demonstra

and uridir

program p

reasonable

entire rang

estimated

of the tech

tetracycline

oxytetracyc

solution.

completely

satisfactori

detection),

solution for

ionic streng

pharmaceut

with a detec

linear range

shown to b

tetracycline

the model for zone dispersion, the temporal width of each solute zone is derived from contributions to variance resulting from longitudinal diffusion and finite injection and detection volumes.

The experimental validation of the computer optimization program was demonstrated for a mixture of the nucleotides adenosine, guanosine, cytidine, and uridine 5'-mono- and di-phosphates in phosphate buffer solution. The program predicted the correct elution order for all nucleotides, and provided a reasonable estimate of the migration time, peak width and resolution within the entire range of pH studied (from 6 to 11). The number of theoretical plates was estimated as 1.4×10^5 plates per meter, which is representative of the efficiency of the technique. The program was then applied to study the separation of tetracycline antibiotics (tetracycline, chlortetracycline, demeclocycline, oxytetracycline, doxycycline, methacycline, and minocycline) in phosphate buffer solution. At the predicted optimum conditions, baseline resolution was not completely achieved for all solutes, however, the separation can be performed satisfactorily with 3×10^4 theoretical plates per meter (UV-absorbance detection), under constant-current conditions of 20 μA, in a phosphate buffer solution formulated at pH 7.5, with 15 mM total sodium concentration, 18.2 mM ionic strength, and 4.29 mM buffer concentration. The analysis of tetracycline pharmaceutical formulations was then performed under the optimized conditions, with a detection limit of 10^{-5} M at a signal-to-noise of approximately 3, and a linear range of two orders of magnitude. Capillary zone electrophoresis is shown to be a suitable alternative method for the analysis of tetracycline, tetracycline derivatives as well as common decomposition products.

to my family

I w
for the gu
would like
Enke. Dr.
discussion
careful rev
(Michigan
acknowled
Científico e
I wa
Evans. Dr.
Chen, Dan
Ogasawara
You
consideratio

ACKNOWLEDGEMENTS

I would like to express my sincere gratitude to my advisor Dr. V. McGuffin for the guidance and encouragement during the development of this work. I also would like to express my appreciation to the members of my committee, Dr. C. Enke, Dr. J. Watson, Dr. C. Chang, and Dr. J. Holland for the helpful discussions. I am indebted to Dr. Faye Ogasawara, and Daniel Hopkins for their careful revisions of this manuscript. I would like to thank Dr. Gerald Larson (Michigan State University) for the pharmaceutical samples. I gratefully acknowledge a fellowship from the Conselho Nacional de Desenvolvimento Científico e Tecnológico (CNPq) of Brazil.

I was honored, throughout these years, with the friendship of Dr. Chris Evans, Dr. Jon Wahl, John Judge, Dr. Jong Shin Yoo, Yiwen Wang, Dr. Shu-Hui Chen, Daniel Hopkins, Patrick Lukulay, Jingpin Jia, Ying Wang, Dr. Faye Ogasawara, and Chomin Lee.

You all, in many ways, touched my soul with your kindness and consideration.

See you in Brazil.

TABLE OF CONTENTS

CHAPTE

CHAPTER

CHAPTER 6

CHAPTE

APPEND

APPENDI

LIST OF TABLES

LIST OF FIGURES

Figure 4

Figure 4

Figure 4.

Figure 4.

Figure 4.1

Figure 4.12

Figure 4.13

Figure A

Figure A

LIST OF SYMBOLS

ROMAN ALPHABET

a_H	hydrogen ion activity
a_{Na}	sodium ion activity
C_j	equilibrium concentration of species j
CT	total buffer concentration
CRS	chromatographic resolution statistic
D_i	effective diffusion coefficient of solute i
F	Faraday constant
g	gravitational acceleration constant
I	current
I	buffer ionic strength
k^{POT}	potentiometric selectivity constant
ℓ_{det}	detection zone length
L_{det}	capillary length to the detector
ℓ_{inj}	injection zone length
$\ell_{inj,hf}$	injection zone length for hydrodynamic injection
$\ell_{inj,ek}$	injection zone length for electrokinetic injection
L_{tot}	total capillary length
n	number of solutes
pH	negative logarithm of hydrogen ion activity
$pK_a buf$	negative logarithm of the dissociation constants of the buffer species
$pK_a sol$	negative logarithm of the dissociation constants of the solute species
r	capillary radius
R	resistance
R_{avg}	average resolution
$R_{i,i+1}$	resolution between adjacent solutes
R_{min}	minimum resolution
R_{opt}	optimum resolution
R_{soln}	solution resistance
R_{surf}	surface resistance
t_i	migration time of solute i
t_{inj}	injection time
T_f	migration time of the last eluting solute
V	applied voltage
v_{ep}	electrophoretic velocity
v_i	velocity of solute i
v_{osm}	electroosmotic velocity
w_i	base width of solute i, in time units

z_{buf}
z_j
z_R
z_{sol}

GREEK

α_j
ΔH
ΔP
ε
ε_0
γ_j
η
κ
μ_0
μ_{buf}
$(\mu_{eff})_j$
μ_{ep}
μ_j
μ_{osm}
μ_{sol}
τ
ρ
σ^2
σ^2_{det}
σ^2_{diff}
σ^2_{inj}
σ^2_n
ζ
ζ_0

z_{buf}	charge of buffer species
z_j	charge of species j
z_R	charge of the counterion
z_{sol}	charge of solute species

GREEK ALPHABET

α_j	distribution function of species j
ΔH	height difference between solution levels at inlet and outlet reservoirs
ΔP	pressure difference along the capillary length
ε	dielectric constant of the solution
ε_0	permittivity of vacuum
γ_j	activity coefficient of species j
η	viscosity of the solution
κ	conductivity of the solution
μ_0	electrophoretic mobility at infinite dilution
μ_{buf}	electrophoretic mobility of buffer species
$(\mu_{eff})_i$	effective mobility of solute i
μ_{ep}	electrophoretic mobility
μ_j	electrophoretic mobility of species j
μ_{osm}	electroosmotic mobility
μ_{sol}	electrophoretic mobility of solute species
τ	standard deviation, in time units
ρ	density of the solution
σ^2	total zone variance
σ^2_{det}	detector contribution to the zone variance
σ^2_{dif}	diffusion contribution to the zone variance
σ^2_{inj}	injection contribution to the zone variance
σ^2_n	individual contribution to the zone variance
ζ	zeta potential
ζ_0	reference potential in the double layer

El
differenti
early 19(
human s
Tiselius v
held an u
the last
electroph
and gaine

Thi
modes, fo
rationale f
advances
sensitivity
electropho
perspective

1.1 Modes

Trad

CHAPTER 1

CAPILLARY ELECTROPHORESIS - FUNDAMENTAL CONCEPTS AND HISTORICAL BACKGROUND

Electrophoresis is the separation of charged molecules based on differential migration in an electric field. Historically, it was introduced in the early 1900s with the moving-boundary method of Tiselius, for the separation of human serum into some of its constituent proteins.[1,2] For this pioneering work, Tiselius was awarded a Nobel prize in 1948. Since then, electrophoresis has held an unique position among the methodologies for biomolecules. But only in the last decade, with the implementation of the capillary techniques,[3-5] has electrophoresis evolved from a manually intensive to a fully automated format and gained acceptance as a routine analytical technique.

This introductory chapter gives a brief description of the electrophoretic modes, followed by a more detailed discussion of zone electrophoresis and the rationale for capillary techniques. This chapter also describes the most recent advances in capillary technology and strategies for enhancement of the detector sensitivity . Finally, the current capabilities and limitations of capillary zone electrophoresis are discussed and the contribution of this work is brought into perspective.

1.1 Modes of Electrophoresis

Traditionally, electrophoresis is performed by one of four basic modes:

moving

1.1 sho

electrop

sample

electric

dictated

Instead,

the othe

analogue

Zo

which the

As the

character

result of

dispersion

no focusi

electropho

In

solutions,

can be ana

the separa

the leading

component

mobility. W

each band

In regions

stronger. Th

moving boundary, zone, isotachophoresis, and isoelectric focusing.[6-8] Figure 1.1 shows schematically the progressive separation of two solutes by each electrophoretic principle. In moving-boundary electrophoresis,[1,2] a long band of sample is placed between buffer solutions in a tube. Upon application of an electric field, the sample components migrate in a direction and at a velocity dictated by each component mobility. Complete separation is never achieved. Instead, only the solutes with the highest mobility can be partially purified while the other components overlap to different degrees. The chromatographic analogue of zone electrophoresis is frontal chromatography.

Zone electrophoresis[9] is, in principle, a moving-boundary technique in which the sample is applied as a narrow band surrounded by the buffer solution. As the electric field is applied, each zone migrates at a constant rate characteristic of its own mobility. The separation is eventually achieved as a result of maximizing the differential rate of migration while minimizing the zone dispersion. In principle, each zone migrates independently from each other and no focusing effects are operative. The chromatographic analogue of zone electrophoresis is elution chromatography.

In isotachophoresis,[10] a sample is inserted between two electrolyte solutions, the leading and the terminating electrolytes. Both cations and anions can be analysed by this mode, however in independent samples. In Figure 1.1, the separation of a mixture of cations is represented. In this particular example, the leading electrolyte contains a cation of higher mobility than any of the sample components, whereas the terminating electrolyte contains a cation of lower mobility. When the electric field is applied, different potential gradients evolve in each band in such a way that all cations eventually migrate at constant velocity. In regions where cations of lower mobility are present, the electric field is stronger. These cations move at the same velocity as the most mobile cations,

Figure 1.1 Schematic representation of the separation of two solutes by the four modes of electrophoresis.

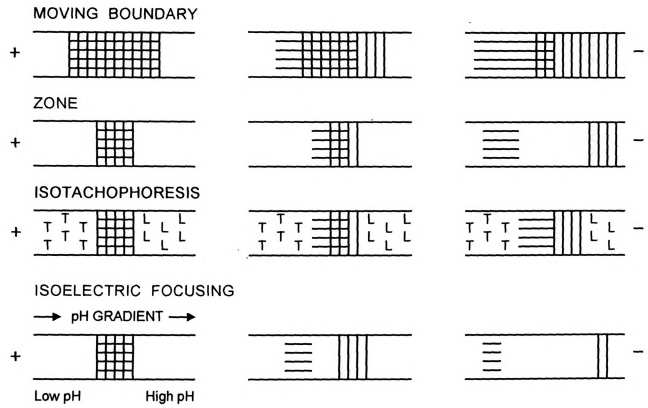
MODES OF ELECTROPHORESIS
MOVING BOUNDARY
+
−
ZONE
+
−
ISOTACHOPHORESIS
+
T
L
−
ISOELECTRIC FOCUSING
pH GRADIENT
+
−
Low pH
High pH

Figure 1.1

which a

electrop

diffuses

its rate

Likewise

rate of

chromat

Is

pH gradi

can be a

a mixture

the gradi

respective

Commerc

from pH

incorporat

medium.

permanen

of anions,

pH at the

field, it en

becomes

ceases to

is equal to

diffuses aw

this charge

and rejoins

which are subjected to weaker electric fields. A characteristic of this mode is the electrophoretic focusing that results at the boundaries of the bands. If a solute diffuses forward into a subsequent band, which is a region of lower electric field, its rate of migration is decreased and the solute rejoins the original band. Likewise, if a solute diffuses backwards into a region of higher electric field, its rate of migration is increased and the solute rejoins its former band. The chromatographic analogue of isotachophoresis is displacement chromatography.

Isoelectric focusing[11] involves the separation of amphoteric solutes in a pH gradient. The key of this technique is the formation of a pH gradient. This can be accomplished by a variety of methods, the most effective being the use of a mixture of ampholytes, whose isoelectric points span the pH range desired for the gradient. When an electric field is applied, the ampholytes migrate to their respective isoelectric point, forming a relatively stable pH gradient. Commercially available ampholyte mixtures allow the generation of gradients from pH 2 to 11. The stability of the pH gradient can be greatly enhanced by incorporating the ampholyte mixture into the molecular structure of a gel-forming medium. Once the gradient is established, the gel is polymerized to yield a permanently immobilized yet porous gradient. Figure 1.1 illustrates the analysis of anions, in which the gradient is established from low pH at the anode to high pH at the cathode. As the negatively charged solute migrates under the electric field, it encounters regions of progressively lower pH and a greater fraction becomes protonated. Eventually, the net charge of the solute is zero and it ceases to migrate. Each sample component migrates to a position where the pH is equal to the solute isoelectric point. If a solute molecule from a focused band diffuses away, it immediately acquires charge by losing or gaining protons. In this charged state, the solute migrates towards the electrode of opposite charge and rejoins the band. An important characteristic of this mode is the

establis

focused

1.2 Ra

T

separati

of electr

uniformly

migration

induce d

convectio

separatio

introducti

analytes.

will move

velocity p

too high, t

The

from Joule

cellulose a

channel.7,8

thermal co

which can

time consu

irreproducib

establishment of a steady state in which the bands are stationary and sharply focused. They will remain so while the electric field is maintained.

1.2 Rationale for Capillary Electrophoresis

The major limitation on the speed, efficiency, and scale of electrophoretic separations is the ability to dissipate Joule heat, which is caused by the passage of electric current through the conducting medium. Since heat is generated uniformly throughout the medium and is dissipated only at the edges of the migration channel, temperature gradients result. The temperature gradients induce density gradients which, in turn, can cause natural convection. Any such convection would serve to remix separated zones, severely reducing the separation performance. A secondary outcome of Joule heating is the introduction of a spatial dependence on the electrophoretic mobility of the analytes. The molecules in the warmer central region of the separation medium will move faster than those at the edges causing a deformation of the initially flat velocity profile. Moreover, if the average temperature of the medium becomes too high, the structural integrity of the sample analyte may be compromised.

The common approach to counteract the convective disturbances arising from Joule heating is to use a solid support, such as paper, starch, agarose, cellulose acetate, or polyacrylamide gels, as an integral part of the migration channel.[7,8] Although the use of a stabilizing medium effectively decreases thermal convection, it increases the surface area available for solute adsorption, which can be detrimental. As an experimental method, manipulation of gels is time consuming and involves intensive preparative work that frequently leads to irreproducibility and poor quantitative results. Even when anticonvective

support
and is c
E
electrop
capillary
is effec
mechani
high fiel
zones a
diffusion.
reported,
highest e
Th
electroph
D. by 36
(approxim
action of
over conv
the same
(50 - 200
culminate
tubes (200
group (Ein
work, the s
plate heigh
1980s, Jorg
contributed

supports are used, the electric field strength can not be substantially increased, and is commonly limited to the range of 10 to 50 V/cm.

Efficient heat dissipation is the primary reason for performing electrophoretic separations in a capillary format.[3-6] The microchannel of a capillary (15 to 100 μm) has such a high surface area-to-volume ratio that heat is effectively transfered through the capillary walls. This heat removal mechanism nearly eliminates convection, so that the application of unusually high field strengths is possible (100 to 500 V/cm). Under these conditions, the zones approach the theoretical limit of being broadened only by longitudinal diffusion.[4-6,12,13] In favorable cases, about 1 million theoretical plates has been reported,[14,15] making capillary electrophoresis the electrophoretic method of highest efficiency.

The earliest demonstration of the use of high electric fields in zone electrophoresis was published in 1967 by Hjertén,[9] who employed a 300 μm I. D. by 36 cm length rotating quartz tube, with an applied voltage of 2.5 – 3 kV (approximately 75 V/cm). In 1974, Pretorius *et al.*[16] demonstrated the pump action of electroosmotic flow and discussed the advantages of this technique over conventional methods of driving solvent in chromatographic separations. At the same time, Virtanen[17] advocated the advantages of small diameter tubes (50 – 200 μm) for electrophoretic separations. This tendency would soon culminate with the first account of zone electrophoresis in narrow-bore teflon tubes (200 μm diameter), which is attributted to Everaerts[3] and his research group (Eindhoven University of Technology, The Netherlands, 1979). In his first work, the separation of a 16-component mixture of anions was peformed, with a plate height of less than 10 μm and analysis time of ten minutes. During the 1980s, Jorgenson and Lukacs,[4-6] followed by several other research groups[18-24] contributed significantly to the initial growth of the technique and investigated the

feasibil

to me

develop

techniq

separat

workers

micellar

formed

chromat

summar

capillary

1.3 Inst

A

presente

most com

as the pre

Capillary

of fused s

material c

dimension

thermal co

wide spect

characteriz

feasibility of capillary electrophoresis as an instrumental technique. Worthwhile to mention are the contributions of Karger and coworkers[25,26] in the development of capillary gel electrophoresis (CGE), which extends the use of the technique to macromolecules, with the inclusion of a size dependence in the separation mechanism. Also significant were the contributions of Terabe and co-workers,[27] who introduced a modified version of capillary zone electrophoresis, micellar electrokinetic capillary chromatography (MECC). In MECC, surfactant-formed micelles are included in the conducting buffer to provide a two-phase chromatographic system for separating neutral molecules. Table 1.1 summarizes the achievements of the earliest workers in the field, and presents capillary electrophoresis in a historical perspective.

1.3 Instrumental Considerations

A detailed description of the instrumental system used in this work is presented in Chapter 2 (*vide* Figure 2.1). In this section, an overview of the most commonly used methods of injection and detection are discussed as well as the present status of the capillary surface technology.

Capillary Technology. Most capillaries used for electrophoresis are composed of fused silica, which is a very pure form of amorphous silicon dioxide. This material confers to the capillaries many convenient properties, such as precise dimensions, a very high dielectric constant, low electrical conductance, high thermal conductivity, mechanical strength, and high optical transmission to a wide spectrum of light (190 to 900 nm).[28] Chemically, the silica capillaries are characterized by the presence of several types of silanol groups (SiOH), which

Table 1.1 *Capillary electrophoresis in a historical perspective.*

YEAR	REFERENCE	

Table 1.1 Capillary electrophoresis in a historical perspective.

YEAR	REFERENCE	ACHIEVEMENT
1967	Hjertén, S. *Chromatogr. Rev.* **1967**, *9*, 122-219	Use of high electric fields (approximately 75 V/cm) in 300 μm I. D. rotating quartz tubes.
1974	Pretorius, V.; Hopkins, B. J.; Schieke, J. D. *J. Chromatogr.* **1974**, *99*, 23-30 Virtanen, R. *Acta Polytech. Scand. Chem. Ind. Metall. Ser.* **1974**, *123*, 1-67	Demonstration that electroosmotic flow acts as a pump. Described the advantages of using tubes of capillary dimensions (50 - 200 μm I. D.).
1979	Mikkers, F. E. P.; Everaerts, F. M.; Verheggen, Th. P. E. M. *J. Chromatogr.* **1979**, *169*, 11-20	First account of zone electrophoresis separations in small-bore capillary tubes (200 μm I. D.) with 35,000 theoretical plates.
1981 1983	Jorgenson, J.; Lukacs, K. D. *Anal. Chem.* **1981**, *53*, 1298-1302 and *Science*, **1983**, *222*, 266-272	Contributed significantly to the initial growth of capillary electrophoresis. By using high field strengths (300 V/cm) in very narrow capillaries (75 μm I. D.) separations with 400,000 theoretical plates were demonstrated. Also developed a simple theory for zone dispersion.
1984	Terabe, S.; Otsuka, K.; Ichikawa, K.; Tsuchiya, A.; Ando, T. *Anal. Chem.* **1984**, *56*, 111-113	Introduction of micellar electrokinetic capillary chromatography.
1987	Cohen, A. S.; Karger, B. L. *J. Chromatogr.* **1987**, *397*, 409-417 and Cohen, A. S.; Paulus, A.; Karger, B. L. *Chromatographia* **1987**, *24*, 15-24	Introduction of capillary gel electrophoresis.

are we

silanol

silanol

which

elabora

silanol

opposit

on the

approac

the cap

silanol g

earliest

purpose

tetradec

By using

reversed

binding c

behavior

of covale

of the

trimethyl

others.35

of time ov

high pH.

stable and

as the o

However,

are weakly acidic in character. In contact with an aqueous medium, some of the silanol groups are ionized causing the surface to be negatively charged. The silanol groups are directly responsible for the phenomenon of electroosmosis,[29] which is the induced flow of solution under an applied electric field. A more elaborate discussion of electroosmotic flow is presented in Chapter 3. The silanol groups also exist in abundant sites for coulombic interaction with oppositely charged solute molecules, and thus can have both an adverse effect on the quality of the separation as well as on the solute detectability. Several approaches have been introduced as a means to control the charge density at the capillary wall and prevent these undesirable effects. Neutralization of the silanol groups by physical adsorption of small cationic molecules is one of the earliest procedures employed. Several molecules have been used with this purpose, including putrescine,[14] cetyltrimethylammonium bromide,[30] tetradecyltrimethylammonium bromide,[31] and s-benzylthiouronium chloride.[32] By using multivalent ions, the direction of electroosmotic flow can even be reversed.[33] The use of cationic molecules has the disadvantage of potential binding of the cations to the analyte molecules, which alters their electrophoretic behavior. A second approach to controlling the surface charge density consists of covalently blocking the silanol groups with polar organosilane ligands. Some of the most commonly used chemical derivatizing agents include trimethylchlorosilane[5] and (γ-methacryloxypropyl)-trimethoxy silane,[34] among others.[35] The bonded coating has proved to be effective for only limited periods of time owing to the reversible hydrolysis of the silyl oxygen bond, particularly at high pH. Recent advances in the technology of wall coating promises more stable and longer lived coatings.[35] The utilization of wall-coated capillaries, such as the ones employed in gas chromatography, has also been attempted. However, these materials have proven to be very hydrophobic, introducing the

phenol

deleter

elimina

reverse

polyam

surface

amount

effectiv

charge

coulom

applicat

layer at

polymer

to 8 with

1.4 Inje

T

dramatic

reproduc

Sample

hydrosta

voltage g

hydrosta

establish

(Beckma

phenomenon of solute partitioning into the electrophoretic process, with causes deleterious effects on resolution and efficiency. A more versatile approach to the elimination of coulombic adsorption of solute analytes is to use a charge-reversed polymeric coating. Recent work with high-molecular-weight polyamines[33] has demonstrated that the negative charge on the fused silica surface, and hence, the electroosmotic flow can be carefully controlled by the amount of polyamine adsorbed. This treatment has been shown to be very effective in eliminating much of the charge-induced adsorption of multiply charged biopolymers, such as proteins and peptides. Furthermore, the coulombic interactions of strongly basic analytes can be nearly eliminated by the application of thicker polymer films and the formation of a positively charged layer at the surface of the capillary. The most important benefit that covalent or polymeric coatings provide is the ability to use buffers in the pH range from 4.5 to 8 without severe solute-wall interaction.

1.4 Injection

The manner by which the sample is introduced into the capillary has dramatic implications on quantitative analysis.[36] The peak area or height reproducibility is a direct function of the precision of the injection technique. Sample injection can be performed either electrokinetically or hydrostatically.[6,19,36-41] Electrokinetic injection is achieved by applying a voltage gradient across the capillary length for a known period of time, whereas hydrostatic injection uses a pressure gradient. The pressure gradient can be established by different mechanisms: head-space pressurization injection (Beckman Instruments, Inc., Fullerton, CA); vacuum injection, in which a

reduce

Divisio

Inc., Sa

the inle

introduc

the ana

injection

the cap

electrok

sample

significa

that is c

preferred

sample c

combina

of mater

electrical

electroos

non-repre

sample c

particular

are near

major app

sample is

modes on

reduced pressure is applied to the outlet end of the capillary (Applied Biosystems Division of The Perkin-Elmer Corporation, Foster City, CA and Spectraphysics, Inc., San Jose, CA); and gravity injection (Dionex, Inc., Sunnyvale, CA), in which the inlet reservoir is elevated with respect to outlet reservoir and the sample is introduced by siphoning action.

Hydrodynamic injection provides a sample plug which is representative of the analyte composition. The injection volume (nL range) depends on the injection time, capillary dimensions, buffer viscosity, and pressure drop across the capillary length.[37] Hydrodynamic injection is usually more precise than electrokinetic injection because it is based strictly on volume loading of the sample (area reproducibility is approximately 3 % RSD).[36,37,41] However, significant broadening of the zone can occur as a result of the parabolic profile that is characteristic of pressure-driven flow.[42] Hydrodynamic injection is the preferred injection method for CZE and MECC applications, particularly when the sample concentration is within the sensitivity limits of the detector.

In electrokinetic injection, sample is introduced in the capillary as a combination of electrophoretic and electroosmotic migration. Thus the amount of material injected is a function of the solute electrophoretic mobility, the electrical conductance of the sample and the conducting medium, and the electroosmotic flow. An important consequence of this mode of injection is that non-representative sampling may result from discrimination in the uptake of sample components with different electrophoretic mobilities.[40] This can be particularly a problem when the sample is composed of low mobility solutes that are near the concentration limit of detection. Electrokinetic injection finds its major application with the use of gel-filled capillaries, where volumetric loading of sample is impossible. A thorough examination of the impact of the injection modes on separation efficiency is presented in Chapter 4.

Sample

zone w

increas

techniq

electrop

detector

electrop

performi

strategie

extensiv

the sam

concentr

field. Ur

greater t

interface

interface,

causing c

electroph

conventio

after a s

injection.

sample zo

of sample

injection

concentrat

stacking c

distribution

Sample Concentration Strategies. The small column dimensions and narrow zone widths in capillary electrophoresis place a high demand on detection. An increase in sensitivity is highly desirable for many applications. Several techniques have been reported to enhance the detectability in capillary electrophoresis.[43] This is usually accomplished through improvement of the detector (*vide* next section). However, the injection features of capillary electrophoresis make it possible to obtain enhanced detection limits by performing on-column sample concentration. Among the pre-concentration strategies, sample stacking with discontinuous buffer systems has found extensive use in many areas of electrophoresis.[44-47] When the conductivity of the sample solution is lower than that of the electrophoretic buffer, a concentration or stacking phenomenon occurs upon application of the electric field. Under these conditions, the electric field in the sample medium is much greater than that in the electrophoretic buffer, and the ions migrate rapidly to the interface between the lower and higher conductivity zones. Upon reaching the interface, the ions experience a lower electric field and slow down (stack), causing contraction of the sample zone. The thin zone then moves through the electrophoretic buffer and separates into individual zones according to conventional zone electrophoresis principles. Sample stacking can be achieved after a sample has been injected hydrodynamically or upon electrokinetic injection. In this latter case, as the stacking proceeds, the concentration in the sample zone increases. Consequently, the conductivity increases and the rate of sample concentration falls off asymptotically during injection time. Thus, the injection length can become larger than desired before a steady-state concentration can be reached in the sample zone. Finally, the effectiveness of stacking depends on the electroosmotic flow velocity. The non uniform distribution of the electric field strength causes differences in the local

electro

across

the sa

relative

electro

flow an

velocity

optimal

where t

overcon

high ele

ions will

migrate

the nega

to migra

sample

created.

using a

isoelectri

lower pH

charged

When th

direction

step, the

charged s

electroosmotic velocities, which in turn generate an electroosmotic pressure across the concentration boundary. When the electroosmotic flow velocity is in the same direction as the analyte migration, the stacking efficiency is decreased relative to the case where the flow is zero. The larger the magnitude of the electroosmotic flow, the worse the stacking efficiency. When the electroosmotic flow and the analyte migration are in opposite directions, with the electrophoretic velocity much larger than the electroosmotic velocity, the stacking efficiency is optimal. This situation is not commonly encountered, particularly at high pH, where the electroosmotic flow can be quite high (*vide* Chapter 3).

The difficulties encountered in applying stacking at high pH can be overcome by using polarity switching during electrokinetic injection.[43] With a high electroosmotic flow and normal polarity (cathode end is grounded), positive ions will stack at the sample-buffer interface, whereas negative ions will tend to migrate out of the injection end of the capillary. Reversing the polarity will cause the negative ions to migrate into the capillary and stack as the positive ions start to migrate out. By appropriately controlling the injection time at each polarity, a sample zone containing both positive and negative ions in a narrow zone can be created.

Another way to achieve stacking, which is applicable to ampholytes, is by using a pH gradient during injection.[47] The injected zone has a pH above the isoelectric point of the solutes, surrounded by an electrophoretic buffer with lower pH. As a result, the solutes in the sample zone are initially negatively charged and migrate towards the anode upon application of the electric field. When the solutes enter the acidic region, the charge reverses and so the direction of migration. This results in a narrowing of the sample zone. In a final step, the pH gradient dissipates and the concentrated zone with positively charged solutes migrates towards the cathode.

amplifi

followe

applica

altered

is hydr

using a

sample

electrop

is subs

indicate

perform

1.5 Det

D

intense

articles

literature

to the

performa

these de

capillarie

benefit fr

variety of

Se

An interesting approach to sample concentration is known as field amplification,[48-51] in which a large fraction of the capillary is filled with sample, followed by focusing of the solute zone prior to separation. This method is applicable to the analysis of either cations (when the capillary surface charge is altered) or anions, but not both simultaneously. For anions, a large sample plug is hydrodynamically injected onto the column in a low-conductivity buffer. By using a voltage polarity opposite to that employed for the electrophoresis, the sample anions are focused at the interface between the sample zone and the electrophoretic buffer, at the cathodic end of the capillary, and the sample zone is substantially contracted. When the focusing step is completed, which is indicated by a change in current, the polarity is reversed and the separation is performed.

1.5 Detection

Detection development for capillary electrophoresis has been an area of intense research since the inceptions of the technique. A series of review articles covering a variety of detection schemes is found in the literature.[18,19,36,43,52] The rapid advance in detection technology is attributable to the relative ease of adaptation of some detectors employed for high-performance liquid chromatography (HPLC). With minor modification some of these detectors have been adapted to accommodate the use of fused-silica capillaries as the detector flow cell. Moreover, the diversity of molecules that benefit from electrophoretic methods has contributed to the implementation of a variety of detection principles.

Several criteria must be considered when choosing the appropriate

detecto
linear
reprodu
should
helpful
Ideally,
of the t
and con
contribu
eliminat

T
property
physical
refractiv
detector
usually
detector
differenc
measure
absorbar
amperom
limit dete
The use
matrix is
interferer
property
noise rati

detector for a particular analysis. These criteria include sensitivity, selectivity, linear range and noise. Detector response should produce a known and reproducible relationship with the amount or concentration of the solute and should have a wide linear-response range. In certain applications, it is more helpful to use a detector that is universal and responds similarly to all solutes. Ideally, the detector for capillary electrophoresis should respond independently of the buffer, should not contribute to band broadening and should be reliable and convenient to use. On-column detection is usually preferable because the contributions to zone dispersion due to joints, fittings and connectors are eliminated. Unfortunately no single detector provides all these properties.

There are two main types of detectors: bulk-property and specific-property detectors. The bulk-property detectors measure the difference in some physical property of the solute relative to that of the buffer alone. These include refractive index,[53,54] conductivity,[3,31,55-58] and indirect methods.[22,59,60] These detectors are generally more universal than the specific-property, however, they usually have lower sensitivities and dynamic ranges. This is because the detector signal depends not on the properties of the solutes but also on the differences in properties of the solute and the buffer. Specific-property detectors measure specific properties of solutes and include ultraviolet (UV) absorbance,[25,27,61-69] fluorescence,[4,20,22,23,70-85] mass spectrometry,[86] amperometric,[87-90] radiometric,[91,92] and Raman detectors.[93,94] These methods limit detection only to those analytes that possess the required specific property. The use of these selective detectors is very advantageous when the sample matrix is complex and in situations where it is desirable to minimize background interferences. This type of detector is normally more sensitive than the bulk-property detector, provides wider linear ranges and more acceptable signal-to-noise ratios, and consequently, is used most often. Table 1.2 compares the

Table

Table 1.2 Comparison between some of the detection schemes available to capillary electrophoresis.

DETECTION MODE	TYPICAL DETECTION LIMITS (M)
REFRACTIVE INDEX[53,54]	$10^{-5} - 10^{-6}$
CONDUCTIVITY[3,31,55-58]	$10^{-5} - 10^{-6}$
ABSORBANCE	
Direct[61-66]	$10^{-5} - 10^{-6}$
Indirect[67-69]	$10^{-4} - 10^{-5}$
FLUORESCENCE	
Direct (lamp-based)[4,70]	$10^{-7} - 10^{-8}$
Direct (laser-based)[20,74-80]	$10^{-9} - 10^{-12}$
Indirect[22,23,84,85]	$10^{-6} - 10^{-7}$
MASS SPECTROMETRY[86]	$10^{-4} - 10^{-9}$
AMPEROMETRIC[87-90]	$10^{-8} - 10^{-9}$
RADIOMETRIC[91,92]	$10^{-9} - 10^{-11}$
RAMAN[93,94]	$10^{-6} - 10^{-7}$

limits

electro

advan

employ

for cap

capillar

Additio

among

detectio

specific

capillari

detectio

perform

sample

affect th

source s

reducing

Illuminat

accompl

absorb li

difficult.

variable

sensitivity

over filter

scan wav

limits of detection for some detection schemes available for capillary electrophoresis. The section that follows describe in more detail the recent advances for the capillary UV-absorbance detector, which is the detector employed in this work.

UV-absorbance detection is by far the most widely used detection scheme for capillary electrophoresis. In fact, all commercially available instruments for capillary electrophoresis employ an ultraviolet-visible absorbance detector. Additionally, there is a broad range of applicability for UV-absorbance detectors among the compounds that can be analysed by electrophoretic methods.

Sensitivity of UV-absorbance detection depends on the pathlength of the detection cell. Hence, detection limits tend to be lower than those of other specific-property detectors. This limits the uselfulness of UV-absorbance to capillaries having inner diameters greater than 25 μm. For UV-absorbance detection, there is a compromise between the use of low cell volumes for high performance and the use of large diameter capillaries for sensitivity. Increased sample loading can overcome the sensitivity problems, but can also adversely affect the electrophoretic separation process. The slit widths for the UV light source should be sufficiently small that only the capillary is illuminated, thereby reducing stray light levels that could result in excessive background noise. Illumination volumes should be smaller than the analyte zones, which is best accomplished by focusing the UV light on the capillary. Finally, many materials absorb light in the UV region, so minimizing background interferences can be difficult. In terms of selectivity, an UV-absorbance detector with continuous variable wavelength is most desirable, even though there may be some loss in sensitivity. With variable-wavelength operation, a monochromator is preferred over filters for wavelength selection since it is more versatile, can be used to scan wavelengths, and produces better resolution. The main disadvantage of

instrum

systen

compo

feature

is usec

gain th

excess

comme

walls o

mercur

is collec

of using

core ca

fibers in

wavelen

detector

unknow

If

obtained

are iden

electroph

obtained

high UV

species a

of the ab

mobilities

instruments utilizing a monochromator is that they are usually less sensitive than systems utilizing filters, which provide more light throughout.

Direct ultraviolet-absorbance detection is useful for a large number of compounds that contain a chromophore. Early work in capillary electrophoresis featured the use of modified HPLC UV-absorbance detectors.[27] Since no pump is used, this detector is modified to obtain shorter response times and higher gain than that needed for HPLC detection, where pump pulses can lead to excessive noise. Another modification included the combination of a commercially available instrument with optical fibers in direct contact with the walls of the electrophoresis capillary.[61] In this approach, the UV radiation of a mercury lamp is filtered before entering the optical fiber, and the transmitted light is collected opposite the incident light using another optical fiber. The advantage of using optical fibers is that the capillary inner diameter and the light conducting core can be matched for optimal sensitivity. The disadvantages of using optical fibers include transmission losses in the fibers and reduced efficiency at low wavelengths. Other approaches include the use of photodiode array detectors.[62] The advantage of this approach is that qualitative information about unknown analytes can be obtained from the absorption spectra.

If the solutes do not contain a chromophore, an absorbance signal can be obtained by indirect detection.[67-69] Optical systems used for indirect detection are identical to those for direct UV-absorbance. The only difference is that the electrophoretic buffer contains a chromophore. The best sensitivities are obtained in low-concentration background electrolytes containing a co-ion with high UV absorption at a given detection wavelength. Non-absorbing ionic species are revealed by changes in light absorption due to charge displacement of the absorbing co-ion. It is desirable that the sample ions have effective mobilities similar to those of the absorbing co-ion. The useful dynamic range is

limited

the op
measu
spectro
charac
perform
capillar
capillar
liquid in
ion lase
nm) se
the cap
solvents
refractiv
sensitivi
pump la
of 50 to
due to s

Detecto
directly
measure
should l
inner dia
resulting
systemat

limited by the linearity and noise of the detector.

The use of high-intensity light sources offers an alternative to extending the optimal path length to obtain greater sensitivity in an absorbance detection measurement. The availability of UV lasers will have an impact on spectroscopic-based instrumentation as costs decrease and optical characteristics improve. Thermooptical detection is another detection technique performed on-column by using two intersecting laser beams focused on the capillary. A pump laser is focused at a right angle to the electrophoresis capillary, and a second laser beam is used to probe the refractive index of the liquid in the capillary. Either a 4 mW HeCd laser (442 nm)[95] or a 130 mW argon ion laser[96] serves as the pump laser, whereas a 1 mW helium-neon laser (632.8 nm) serves as the probe laser. Absorbance of the pump beam by analytes in the capillary produces a temperature rise. Since the refractive index of most solvents change with temperature, absorbance of the pump beam produces refractive index changes that are monitored by the probe laser. The absorbance sensitivity for the thermooptical detection is proportional to the power of the pump laser, and the signal is independent of the capillary diameter in the range of 50 to 500 μm. Unlike typical absorbance measurements, sensitivity is not lost due to short detection path lengths.

Detector Cell Designs. According to Beer's law, the absorbance of a sample is directly proportional to the path length through which the absorbance measurement is performed. Therefore, extension of the optical path length should lead to improved detection sensitivity. However, simply increasing the inner diameter of the capillary is not always an attractive alternative because the resulting Joule heating may lead to a loss of resolution. Bruin *et al.*[97] have systematically investigated alternative flow cell designs and capillary diameters.

All flo

effect

length

the m

the ce

bendir

have r

optical

increas

sensitiv

backgr

With ap

maintai

limitatio

substan

A

path len

and rec

employe

geometr

efficient

detection

Th

using mi

capillary

while the

All flow cell designs, including the standard cylindrical capillary, require an effective means of coupling the excitation light into and through the capillary path length. A ball lens made from saphire or quartz, placed closed to the capillary is the most effective approach.[41] This configuration provides radial illumination of the center of the capillary, optimizing light throughput and minimizing stray light.

The short optical path lengths in microcapillaries can be extended by bending the capillary (Z-cell) and illuminating through the bend. Chervet et al.[98] have manufactured Z-cells for capillary electrophoresis that provide a 3-mm optical path length. However, in spite of the fact that the pathlength was increased by 40-fold over a 75 μm inner-diameter capillary, only about a 5-fold sensitivity enhancement occured. This was attributed to an increased background noise level and poor efficiency in light throughput at the 3-mm bend. With appropriate optics, the noise level can be reduced, while the signal gain is maintained. The extended optical path length in the Z-cell contains an inherent limitation: the contribution of the finite detector volume to the zone variance is substantially increased.

An alternative to bending a cylindrical capillary to gain a longer optical path length is to perform electrophoresis in flattened channels. Several square and rectangular capillaries of varying dimensions and materials have been employed for this purpose.[99-100] The advantage provided by flattened geometries is that the narrow separation channel dimension is maintained for efficient heat dissipation, while longer optical paths are obtained for enhanced detection sensitivity.

The optical path length of the capillary can be effectively multiplied by using mirrors (silver coated capillary) to reflect the incident light inside the capillary prior to detection.[101] In this approach, the optical path length increases while the narrow separation dimension is maintained. A critical parameter in

such

inter

and

effici

detec

width

is to

length

intern

result

the to

Samp

electr

deal o

and id

collect

employ

mainta

Severa

been d

from c

approa

the use

can be

with re

such cell construction is the incident light angle, which controls the number of internal reflections and the path length per reflection. The number of reflections, and hence the ultimate sensitivity, must be restricted to minimize the loss in efficiency caused by the flow cell size. The distance between incident light and detection should be less than the standard deviation of the narrowest zone width.

An interesting approach to increase sensitivity in capillary electrophoresis is to select the entire capillary length as the light path rather than the radial length.[102,103] In this format, light is transmitted through the capillary by total internal reflection. The absorbance indicates the sum of the absorbance signals resulting from all analyte components. As components elute from the column, the total absorbance decreases in a steplike manner.

Sample Collection Strategies. The most commonly used detectors in capillary electrophoresis do not provide structural information. Therefore, there is a great deal of interest, particularly in biotechnological applications, for sample collection and identification, after the separation has occurred. The process of fraction collection in capillary electrophoresis is fundamentally different from that employed in other separation techniques, because the electric field must be maintained during sampling, in order to transport the solutes out of the capillary. Several strategies to perform sample collection in capillary electrophoresis have been described.[104-107] Devices have been designed where the capillary moves from one collection vessel to another in a programmable manner. Other approaches include the use of a frit structure at the side wall of the capillary and the use of multiple capillaries arranged in bundles. The amount of material that can be collected by these schemes range from nanogram to tenth of microgram with repetitive cycles. The shortcomings of sample collection for capillary

elect

incre

the s

1.6 C

chara

applic

speed

descri

injecti

over t

fundar

physic

not po

electro

devise

incorpo

constitu

progra

compos

injectio

integral

favorab

electrophoresis are loss of efficiency due to either mixing of the solute zones, or increased capillary diameter. Moreover, there might be a substantial dilution of the sample during the collection process.

1.6 Conclusions

Throughout this first chapter, capillary electrophoresis has been characterized as a versatile technique for routine biomedical and industrial applications, capable of achieving high efficiencies, superior resolution and high speed separations. The present state-of-the-art of the technique has been described in areas such as capillary technology, enhancement of sensitivity, injection and detection schemes. However, despite the impressive advances over the past ten years of capillary electrophoresis, there is still a scarcity of fundamental studies that would lead to a greater understanding of the physicochemical nature of the separation process. Without this knowledge, it is not possible to model important parameters, and most importantly, to design electrophoretic separations.

In this work, a novel approach to capillary zone electrophoresis has been devised through the development of a computer routine. The program incorporates simple but reliable models for zone migration and dispersion, and constitutes a comprehensive description of electrophoretic separations. The program includes many versatile features, such as the choice of buffer composition, capillary dimensions, and instrumental parameters related to injection, detection, and power supply operation. This program serves as the integral part of a systematic optimization strategy to search and identify the most favorable conditions for a separation. Chapter 2 organizes the experimental

methods and instrumental details for the elaboration of the program constituent models and validation of the overall optimization strategy. Chapter 3 describes the development of a theoretical model for electroosmotic flow, and contrasts the features of separations under constant-current and constant-voltage conditions. Chapter 4 presents the mathematical background of the computer optimization routine, and describes the usage of the computer program as a pedagogical tool to examine the effect of a variety of parameters on electrophoretic separations. Chapter 5 applies the methodology developed to determine dissociation constants and electrophoretic mobilities to nucleotides and provides the experimental validation of the optimization routine. Chapter 6 describes the use of the optimization program to study the separation of tetracycline antibiotics and explores the analytical capabilities of capillary zone electrophoresis as an alternative method for the determination of tetracyclines. Chapter 7 summarizes the overall accomplishments of the present work and introduces ideas for further improvement of the optimization strategy. Finally, two appendices are incorporated to detail the buffer preparation and the optimization computer programs.

1.7 R

1.

2.

3.

4.

5.

6.

7.

8.

9.

10.

11.

12.

13.

14.

15.

16.

17.

18.

19.

20.

1.7 References

1. Tiselius, A.; Thesis; *Nova Acta Regiae Societatis Scientiarum Uppsaliensis*, Ser. IV, Vol. 7, pp. 1-107; Almqvist & Wiksell: Uppsala, Sweden, 1930.

2. Tiselius, A. *Trans. Faraday Soc.* **1937**, *33*, 524-531.

3. Mikkers, F. E. P.; Everaerts, F. M.; Verheggen, Th. P. E. M. *J. Chromatogr.* **1979**, *169*, 11-20.

4. Jorgenson, J.; Lukacs, K. D. *Anal. Chem.* **1981**, *53*, 1298-1302.

5. Jorgenson, J.; Lukacs, K. D. *Science* **1983**, *222*, 226-272.

6. Jorgenson, J. W.; Phillips, M., Eds.; *New Directions in Electrophoretic Methods; ACS Symposium Series*; American Chemical Society: Washington, DC, 1987.

7. Bier, M., Ed.; *Electrophoresis - Theory, Methods and Applications*; Academic Press Inc.; New York, 1959.

8. Deyl, Z., Ed.; *Electrophoresis; J. Chromatogr. Lib.*, Vol. 18; Elsevier Scientific Publlishing Co.: Amsterdam, 1979.

9. Hjertén, S. *Chromatogr. Rev.* **1967**, *9*, 122-219.

10. Bocek, P.; Deml. M.; Gebauer, P.; Dolnik, V. *Analytical Isotachophoresis*; *Electrophoresis Library*, Vol.1; VCH Publishers: New York, 1988.

11. Righetti, P. G. *J. Chromatogr.* **1984**, *300*, 165-223.

12. Giddings, J. C. *J. Sep. Sci.* **1969**, *4*, 181-189.

13. Lauer, H. H.; McManigill, D. *Trends Anal. Chem.* **1986**, *5*, 11-15.

14. Lauer, H. H.; McManigill, D. *Anal. Chem.* **1986**, *58*, 166-170.

15. Smith, R. D.; Olivares, J. A.; Nguyen, N. T.; Udseth, H. R. *Anal. Chem.* **1988**, *60*, 436-441.

16. Pretorius, V.; Hopkins, B. J.; Schieke, J. D. *J. Chromatogr.* **1974**, *99*, 23-30.

17. Virtanen, R. *Acta Polytech. Scand. Chem. Ind. Metall. Ser.* **1974**, *123*, 1-67.

18. Kuhr, W. G. *Anal. Chem.* **1990**, *62*, 403R-414R.

19. Wallingford, R. A.; Ewing, A. G. *Adv. Chromatogr.* **1989**, *29*, 1-77.

20. Gassmann, E.; Kuo, J. E.; Zare, R. N. *Science* **1985**, *230*, 813-814.

21.

22.

23.

24.

25.

26.

27.

28.

29.

30.

31.

32.

33.

34.

35.

36.

37.

38.

39.

40.

41.

42.

21. Gordon, M. J.; Huang, X.; Pentoney, S. L.; Zare, R. N. *Science* **1988**, *242*, 224-228.

22. Kuhr, W. G.; Yeung, E. S. *Anal. Chem.* **1988**, *60*, 1832-1834.

23. Kuhr, W. G.; Yeung, E. S. *Anal. Chem.* **1988**, *60*, 2642-2646.

24. Smith, R. D.; Barinaga, C. J.; Udseth, H. R. *Anal. Chem.* **1988**, *60*, 1948-1952.

25. Cohen, A. S.; Karger, B. L. *J. Chromatogr.* **1987**, *397*, 409-417.

26. Cohen, A. S.; Paulus, A.; Karger, B. L. *Chromatographia* **1987**, *24*, 15-24.

27. Terabe, S.; Otsuka, K.; Ichikawa, K.; Tsuchiya, A.; Ando, T. *Anal. Chem.* **1984**, *56*, 111-113.

28. Unger, K. K. *Porous Silica; J. Chromatogr. Lib.*, Vol. 16; Elsevier Scientific Publishing Company: New York, 1990.

29. Hiemenz, P. C. *Principles of Colloid and Surface Chemistry*, 2nd ed.; Marcel Dekker: New York, 1959.

30. Altria, K.; Simpson, C. *Anal. Proc.* **1986**, *23*, 453-454.

31. Huang, X.; Luckey, J. A.; Gordon, M. J.; Zare, R. N. *Anal. Chem.* **1989**, *61*, 766-770.

32. Altria, K.; Simpson, C. *Chromatographia* **1987**, *24*, 527-532.

33. Wiktorowicz, J. E.; Colburn, J. C. *Electrophoresis* **1990**, *11*, 769-773.

34. Hjérten, S. *J. Chromatogr.* **1985**, *347*, 191-198.

35. McCormick, R. *Anal. Chem.* **1988**, *60*, 2322-2328.

36. Grossman, P. D.; Colburn, J. C., Eds.; *Capillary Electrophoresis - Theory and Practice*; Academic Press Inc.: San Diego, CA, 1992.

37. Rose, D. J., Jr.; Jorgenson, J. W. *Anal. Chem.* **1988**, *60*, 642-648.

38. Olechno, J. D.; Tso, J. M. Y.; Thayer, J. Wainright, A. *Am. Lab.* **1990**, 12, 30-37.

39. Burton, D. E.; Sepaniak, M. J.; Maskarinec, M. P. *Chromatographia* **1986**, *21*, 583-586.

40. Huang, X.; Gordon, M. J.; Zare, R. N. *Anal. Chem.* **1988**, *60*, 337-380.

41. Moring, S. E.; Colburn, J. C.; Grossman, P. D.; Lauer, H. H. *LC/GC* **1990**, *8*, 34-46.

42. Giddings,J. C. *Unified Separation Science*; Wiley-Interscience Publication: New York, 1991.

43.

44.

45.

46.

47.

48.

49.

50.

51.

52.

53.

54.

55

56

57

58

59

60

61

62.

63.

64.

65.

43. Albin, M.; Grossman, P. D.; Moring, S. E. *Anal. Chem.* **1993**, *65*, 489A-497A.

44. Burgi, D. S.; Chien, R. *Anal. Chem.* **1991**, *63*, 2042-2047.

45. Schwer, C.; Lottspeich, F. *J. Chromatogr.* **1992**, *623*, 345-355.

46. Gebauer, P.; Thormann, W.; Bocek, P. *J. Chromatogr.* **1992**, *608*, 47-57.

47. Aebersold, R.; Morrison, H. D. *J. Chromatogr.* **1990**, *516*, 79-88.

48. Chien, R.; Helmer, J. C. *Anal. Chem.* **1991**, *63*, 1354-1361.

49. Chien, R.; Burgi, D. S. *J. Chromatogr.* **1991**, *559*, 153-161.

50. Burgi, D. S.; Chien, R. *Anal. Biochem.* **1992**, *202*, 306-309.

51. Chien, R.; Burgi, D. S. *Anal. Chem.* **1992**, *64*, 489A-496A.

52. Ewing, A. G.; Wallingford, R. A.; Olefirowicz, T. M. *Anal. Chem.* **1989**, *61*, 292A-303A.

53. Bornhop, D. J.; Dovichi, N. J. *Anal. Chem.* **1987**, *59*, 1632-1636.

54. Chen, C.; Demana, T.; Huang, S.; Morris, M. D. *Anal. Chem.* **1989**, *61*, 1590-1593.

55 Huang, X.; Pang, T. J.; Gordon, M. J.; Zare, R. N. *Anal. Chem.* **1987**, *59*, 2747-2749.

56 Huang, X.; Gordon, M. J.; Zare, R. N. *J. Chromatogr.* **1988**, *425*, 385-390.

57 Huang, X.; Gordon, M. J.; Zare, R. N. *J. Chromatogr.* **1989**, *480*, 285-288.

58 Ackermans, M. T.; Everaerts, F. M.; Beckers, J. L. *J. Chromatogr.* **1991**, *549*, 345-355.

59 Yeung, E. *Acc. Chem. Res.* **1989**, *22*, 125-130.

60 Hogan, B. L.; Yeung, E. S. *Appl. Spectrosc.* **1989**, *43*, 349-350.

61 Foret, F.; Deml, M.; Kahle, V.; Bocek, P. *Electrophoresis* **1986**, *7*, 430-432.

62. Kobayashi, S.; Ueda, T.; Kikumoto, M. *J. Chromatogr.* **1989**, *480*, 179-184.

63. Sepaniak, M. J.; Swaile, D. F.; Powell, A. C. *J. Chromatogr.* **1989**, *480*, 185-196.

64. Aguilar, M.; Huang, X.; Zare, R. N. *J. Chromatogr.* **1989**, *480*, 427-432.

65. Walbroehl, Y.; Jorgenson, J. W. *J. Chromatogr.* **1984**, *315*, 135-143.

66.

67.

68.

69.

70.

71.

72.

73.

74.

75.

76.

77.

78.

79.

80.

81.

82.

83.

84.

85.

86.

87.

88.

66. Green, J. S.; Jorgenson, J. W. *J. Liq. Chromatogr.*, **1989**, *12*, 2527-2561.

67. Hjérten, S.; Elenbring, K.; Kilar, F.; Ilao, J.; Chen, A. J. C.; Siebert, C. J.; Zhu, M. *J. Chromatogr.* **1987**, *403*, 47-61.

68. Foret, F.; Fanali, S.; Ossicini, L.; Bocek, P. *J. Chromatogr.* **1989**, *470*, 299-308.

69. Grant, I. H.; Steuer, W. *J. Microcol. Sep.*, **1990**, *2*, 74-79.

70. Green, J. S.; Jorgenson, J. W. *J. Chromatogr.* **1986**, *352*, 337-343.

71. Lawrence, J. F. *J. Chromatogr. Sci.* **1979**, *17*, 147-151.

72. Ohkura, Y.; Nohta, H. *Advances in Chromatography*, Vol. 29, pp. 221-258; Marcel Dekker: New York, 1989.

73. Kasper, T. J.; Melera, M.; Gozel, P.; Brownlee, R. G. *J. Chromatogr.* **1988**, *458*, 303-312.

74. Toulas, C.; Hernadez, L. *LC/GC* **1992**, *10*, 471-476.

75. Gozel, P.; Gassmann, E.; Michelsen, H.; Zare, R. N.; *Anal. Chem.* **1987**, *59*, 44-49.

76. Roach, M. C.; Gozel, P.; Zare, R. N. *J. Chromatogr. Biomed. Appl.* **1988**, *426*, 129-140.

77. Nickerson, B.; Jorgenson, J. W. *J. High Res. Chromatogr.* **1988**, *11*, 533-534.

78. Cheng, Y.; Dovichi, N. J. *Science* **1988**, *242*, 562-564.

79. Wu, S.; Dovichi, N. J. *J. Chromatogr.* **1989**, *480*, 141-155.

80. Hernadez, L.; Marquina, R.; Escalona, J.; Guzman, N. A. *J. Chromatogr.* **1990**, *502*, 247-255.

81. Swaile, D. F.; Sepaniak, M. J. *J. Microcol. Sep.* **1989**, *1*, 155-158.

82. Rose, D. J., Jr.; Jorgenson, J. W. *J. Chromatogr.* **1988**, *447*, 117-131.

83. Nickerson, B.; Jorgenson, J. W. *J. Chromatogr.* **1989**, *480*, 157-168.

84. Gross, L.; Yeung, E. S. *J. Chromatogr.* **1989**, *480*, 169-178.

85. Hogan, B. L.; Yeung, E. S. *J. Chromatogr. Sci.* **1990**, *28*, 15-18.

86. Smith, R. D.; Wahl, J. H.; Goodlett, D. R.; Hofstadler, S. A. *Anal. Chem.* **1993**, *65*, 574A-584A.

87. Wallingford, R. A.; Ewing, A. G. *Anal. Chem.* **1987**, *59*, 1762-1766.

88. Wallingford, R. A.; Ewing, A. G. *Anal. Chem.* **1988**, *60*, 258-263.

89.

90.

91.

92.

93.

94.

95.

96.

97.

98.

99.

100.

101.

102.

103.

104.

105.

106.

107.

89. Wallingford, R. A.; Ewing, A. G. *Anal. Chem.* **1988**, *60*, 1972-1975.

90. Olefirowicz, T. M.; Ewing, A. G. *J. Chromatogr.* **1990**, *499*, 713-719.

91. Pentoney, S. L., Jr.; Zare, R. N.; Quint, J. F. *J. Chromatogr.* **1989**, *480*, 259-270.

92. Pentoney, S. L., Jr.; Zare, R. N.; Quint, J. F. *Anal. Chem.* **1989**, *61*, 1642-1647.

93. Chen, C.; Morris, M. D. *Appl. Spectrosc.* **1988**, *42*, 515-518.

94. Chen, C.; Morris, M. D. *J. Chromatogr.* **1991**, *540*, 355-363.

95. Yu, M.; Dovichi, N. J. *Mikrochim. Acta* **1988**, *3*, 41-56.

96. Yu, M.; Dovichi, N. J. *Anal. Chem.* **1989**, *61*, 37-40.

97. Bruin, G. J. M.; Stegeman, G.; van Asten, A. C.; Xu, X.; Kraak, J. C.; Poppe, H. *J. Chromatogr.* **1991**, *559*, 163-181.

98. Chervet, J. P.; van Soest, R. E. J.; Ursem, M. *J. Chromatogr.* **1991**, *543*, 439-449.

99. Izumi, T.; Nagahori, T.; Okuyama, T. *J. High Chromatogr. Chromatogr. Commun.* **1991**, *14*, 351-357.

100. Tsuda, T.; Sweedler, J. V.; Zare, R. N. *Anal. Chem.* **1990**, *62*, 2149-2152.

101. Wang, T.; Aiken, J. H.; Huie, C. W.; Hartwick, R. A. *Anal. Chem.* **1991**, *63*, 1372-1376.

102. Xi, X.; Yeung, E. S. *Appl. Spectrosc.* **1991**, *45*, 1199-1203.

103. Taylor, J. A.; Yeung, E. S. *J. Chromatogr.* **1991**, *550*, 831-837.

104. Rose, D. J., Jr.; Jorgenson, J. W. *J. Chromatogr.* **1988**, *438*, 23-34.

105. Huang, X.; Zare, R. *J. Chromatogr.* **1990**, *516*, 185-189.

106. Guzman, N. A.; Trebilcock, M. A.; Advis, J. P. *J. Liq. Chromatogr.* **1991**, *14*, 997-1015.

107. Guzman, N. A.; Trebilcock, M. A. *Anal. Chim. Acta* **1991**, *249*, 247-255.

meth

elect

(Cha

inclu

condi

devel

the vi

(Chap

prese

and s

2.1 C

repres

supply

Station

voltage

high vo

safety i

CHAPTER 2

EXPERIMENTAL METHODS

In this chapter, an overall view of the experimental apparatus and methods used throughout this dissertation is provided. The capillary electrophoresis system was basically the same for all developmental studies (Chapters 3 and 4) and practical applications (Chapters 5 and 6). This chapter includes a detailed description of the procedure used for capillary surface conditioning, a process essential for migration time reproducibility. The method developed for the electroosmotic flow determination and the measurements of the viscosity and dielectric constant, needed in the model of electrosmotic flow (Chapter 3), are also included. A descriptive list of all reagents and solutions is presented. Finally, brief descriptions of data processing, computer hardware and software are provided.

2.1 Capillary Zone Electrophoresis System

The capillary zone electrophoresis system used in this work is represented schematically in Figure 2.1. A regulated high-voltage DC power supply (Model EH50R0.19XM6, Glassman High Voltage Inc., Whitehouse Station, NJ) is operated in either constant-current (0 – 190 μA) or constant-voltage (0 – 50 kV) mode. The operator is protected from accidental exposure to high voltage by enclosing the CZE system in a Plexiglas® box equipped with safety interlocks. The power supply is connected via platinum rod electrodes to

Figure 2.1 Schematic representation of the capillary zone electrophoresis system.

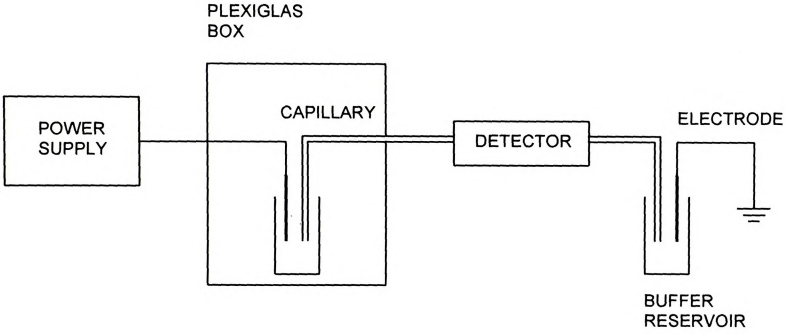
PLEXIGLAS
BOX
POWER
SUPPLY
CAPILLARY
DETECTOR
ELECTRODE
BUFFER
RESERVOIR

Figure 2.1

two

capil

i.d.,

soluti

maint

water

differe

min p

sampl

prefer

repres

particu

injectio

injecte

lower

quantit

spectro

wavele

removi

2.2 Cap

T

of migra

two small reservoirs containing the solution under investigation. Fused-silica capillary tubing (Polymicro Technologies, Phoenix, AZ), with dimensions 75 μm i.d., 375 μm o.d., and 110 cm total length, is immersed at each end in the solution reservoirs. In order to minimize thermal effects, the capillary is maintained at 25.0° C during operation by means of a thermostatically controlled water bath (Model RTE 9B, Neslab Instruments, Portsmouth, NH).

Injection was performed hydrodynamically, by maintaining a 2-cm difference between the liquid levels at the inlet and outlet reservoirs, during a 1-min period. Under typical operating conditions, this procedure introduces a sample volume of approximately 9 nL. The hydrodynamic injection method was preferred over electrokinetic injection because it provides a sample that is representative of the analyte composition. The choice of injection method was particularly critical in the studies with nucleotides. During electrokinetic injection, the nucleotides of higher electrophoretic mobility were preferentially injected into the capillary. As a result, the sample zone was depleted from the lower mobility nucleotides, which compromised their apparent detectability and quantitative determination.

Detection was performed by means of an on-column UV-absorbance spectrophotometer (Model UVIDEC-100-V, Jasco, Tokyo, Japan), at a fixed wavelength of 260 nm. A detection window of 0.5 cm length was created by removing the polyimide coating from the capillary at a distance of 43.4 cm.

2.2 Capillary Surface Treatment

The conditioning of the capillary surface is critical to assure reproducibility f migration time measurements. In the series of studies presented in Table 2.1,

Tab

C_{Na}
AVE
R
1
AVER
RS

Table 2.1 Comparison of the reproducibility of electroosmotic flow measurements in sodium chloride solutions, using two capillary conditioning methods. The electroosmotic flow was determined under constant-voltage conditions of 30 kV in a capillary with 109.0 cm total length.

C_{NaCl} (mM)	MIGRATION TIME (min)	
	METHOD 1	METHOD 2
5	12.4 ± 0.3	7.9 ± 0.3
	10.7 ± 0.6	7.7 ± 0.4
	8.1 ± 0.3	8.1 ± 0.5
	9.3 ± 0.1	7.8 ± 0.3
	12 ± 1	8.1 ± 0.2
	12.1 ± 0.9	
AVERAGE	10.8 ± 1.7	7.9 ± 0.18
RSD	16 %	2.3 %
10	12.2 ± 0.9	8.13 ± 0.06
	11 ± 1	8.3 ± 0.3
	9.3 ± 0.1	8.3 ± 0.2
	9.2 ± 0.2	8.6 ± 0.1
	11 ± 2	
AVERAGE	10.5 ± 1.3	8.3 ± 0.20
RSD	12 %	2.4 %

the

con

infra

NaC

inve

mea

repro

capil

solut

Unde

and f

six m

condi

electr

perfo

hydro

standa

was c

and d

2.3 El

introdu

filled w

then re

the electroosmotic flow of sodium chloride solutions was measured under constant-voltage conditions by means of the resistance-monitoring method (*vide infra*). For the first conditioning method, the capillary was flushed with 0.1 M NaOH solution (10 capillary volumes) followed by the solution under investigation. Under these conditions, the electroosmotic flow could be measured in the same day with approximately ±10 % RSD and the day-to-day reproducibility was ±15 % RSD. For the second conditioning method, the capillary was washed with 1 M NaOH solution, followed by flushing with the solution under investigation, preferably overnight but at least for a 2-h period. Under these conditions, the single-day reproducibility was better than ±5 % RSD and the day-to-day reproducibility was better than ±3 % RSD, over a period of six months. Therefore, this method was selected as the standard procedure to condition the capillary surface. In the studies on the effect of cation type on electroosmotic flow (Chapter 3), an acid wash with 10^{-2} M hydrochloric acid was performed prior to the alkaline wash with a solution of the appropriate cation hydroxide. In all the studies involving phosphate buffers (Chapters 3 to 6), the standard conditioning procedure was performed only when the pH of the buffer was changed. When not in use, the capillary was rinsed with deionized water and dried under helium.

2.3 Electroosmotic Flow Determination

The electroosmotic flow was measured by a modification of the procedure introduced by Huang *et al.*[1] Initially, the capillary and the outlet reservoir are filled with an electrolyte solution of a certain concentration. The inlet reservoir is then replenished with a solution of the same composition but diluted by a factor

of

mig

cor

sup

be

ope

follo

prop

kV)

subs

Hew

pow

typic

conc

time

signa

moni

inflec

capill

the e

2.4 R

Electr

NaNO

predis

of 4% in volume. Under the applied electric field, the dilute solution continuously migrates into the capillary and displaces an equivalent volume of the more concentrated solution, thereby causing the resistance to change. If the power supply is operated in the constant-voltage mode, the changes in resistance can be followed by recording the changes in current. Conversely, if the instrument is operated in the constant-current mode, the changes in resistance can be followed by recording the changes in voltage. A 0 – 10 V DC signal, in direct proportion to either the output current (0 – 190 μA) or the output voltage (0 – 50 kV) is available at the remote terminal of the power supply. This signal is subsequently divided to 0 – 1 V and displayed on a recorder (Model 3392A, Hewlett-Packard Co., Avondale, PA). The voltage divider that interfaces the power supply remote terminal and the recorder is displayed in Figure 2.2. A typical output of the recorder is shown in Figure 2.3, under both operating conditions. Note that when the current is monitored, the signal decreases with time until the entire capillary is filled with the dilute solution, after which the signal becomes constant. Under the same conditions, when the voltage is monitored, the signal initially increases and then becomes constant. The inflection point represents the time (T) required to complete the filling of the capillary by electroosmosis. Thus, with knowledge of the capillary length (L_{tot}), the electroosmotic velocity can be calculated ($v_{osm} = L_{tot} / T$).

2.4 Reagents and Solutions

Electrolyte Solutions. All electrolyte solutions (LiCl, NaCl, KCl, NaBr, NaI, $NaNO_3$, and $NaClO_4$) were prepared from analytical-grade reagents and predistilled-deionized water (Corning Mega-Pure™ System, Corning, NY),

Figure 2.2 Voltage divider used to interface the power supply remote terminal and the recorder.

Figure 2.2

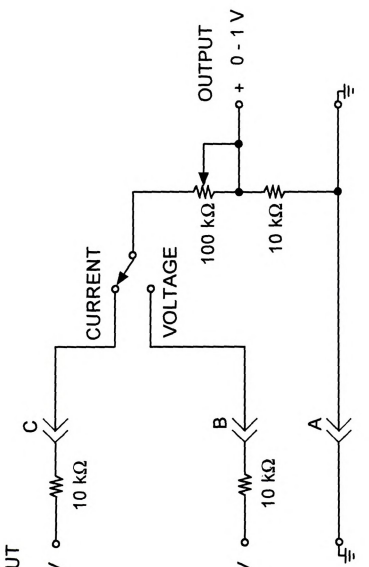
INPUT
0 - 10 V
10 kΩ
C
CURRENT
VOLTAGE
0 - 10 V
10 kΩ
B
100 kΩ
10 kΩ
A
OUTPUT
+ 0 - 1 V

Figure 2.3 Schematic of typical recorder outputs during the measurement of electroosmotic flow by the resistance-monitoring method. (A) Constant-current conditions of 9 μA; pH 7 phosphate buffer solution with 12.5 mM sodium concentration. (B) Constant-voltage conditions of 20 kV; 3 mM sodium chloride solution.

Figure 2.3

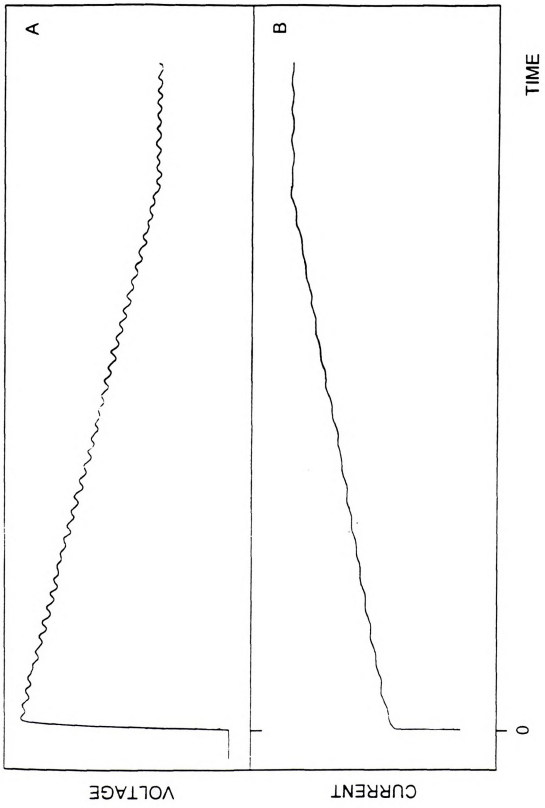

Figure 2.3 Schematic of typical recorder outputs during the measurement of electroosmotic flow by the resistance-monitoring method. (A) Constant-current conditions of 9 μA; pH 7 phosphate buffer solution with 12.5 mM sodium concentration. (B) Constant-voltage conditions of 20 kV; 3 mM sodium chloride solution.

Figure 2.3

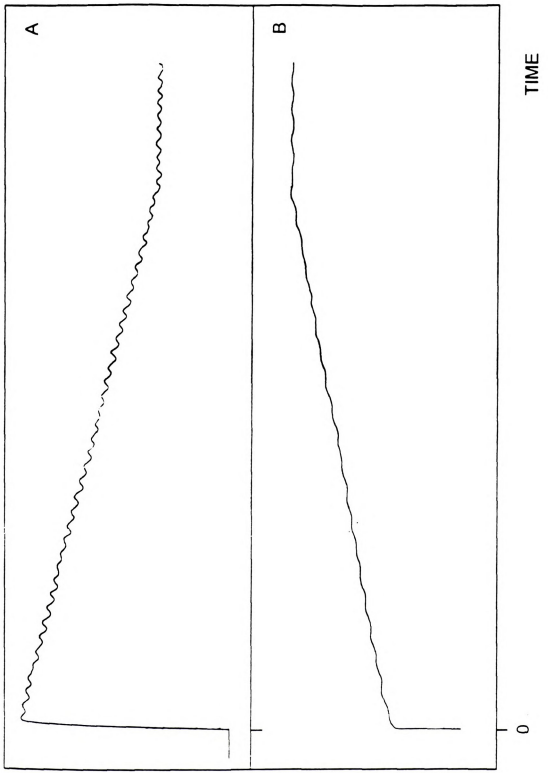

preadjusted to pH 9 with 0.1 M NaOH solution.

Phosphate Buffers. The phosphate buffer solutions were prepared from reagent-grade chemicals and predistilled-deionized water (Corning). The buffers were formulated to contain appropriate amounts of sodium chloride in addition to the sodium buffer salts and phosphoric acid. For the entire pH range from 4 to 11, the total concentration of sodium was maintained constant (5 – 15 mM) and the ratio of sodium from each source, sodium chloride and buffer salts, was equal to unity. Appendix 1 describes in greater detail the mathematical basis of the computer program for buffer preparation.

Nucleotides. The nucleotides adenosine, guanosine, cytidine and uridine 5'-mono and diphosphates (AMP, ADP, GMP, GDP, CMP, CDP, UMP and UDP) were obtained as reagent-grade chemicals (Sigma, St. Louis, MO). Stock aqueous solutions were prepared at 5 mM concentration. Analytical solutions of 0.1 mM concentration were prepared freshly as needed, by dilution of the stock solutions with phosphate buffer of the appropriate pH.

Tetracyclines. The antibiotics tetracycline (TC), chlortetracycline (CTC), demechlocycline (DMCC), oxytetracycline (OTC), doxycycline (DOC), methacycline (MTC) and minocycline (MNC) were obtained as reagent-grade chemicals (Sigma). Stock aqueous solutions were prepared at 25 mM nominal concentration. At this concentration, TC, CTC and OTC solutions were saturated. In order to provide a similar response from the UV-absorbance detector, decanted aliquots of the stock solutions, in the ratio 2 TC : 3 CTC : 1 DMCC : 2 OTC : 1 DOC : 1 MTC : 1 MNC, were diluted with the phosphate buffer solution of appropriate pH, to give approximately 5 mM standard solutions.

Individual tetrac
combinations of
calibration curv
consecutively to
the dissolution o
to prevent losses

Pharmace
and Warner Ch
obtained as harc
drug was dissolv
nominal concent
removed by cer
supernatant solu
phosphate buffer

A common
is the control of t
order to study the
by complete disso
acid at pH 2. Th
period, the sampl
pH 7.5 phosphate

2.5 Physical Mea

The absolu
measurements of

Individual tetracycline standards and also mixtures containing different combinations of the standards were prepared by the above procedure. For the calibration curve, a 1 mM standard solution of tetracycline was diluted consecutively to 0.5, 0.1, 0.05, and 0.01 mM with the same buffer employed in the dissolution of the standard solution (pH 7.5), and was analysed immediately to prevent losses by adsorption on the glassware.[2]

Pharmaceutical drugs, manufactured by Rugby (methacycline 500 mg) and Warner Chilcott (tetracycline 250 mg and doxycycline 100 mg), were obtained as hard-filled capsules. An appropriate weight of the pharmaceutical drug was dissolved in pH 7.5 phosphate buffer to make a solution of 25 mM nominal concentration. The undissolved filler and binder materials were removed by centrifugation for approximately 15 min. An aliquot of the supernatant solution was then diluted to 5 mM concentration with pH 7.5 phosphate buffer solution and analysed immediately.

A common concern in the manufacture industry of tetracycline antibiotics is the control of toxic impurities that result from decomposition during storage. In order to study the decomposition of tetracycline, a 25 mM solution was prepared by complete dissolution of an appropriate weight of the standard in hydrochloric acid at pH 2. This sample was submitted to heating at 70°C for 1 h. After this period, the sample was cooled in an ice bath, diluted to 5 mM concentration with pH 7.5 phosphate buffer solution and analysed immediately.

2.5 Physical Measurements

The absolute viscosity of sodium chloride solutions was determined by measurements of kinematic viscosity and density.[3] The kinematic viscosity

measurements v

25). The dens

constant absolut

for all solutions i

The diele

heterodyne-beat

Wiss. - Tech. -

frequency of a cr

in a mixer resulti

composed of a fi

precision air cap

as detector, with

ray tube and the

Lissajous figure

capacitance can

air capacitor that

with the dielectri

standard liquids

accurate measur

capacitance (few

method. Howeve

solutions of high

of the sodium cl

greater than 0.1

techniques for

appropriate, but th

± 1 at 25° C was

measurements were performed in a Cannon-Ubbelhode viscometer (ASTM size 25). The density measurements utilized standard 10 mL pycnometers. A constant absolute viscosity value of 0.8755 ± 0.0017 cP at 25° C was obtained for all solutions in the concentration range from 1 to 10 mM.

The dielectric constant of sodium chloride solutions was evaluated by the heterodyne-beat method[3,4] using a beat-frequency oscillator (Model DM01, Wiss. - Tech. - Werkstatten, Weilheim Obb., Germany). In this method, the frequency of a crystal-controlled oscillator and a variable oscillator are combined in a mixer resulting in a beat-frequency output signal. The variable oscillator is composed of a fixed inductor and several capacitors including the cell, a variable precision air capacitor, etc, combined in parallel. An oscilloscope can be used as detector, with the beat-frequency applied to the vertical plates of the cathode-ray tube and the 60-Hz line frequency applied to the horizontal plates. A simple Lissajous figure serves as the indicator of balance. Changes in the cell capacitance can be determined by noting the changes in the variable precision air capacitor that are needed to restore balance. These readings are associated with the dielectric constant by means of a calibration curve, determined using standard liquids of known dielectric constant. For solutions of low conductance, accurate measurements of beat-frequency (less than 1 Hz) or changes in capacitance (few parts per million) can be performed by the beat-frequency method. However, due to inherent limitations of this method when applied to solutions of high electrical conductance, the determination of dielectric constant of the sodium chloride solutions could not be performed at concentrations greater than 0.1 mM. For such solutions, resonance methods and bridge techniques for measuring capacitive reactance[3] would have been more appropriate, but this instrumentation was not available. A constant value of 78.5 ± 1 at 25° C was obtained for all sodium chloride solutions in the concentration

range from 0.00

2.6 Data Proce

All data p

386 microproces

version 4.0, Mic

and the optimiz

language Asyst (

80-286 micropro

The buffe

required to pr

thermodynamic

buffer species.

constant ionic st

capacity. This p

incorporates ioni

Davies equation.

magnitude of the

The optimi

Chapter 4, inclu

phosphate buffers

buffer concentrati

buffer formulation

prepare the buffe

separation of the

range from 0.001 to 0.1 mM.

2.6 Data Processing

All data processing and numerical calculations were performed on a 80-386 microprocessor-based computer in a spreadsheet format (Microsoft Excel, version 4.0, Microsoft Corp., Redmond, WA). The buffer formulation program and the optimization program were written in the Forth-based programming language Asyst (version 2.1, Keithley Asyst, Rochester, NY) to be executed on a 80-286 microprocessor-based computer.

The buffer formulation program (Appendix 1) performs the calculations required to prepare phosphate buffers at a specified pH, given the thermodynamic dissociation constants[5] and the ionic charge of the individual buffer species. Options are available to prepare buffers under conditions of constant ionic strength, constant buffer concentration, and/or constant buffer capacity. This program is based on classical equilibrium calculations,[6-8] and incorporates ionic strength corrections that are valid up to 0.5 M by means of the Davies equation.[7] No simplifying assumptions are made regarding the relative magnitude of the equilibrium concentration of the buffer species.

The optimization program (Appendix 2), which is described in detail in Chapter 4, includes a buffer calculation subroutine. In this subroutine, phosphate buffers are formulated with both constant ionic strength and constant buffer concentration, which requires the addition of an inert electrolyte. The buffer formulation subroutine provides the analytical concentrations necessary to prepare the buffer solution correspondent to the optimal conditions for the separation of the solutes under investigation.

2.7 References

1. Huang, X

2. Ciarlone,
255.

3. Weissber
Interscier

4. Shoemak
Physical

5. Hirokawa,

6. Butler, J.
Wesley P

7. Lambert,

8. Rilbe, H.

2.7 References

1. Huang, X.; Gordon, M. J.; Zare, R. N. *Anal. Chem.* **1988**, *60*, 1837-1838.
2. Ciarlone, A. E.; Fry, B. W.; Ziemer, D. M. *Microchem. J.* **1990**, *42*, 250-255.
3. Weissberger, A. *Physical Methods of Organic Chemistry*, 3rd ed.; Interscience Publishers Inc.: New York, 1959.
4. Shoemaker, D. P.; Garland, C. W. and Steinfeld, J. I. *Experiments in Physical Chemistry*; McGraw-Hill: New York, 1989.
5. Hirokawa, T.; Kobayashi, S.; Kiso, Y. *J. Chromatogr.* **1985**, *318*, 195-210.
6. Butler, J. N. *Ionic Equilibrium - A Mathematical Approach*; Addison-Wesley Publishing Company, Inc.: Massachusetts, 1964.
7. Lambert, W. J. *J. Chem. Ed.* **1990**, *67*, 150-153.
8. Rilbe, H. *Electrophoresis* **1992**, *13*, 811-816.

THEORI

3.1 Introductio

Over the
emerged as a v
biomolecules.
resolving power
detection schem
technological de
has been direct
routine applicati
characterization
fundamental stu
nature of the sep

In capillar
buffering proper
influence of a ta
occur.[1,4,5] The
migrate with a c
size, and shape.
as a bulk is in
electroosmosis,

CHAPTER 3

THEORETICAL MODEL OF ELECTROOSMOTIC FLOW

3.1 Introduction

Over the past ten years, capillary zone electrophoresis (CZE) has emerged as a very resourceful alternative method for the separation of charged biomolecules. Relevant aspects of the technique such as high efficiency, high resolving power, high speed, full automation, and a variety of injection and detection schemes have been extensively investigated.[1] In addition to these technological developments, much research in capillary zone electrophoresis has been directed towards demonstrating the versatility of the technique for routine applications.[2,3] However, despite the past considerable effort on the characterization of the electrokinetic phenomena,[4,5] there is still a scarcity of fundamental studies to provide greater understanding of the physicochemical nature of the separation process at the capillary surface and in solution.

In capillary zone electrophoresis, a background electrolyte with adequate buffering properties forms a continuum along the migration path. Under the influence of a tangentially applied electric field, two mechanisms of migration occur.[1,4,5] The field exerts an electric force on charged molecules, which migrate with a constant velocity that is characteristic of the molecular charge, size, and shape. Concomitant to the electrophoretic migration, a flow of solution as a bulk is induced by the electric field. This migration, regarded as electroosmosis, is dependent on the characteristics of the capillary surface as

well as the com

The exi

contributed sig

allowing for on

analysis of cati

has a substant

However, beca

introduces no b

molecules, rega

efficiency benef

compromised.

The und

implications in

several strateg

electroosmotic f

and physical pro

concentration, a

an inert electrol

viscosity, dielec

demonstrated.

electroosmotic f

capillary materia

and teflon capill

capillaries, the r

coating and chem

application of an

well as the composition of the conducting medium.

The existence of electroosmotic flow in fused-silica capillaries has contributed significantly to the full automation of capillary electrophoresis, allowing for on-line sample injection and detection as well as for simultaneous analysis of cations and anions in favorable cases.[1-3] The electroosmotic flow has a substantial influence on the time the analytes reside in the capillary. However, because of the flat velocity profile, electroosmotic flow theoretically introduces no broadening. The same velocity component is added to all solute molecules, regardless of their radial position. Consequently, analysis time and efficiency benefit from a rapid electroosmotic flow, although resolution may be compromised.

The understanding and control of electroosmotic flow have critical implications in the design of electrophoretic separations. In recent years, several strategies have been developed to exert proper control of the electroosmotic flow. Perhaps the most effective means is to alter the chemical and physical properties of the buffer solution. In this context, changes in the pH, concentration, and ionic strength of the buffer,[6,7] the type and concentration of an inert electrolyte or organic additive,[8-11] as well as changes in the solvent viscosity, dielectric constant,[12] and temperature[13] have all been successfully demonstrated. Another simple approach to alter or ultimately inhibit the electroosmotic flow consists of changing the chemical composition of the capillary material and, hence, the surface charge density. Fused-silica, glass, and teflon capillaries have been employed for this purpose.[14] In fused-silica capillaries, the nature of the capillary wall can be further modified by physical coating and chemical derivatization methods.[15-17] Other strategies, such as the application of an external electric field across the capillary wall, can also be

used to influen

At the p

been achieved

and chemical

parameters rel

resulting equati

computationally

practical means

In this

capillaries is e

physically mear

surface to chan

ion-selective ele

both constant-v

is confirmed usi

a controlled con

3.2 Theory

Ion-Selective M

have been explo

Among the man

one of the mos

membrane seale

solution and an

used to influence the electroosmotic flow.[18,19]

At the present time, mathematical modelling of electroosmotic flow has been achieved by solution of the fundamental laws describing mass transport and chemical equilibria.[20,21] Other approaches rely on the estimation of parameters related to the electrical double layer.[22] In most instances, the resulting equations are not trivial and their solution can only be approached by computationally intensive numerical methods. Therefore, a simpler and more practical means of describing the migration process is highly desirable.

In this work, the nature of electroosmotic migration in fused-silica capillaries is examined from a theoretical and experimental perspective. A physically meaningful model is proposed, where the response of the capillary surface to changes in buffer composition and pH is treated as an analogy to an ion-selective electrode. The prediction of electroosmotic flow is evaluated under both constant-voltage and constant-current conditions. The validity of the model is confirmed using phosphate buffer solutions in the pH range from 4 to 10, with a controlled concentration of sodium ions.

3.2 Theory

Ion-Selective Membranes. The ion-selective properties of glass membranes have been exploited for the construction of a variety of chemical sensors.[23-25] Among the many representative examples, the pH-sensing glass electrode is one of the most common. A typical pH electrode consists of a thin glass membrane sealed at the end of a tube containing an appropriate standard solution and an internal reference electrode. During the measurements, the

complete asse
registered with
of the glass me
solution is show

Many of
membranes are
glasses are co
oxygen atoms
structure are o
attraction to the
are strongly hel
the glass. How
lattice, are prim
membrane.

Exposure
layer. At the o
charged sites a
layer, there is a
increase in the
are occupied ex

The exch
solution is res
characteristic of
cation in the me

$H^+(glass) + Na$

complete assembly is immersed into a test solution and the potential is registered with respect to an external reference electrode. A schematic diagram of the glass membrane in contact with the internal reference solution and the test solution is shown in the top part of Figure 3.1.

Many of the properties that confer selectivity and sensitivity to such membranes are associated with the chemical structure of the glass.[24] Silicate glasses are composed of an irregular three-dimensional network of silicon and oxygen atoms with nominal composition $(SiO_2)_x$. The holes or defects in this structure are occupied by cations, held more or less strongly by electrostatic attraction to the neighboring oxygen atoms. Doubly and triply charged cations are strongly held and do not contribute to the electrical conduction properties of the glass. However, singly charged cations, which are quite mobile within the lattice, are primarily responsible for charge transport in the interior of the glass membrane.

Exposure of the glass to water causes the formation of a hydrated gel layer. At the outer edge of this layer in contact with the solution, the singly charged sites are predominantly occupied by hydrogen ions. Within the gel layer, there is a continuous decrease of the number of hydrogen ions and an increase in the number of other cations. In the interior of the glass, such sites are occupied exclusively by cations.

The exchange of cations in the hydrated gel layer with cations in the solution is responsible for the pH response and alkaline error that are characteristic of glass membranes. If sodium is considered to be the only active cation in the membrane, the ion-exchange reaction can be written as:

$$H^+(glass) + Na^+(soln) \leftrightarrow H^+(soln) + Na^+(glass) \qquad [3.1]$$

Figure 3.1 Schematic diagram of an ion-selective glass membrane (top) and the electrical double-layer structure at silica surfaces (bottom).

Figure 3.1

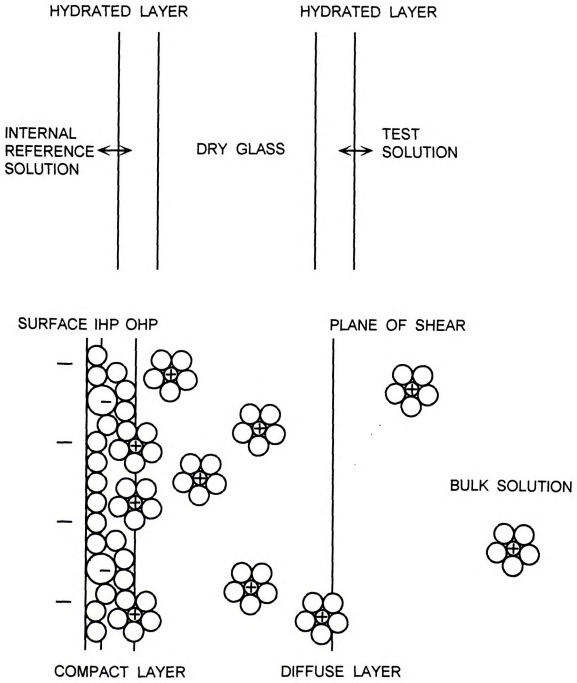
HYDRATED LAYER
HYDRATED LAYER
INTERNAL REFERENCE SOLUTION
DRY GLASS
TEST SOLUTION
SURFACE IHP OHP
PLANE OF SHEAR
BULK SOLUTION
COMPACT LAYER
DIFFUSE LAYER

with the associa

$$K = \frac{a_H\,(sol}{a_H\,(gla}$$

where a_H and
respectively, in
The equilibriu
incorporation of
contact with the

When a
reference soluti
This boundary p
the contribution

$$E_b = E' + \frac{2.3}{}$$

where T is the a
and F is the Fa
the boundary po
solution, as well
Equation [3.3] s
sodium ions in th
magnitude of kP
of the determin
values that rang

with the associated equilibrium constant:

$$K = \frac{a_H\,(soln)\;\; a_{Na}\,(glass)}{a_H\,(glass)\;\; a_{Na}\,(soln)} \qquad [3.2]$$

where a_H and a_{Na} represent the activities of hydrogen and sodium ions, respectively, in solution (soln) and in the interior of the glass membrane (glass). The equilibrium constant for this reaction is quite small, favoring the incorporation of hydrogen rather than sodium ions into the silicate lattice in close contact with the solution.[26]

When a difference in pH exists between the test and the internal reference solutions, a boundary potential develops across the glass membrane. This boundary potential (E_b) is given by the Nernst equation, modified to include the contribution of the sodium ions to the pH response:[23]

$$E_b = E' + \frac{2.303\;R\;T}{z\;F}\;\log\;[\,a_H\,(soln) + k^{POT}\,a_{Na}\,(soln)] \qquad [3.3]$$

where T is the absolute temperature, z is the ionic charge, R is the gas constant and F is the Faraday constant. The constant term (E') includes contributions to the boundary potential from hydrogen and sodium ions in the internal reference solution, as well as the reference electrode, junction, and asymmetry potentials. Equation [3.3] shows that the membrane is responsive to both hydrogen and sodium ions in the test solution, where the degree of selectivity is dictated by the magnitude of k^{POT}. The quantity k^{POT} is defined as the potentiometric constant of the determinand H^+ with respect to the interferent Na^+ and may assume values that range from zero (no interference) to greater than unity, depending

upon the compo

comprised of th

exchange equilib

$$k^{POT} = K \frac{\mu_{Na}}{\mu_H}$$

Equation [3.3] lea

response. If the

the membrane is

selective glass e

surpasses a_H, the

sodium-selective g

Electrical double

presence of sever

character.[27] In co

ionized and cause

homogeneous spa

immediate proximit

Much theoretical

between the surfac

concentration profi

accepted features

bottom part of Figur

The region

oriented water mole

upon the composition of the membrane.[24,25] The potentiometric constant is comprised of the ratio of ionic mobilities (μ) in the membrane as well the exchange equilibrium constant defined by Equation [3.2]:

$$k^{POT} = K \frac{\mu_{Na}\,(glass)}{\mu_{H}\,(glass)} \qquad [3.4]$$

Equation [3.3] leads to interesting predictions concerning the glass membrane response. If the product of k^{POT} and a_{Na} is sufficiently small compared to a_H, the membrane is primarily responsive to hydrogen ions, constituting a pH-selective glass electrode. Conversely, when the product of k^{POT} and a_{Na} surpasses a_H, the membrane responds primarily to sodium ions, constituting a sodium-selective glass electrode.

Electrical double-layer structure. Silica surfaces are characterized by the presence of several types of silanol groups (SiOH), which are weakly acidic in character.[27] In contact with an aqueous medium, some of the silanol groups are ionized and cause the surface to be negatively charged.[28] As a result, a non-homogeneous spatial distribution of charge originates within the solution in immediate proximity to the surface, designated as the electrical double layer. Much theoretical work has been concerned with describing the interface between the surface and the solution, including evaluation of the potential and concentration profiles as a function of distance.[4,5,23] Some of the presently accepted features of the electrical double-layer structure are illustrated in the bottom part of Figure 3.1.

The region adjacent to the surface is occupied by layers of strongly oriented water molecules and some ions, presumably dehydrated, tightly held to

the surface by

center of these

Hydrated ions

hydration radiu

surface is inde

The plane defi

Helmholtz plan

double layer.

motion, some c

surface increa

approaches the

double layer.

When an

forces act upon

a unilateral mo

During their mig

inducing the ov

differences in th

layer, a velocity

increases inside

certain, very sm

solution migrate

portion of the

characterized a

shear is known

important impl

the surface by electrostatic and other cohesive forces (specific adsorption). The center of these ions defines a plane known as the inner Helmholtz plane (IHP). Hydrated ions approach the surface by a distance corresponding to their hydration radius. These ions are loosely bound and their interaction with the surface is independent of their chemical properties (non-specific adsorption). The plane defined by the center of the hydrated ions is known as the outer Helmholtz plane (OHP), or Stern layer, and delimits the compact region of the double layer. Due to the finite temperature and associated random thermal motion, some of the ions diffuse farther into solution. As the distance from the surface increases, the counterion concentration decreases and ultimately approaches the bulk value. This region is referred to as the diffuse part of the double layer.

When an electric field is imposed tangentially to the surface, the electrical forces act upon the spatial distribution of charge within the diffuse layer, causing a unilateral movement of ions towards the oppositely charged electrode.[4,5] During their migration, these ions transport the surrounding solvent molecules, inducing the overall movement of solution known as electroosmotic flow. Due to differences in the magnitude of electrical and frictional forces within the double layer, a velocity gradient originates. The flow velocity is zero at the surface, increases inside the double-layer region and reaches a maximum value at a certain, very small distance from the charged surface. The remainder of the solution migrates with this maximum velocity. The location at which the mobile portion of the diffuse layer can slip or flow past the charged surface is characterized as the plane of shear. The potential developed at the plane of shear is known as the electrokinetic or zeta potential. Its magnitude has important implications on the development and characterization of

electroosmotic

The pot

Poisson-Boltzr

sufficiently lo

approximated

$$\Psi = \Psi_0 \exp$$

One of the mo

the parameter

dimensions:

$$\chi^2 = \frac{1000}{\varepsilon}$$

where z_i is the

constant of the

is Boltzmann's

known as the D

double layer.

Analogy betwe

Silica Surface

behavioral anal

structure at the

analogy to the

compact region

electroosmotic flow (*vide infra*).

The potential distribution in the double layer can be derived by solving the Poisson-Boltzmann equation for limiting cases. If the surface potential (Ψ_0) is sufficiently low (< 50 mV), the potential profile with distance (x) can be approximated by the Debye-Huckel theory:[4,23]

$$\Psi = \Psi_0 \exp(-\kappa x) \qquad [3.5]$$

One of the most important quantities to emerge from the Debye-Huckel theory is the parameter κ, which correlates properties of the solution with the double-layer dimensions:

$$\kappa^2 = \frac{1000\, e^2\, N_A}{\varepsilon\, k\, T} \sum z_i^2\, M_i \qquad [3.6]$$

where z_i is the charge and M_i is the molarity of the i^{th} ion, ε is the dielectric constant of the medium, e is the elemental charge, N_A is Avogadro's number, k is Boltzmann's constant, and T is the absolute temperature. The quantity κ^{-1}, known as the Debye length, is often used to characterize the thickness of the double layer.

Analogy between Ion-Selective Membranes and Double-Layer Structure at Silica Surfaces. The proposed model for electroosmotic flow is based on behavioral analogies between an ion-selective membrane and the double-layer structure at the fused-silica capillary surface, as illustrated in Figure 3.1. In analogy to the internal reference solution of a pH-sensing glass electrode, the compact region of the double layer is modelled as a reference layer for the bulk

solution. Th
extent of ioni
the ionic cha
within the con
the plane of
mobile parts
sodium ions
potential, is re
a mechanism
membranes.
manipulate el
choice of pH
concentration

3.3 Results a

The cha
effect of a giv
proper selectio
extremely impo
most commonly
of pH on the ex
the complexity
can be formula
as pH, from o

solution. The establishment of the compact layer is dictated primarily by the extent of ionization of the silica surface, which is affected by the pH but not by the ionic character and content of the bulk solution. Therefore, the potential within the compact layer responds only to changes in pH of the bulk solution. At the plane of shear, which is a physical boundary between the immobile and mobile parts of the solution, an exchange equilibrium between hydrogen and sodium ions occurs. Therefore, the potential at the plane of shear, the zeta potential, is responsive to both hydrogen and sodium ions in the bulk solution, in a mechanism analogous to that which accounts for the alkaline error in glass membranes. The proposed model thus comprises two fundamental ways to manipulate electroosmotic flow in capillary zone electrophoresis: the judicious choice of pH (a coarse adjustment) and the selection of an appropriate sodium concentration (a fine adjustment).

3.3 Results and Discussion

The characterization of electroosmotic flow depends on how distinctly the effect of a given variable can be isolated from others. For this reason, the proper selection of the conducting medium and the control of its composition is extremely important. Conducting media with buffering properties are among the most commonly used in capillary zone electrophoresis because of the dual effect of pH on the extent of ionization of the solutes and the silanol groups. However, the complexity of buffer systems and the diversity with which a buffer solution can be formulated make it difficult to isolate the effect of a single variable, such as pH, from other changes that may occur concomitantly when pH is varied,

such as ionic

Therefore, in

system seem

studies were

later studies,

system and

magnitude un

The ex

and accuracy

accepted[7,12,2

manner in whi

systematic pro

day with appr

± 20 % RSD (

described prev

and the day-to

six months.

The reli

the method se

most common

the weighing

large range of

conducting m

modifications o

method to both

the direct co

such as ionic strength, buffer concentration and capacity, cation and anion type. Therefore, in order to characterize the electroosmotic flow, a simpler electrolyte system seems to be a more appropriate choice. In this work, the preliminary studies were performed using solutions of singly-charged, strong electrolytes. In later studies, the electroosmotic flow was characterized in the phosphate buffer system and a comprehensive model was developed to predict the flow magnitude under a variety of operational conditions.

The experimental validation of the proposed model relies on the precision and accuracy with which the electroosmotic flow can be determined. It is well accepted[7,12,29,30] that the electroosmotic flow is strongly dependent on the manner in which the capillary surface has been conditioned. In the absence of a systematic procedure, the electroosmotic flow could be measured in the same day with approximately ± 10 % RSD and the day-to-day reproducibility was ± 20 % RSD (*vide* Chapter 2). By conditioning properly the capillary surface, as described previously, the single-day reproducibility was better than ± 1 % RSD and the day-to-day reproducibility was better than ± 3 % RSD, over a period of six months.

The reliability of the model for the electroosmotic flow also depends on the method selected to evalute the flow magnitude. In this work, several of the most common methods were compared, including the neutral-marker method,[14] the weighing procedure,[31] and the resistance-monitoring method.[32] When a large range of pH was inspected, the monitoring of resistance changes in the conducting medium was found to be the most reliable method. The modifications described in Chapter 2 extend the use of the resistance-monitoring method to both constant-voltage and constant-current conditions. This enables the direct comparison of results obtained under both conditions for the

development a

Preliminary

Conditions.

electroosmotic

equation,[4,5] w

(E) according

$$v_{osm} = -\frac{\varepsilon}{}$$

where V is t

proportionality

comprised of

viscosity (η)

potential (ζ).

the capillary (r

[3.6]), or when

theoretical deri

structure of the

implied, howev

are applicable

velocity and el

zeta potential is

Accordin

between the el

when the veloc

development and evaluation of the proposed model of electroosmotic flow.

Preliminary Studies of Electroosmotic Flow under Constant-Voltage Conditions. In the constant-voltage operation of the power supply, the electroosmotic flow is evaluated by means of the Helmholtz-Smoluchowski equation,[4,5] which relates the linear velocity (v_{osm}) and the electric field strength (E) according to:

$$v_{osm} = -\frac{\varepsilon\ \varepsilon_0\ \zeta}{\eta} E = \mu_{osm} \frac{V}{L} \qquad [3.7]$$

where V is the applied voltage and L is the total capillary length. The proportionality term, which represents the electroosmotic mobility (μ_{osm}), is comprised of several constants such as the dielectric constant (ε) and the viscosity (η) of the medium, the permittivity of a vacuum (ε_0), and the zeta potential (ζ). The Helmholtz-Smoluchowski equation is valid when the radius of the capillary (r) is large compared to the double-layer thickness (κ^{-1}, Equation [3.6]), or when the product (κ r) is much larger than one hundred. In the theoretical derivation of Equation [3.7], no assumptions are made regarding the structure of the double layer except for the existence of a plane of shear. It is implied, however, that the dielectric constant and viscosity of the bulk solution are applicable within the double layer. It is interesting to note that when the velocity and electric field vectors are in the same direction, a negative value for zeta potential is required.

According to the Helmholtz-Smoluchowski equation, a linear relationship between the electroosmotic velocity and field strength is expected. However, when the velocity is displayed as a function of the applied voltage (Figure 3.2),

Figure 3.2 Dependence of electroosmotic velocity on the applied voltage for aqueous sodium chloride solutions of concentration (△) 1 mM, (○) 2 mM, (□) 3 mM, (▽) 4 mM.

Figure 3.2

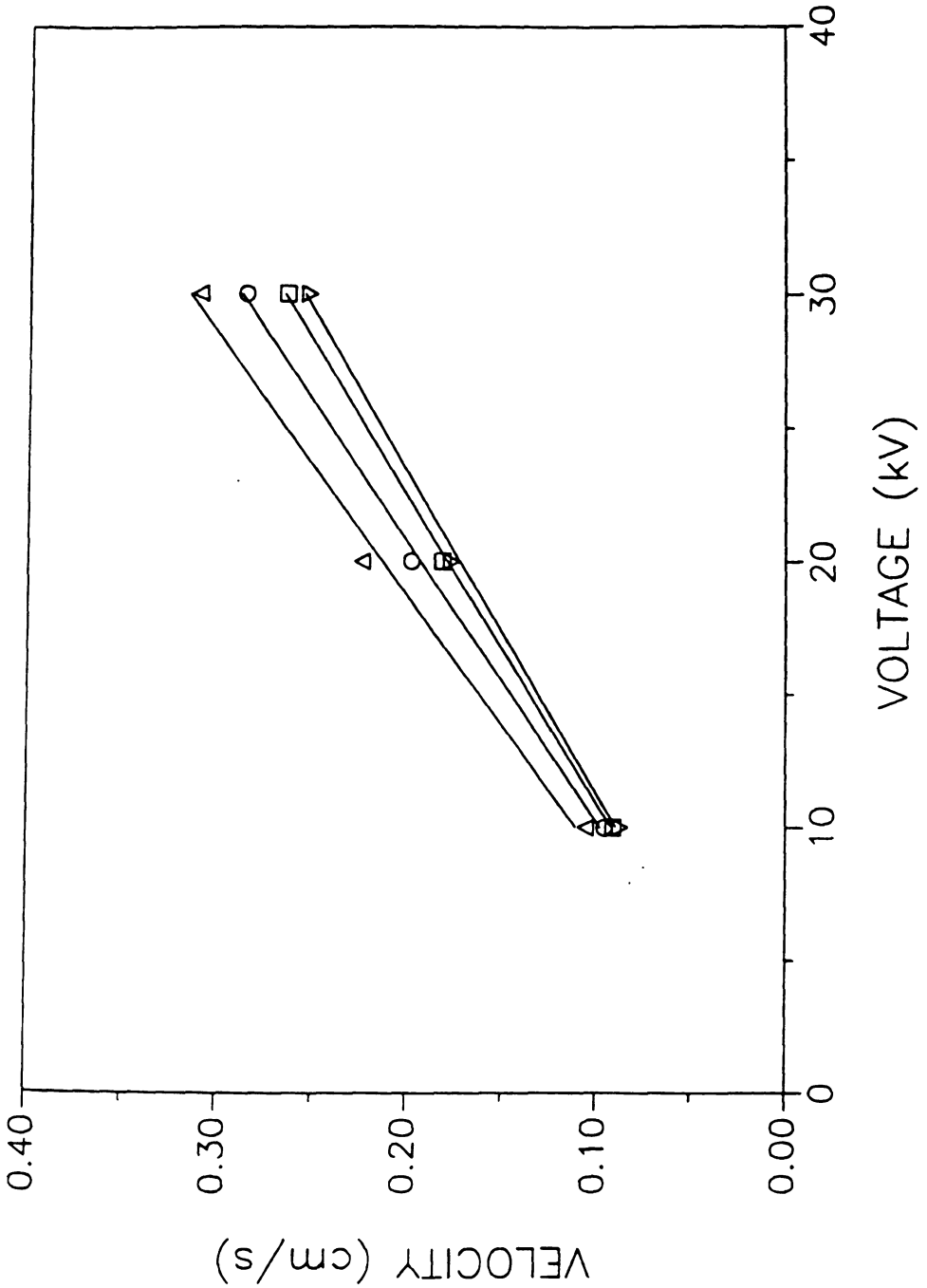

ed voltage for
n (Δ) 1 mM,

the slope sh
aqueous solu
of concentrati
equation. In c
results are p
properties of
be dependen
concentration
be fairly cons
was calculate
electroosmotic
measured valu
the zeta poten
and the surfa
marked depen
results identif
development c
responds to
dependence o
characterizes a

With the
capillary surfa
electrolyte syst
magnitude of t
potassium chlo
varied linearly

the slope shows a dependence on the concentration of sodium chloride in aqueous solutions. Therefore, it is important to examine in more detail the effect of concentration on each constant in the slope of the Helmholtz-Smoluchowski equation. In order to accommodate the large range of concentration studied, the results are plotted in a semi-logarithmic manner in Figure 3.3. As intrinsic properties of the solution, the dielectric constant and viscosity are expected to be dependent on the solution composition.[33] However, within the range of concentration studied, both the dielectric constant and the viscosity are shown to be fairly constant and approach the values for pure water. The zeta potential was calculated from Equation [3.7], where the slope of the graph of electroosmotic velocity *versus* applied voltage was used, together with the measured values of viscosity and dielectric constant. As an interface potential, the zeta potential is expected to be influenced by both the solution composition and the surface characteristics as well. Indeed, the zeta potential shows a marked dependence on the concentration of the solution in Figure 3.3. These results identify the zeta potential as the most significant parameter in the development of electroosmotic flow and the mechanism by which the surface responds to changes in the electrolyte composition. Furthermore, the dependence of the zeta potential on the logarithm of the sodium concentration characterizes an ion-selective type of response.

With the intent of exploring in more detail the ion-selective behavior of the capillary surface, the zeta potential was determined in other singly charged electrolyte systems. Figure 3.4 presents the influence of the cation type on the magnitude of the zeta potential for aqueous solutions of lithium, sodium, and potassium chloride. Within the range of concentration studied, the zeta potential varied linearly with the logarithm of the cation concentration, which verifies that

Figure 3.3 Evaluation of dielectric constant, viscosity, and zeta potential of aqueous sodium chloride solutions at pH 9. The zeta potential was evaluated under constant-voltage conditions at (△) 10 kV, (○) 20 kV, (□) 30 kV.

Figure 3.3

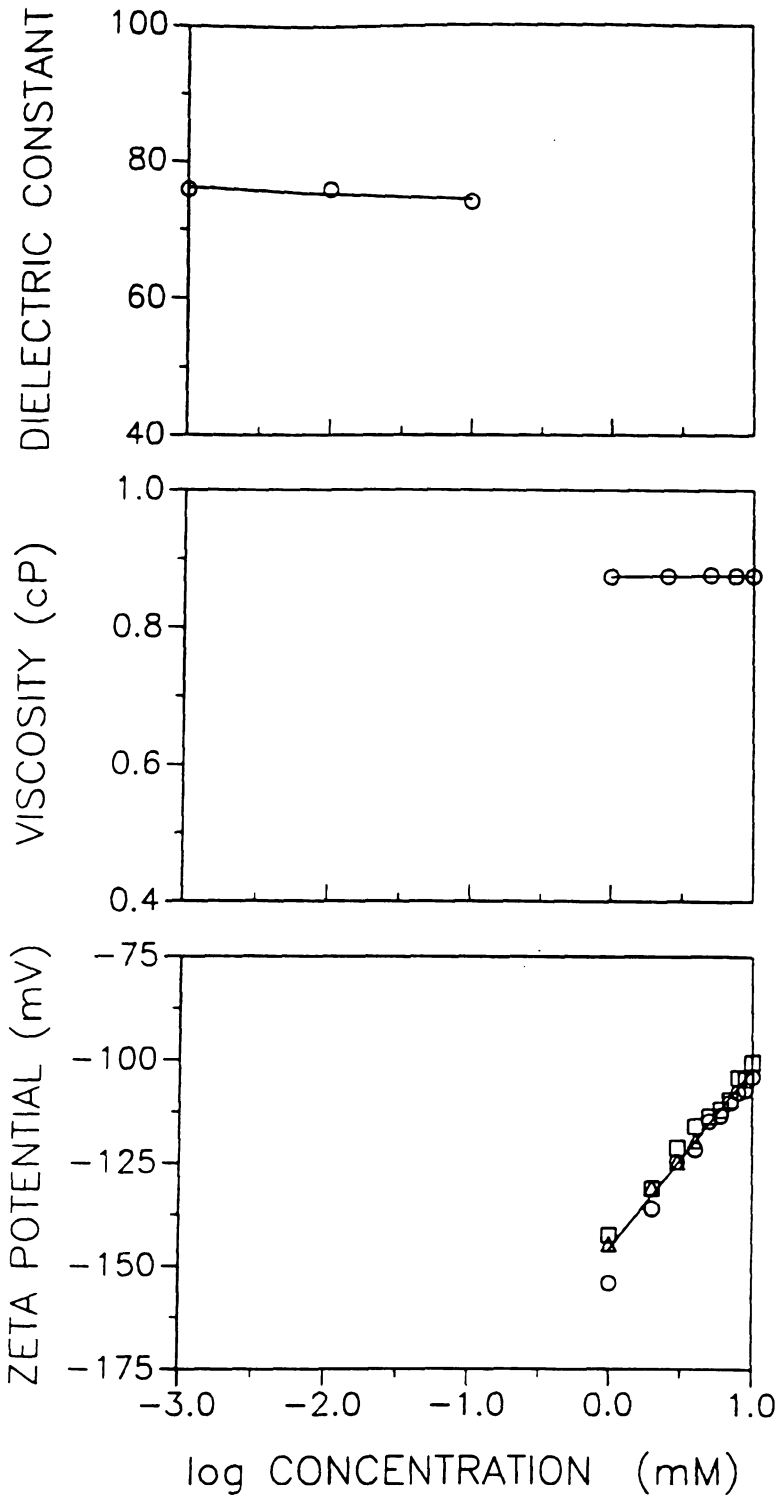

a potential of
potential was
10 kV, (O)

Figure 3.4 Effect of cation type on the magnitude of the zeta potential under constant-voltage conditions at 20 kV. Aqueous solutions at pH 9 of (△) LiCl,(□) KCl, (○) NaCl.

Figure 3.4

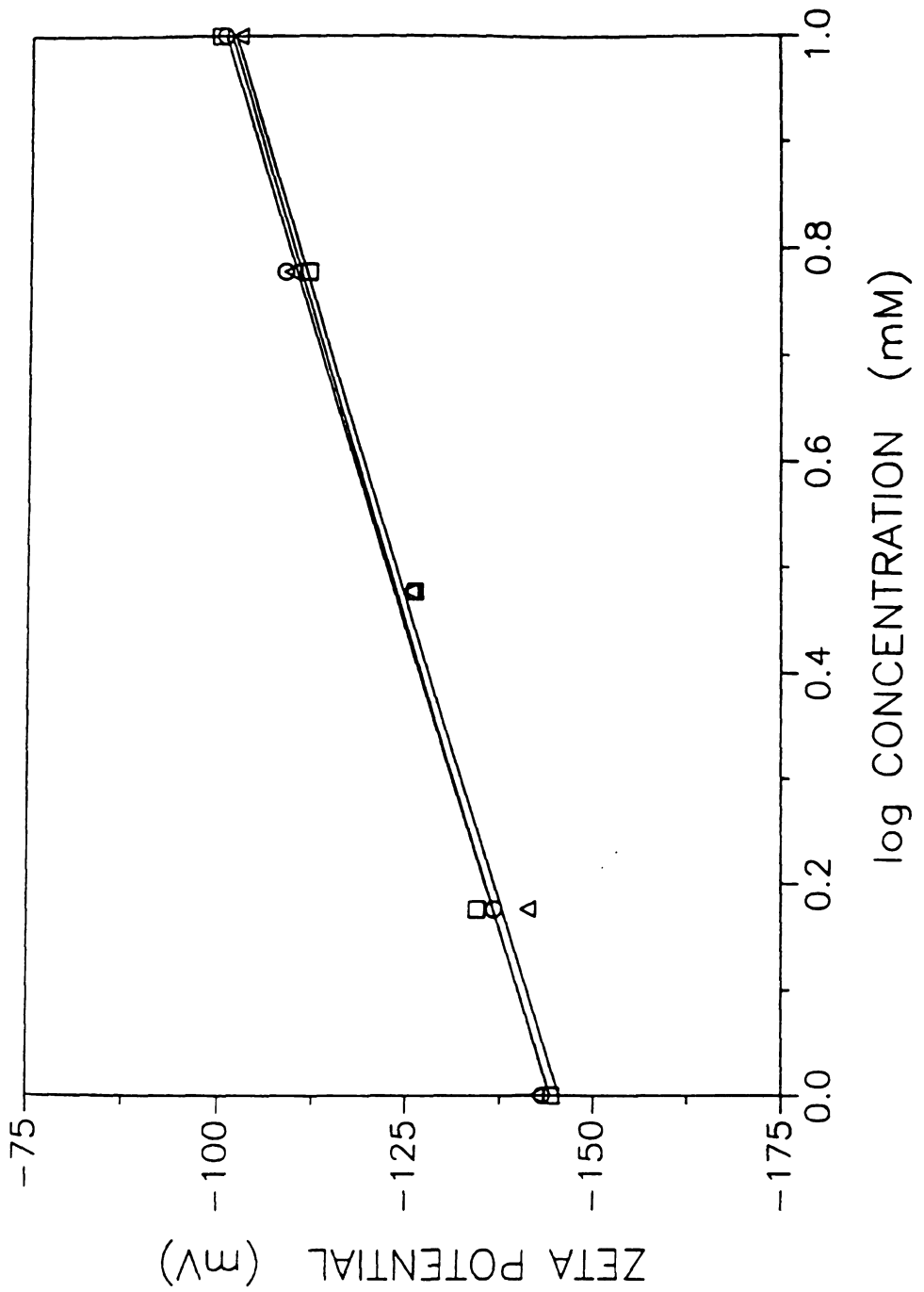

tential under
ns at pH 9 of

the capillary
at any given
of the zeta p
not distingu
These result
the complete
This conclus
radiometric
ions only in
studies in c
from those re
increased w
observed th
conditioning
altered. An a
of the diffuse
cation during
composition
the reliability

Figure
the zeta pot
nitrate, and p
particularly in
is involved, i
The exact or
correlation o

the capillary surface responds to each cation in a Nernstian fashion. However, at any given concentration, no statistically significant variation in the magnitude of the zeta potential was observed. This behavior implies that the surface does not distinguish between cation types, regardless of their chemical diversity. These results preclude the possibility of specific adsorption and, in fact, suggest the complete absence of cations other than hydrogen ion in the compact layer. This conclusion is supported by the previous work of Li and Bruyn,[34] where radiometric measurements at quartz surfaces revealed the presence of sodium ions only in the diffuse region of the double layer. However, several recent studies in capillary zone electrophoresis have reached conclusions different from those reported here. Salomon *et al.*[22] reported that electroosmotic velocity increased with the hydrated radius of the cation, whereas Atamna *et al.*[8] observed the opposite behavior. Based on our experience, the method of conditioning the capillary surface is particularly important when the cation type is altered. An acid wash is necessary to remove the cations in the immobile region of the diffuse layer, so that they can be replaced completely with the appropriate cation during the alkaline wash. In the absence of this treatment, a mixed composition of cations is obtained at the capillary surface which compromises the reliability and long-term reproducibility of the electroosmotic flow.

Figure 3.5 presents the influence of the anion type on the magnitude of the zeta potential for aqueous solutions of sodium chloride, bromide, iodide, nitrate, and perchlorate. The zeta potential varied markedly with the anion type, particularly in the low concentration range. These results suggest that the anion is involved, in some manner, in the development of the double-layer structure. The exact origin of this effect is not known, however, as there is no apparent correlation of the zeta potential with either the hydrated radius[35,36] or the

Figure 3.5 Effect of anion type on the magnitude of the zeta potential under constant-voltage conditions at 20 kV. Aqueous solutions at pH 9 of (○) NaCl, (△) NaBr, (■) NaI, (□) $NaNO_3$, (▽) $NaClO_4$.

Figure 3.5

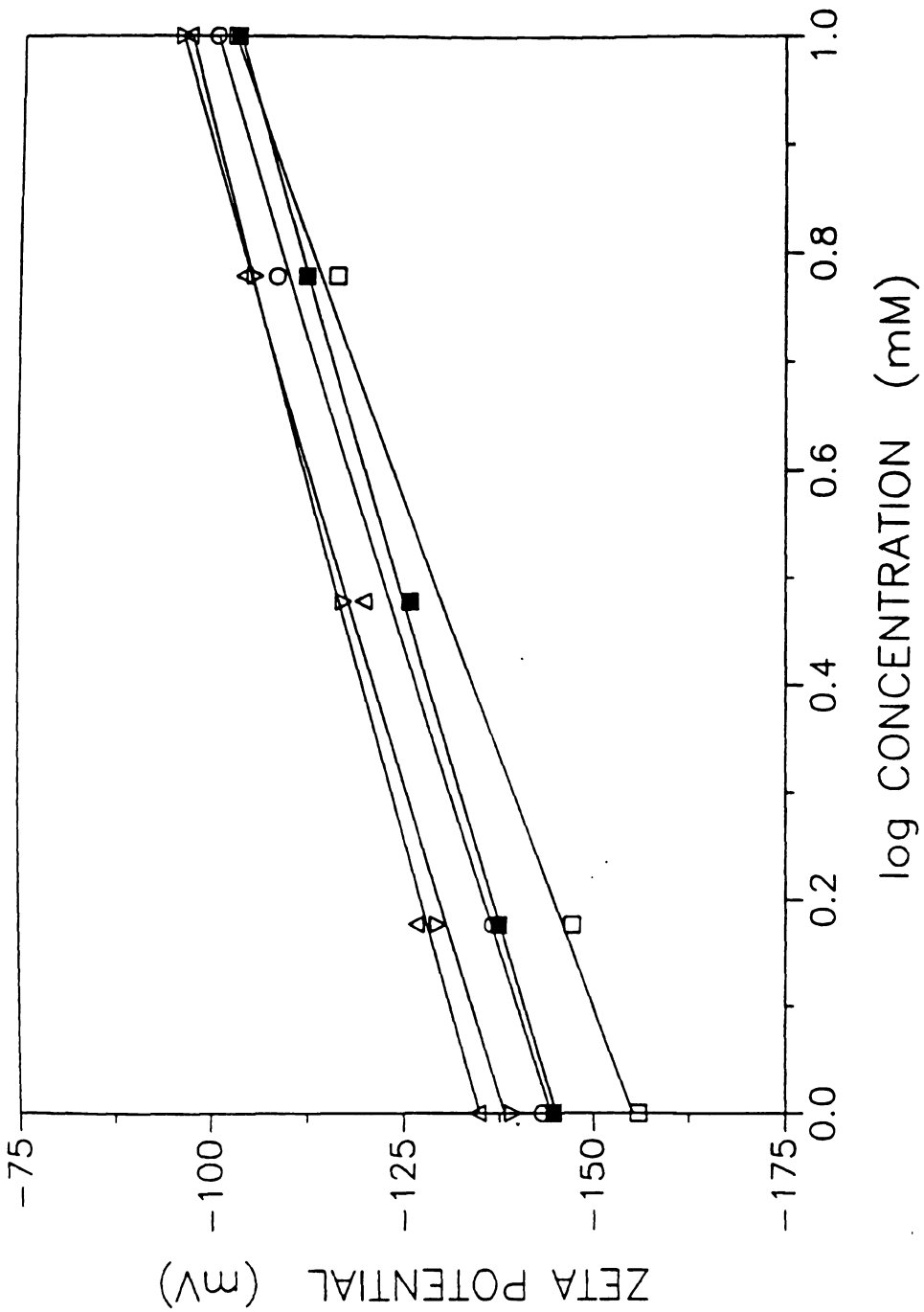

potential under
ions at pH 9 of
') $NaClO_4$.

mobility[23] of
literature to
electroosmot
electroosmot
found that b
electroosmot
Green and
unimportant
higher than
observations
controlled io
electroosmot

In cor
of predicting
the logarithm
surface resp
of the electro
towards the
anion identit
electroosmot
system.

Preliminary
Conditions.
conditions, C
equation (Eq

mobility[23] of the anion. There appears to be a great deal of controversy in the literature to date regarding the effect of anion type on the development of the electroosmotic flow. Atamna *et al.*[9] observed strong differences in the electroosmotic flow using common sodium buffer solutions. VanOrman *et al.*[7] found that buffers with several different anion types can produce the same electroosmotic velocity provided that the ionic strength is carefully controlled. Green and Jorgenson[10] concluded that differences in anion type are unimportant if the concentration of an inert electrolyte is at least three-fold higher than the concentration of the operating buffer. Despite these prior observations, our data suggest that even solutions of inert electrolytes with well-controlled ionic strength exhibit a distinct influence of the anion type on the electroosmotic flow.

In conclusion, the results presented herein clearly sustain the possibility of predicting electroosmotic flow by modelling the zeta potential as a function of the logarithm of the cation concentration. It has been shown that the capillary surface responds to the solution concentration in a Nernstian fashion, regardless of the electrolyte type employed. There is no apparent selectivity of the surface towards the cation, however, the zeta potential magnitude is affected by the anion identity. Therefore, under constant-voltage conditions, the prediction of electroosmotic flow is determined by the ionic character of the electrolyte system.

Preliminary Studies of Electroosmotic Flow under Constant-Current Conditions. In order to describe electroosmotic flow under constant-current conditions, Ohm's law must be incorporated into the Helmholtz-Smoluchowski equation (Equation [3.7]):

$v_{osm} = -$

where R is t

variables are

$$\frac{1}{R} = k -$$

where A is th

the solution.

individual ior

$k = F \Sigma | z$

By combining

$$v_{osm} = - \frac{\varepsilon}{}$$

Equation [3.

and the app

properties, a

derivation of

Accord

intrinsic cha

electroosmoti

velocities of

$$v_{osm} = - \frac{\varepsilon \varepsilon_0 \zeta}{\eta} \frac{R I}{L} \qquad [3.8]$$

where R is the resistance of the medium and I is the applied current. All other variables are as previously defined. The resistance is given by:

$$\frac{1}{R} = k \frac{A}{L} \qquad [3.9]$$

where A is the cross-sectional area of the capillary and k is the conductivity of the solution. The conductivity is related to the electrophoretic mobility (μ_i) of the individual ionic species as follows:

$$k = F \Sigma |z_i| \mu_i M_i \qquad [3.10]$$

By combining Equations [3.8], [3.9], and [3.10], the following expression results:

$$v_{osm} = - \frac{\varepsilon \varepsilon_0 \zeta}{\eta} \frac{I}{A k} = \frac{\mu_{osm}}{A F \Sigma |z_i| \mu_i M_i} I \qquad [3.11]$$

Equation [3.11] predicts a linear relationship between electroosmotic velocity and the applied current. The influence of the capillary dimensions, solution properties, as well as the surface characteristics are clearly evident in the derivation of Equation [3.11].

According to Equation [3.11], the electrophoretic mobility is one of the intrinsic characteristics of the electrolyte that is expected to affect the electroosmotic velocity. To examine the extent of this effect, the electroosmotic velocities of sodium nitrate and sodium bromide solutions were measured in

reference to
whose soluti
the previous
velocity und
with the app
Therefore, it
sufficiently l
conditions er

As sh
flow is by al
when studyir
buffer syster
likely to be p
charged elec
controlled.
buffer solutio
with increasi
chloride exce
approaches f

The s
selective beh
solutions as
differences i
addition of a
carefully co
electroosmot

reference to sodium chloride solutions. Nitrate and bromide are the anions whose solutions presented the greatest difference in electroosmotic behavior in the previous study under constant-voltage conditions. The electroosmotic velocity under constant-current conditions, shown in Figure 3.6, varied linearly with the applied current and seems to be independent of the type of anion. Therefore, it is valid to conclude that the differences in anion mobility[23] were not sufficiently large to affect the electroosmotic velocity under the experimental conditions employed in this work.

As shown in Equation [3.11], another means to affect the electroosmotic flow is by altering the charge of the electrolyte. This is particularly important when studying the electroosmotic behavior of more complex electrolytes such as buffer systems, where several species with different charge and mobility are likely to be present. However, by addition of a substantial amount of a singly charged electrolyte, the electroosmotic velocity of the buffer solution can be controlled. Figure 3.7 shows the results of flow measurements in phosphate buffer solutions at pH 9 (where the highly charged PO_4^{3-} species predominates), with increasing amounts of sodium chloride. When the concentration of sodium chloride exceeds the concentration of the buffer salts, the electroosmotic velocity approaches that of a sodium chloride solution.

The studies under constant-current conditions have shown that the ion-selective behavior of the capillary surface applies to singly charged electrolyte solutions as well as to buffer systems. In buffer solutions, however, the differences in charge and mobility of the individual species must be masked by addition of an excess of a singly charged strong electrolyte. Therefore, under carefully controlled experimental conditions, the proposed model of electroosmotic flow can be explored in more detail to represent the behavior of

Figure 3.6 Effect of anion type on the electroosmotic velocity under constant-current conditions. Aqueous solutions at pH 9 with 3 mM concentration of (○) NaCl, (△) NaBr, (□) $NaNO_3$.

Figure 3.6

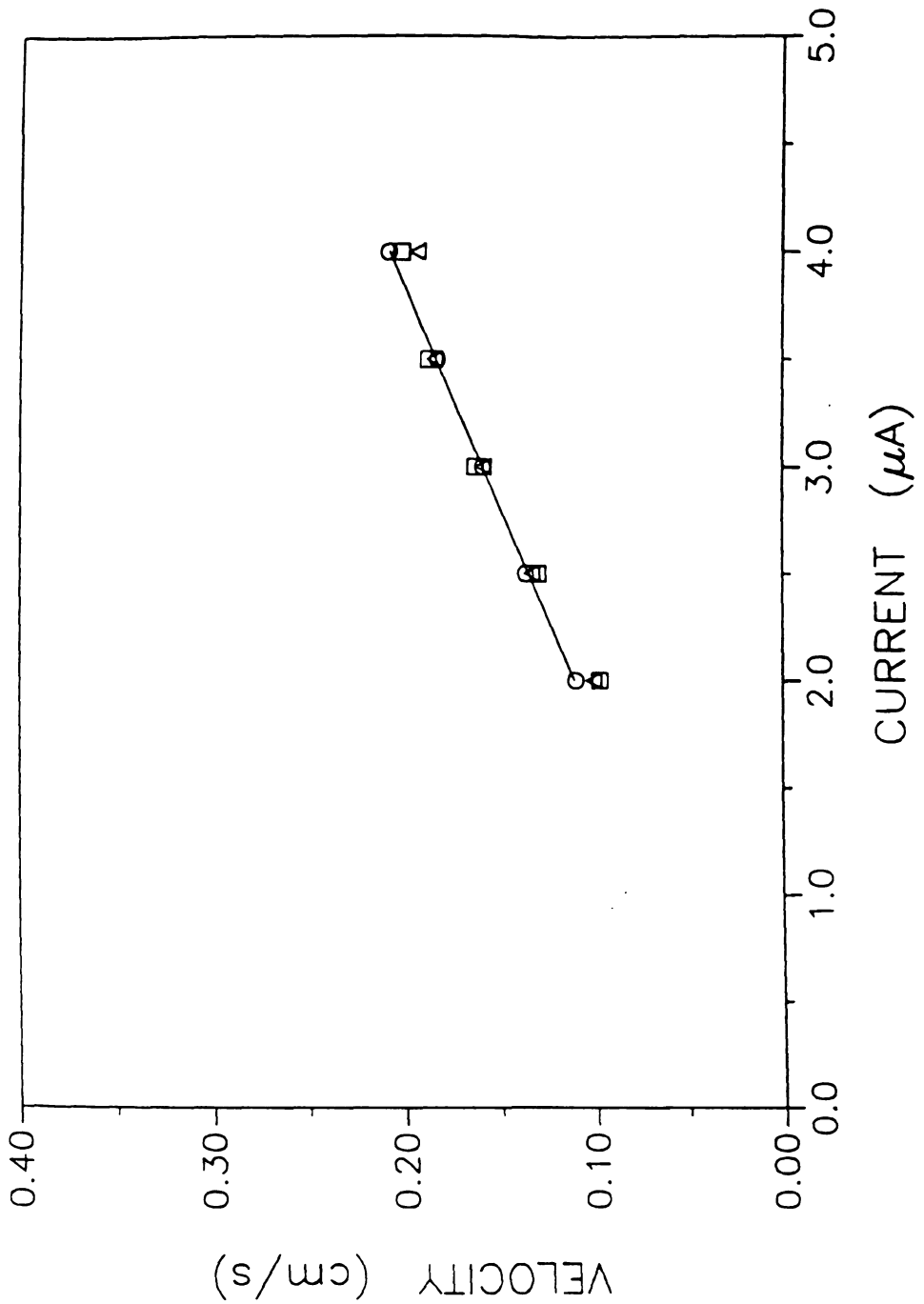

nder constant-
with 3 mM
3·

Figure 3.7 Effect of the ratio of Na(NaCl) to Na(buffer salts) on electroosmotic velocity under constant-current conditions for phosphate buffer solutions at pH 9 with 10 mM total sodium concentration. (▽) 0 : 10, (○) 5 : 5, (□) 6.5 : 3.5, (△) 10 : 0.

Figure 3.7

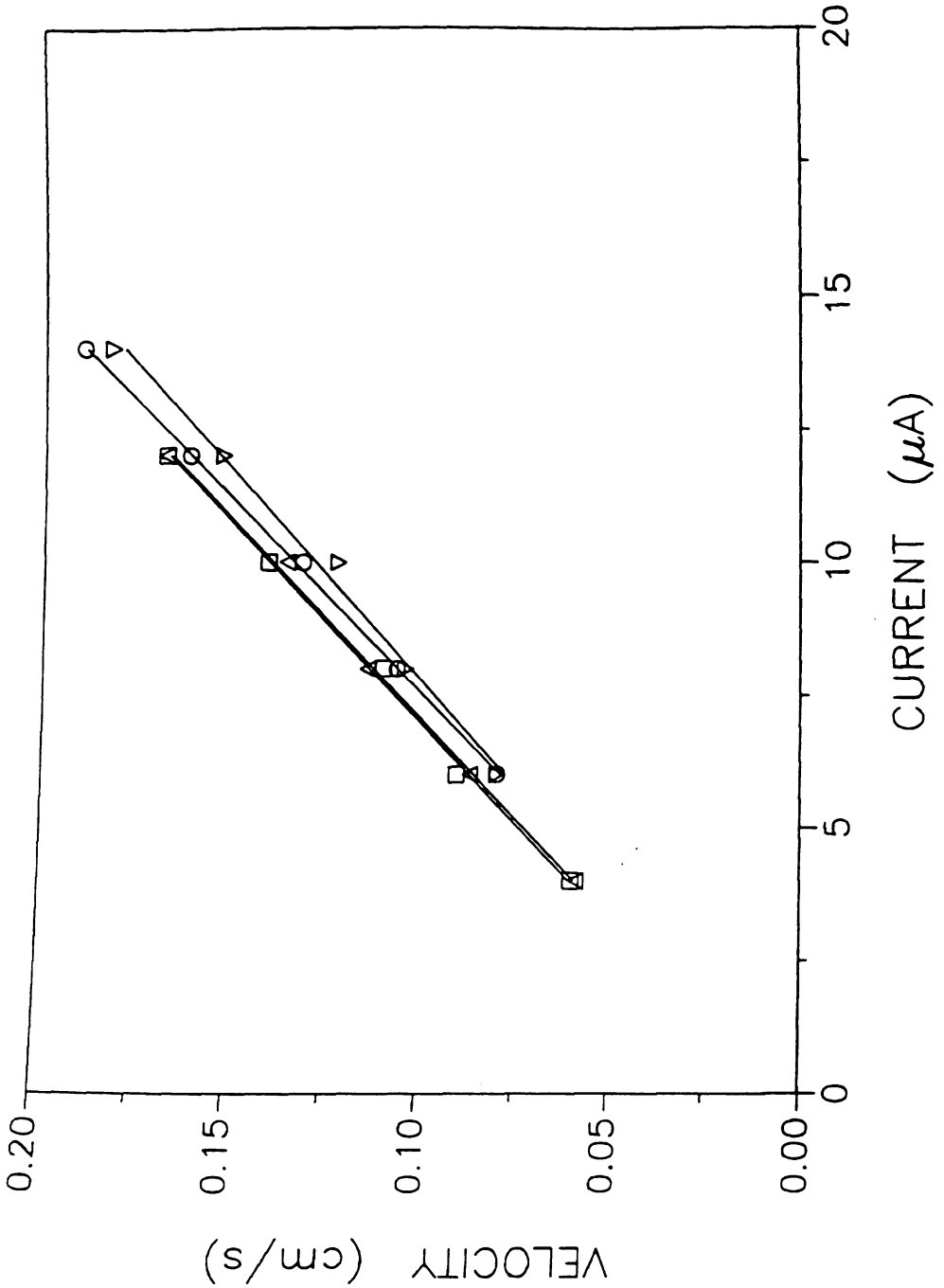

electroosmotic
sphate buffer
on.

complex bu

Validation

phosphate

conditions.

sodium from

and equal

representati

nonlinearly

influencing t

potential.

extensive pr

density in th

electroosmo

produced th

3.9. For a c

electroosmot

concentratio

increases, c

decreases.

The c

magnitude of

data were fi

behavior of g

$\zeta = \zeta_0 + S$

complex buffer systems.

Validation of the Ion-Selective Model. The effects of pH and composition of phosphate buffer solutions were examined separately under constant-current conditions. These solutions were prepared in such a way that the ratio of sodium from sodium chloride and the sodium buffer salt was maintained constant and equal to unity. For a constant concentration of sodium, shown for a representative case in Figure 3.8, the electroosmotic velocity increased nonlinearly from pH 4 to 10. The pH affects the electroosmotic flow by influencing the extent of ionization of the silica surface, thus altering the surface potential. When the pH is much lower than the pK_a of the silica surface, extensive protonation of the silanol groups occurs, which reduces the charge density in the double layer. Consequently, the zeta potential is lowered and the electroosmotic flow decreases. A change in the electrolyte concentration produced the opposite effect, as illustrated for a representative case in Figure 3.9. For a constant value of pH, which defines a constant surface potential, the electroosmotic velocity decreased proportionately with the total sodium concentration from 5 to 15 mM. As the concentration of the bulk solution increases, compression of the double layer occurs and the electroosmotic flow decreases.

The combined effect of pH and composition of the buffer solution on the magnitude of the zeta potential is illustrated in Figure 3.10. These experimental data were fit to an equation analogous to that describing the ion-selective behavior of glass membranes (Equation [3.3]):

$$\zeta = \zeta_0 + \text{SLOPE} \log (a_H + k^{POT} a_{Na}) \qquad [3.12]$$

Figure 3.8 Effect of pH on electroosmotic velocity under constant-current conditions for phosphate buffer solutions with 10 mM total sodium concentration and 1:1 ratio of Na(NaCl) to Na(buffer salts). (▲) pH 4, (■) pH 5, (●)pH 6, (▽) pH 7, (○) pH 8, (□) pH 9, (△) pH 10.

Figure 3.8

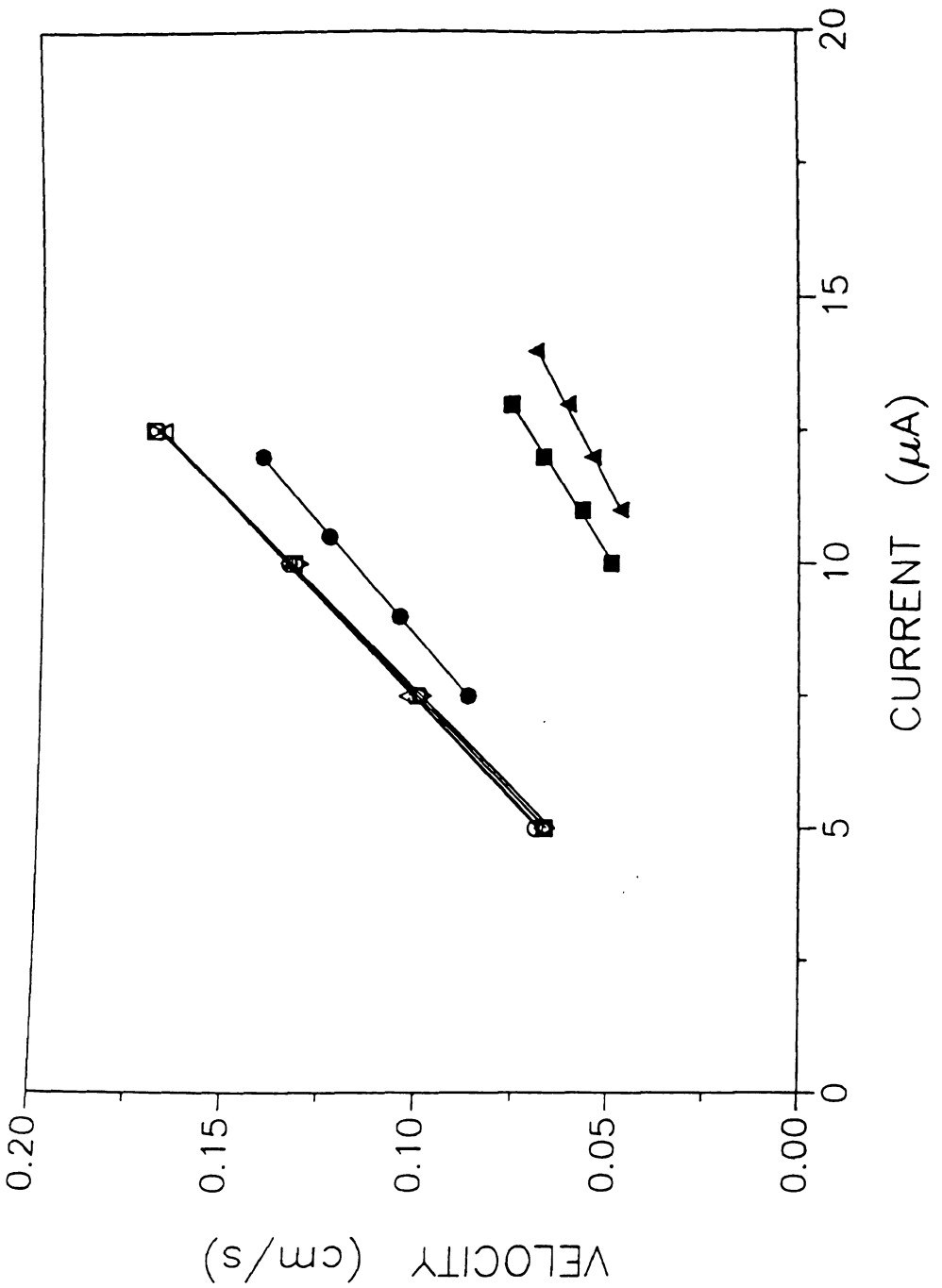

nstant-current
M total sodium
salts). (▲)
3, (□) pH 9,

Figure 3.9 Effect of total sodium concentration on electroosmotic velocity under constant-current conditions for phosphate buffer solutions at pH 7 with 1:1 ratio of Na (NaCl) to Na (buffer salts). (○) 5 mM, (△) 7.5 mM, (■) 10 mM, (□) 12.5 mM, (▽) 15 mM.

Figure 3.9

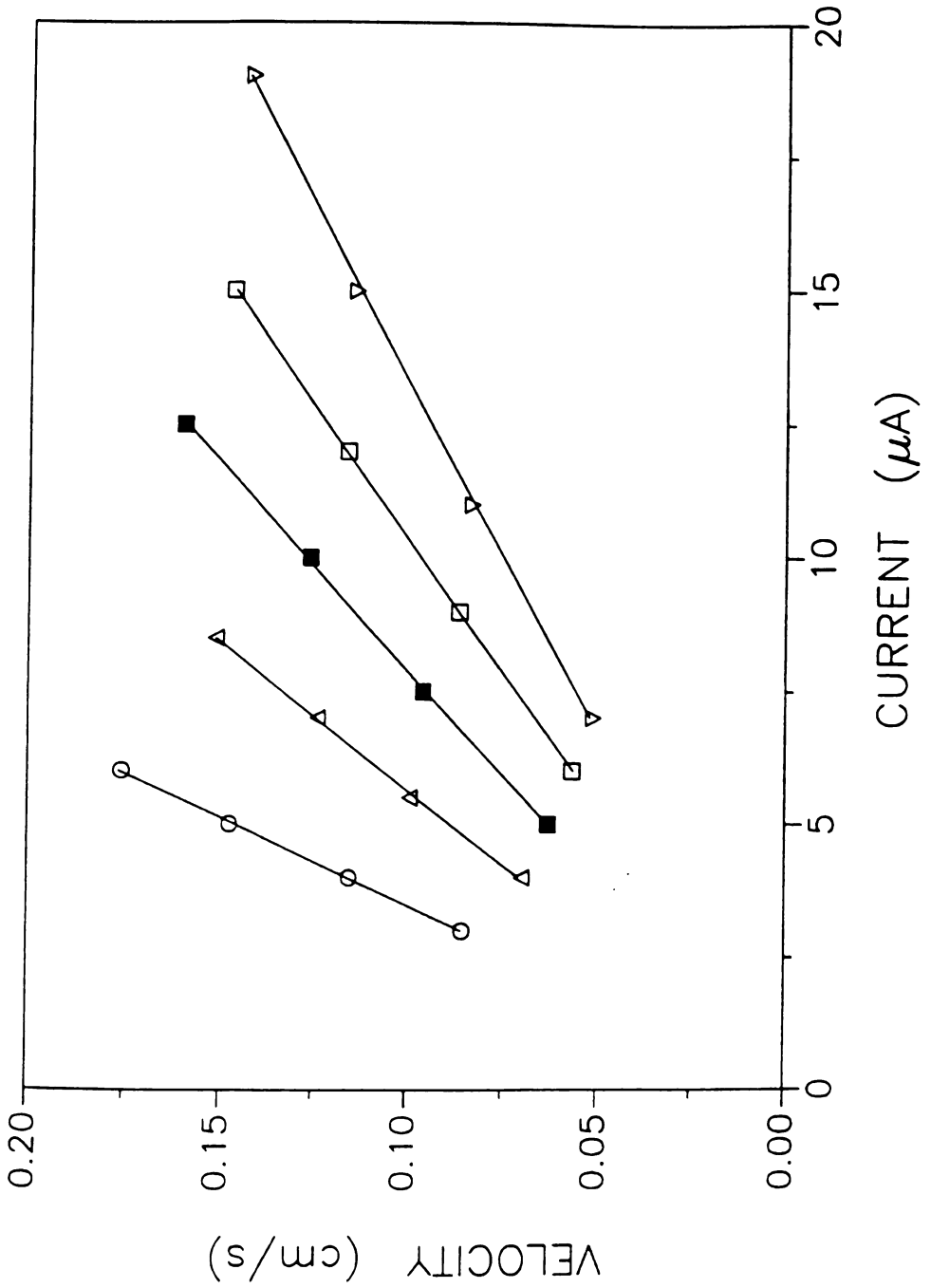

smotic velocity
fer solutions at
(O) 5 mM,
mM.

Figure 3.10 Comparison of experimental data with the ion-selective model for zeta potential as a function of pH from 4 to 10 and total sodium concentration from 5 to 15 mM (bottom to top curves). Experimental conditions as given in Figures 3.8 and 3.9.

Figure 3.10

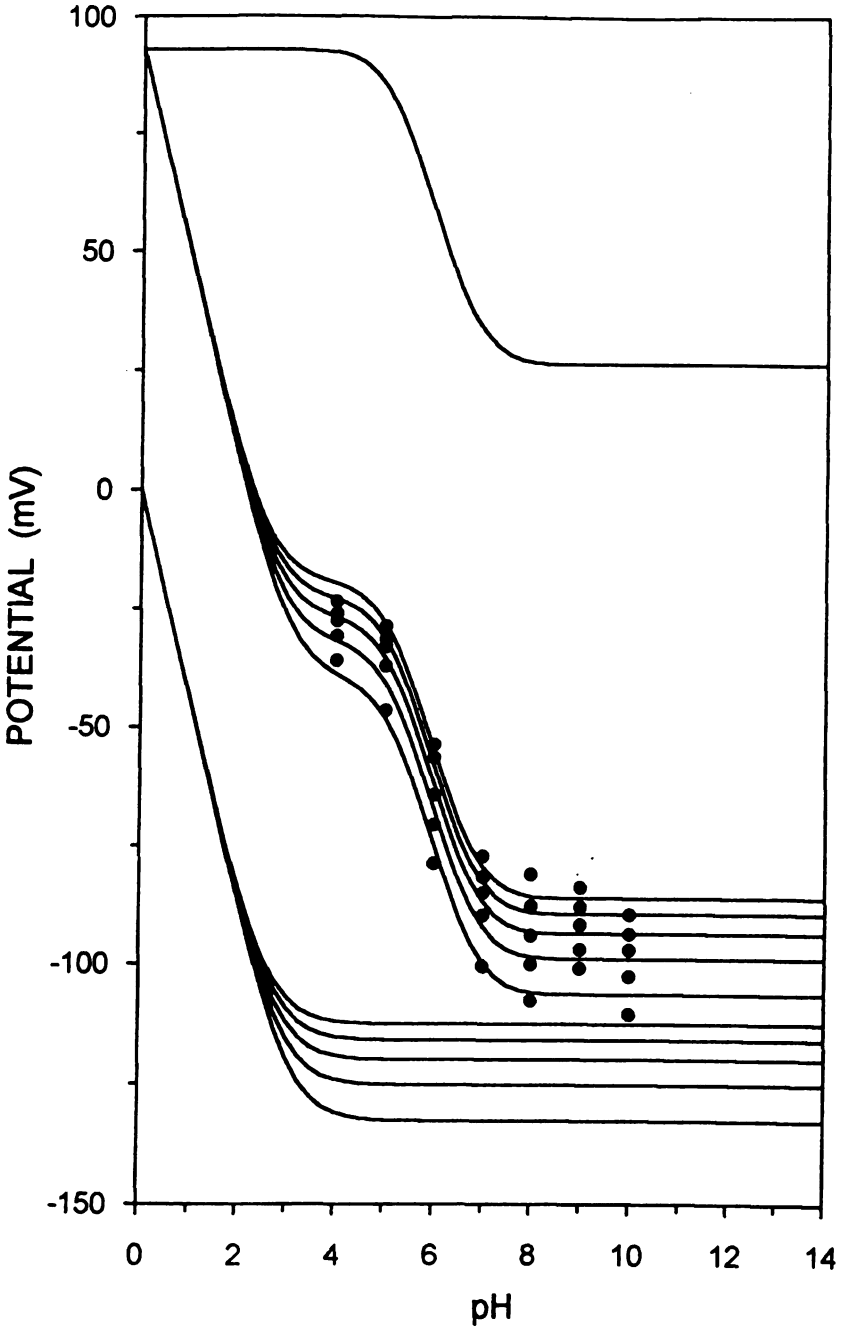

ctive model for
d total sodium
top curves).
3.9.

ζ_0 is mat
function (E

ζ_0 = [ERI

The param
distributio
parameter
unknown
and the b
magnitude
(SSE) are
ion-select
interpretin

Th
surface, i
potential
the pH in
dramatica
part to th
primarily
proposed
sodium a
higher th
which is
significan

ζ_0 is mathematically described by a Gaussian probability integral or error function (ERF), which is sigmoidal in shape:[37]

$$\zeta_0 = [\mathrm{ERF}\,(A_0\,\mathrm{pH} + B_0)]\,C_0 + D_0 \qquad [3.13]$$

The parameters A_0 and B_0 are related to the mean and standard deviation of the distribution. The parameter C_0 confers the height to the sigmoidal curve and the parameter D_0 is needed for displacement in the zeta potential axis. The unknown parameters of Equation [3.12] and [3.13] were searched numerically and the best fit was determined by means of the least-square method.[38] The magnitude of these parameters as well as the sum of the squared residuals (SSE) are presented in Table 3.1. In Table 3.2, an statistical evaluation of the ion-selective model is presented. These results can be understood by interpreting separately the contribution of each term in Equation [3.12].

The logarithm term, which represents the ion-selective behavior of the surface, is shown in the bottom part of Figure 3.10. At very low pH, the zeta potential responds exclusively to the logarithm of the hydrogen ion activity. As the pH increases, the contribution of sodium to the overall potential increases dramatically and predominates shortly after pH 4. This behavior is attributed in part to the relative magnitude of the hydrogen and sodium ions activity, but primarily to the magnitude of the potentiometric constant. According to the proposed model, k^{POT} carries information on the exchange equilibrium between sodium and hydrogen ions at the plane of shear. The value 0.22 is appreciably higher than the potentiometric constant of a pH-sensing glass electrode,[25,26] which is on the order of 10^{-12}. This result suggests that sodium ions contribute significantly to the transport of charge across the plane of shear.

Table 3.1 P

PARA
SI
K
S

Table 3.1 Parameters of the ion - selective model.

PARAMETERS	VALUES
A_0	–0.86
B_0	5.11
C_0	33.2
D_0	59.7
SLOPE	44.4
k^{POT}	0.22
SSE	247

Table 3.2 C
v

pH	
4	
5	
6	
7	
8	
9	
10	

* Equation
** % ERRC

Table 3.2 Comparison of the experimentally determined zeta potential with values calculated from the ion-selective model.

pH	a_{Na^+}	ZETA POTENTIAL (mV) EXPERIMENTAL	CALCULATED*	% ERROR**
4	4.63×10^{-3}	−35.7 ± 1.2	−38.5	−7.8
	6.84×10^{-3}	−30.6 ± 1.1	−31.6	−3.3
	9.00×10^{-3}	−27.3 ± 0.75	−26.6	2.6
	1.11×10^{-2}	−25.7 ± 0.68	−22.7	12
	1.32×10^{-2}	−23.3 ± 0.42	−19.5	16
5	4.63×10^{-3}	−46.3 ± 1.3	−47.9	−3.5
	6.84×10^{-3}	−36.8 ± 1.5	−40.7	−11
	9.00×10^{-3}	−32.8 ± 0.94	−35.2	−7.3
	1.11×10^{-2}	−31.1 ± 0.77	−31.1	0.0
	1.32×10^{-2}	−28.5 ± 0.85	−27.8	2.5
6	4.63×10^{-3}	−78.7 ± 2.3	−74.8	5.0
	6.83×10^{-3}	−70.5 ± 1.8	−67.3	4.5
	8.99×10^{-3}	−64.2 ± 2.1	−62.0	3.4
	1.11×10^{-2}	−56.3 ± 2.3	−57.9	−2.8
	1.32×10^{-2}	−53.6 ± 2.9	−54.6	−1.9
7	4.61×10^{-3}	−100.3 ± 1.6	−99.6	7.0
	6.80×10^{-3}	−89.7 ± 1.5	−92.1	−2.7
	8.94×10^{-3}	−85.0 ± 1.5	−86.8	−2.1
	1.10×10^{-2}	−81.6 ± 1.5	−82.7	−1.3
	1.31×10^{-2}	−77.3 ± 1.8	−79.4	−2.7
8	4.60×10^{-3}	−107.5 ± 1.6	−105.8	1.6
	6.78×10^{-3}	−99.9 ± 1.4	−98.3	1.6
	8.91×10^{-3}	−93.7 ± 1.3	−93.0	0.75
	1.10×10^{-2}	−87.6 ± 1.2	−88.9	−1.5
	1.31×10^{-2}	−81.0 ± 1.2	−85.6	−5.7
9	4.60×10^{-3}	−100.8 ± 2.8	−106.2	−5.4
	6.78×10^{-3}	−96.7 ± 1.5	−98.7	−2.1
	8.91×10^{-3}	−91.6 ± 1.6	−93.4	−2.0
	1.10×10^{-2}	−87.8 ± 2.0	−89.3	−1.7
	1.31×10^{-2}	−83.7 ± 2.4	−86.0	−2.7
10	4.60×10^{-3}	−110.4 ± 2.1	−106.2	3.8
	6.78×10^{-3}	−102.3 ± 2.1	−98.7	3.5
	8.91×10^{-3}	−96.8 ± 1.9	−93.4	3.5
	1.10×10^{-2}	−93.4 ± 2.0	−89.3	4.4
	1.31×10^{-2}	−89.4 ± 1.7	−86.0	3.8

* Equation [3.12]

** % ERROR = 100 (EXP − CALC) / EXP

The io
phosphate bu
change in cor
observed in th
of electrolyte c
subject of mar
departure of th
Several model
rate of chang
($d\zeta/d(\log C)$) i
explanation pr
surface alters
describing the
applicable. T
Lyklema,[28] wh
surface in whic
cations.

The ion
second term o
of the experim
zeta potential
many possible
was chosen be
potential curve
curve of the
characterized

The ion-selective model in Equation [3.12], when applied to the phosphate buffer system, gives a value for SLOPE of 44.4 mV per tenfold change in concentration. It is noteworthy that a slope of 43.7 mV was also observed in the studies with pure electrolyte systems (Figure 3.3). The influence of electrolyte concentration on the zeta potential of silica surfaces has been the subject of many studies,[39-43] and there is substantial evidence to support the departure of the slope from the value of 59 mV expected for Nernstian behavior. Several models have been proposed to account for this phenomenon, where the rate of change of the zeta potential with the logarithm of concentration ($d\zeta/d(\log C)$) is correlated with important parameters of the double layer. An explanation proposed by Hunter and Wright[42] is that conductance at the silica surface alters the surface charge density, such that the classical equations[23] describing the potential profile in the double layer are no longer strictly applicable. This concept is further supported by the theoretical model of Lyklema,[28] who postulated the existence of an amorphous gel layer at the silica surface in which the potential is affected by the degree of penetration of certain cations.

The ion-selective behavior of the surface alone, as represented by the second term of Equation [3.12], is not sufficient to explain the sigmoidal contour of the experimental data. It is the first term, ζ_0, that imparts this feature to the zeta potential curve, as demonstrated in the top part of Figure 3.10. Among the many possible mathematical functions with sigmoidal shape,[37] the error function was chosen because of its physical meaning. Another way to interpret the zeta potential curve as a function of pH is to recognize that it represents a titration curve of the acidic sites at the silica surface. These acidic sites are characterized by different types of silanol groups, whose abundance is assumed

to be normally

overall pK_a wh

experimentally

reported valu

spectroscopic,[4

found a pK_a

Likewise, Luka

versus pH with

provided a pK_a

groups by com

oxides.[45] Prev

values betwee

used as titrant.

The mod

membrane lead

3.10 reveals t

approaches ze

infinitesimally

corresponding

point of zero c

approximately

from this mode

should be exe

predicts positiv

practice, for tha

the surface, re

to be normally distributed. The inflection point of the titration curve gives an overall pK_a which is representative of the average acidity of the surface. The experimentally determined pK_a of 5.9 is in good agreement with previously reported values for silica materials determined by electrophoretic,[12,14] spectroscopic,[45] and potentiometric methods.[39,46] Schwer and Kenndler[12] found a pK_a of 5.3 by electrophoretic measurements in aqueous solutions. Likewise, Lukacs and Jorgenson[14] presented a curve of electroosmotic mobility *versus* pH with an inflection point around pH 6. Spectroscopic measurements provided a pK_a of 7.1, which was attributted to the various silica surface hydroxyl groups by comparing the hydroxyl band frequency shifts of alcohols and silica oxides.[45] Previous reports on titration curves of silica gels and sols have given values between 5.2 and 5.7[39] and 6.5 to 7.7,[46] depending on the type of base used as titrant.

The modelling of the response of the capillary surface as an ion-selective membrane leads to interesting observations. For instance, inspection of Figure 3.10 reveals that all curves tend to the same point as the zeta potential approaches zero. At this point, the double layer has collapsed to an infinitesimally thin layer of ions and the electroosmotic flow ceases. The pH corresponding to the point where the zeta potential reaches zero is known as the point of zero charge (PZC). For colloidal silica, the PZC is believed to occur approximately at pH 2.5,[39,43] which is in good agreement with that predicted from this model. It is necessary to emphasize that beyond the PZC caution should be exercized in the physical interpretation of the model. The model predicts positive values for the zeta potential at pH values less than the PZC. In practice, for that to occur, a layer of cations would have to adsorb specifically at the surface, reversing its charge.

3.4 Conclusio

The det
under both
successfully a
meaningful mo
potential as a
which describ
potential toget
can then be u
Smoluchowski
data in the p
electrophoresi
potential.

3.4 Conclusions

The determination of electroosmotic flow in capillary zone electrophoresis under both constant-voltage and constant-current conditions has been successfully achieved through the development of a simple but physically meaningful model. The proposed model is based on the evaluation of the zeta potential as a function of the buffer composition in a manner analogous to that which describes the ion-selective behavior of glass membranes. The zeta potential together with the dielectric constant and viscosity of the buffer solution can then be used to calculate the electroosmotic velocity from the Helmholtz-Smoluchowski equation. The model has been fully supported by experimental data in the pH range from 4 to 10, which is most useful in capillary zone electrophoresis, resulting in approximately 5 % error in the prediction of the zeta potential.

3.5 Referenc

1. Grossm
and Pra
2. Kuhr, W
3. McLaug
K. W.;
1992, *1*
4. Hiemen
Marcel
5. Bier, M
Acaden
6. Vindevo
7. VanOm
Ewing,
8. Atamna
Chroma
9. Atamna
Chroma
10. Green
11. Fujiwar
12. Schwe
13. Kurosu
1991,
14. Lukacs
15. Schom
16. Hjerten
17. McCon
18. Lee, C
1519-1
19. Hayes,
20. Dose,

3.5 References

1. Grossman, P. D.; Colburn, J. C., Eds.; *Capillary Electrophoresis - Theory and Practice*; Academic Press Inc.: San Diego, CA, 1992.

2. Kuhr, W. G.; Monnig, C. A. *Anal. Chem.* **1992**, *64*, 389R-407R.

3. McLaughlin, G. M.; Nolan, J. A.; Lindahl, J. L.; Palmieri, R. H.; Anderson, K. W.; Morris, S. C.; Morrison, J. A.; Bronzert, T. J. *J. Liq. Chromatogr.* **1992**, *15*, 961-1021.

4. Hiemenz, P. C. *Principles of Colloid and Surface Chemistry*, 2nd ed.; Marcel Dekker: New York, 1986.

5. Bier, M., Ed.; *Electrophoresis - Theory, Methods and Applications*; Academic Press Inc.: New York, 1959.

6. Vindevogel, J.; Sandra, P. *J. Chromatogr.* **1991**, *541*, 483-488.

7. VanOrman, B. B.; Liversidge, G. G.; McIntire, G. L.; Olefirowicz, T. M.; Ewing, A. G. *J. Microcol. Sep.* **1990**, *2*, 176-180.

8. Atamna, I. Z.; Metral, C. J.; Muschik, G. M.; Issaq, H. J. *J. Liq. Chromatogr.* **1990**, *13*, 2517-2527.

9. Atamna, I. Z.; Metral, C. J.; Muschik, G. M.; Issaq, H. J. *J. Liq. Chromatogr.* **1990**, *13*, 3201-3210.

10. Green J. S.; Jorgenson, J. W. *J. Chromatogr.* **1989**, *478*, 63-70.

11. Fujiwara, S.; Honda, S. *Anal. Chem.* **1987**, *59*, 487-490.

12. Schwer, C.; Kenndler, E. *Anal. Chem.* **1991**, *63*, 1801-1807.

13. Kurosu, Y.; Hibi, K.; Sasaki, T.; Saito, M. *J. High Resol. Chromatogr.* **1991**, *14*, 200-203.

14. Lukacs, K. D.; Jorgenson, J. W. *J. Chromatogr.* **1985**, *8*, 407-411.

15. Schomburg, G. *Trends Anal. Chem.* **1991**, *10*, 163-169.

16. Hjerten, S. *J. Chromatogr.* **1985**, *347*, 191-198.

17. McCormick, R. *Anal. Chem.* **1988**, *60*, 2322-2328.

18. Lee, C. S.; McManigill, D.; Wu, C. T.; Patel, B. *Anal. Chem.* **1991**, *63*, 1519-1523.

19. Hayes, M. A.; Ewing, A. G. *Anal. Chem.* **1992**, *64*, 512-516.

20. Dose, E. V.; Guiochon, G. A. *Anal. Chem.* **1991**, *63*, 1063-1072.

21. Bier, M
219, 12

22. Salomo

23. Bard, A
Applica

24. Koryta
London

25. Freiser,
York, 1

26. Buck, R
46, 255

27. Unger,
Publish

28. Lyklem

29. Lambe

30. Smith,
57-68.

31. Altria,

32. Huang,

33. Weissb
Intersci

34. Li, H. C

35. McCon
Dugge

36. Melchi
ACS S
1990.

37. Spanie
Washi

38. Devore
2nd ed

39. Parks,

40. Wiese,
1971,

21. Bier, M.; Palusinski, O. A.; Mosher, R. A.; Saville, D. A. *Science* **1983**, *219*, 1281-1287.

22. Salomon, K.; Burgi, D. S.; Helmer, J. C. *J. Chromatogr.* **1991**, *559*, 69-80.

23. Bard, A. J.; Faulkner, L. R. *Electrochemical Methods - Fundamentals and Applications*; John Wiley & Sons: New York, 1980.

24. Koryta J. *Ion-Selective Electrodes*, 2nd ed.; Cambridge University Press: London, 1975.

25. Freiser, H. *Ion-Selective in Analytical Chemistry*; Plenum Press: New York, 1978.

26. Buck, R. P.; Boles, J. H.; Porter, R. D.; Margolis, J. A. *Anal. Chem.* **1974**, *46*, 255-261.

27. Unger, K. K. *Porous Silica, J. Chromatogr. Lib.*, Vol. 16, Elsevier Scientific Publishing Company: New York, 1979.

28. Lyklema, J. *J. Electroanal. Chem.* **1968**, *18*, 341-348.

29. Lambert, W. J.; Middleton, D. L. *Anal. Chem.* **1990**, *62*, 1585-1587.

30. Smith, S. C.; Strasters, J. K.; Khaledi, M. G. *J. Chromatogr.* **1991**, *559*, 57-68.

31. Altria, J. D.; Simpson, C. F. *Anal. Proc.* **1986**, *23*, 453-454.

32. Huang, X.; Gordon, M. J.; Zare, R. N. *Anal. Chem.* **1988**, *60*, 1837-1838.

33. Weissberger, A. *Physical Methods of Organic Chemistry*, 3rd ed.; Interscience Publishers Inc.: New York, 1959.

34. Li, H. C.; Bruyn, P. L. *Surface Sci.* **1966**, *5*, 203-220.

35. McConnell, B. L.; Williams, K. C.; Daniel, J. L.; Stanton, J. H.; Irby, B. N.; Dugger, D. L.; Maatman, R. W. *J. Phys. Chem.* **1964**, *68*, 2941-2946.

36. Melchior, D. C.; Bassett, R. L. *Chemical Modeling of Aqueous Systems II, ACS Symp. Ser.,* Vol. 416, American Chemical Society: Washington, DC, 1990.

37. Spanier, J.; Oldham, K. *An Atlas of Functions*; Hemisphere Pub. Corp.: Washington, DC, 1987.

38. Devore, J. L. *Probability and Statistics for Engineering and the Sciences*, 2nd ed.; Brooks/Cole Publishing Company: Monterey, CA, 1987.

39. Parks, G. A. *Chem. Rev.* **1965**, *65*, 177-198.

40. Wiese, G. R.; James, R. O.; Healy, T. W. *Faraday Discuss. Chem. Soc.* **1971**, *52*, 302-311.

41. Rutgers
42. Hunter,
43. Churae
Interfac
44. Tadros,
45. Hair, M
46. Strazhe
Chroma

41. Rutgers, A. J.; De Smet, M. *Trans. Faraday Soc.* **1945**, *41*, 758-771.

42. Hunter, R. J.; Wright, H. J. L. *J. Colloid Interface Sci.* **1971**, *37*, 564-580.

43. Churaev, N. V.; Sergeeva, I. P.; Sobolev, V.D.; Derjaguin, B. V. *J. Colloid Interface Sci.* **1981**, *84*, 451-460.

44. Tadros, T. F.; Lyklema, J.; *J. Electroanal. Chem.* **1968**, *17*, 267-275.

45. Hair, M. L.; Hertl, W. *J. Phys. Chem.* **1970**, *74*, 91-94.

46. Strazhesko, D. N.; Strelko, V. B.; Belyakov, V. N.; Rubanik, S. C. *J. Chromatogr.* **1974**, *102*, 191-195.

4.1. Introduct

The ca
resolution sep
industrial and
of separation
strategy utiliz
parameter is
constant.[3,4]
misleading in
methods whe
diversity and
complexity of
approaches
procedures,
variables of
procedures,
experimental
the optimizati
assisted opti
regarding the

CHAPTER 4

OPTIMIZATION OF SEPARATIONS IN CAPILLARY ZONE ELECTROPHORESIS

4.1. Introduction

The capability of capillary zone electrophoresis (CZE) to achieve high-resolution separations has been demonstrated for a variety of substances of industrial and biomedical importance.[1,2] However, to a large extent, optimization of separations has been approached in an empirical manner. A common strategy utilizes univariate sequential methods, where the effect of each parameter is assessed individually while all other parameters are held constant.[3,4] Such procedures are inherently time consuming and often misleading in the search for the global optimum. The reliability of univariate methods when applied to CZE separations is further compromised by the diversity and interactive nature of the system variables as well as by the complexity of typical CZE samples. In the literature to date, several systematic approaches to optimization have been proposed.[5-10] Some of these procedures, however, are rather simplistic and do not consider all important variables of the system.[5,8] Other approaches utilize resolution mapping procedures, which may demand the initial inspection of a large set of experimental conditions.[6,9,10] Therefore, a more comprehensive approach to the optimization of electrophoretic separations is highly desirable. A computer-assisted optimization routine fulfills this need in many respects, especially regarding the speed and accuracy with which a variety of conditions can be

evaluated. F
our understa
develop such
for zone migr

During
electrophores
mathematical
incorporates
This approac
computationa
rigorous and
simplified att
inherent assu
applications.5

In com
have receive
CZE, longitu
broadening.2
broadening,
expected. I
because add
the most co
finite volum
broadening
profile cause
contributions
zone and th

evaluated. Furthermore, the resulting simulation data can add substantially to our understanding of fundamental electrokinetic phenomena. In order to develop such an optimization procedure, however, proper and reliable models for zone migration and dispersion processes are required.

During the past decades, the simulation of migration processes in electrophoresis has been a subject of considerable interest.[11-18] The mathematical description of the temporal evolution of the zone profile incorporates the fundamental laws of chemical equilibrium and mass transport. This approach generates complex equations, whose solution often demands computationally intensive numerical methods. Although these models are rigorous and exact, they may not be practical for routine implementation. Other simplified attempts to describe zone migration have been proposed, but the inherent assumptions and limitations of these models restrict their use to specific applications.[5,8,16]

In comparison to zone migration, dispersive processes in electrophoresis have received significantly less attention. Since the initial implementation of CZE, longitudinal diffusion has been considered as the major cause of zone broadening.[2] If the technique truly approached the theoretical limit of diffusional broadening, a number of theoretical plates on the order of 10^6 would be expected. In practice, however, such high plate numbers are rarely achieved because additional factors contribute to the loss of separation efficiency. Among the most common sources of broadening are instrumental contributions due to finite volumes for injection and detection.[19,20] In addition, detrimental broadening may result from deviation from the theoretically expected flat velocity profile caused by either laminar flow or thermal effects.[2,20,21] Sample-specific contributions may arise from differences in conductivity between the sample zone and the conducting medium[2] as well as from solute adsorption to the

capillary wall.

In this

through the

incorporates

migration as

the buffer co

judiciously ch

solute zones

assessed by

varying the

optimum con

program mo

phosphate bu

4.2 Optimiz

The c

separations

separation is

chromatogra

statistic (CRS

$$CRS = \left\{ \sum_{i=} \right.$$

where $R_{i,i+1}$

capillary wall.[2,20,21]

In this work, a systematic approach to CZE separations has been devised through the development of a computer optimization routine. The program incorporates theoretical models for both electroosmotic and electrophoretic migration as well as a simple rationale for zone dispersion. Variables related to the buffer composition, capillary dimensions, and instrumental parameters are judiciously chosen as input to the program. The resolution between adjacent solute zones is then calculated and the overall quality of the separation is assessed by means of an appropriate response function. By systematically varying the input parameters and evaluating the resultant separation, the optimum conditions may be identified. The experimental validation of the program models has been demonstrated for a mixture of nucleotides in phosphate buffer solutions.

4.2 Optimization Strategy

The computer routine developed for the optimization of electrophoretic separations is presented schematically in Figure 4.1. The quality of the entire separation is assessed by means of a response function developed originally for chromatographic separations,[22] designated the chromatographic resolution statistic (CRS):

$$CRS = \left\{ \sum_{i=1}^{n-1} \left[\frac{(R_{i,i+1} - R_{opt})^2}{(R_{i,i+1} - R_{min})^2 R_{i,i+1}} \right] + \sum_{i=1}^{n-1} \frac{R^2_{i,i+1}}{(n-1) R^2_{avg}} \right\} \frac{T_f}{n} \quad [4.1]$$

where $R_{i,i+1}$ is the resolution between adjacent solute pairs, R_{avg} is the average

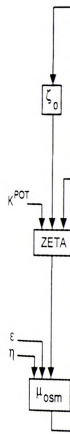

Figure 4.1 Schematic diagram of the computer optimization program for capillary electrophoresis.

Figure 4.1

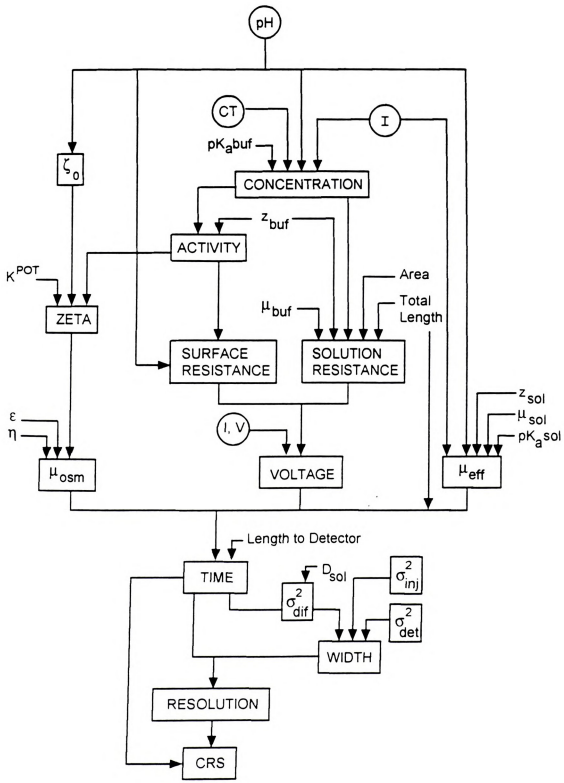
pH
CT
I
pKabuf
ζ0
CONCENTRATION
zbuf
ACTIVITY
KPOT
Area
Total Length
μbuf
ZETA
SURFACE RESISTANCE
SOLUTION RESISTANCE
zsol
μsol
pKasol
ε
η
I, V
μosm
VOLTAGE
μeff
Length to Detector
TIME
Dsol
σ2inj
σ2dif
σ2det
WIDTH
RESOLUTION
CRS

resolution of a
minimum acce
is the number
considers the
resolved pair,
first term in Eq
between all a
optimum and
approaches R
equal to R_{op}
improvement
maintained at
rapidly as $R_{i,i+}$
equal to R_{min}
considers the
approaches a
equal to the a
spaced. The
analysis time a

In capil
zones is defin
by their averag

$$R_{i,i+1} = \frac{2 (}{w}$$

The migration

resolution of all solute pairs, R_{opt} is the optimum desired resolution, R_{min} is the minimum acceptable resolution, T_f is the migration time of the last solute, and n is the number of solutes in the sample. The chromatographic resolution statistic considers the resolution of all solutes in the sample, rather than solely the least-resolved pair, and incorporates three important aspects of the separation. The first term in Equation [4.1], named the resolution term, evaluates the resolution between all adjacent solute pairs in comparison to the defined values for optimum and minimum resolution. The resolution term decreases as $R_{i,i+1}$ approaches R_{opt} and reaches the minimum value of zero when $R_{i,i+1}$ is exactly equal to R_{opt}. Any further increase in resolution offers no additional improvement in the quality of the separation, hence the resolution term is maintained at a constant value close to zero. The resolution term increases rapidly as $R_{i,i+1}$ approaches R_{min} and becomes undefined when $R_{i,i+1}$ is exactly equal to R_{min}. The second term of Equation [4.1], named the distribution term, considers the relative spacing of the solute zones. The distribution term approaches a minimum value of one when the resolution of each solute pair is equal to the average resolution, which is the case when all zones are uniformly spaced. The final multiplier term in Equation [4.1] takes into consideration the analysis time and the complexity of the sample.

In capillary zone electrophoresis, the resolution between adjacent solute zones is defined as the difference between their mean migration time (t) divided by their average temporal base width (w):

$$R_{i,i+1} = \frac{2\,(t_{i+1} - t_i)}{w_i + w_{i+1}} \qquad [4.2]$$

The migration time of each zone to the detector position (L_{det}) is determined by

the net rate
electroosmoti

$$t_i = \frac{L_{det}}{v_i} =$$

where μ_{osm}
respectively, V

For a n
deviation of th

$$w_i = 4\ \tau$$

where τ is exp
the spatial dis

$$\tau = \frac{\sigma}{v_i}$$

The variance
phenomena th
these process

$$\sigma^2 = \Sigma \sigma^2_n$$

where σ^2_n rep

An ov
appropriately
the compute

the net rate of zone migration (v_i), which is a vectorial summation of the electroosmotic (v_{osm}) and electrophoretic (v_{ep}) velocities:

$$t_i = \frac{L_{det}}{v_i} = \frac{L_{det}}{v_{osm} + v_{ep}} = \frac{L_{det}\ L_{tot}}{(\mu_{osm} + \mu_{ep})\ V} \qquad [4.3]$$

where μ_{osm} and μ_{ep} are the electroosmotic and electrophoretic mobilities, respectively, V is the applied voltage, and L_{tot} is the total capillary length.

For a normally distributed zone, the base width is related to the standard deviation of the temporal distribution (τ):

$$w_i = 4\ \tau \qquad [4.4]$$

where τ is expressed in units of time, and is related to the standard deviation of the spatial distribution (σ) by means of the zone velocity:

$$\tau = \frac{\sigma}{v_i} \qquad [4.5]$$

The variance of the spatial distribution (σ^2) arises from several dispersive phenomena that occur during the migration of the solute zone in the capillary. If these processes are independent, then the variances are statistically additive:[23]

$$\sigma^2 = \Sigma\, \sigma^2_n \qquad [4.6]$$

where σ^2_n represents the individual contributions to the total variance.

An overall expression for resolution can be derived by combining appropriately Equations [4.2] to [4.6]. In order to incorporate these equations in the computer optimization routine, independent models for voltage,

electroosmoti
These mode
described in g

Model for Vo
conditions, th
constant-curre
means of Ohm
the conducting

$$\frac{1}{R_{soln}} = \kappa \frac{\pi}{L}$$

where r is the
conductivity is
all ionic specie

$$\kappa = F \sum |z_j$$

where F is the

Figure
solutions at c
determined va
and [4.8], usin
of the system
Ohm's law cu
resulting volta
resistance is s

electroosmotic mobility, electrophoretic mobility, and zone variance are required. These models and their correlation with the experimental variables are described in greater detail in the following sections.

Model for Voltage. When the power supply is operated under constant-voltage conditions, the system voltage is an experimentally available parameter. Under constant-current conditions, however, the voltage must be predicted indirectly by means of Ohm's law. This may be accomplished by evaluating the resistance of the conducting medium (R_{soln}), which is given by:[24]

$$\frac{1}{R_{soln}} = \kappa \frac{\pi r^2}{L_{tot}} \qquad [4.7]$$

where r is the capillary radius and κ is the conductivity of the solution. The conductivity is related to the charge (z_j), mobility (μ_j), and concentration (C_j) of all ionic species in solution by:

$$\kappa = F \Sigma |z_j| \mu_j C_j \qquad [4.8]$$

where F is the Faraday constant.

Figure 4.2 presents the resistance calculated for phosphate buffer solutions at different pH and concentration, in comparison with experimentally determined values. The calculated resistance was derived from Equations [4.7] and [4.8], using literature values of ionic mobility[25] and other known parameters of the system. The experimental resistance was obtained from the slope of an Ohm's law curve (not shown), by applying a constant current and measuring the resulting voltage. The results shown in Figure 4.2 indicate that the prediction of resistance is satisfactory for acidic solutions. However, as the pH increases, the

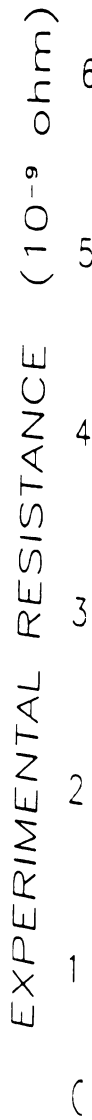

Figure 4.2 Comparison of experimental resistance of phosphate buffer solutions with theoretical calculations according to Equations [4.7] and [4.8]. (▲) pH 4, (■) pH 5, (●) pH 6, (▽) pH 7, (○) pH 8, (□) pH 9, and (△) pH 10.

Figure 4.2

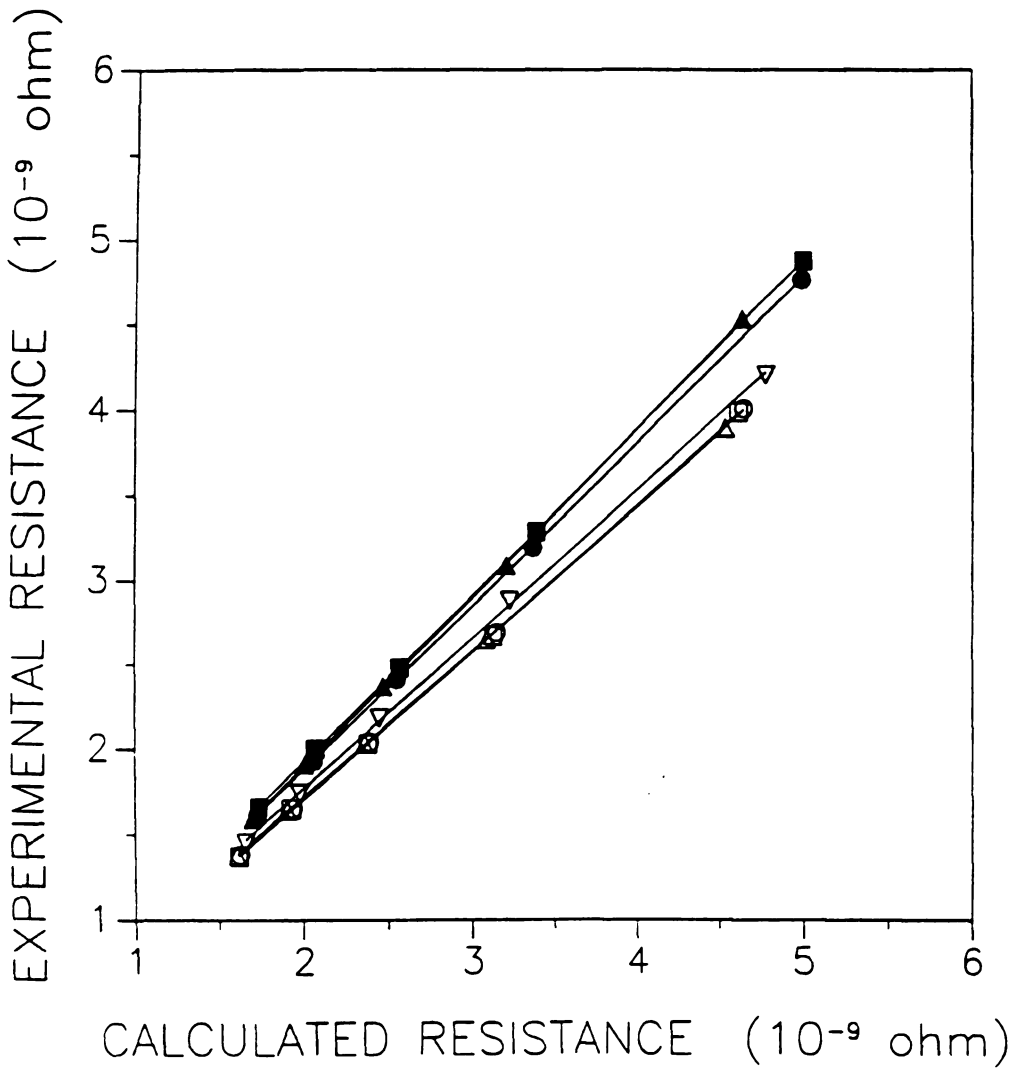

sphate buffer
Equations [4.7]
) pH 7, (O)

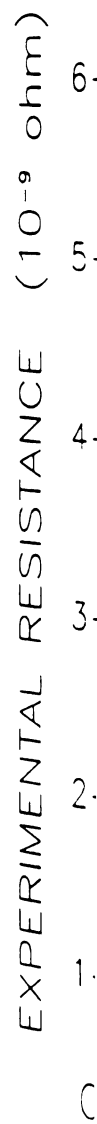

Figure 4.2 Comparison of experimental resistance of phosphate buffer solutions with theoretical calculations according to Equations [4.7] and [4.8]. (▲) pH 4, (■) pH 5, (●) pH 6, (▽) pH 7, (○) pH 8, (□) pH 9, and (△) pH 10.

Figure 4.2

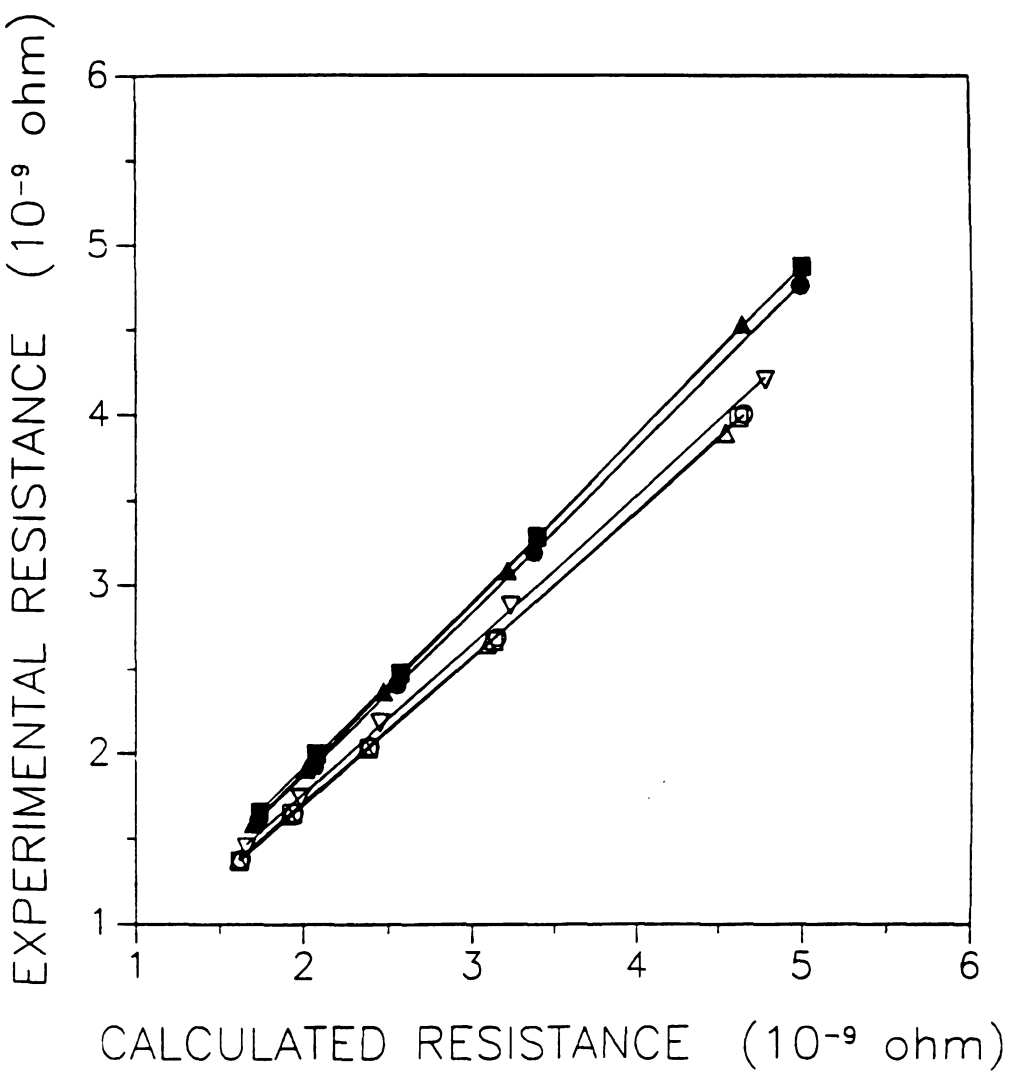

osphate buffer
Equations [4,7]
7) pH 7, (O)

experimental

by the model

the current,

magnitude of

but may beco

area to volum

an equivalen

resistors con

(R) can be e

$$\frac{1}{R} = \frac{}{R}$$

where R_{surf}

therefore de

system and

The curve

solution (a_N

manner:

$$\frac{1}{R_{surf}} = \{$$

where A, B

data presen

5.25×10^{-9}

Figu

silica capill

experimental resistance gradually becomes lower than the resistance predicted by the model. This observation suggests the existence of a secondary path for the current, other than the solution, possibly the capillary surface. The magnitude of surface conductance in silica capillaries is usually negligible,[26,27] but may become significant for capillaries because of their high ration of surface area to volume. The mathematical description of surface conductance invokes an equivalent electric circuit, where the solution and surface are treated as resistors combined in parallel. Therefore, the overall resistance of the system (R) can be evaluated according to:

$$\frac{1}{R} = \frac{1}{R_{soln}} + \frac{1}{R_{surf}} \qquad [4.9]$$

where R_{surf} represents the surface resistance. The surface resistance is therefore derived from experimental measurements of the total resistance of the system and the evaluation of the solution resistance by Equations [4.7] and [4.8]. The curve $1/R_{surf}$ versus pH and the activity of the sodium ion in the buffer solution (a_{Na}) can be numerically fit to an error function[28] in the following manner:

$$\frac{1}{R_{surf}} = \{ [ERF (A\,pH + B)] C + D \}\, a_{Na} \qquad [4.10]$$

where A, B, C, and D are fitting parameters. Typical values obtained from the data presented in Figure 4.2 are: A = 1.16, B = –7.75, C = 3.00×10^{-9}, and D = 5.25×10^{-9}.

Figure 4.3 presents the estimate of the surface conductance of fused-silica capillaries in comparison to the solution conductance for phosphate buffer

Figure 4.3 Conductance of phosphate buffer solutions (a) and silica capillary surface (b) as a function of pH and sodium concentration (5, 7.5, 10, 12.5, and 15 mM from bottom to top).

Figure 3a

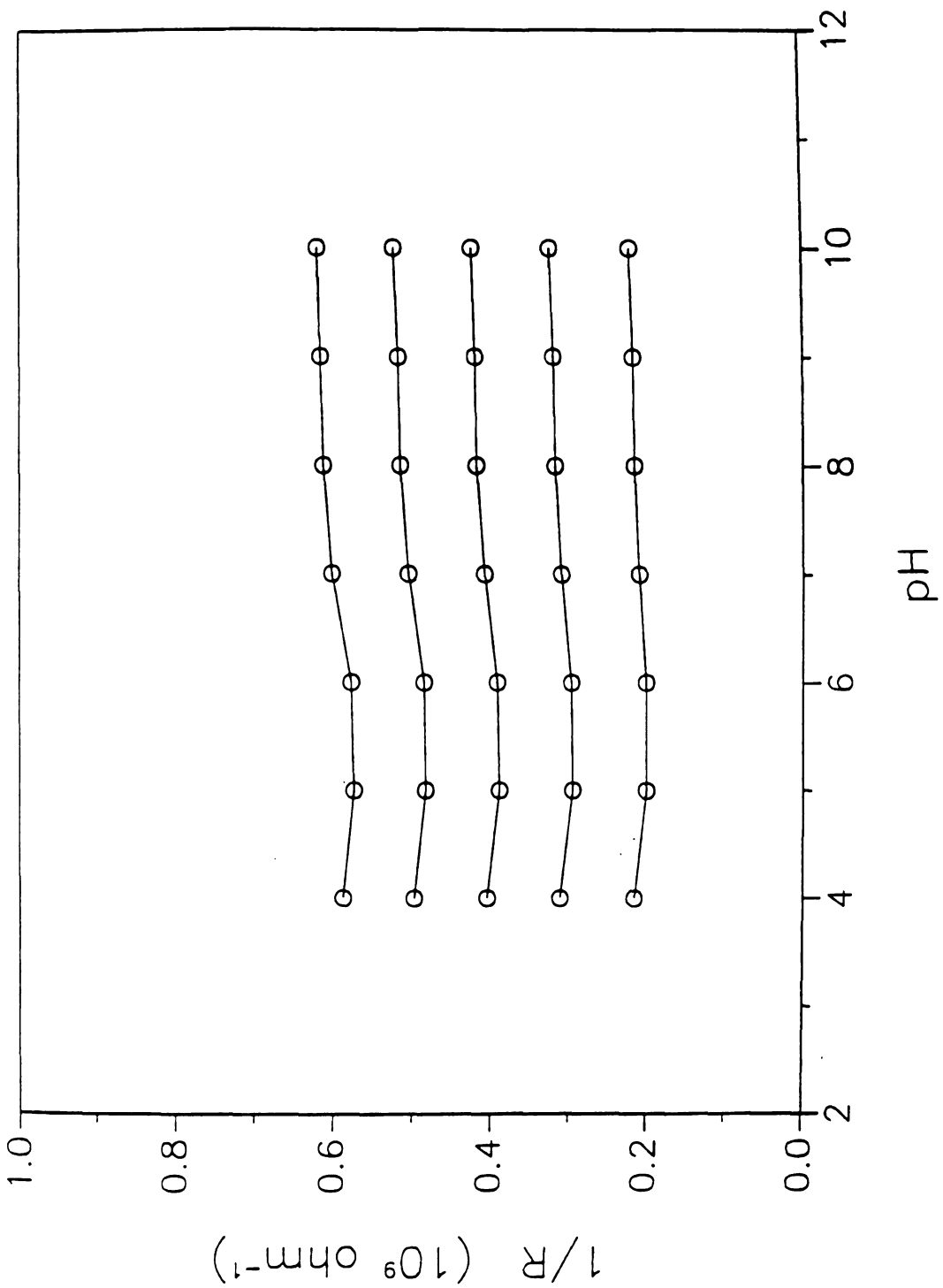

silica capillary
ration (5, 7.5,

Figure 3b

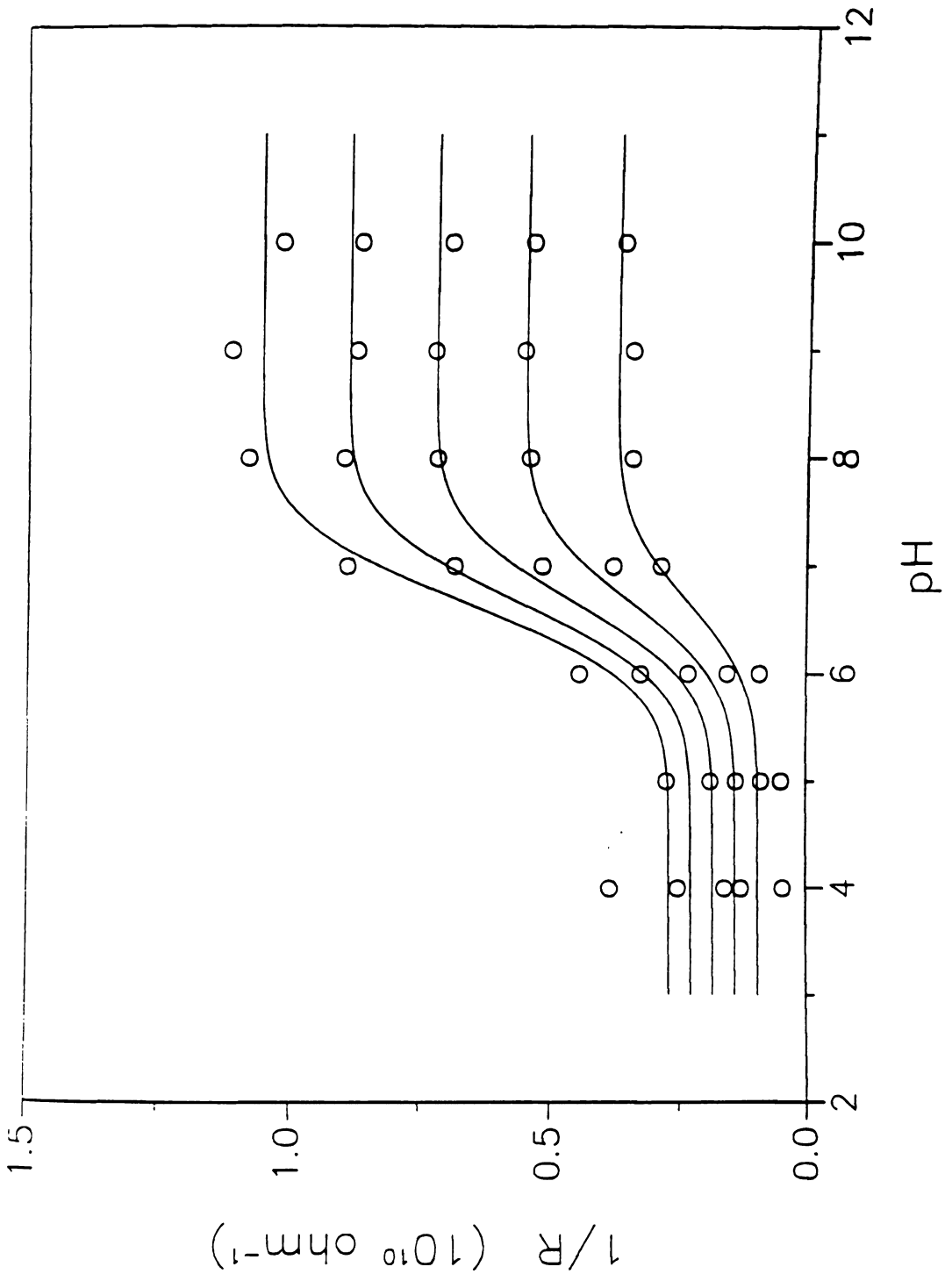

solutions. T
buffer soluti
consequence
concentration
increases, th
compensated
buffer soluti
conductance
dependence
mechanism
subject to sp
of ionized s
increase with
groups on th
providing few
conductance
be transporte
solution imm
might occur i
gel layer at t
for conducti
considerably

In Tab
which incorp
[4.7] to [4.10
concentration
voltage and th

solutions. The solution conductance increases with the sodium content of the buffer solution, but does not vary significantly with pH. This result is a consequence of the manner in which the buffers are prepared, with a constant concentration of sodium ion regardless of the pH. Therefore, as the pH increases, the decrease in the concentration of the highly mobile hydrogen ion is compensated by an increase in the ionic strength of the buffer. As a result, all buffer solutions with the same total sodium concentration possess a similar conductance. In contrast, the surface conductance shows a marked dependence not only on pH, but also on the sodium concentration. The mechanism by which the current is conducted along the capillary surface is subject to speculation. If the mechanism of conduction is related to the presence of ionized silanol groups, the surface conductance would be expected to increase with pH, as observed in Figure 4.3. At low pH, protonation of the silanol groups on the capillary surface occurs to a greater extent (*vide* Chapter 3), providing fewer sites for conduction. However, the dependence of the surface conductance on the sodium concentration suggests that charge might actually be transported by the ions in the electrical double layer. Although the layer of solution immediately adjacent to the surface is immobile, transport of charge might occur in a manner similar to a semi-conductor. Alternatively, the hydrated gel layer at the capillary surface would constitute another appropriate medium for conduction of charge, given that the mobility of ions in this layer is considerably greater than that in the dry silica.[29]

In Table 4.1, the prediction of voltage under constant-current conditions, which incorporates the solution and surface resistance according to Equations [4.7] to [4.10], is evaluated for phosphate buffer solutions at different pH and concentration. A good agreement is observed between the proposed model for voltage and the experimental results, with a typical error of approximately 1.2 %.

Table 4.1

pH
6
7
8
9
10
11

* % ERROR =

Table 4.1 Prediction of voltage in phosphate buffer solutions with total sodium concentration of 10 mM under constant-current conditions of 12.5 μA.

pH	VOLTAGE (kV)		% ERROR*
	EXPERIMENTAL	CALCULATED	
6	29.6	29.9	1.0
7	27.4	26.9	–1.8
8	25.8	25.5	–1.2
9	25.6	25.4	–0.78
10	25.3	25.2	–0.39
11	22.9	23.3	1.7

* % ERROR = (CALC – EXP) x 100 / EXP

Model for El

electroosmot

has been es

4.1. The re

composition

mathematica

composition

ion-selective

$\zeta = \zeta_0 + S$

where a_H an

solution, resp

reference p

mathematica

(ERF) accord

$\zeta_0 = [ERF ($

where A_0, $B_$

mathematica

because of i

versus pH as

acidic sites

abundance is

are related

parameter $C_$

needed for di

Model for Electroosmotic Mobility. A systematic approach to the prediction of electroosmotic flow under both constant-voltage and constant-current conditions has been established in Chapter 3 and is represented schematically in Figure 4.1. The response of the fused-silica capillary surface to changes in buffer composition and pH is modelled in analogy to an ion-selective electrode.[24] The mathematical model predicts the zeta potential (ζ) as a function of the composition of the solution with the corresponding modified Nernst equation for ion-selective electrodes:

$$\zeta = \zeta_0 + \text{SLOPE} \log (a_H + k^{POT} a_{Na}) \qquad [4.11]$$

where a_H and a_{Na} are the activities of hydrogen and sodium ions in the buffer solution, respectively, k^{POT} is the potentiometric selectivity constant, and ζ_0 is a reference potential in the double layer. The potential ζ_0 has been mathematically described by a Gaussian probability integral or error function (ERF) according to:

$$\zeta_0 = [\text{ERF} (A_0 \text{pH} + B_0)] C_0 + D_0 \qquad [4.12]$$

where A_0, B_0, C_0, and D_0 are fitting parameters. Among the many possible mathematical functions with sigmoidal shape,[28] the error function was chosen because of its physical meaning. It is possible to interpret the zeta potential *versus* pH as a titration curve of the acidic sites at the silica surface. These acidic sites are characterized by different types of silanol groups, whose abundance is assumed to be normally distributed. The parameters A_0 and B_0 are related to the mean and standard deviation of the distribution. The parameter C_0 confers the height to the sigmoidal curve and the parameter D_0 is needed for displacement in the zeta potential axis.

The u

by regressio

for fused-silic

= 44.4 mV/p

With knowle

accurately pr

$\mu_{osm} = -$

where η an

respectively,

The p

mobility in pl

increasing a

model deper

buffer soluti

mobility from

phosphate b

between pre

However, er

used for six

irreversible a

during the all

Model for E

several ioni

The unknown parameters in Equation [4.11] and [4.12] were determined by regression analysis using the least-square method. Typical values obtained for fused-silica capillaries with phosphate buffer solutions are as follows: SLOPE = 44.4 mV/pH, k^{POT} = 0.22, A_0 = –0.86, B_0 = 5.11, C_0 = 33.2, and D_0 = 59.7. With knowledge of the zeta potential, the electroosmotic mobility can be accurately predicted by means of the Helmholtz-Smoluchowski equation:[26]

$$\mu_{osm} = - \frac{\varepsilon \, \varepsilon_0 \, \zeta}{\eta} \qquad [4.13]$$

where η and ε are the viscosity and the dielectric constant of the medium, respectively, and ε_0 is the permittivity of the vacuum.

The proposed model has been applied to the prediction of electroosmotic mobility in phosphate buffer solutions in the pH range from 4 to 10, containing increasing amounts of sodium chloride from 5 to 15 mM. The success of the model depends on the rigorous control of the sodium content and pH of the buffer solution. Table 4.2 compares the predicted values of electroosmotic mobility from Equations [4.11] to [4.13] with experimental measurements using phosphate buffer solutions in both new and used capillaries. The agreement between predicted and experimental values for new capillaries is typically 2.3 %. However, errors as large as 9.6 % are obtained with capillaries that have been used for six months. The observed loss of accuracy may be attributed to irreversible alteration of the capillary surface caused by continuous etching during the alkaline solution rinses.

Model for Effective Electrophoretic Mobility. For a solute (i) that consists of several ionic and neutral species (j) interacting by a dynamic acid-base

Table 4.2

pH	
6	
7	
8	
9	
10	
11	

* % ERROR =

Table 4.2 Prediction of the electroosmotic mobility in new and six-month used capillaries, using phosphate buffer solutions with total sodium concentration of 10 mM under constant-current conditions of 12.5 μA.

pH	ELECTROOSMOTIC MOBILITY ($\times 10^5$ $cm^2 V^{-1} s^{-1}$)			% ERROR*	
	EXPERIMENTAL		CALCULATED		
	NEW	USED		NEW	USED
6	50.9	54.4	49.2	–3.3	–9.6
7	67.4	70.1	69.0	2.4	–1.6
8	74.5	75.8	73.9	–0.81	–2.5
9	72.8	81.0	74.3	2.1	–8.3
10	76.7	82.0	74.3	–3.1	–9.4
11	——	81.1	74.2	——	–8.5

* % ERROR = (CALC – EXP) x 100 / EXP

equilibrium, t

$(\mu_{eff})_i = \Sigma$

where α_j re
dissociation
each individu

The p
dissociation
experimenta
advantageou
constants a
composed o
experimenta
more comp
conceptual
distribution
function of p
of each dis
individual sp
curve that a
of two distri
species, whe
point in the
the effectiv
regression,
the individua

equilibrium, the effective electrophoretic mobility (μ_{eff}) is defined as:

$$(\mu_{eff})_i = \Sigma (\alpha_j \mu_j) \qquad [4.14]$$

where α_j represents the distribution functions,[30] which are related to the dissociation constants (K_a) of the solutes, and μ_j is the electrophoretic mobility of each individual species.

The prediction of effective mobility relies on accurate values of the dissociation constants and electrophoretic mobilities. Although there are many experimental methods for the determination of these parameters,[31,32] it is advantageous to use electrophoretic methods because both dissociation constants and mobilities can be derived simultaneously.[33] For solutes composed of less than three species, these parameters may be determined from experimental data by direct solution of the equations of mass balance;[8,34,35] for more complex solutes, a numerical procedure may be employed. The conceptual basis of this procedure is illustrated in Figure 4.4, where the distribution functions for guanosine 5'-monophosphate are represented as a function of pH (mobility and pK_a data from Table 5.1, Chapter 5). The maximum of each distribution function defines the pH region of predominance for an individual species. In this region, a plateau is observed in the effective mobility curve that approximates the mobility of that individual species. The intersection of two distribution functions defines the point of equal concentration for two species, where the pH is equal to the pK_a. This point coincides with an inflection point in the effective mobility curve. Therefore, experimental measurements of the effective mobility as a function of pH can be analyzed by numerical regression, where the plateaus and inflection points serve as initial estimates of the individual mobilities and dissociation constants (pK_a), respectively. The best

Figure 4.4 Distribution functions of guanosine 5'-monophosphate in phosphate buffer solution, together with individual and effective electrophoretic mobilities.

Figure 4.4

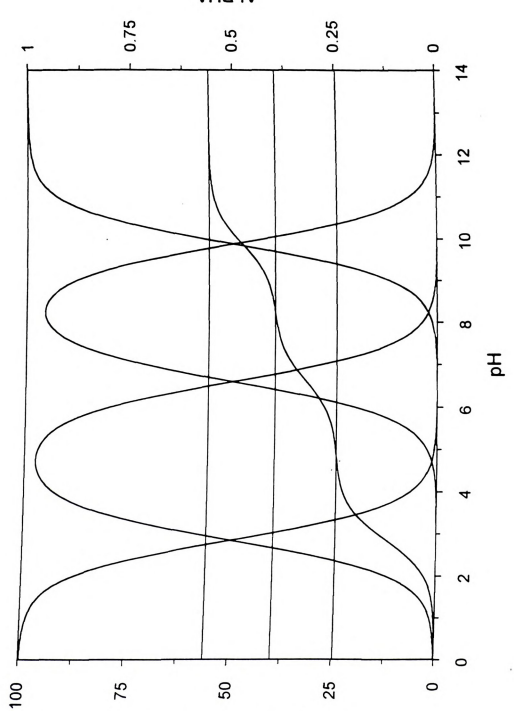

te in phosphate
and effective

values for

method.[3,4]

number of

determine th

the dissocia

data in the a

values is mo

mobilities is

likely to be s

The

and individu

Therefore, t

thermodyna

of activity co

$$-\log \gamma_i = 0$$

where I is

mobility can

$$\mu = \mu_0 -$$

where μ_0 is

counterion.

Table

adenosine r

values for these parameters can then be determined by the least-square method.[3,4] This procedure, in principle, is applicable to solutes consisting of any number of species. However, the ability to differentiate and accurately determine the parameters for all species depends on the relative magnitude of the dissociation constants and mobilities, as well as the number of experimental data in the appropriate pH region. In general, if the difference between the pK_a values is more than two pH units and the difference between the electrophoretic mobilities is more than 10^{-4} cm^2 V^{-1} s^{-1}, the numerical regression procedure is likely to be successful.

The optimization program uses thermodynamic dissociation constants and individual electrophoretic mobilities at the condition of infinite dilution. Therefore, both parameters must be corrected for ionic strength effects. The thermodynamic constants are related to the stoichiometric constants by means of activity coefficients (γ_i), which are calculated by the Davies equation:[24,36]

$$-\log \gamma_i = 0.509\ z_i^2 \left[\frac{\sqrt{I}}{1 + \sqrt{I}} - 0.15\ I \right] \qquad [4.15]$$

where I is the ionic strength and z_i is the charge of the individual species. The mobility can be corrected by means of the Onsager equation:[25]

$$\mu = \mu_0 - (0.23\ \mu_0\ |\ z_i\ z_R\ |\ +\ 31.3 \times 10^{-9}\ |\ z_i\ |\ ) \frac{\sqrt{I}}{1 + \sqrt{I}} \qquad [4.16]$$

where μ_0 is the mobility at zero ionic strength and z_R is the charge of the counterion.

Table 4.3 compares the experimentally determined effective mobility of adenosine monophosphate with predicted values. The predicted values of the

Table 4.3

pH
6
7
8
9
10
11

* % ERROR =

Table 4.3 Prediction of the effective electrophoretic mobility of adenosine monophosphate in phosphate buffer solutions with total sodium concentration of 10 mM under constant-current conditions of 12.5 μA.

pH	EFFECTIVE MOBILITY ($\times 10^5$ $cm^2 V^{-1} s^{-1}$)		% ERROR*
	EXPERIMENTAL	CALCULATED	
6	–22.4	–23.1	3.1
7	–30.0	–28.9	–3.7
8	–31.0	–31.5	1.6
9	–33.0	–31.8	–3.6
10	–32.7	–31.9	–2.4
11	–31.1	–32.0	2.9

* % ERROR = (CALC – EXP) x 100 / EXP

effective mo

mobility of r

entire pH ra

experimenta

Model for Z

considered:

volumes (σ^2

The v

equation:[23]

$$\sigma^2_{dif} = 2 D$$

where D_i is

the residenc

exclusively

and other in

Equation [4.

$$\sigma^2_{dif} = \frac{2}{(\mu_0}$$

The

approximate

zone profile:

$$\sigma^2_{inj} = \frac{\ell^2_{in}}{12}$$

effective mobility were calculated from the pK_a and individual electrophoretic mobility of nucleotides determined in Chapter 5 (*vide* Table 5.1). Within the entire pH range, the prediction of effective mobility is in good agreement with the experimental results, with an average relative error of 2.9 %.

Model for Zone Variance. In this work, three sources of broadening were considered: longitudinal diffusion (σ^2_{dif}), and finite injection and detection volumes (σ^2_{inj} and σ^2_{det}, respectively).

The variance resulting from longitudinal diffusion is given by the Einstein equation:[23]

$$\sigma^2_{dif} = 2\ D_i\ t_i \qquad [4.17]$$

where D_i is the diffusion coefficient of the solute i. The variance is a function of the residence time of the solute in the capillary and, hence, does not depend exclusively on the solute characteristics but also on the electroosmotic mobility and other instrumental parameters. By substituting the migration time given by Equation [4.3] into Equation [4.17], this influence becomes explicitly clear:

$$\sigma^2_{dif} = \frac{2\ D_i\ L_{det}\ L_{tot}}{(\mu_{osm} + \mu_{ep})\ V} \qquad [4.18]$$

The contribution to variance caused by a finite injection volume is approximated by the expression developed by Sternberg[37] for a rectangular zone profile:

$$\sigma^2_{inj} = \frac{\ell^2_{inj}}{12} \qquad [4.19]$$

In order to e

must be co

establishing

Under the co

by means of

$$\ell_{inj,hf} = \frac{\Delta}{8}$$

where t_{inj} is

difference al

by applying

pressure diff

achieved by

$$\Delta P = \rho g$$

where ΔH is

outlet reser

acceleration

which is cha

[4.19] and [4

In ele

voltage grad

injection zo

mobilities an

In order to evaluate the length of the injection zone (ℓ_{inj}), the mode of injection must be considered. In hydrodynamic injection, the sample is introduced by establishing a pressure gradient along the capillary for a brief period of time. Under the condition of laminar flow, the length of the injection zone is determined by means of the Hagen-Poiseuille equation:[23]

$$\ell_{inj,hf} = \frac{\Delta P \; r^2}{8 \; \eta \; L_{tot}} \; t_{inj} \qquad [4.20]$$

where t_{inj} is the injection time, η is the fluid viscosity, and ΔP is the pressure difference along the capillary length. When hydrodynamic injection is performed by applying pressure at the capillary inlet or vacuum at the capillary outlet, the pressure difference along the capillary is a known parameter. When injection is achieved by siphoning action, the pressure difference can be calculated as:

$$\Delta P = \rho \; g \; \Delta H \qquad [4.21]$$

where ΔH is the height difference between the solution level at the inlet and outlet reservoirs, ρ is the density of the solution, g is the gravitational acceleration constant. The dispersion caused by a parabolic velocity profile, which is characteristic of pressure-driven flow, was disregarded in Equations [4.19] and [4.20].

In electrokinetic injection, the sample is introduced by establishing a voltage gradient along the capillary for a brief period of time. The length of the injection zone is determined from the electroosmotic and electrophoretic mobilities and the injection time:

$\ell_{inj,ek}$ = (μ

In an
transducer
transducer h
the zone d
approximate

$$\sigma^2_{det} = \frac{\ell^2_d}{12}$$

where ℓ_{det} i

The
therefore, th
spatial distri
appear to b
4.4, with an

Chromatog
various res
separation,3
advantageou
resolution, d
function eva
of the nucle
qualitative in
the best sep

$$\ell_{inj,ek} = (\mu_{osm} + \mu_{ep}) \frac{V}{L_{tot}} t_{inj} \qquad [4.22]$$

In any detector device, a finite volume of solution is in contact with the transducer and the output signal represents an average response. If the transducer has distinct spatial boundaries and uniform response along its length, the zone distribution is rectangular in profile, so that the variance can be approximated by the Sternberg equation:[37]

$$\sigma^2_{det} = \frac{\ell^2_{det}}{12} \qquad [4.23]$$

where ℓ_{det} is the length of the detector window.

The processes of diffusion, injection, and detection are independent; therefore, their variances can be added to represent the overall variance of the spatial distribution, as expressed by Equation [4.6]. These sources of variance appear to be sufficient to describe the experimental results, as shown in Table 4.4, with an average relative error of 9.4 %.

Chromatographic Resolution Statistic as a Response Function. Among the various response functions used to numerically assess the quality of a separation,[38-40] the chromatographic resolution statistic (CRS)[22] is advantageous because it comprises three important features of the separation: resolution, distribution, and analysis time. In order to understand how the CRS function evaluates a separation, several computer-simulated electropherograms of the nucleotide mono- and di-phosphates are displayed in Figure 4.5. By qualitative inspection, the electropherogram at pH 10 may be easily identified as the best separation, whereas that at pH 11 is the second best. In both of these

Table 4.4

pH
6
7
8
9
10
11

* % ERROR

Table 4.4 Prediction of the zone variance for adenosine monophosphate in phosphate buffer solutions with total sodium concentration of 10 mM under constant-current conditions of 12.5 μA.

pH	ZONE VARIANCE (cm^2)		% ERROR*
	EXPERIMENTAL	CALCULATED	
6	0.0372	0.0353	–5.1
7	0.0276	0.0335	21
8	0.0295	0.0331	12
9	0.0314	0.0327	4.1
10	0.0292	0.0325	11
11	0.0344	0.0334	–2.9

* % ERROR = (CALC – EXP) x 100 / EXP

Figure 4.5 Computer-simulated electropherograms of the nucleotides (1) AMP, (2) CMP, (3) GMP, (4) UMP, (5) ADP, (6) CDP, (7) GDP, and (8) UDP at different pH conditions.

Figure 4.5

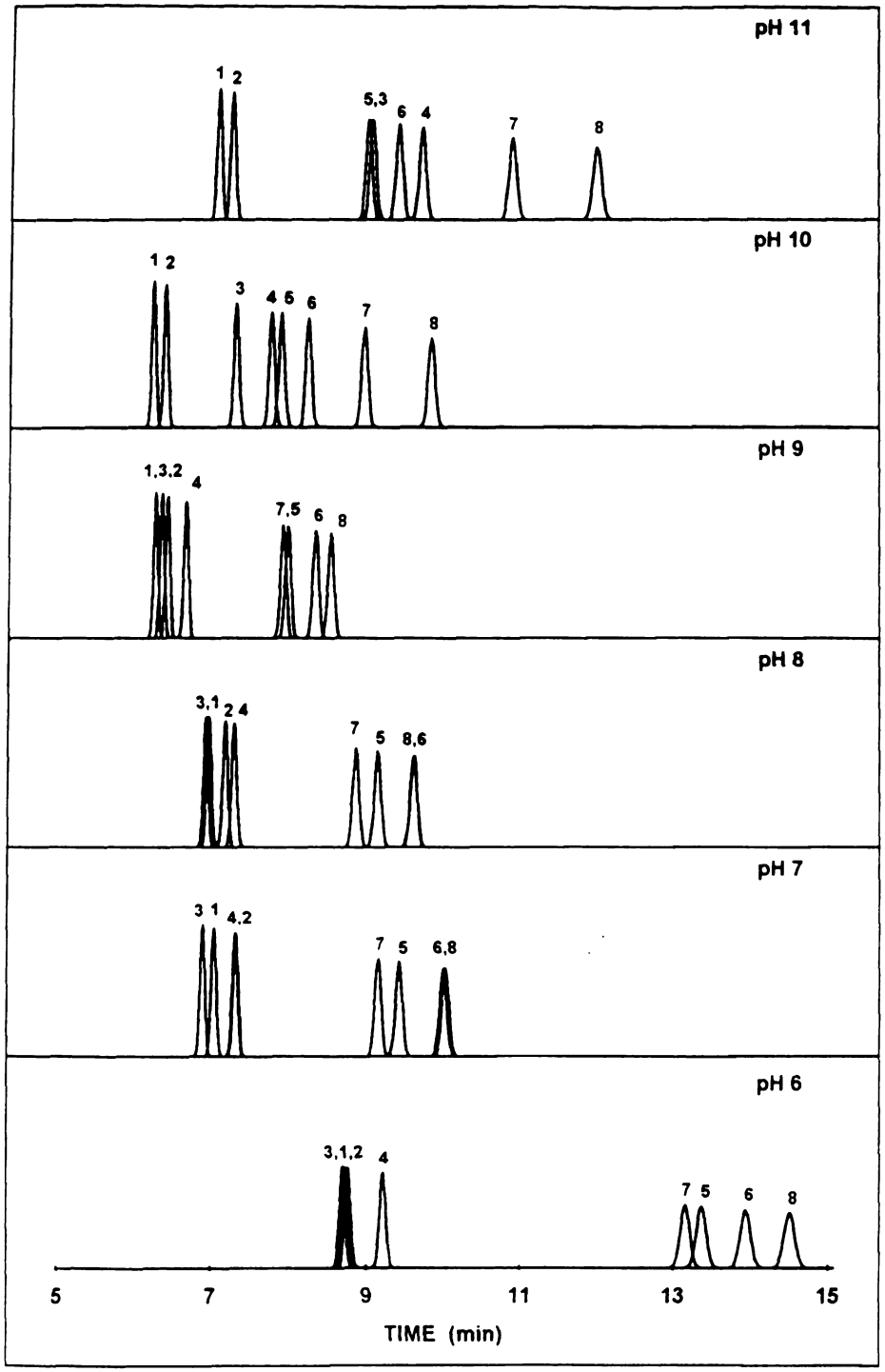

nucleotides (1)
) CDP, (7) GDP,

electrophere
remaining
unresolved
would be c
unambiguou
be conside
accurate de
in principle,
mathematic

For
correspondi
[4.1] are su
CRS value,
distinctly su
still conside
term and th
optimum co
of peak spa
value becau
in good acc

Upon
function are
range of v
separations
separation
separation,
goals that

electropherograms, a single pair of solutes is overlapped ($R_{i,i+1} \leq 1.5$). In the remaining electropherograms from pH 6 to 9, three pairs of solutes are unresolved to different degrees. Among these latter electropherograms, pH 9 would be considered the most desirable if qualitative analysis is the goal, since unambiguous identification of all eight solutes is possible. However, pH 6 would be considered the most desirable if quantitative analysis is the goal, since accurate determination of five solutes is possible. The response function should, in principle, be able to represent these subjective evaluations in an objective mathematical manner.

For each of the electropherograms shown in Figure 4.5, the corresponding values of the CRS function and its individual terms from Equation [4.1] are summarized in Table 4.5 ($R_{opt} = 1.5$, $R_{min} = 0$). According to the total CRS value, the overall quality of the separations at pH 9 to 11 is ranked as distinctly superior. The separation at pH 6, while significantly less desirable, is still considered to be of higher quality than those at pH 7 and 8. The resolution term and the distribution term correctly identify the separation at pH 10 as the optimum condition, because of the high degree of resolution and the uniformity of peak spacing. The multiplier term assigns the separation at pH 9 the smallest value because of the comparatively short analysis time. These conclusions are in good accord with the subjective evaluation of the separation.

Upon inspection of Table 4.5, several important features of the CRS function are apparent. First, the resolution term has the greatest magnitude and range of values and, hence, generally controls the relative ranking of the separations. This is intuitively desirable, since the primary goal of any separation is to achieve resolution of all solutes. The other aspects of the separation, spatial distribution of the zones and analysis time, are secondary goals that become important only when all solutes have been adequately

Table 4.5

pH
6
7
8
9
10
11

Table 4.5 Evaluation of the chromatographic resolution statistic (CRS) as a response function using optimum resolution (R_{opt}) of 1.5 and minimum resolution (R_{min}) of 0.

pH	CHROMATOGRAPHIC RESOLUTION STATISTIC			
	RESOLUTION TERM	DISTRIBUTION TERM	MULTIPLIER TERM	TOTAL CRS
6	228	3.5	1.8	420
7	4478	2.8	1.3	5612
8	2745	2.7	1.2	3304
9	19	2.5	1.1	23
10	0.89	1.4	1.2	2.8
11	48	1.8	1.5	74

selected va

in Table 4.5

Table 4.6 (F

resolution t

passes thro

becomes

separation

example, th

and 0.73 a

in Table 4.

whether hi

4.7 (R_{opt} =

the CRS fu

the judiciou

the separa

4.3 Use

Cap

The

separation

evaluated

learning t

critical pa

order to il

and uridir

selected values of R_{opt} and R_{min}. The relative ranking of the separations shown in Table 4.5 (R_{opt} = 1.5, R_{min} = 0) is completely different from that shown in Table 4.6 (R_{opt} = 1.5, R_{min} = 0.75). Because of the mathematical features of the resolution term, $(R_{i,i+1} - R_{opt})^2$ passes through a minimum and $1/(R_{i,i+1} - R_{min})^2$ passes through a maximum as $R_{i,i+1}$ increases. As a result, the CRS value becomes extremely high and is no longer representative of the overall separation quality when any individual value of $R_{i,i+1}$ approaches R_{min}. For example, the separation at pH 9 contains individual resolution elements of 0.70 and 0.73 and, therefore, is ranked as the second best in Table 4.5 but the worst in Table 4.6. More importantly, values of $R_{i,i+1}$ that are equidistant from R_{min}, whether higher or lower in magnitude, are ranked equally. As shown in Table 4.7 (R_{opt} = 1.5, R_{min} = 1.0), the resolution term becomes relatively constant and the CRS function provides little discrimination of the separation quality. Hence, the judicious choice of these parameters is critical to the objective assessment of the separation and the correct identification of the optimum conditions.

4.3 Use of the Optimization Program as a Pedagogical Approach to Capillary Zone Electrophoresis

The optimization program developed to assess electrophoretic separations can be operated in such a way that one single set of conditions is evaluated at a time. With this approach, the program becomes a powerful learning tool that can be used advantageously to examine the influence of critical parameters on the separation efficiency, resolution, and analysis time. In order to illustrated this concept, the nucleotides adenosine, guanosine, cytidine, and uridine 5'-mono- and di-phosphates were chosen as model solutes and their

Table 4.6

pH
6
7
8
9
10
11

Table 4.6 Evaluation of the chromatographic resolution statistic (CRS) as a response function using optimum resolution (R_{opt}) of 1.5 and minimum resolution (R_{min}) of 0.75.

pH	CHROMATOGRAPHIC RESOLUTION STATISTIC			
	RESOLUTION TERM	DISTRIBUTION TERM	MULTIPLIER TERM	TOTAL CRS
6	136	3.5	1.8	252
7	91	2.8	1.3	117
8	102	2.7	1.2	126
9	2422	2.5	1.1	2600
10	16	1.4	1.2	21
11	24	1.8	1.5	39

Table 4.7

pH
6
7
8
9
10
11

Table 4.7 Evaluation of the chromatographic resolution statistic (CRS) as a response function using optimum resolution (R_{opt}) of 1.5 and minimum resolution (R_{min}) of 1.0.

pH	CHROMATOGRAPHIC RESOLUTION STATISTIC			
	RESOLUTION TERM	DISTRIBUTION TERM	MULTIPLIER TERM	TOTAL CRS
6	42	3.5	1.8	82
7	48	2.8	1.3	64
8	66	2.7	1.2	82
9	31	2.5	1.1	36
10	48	1.4	1.2	61
11	10	1.8	1.5	18

separation
4.6a, a typ
initial stand
This outpu
under the
electropho
electroosm
resistance)
dimensions
necessary
the comp
correspond
completed
plates per
the least-re

As a
CZE syste
and length
are include
will be eva
outlet rese
next studie
ionic stren
capillary s
magnitude

separation is simulated and compared under a variety of conditions. In Figure 4.6a, a typical output of the program illustrates the set of parameters chosen as initial standard conditions (current, buffer pH, ionic strength and concentration). This output also gives the complete characterization of the separation achieved under the stated conditions (resolution, variances, and efficiency), the solute electrophoretic behavior (migration time and effective mobility), the electroosmotic flow properties (zeta potential, electroosmotic mobility, resistance) as well as other instrumental related parameters (voltage, capillary dimensions, injection characteristics). Finally, the analytical concentrations necessary to prepare the phosphate buffer solution is provided. In Figure 4.6b, the computer-generated electropherogram of the mixture of nucleotides corresponding to the standard conditions is presented. The separation is completed in about 10 min, with an average efficiency of 1.4×10^5 theoretical plates per meter. Also, all solutes have been completely resolved (resolution of the least-resolved pair is 1.88).

As an initial comparative study, the effect of the parameters related to the CZE system is evaluated. In this category, the capillary dimensions of diameter and length, as well as the detection position and window length exposed to light are included. Next, some characteristics of the hydrodynamic injection method will be evaluated, such as the height difference between the capillary inlet and outlet reservoirs and also the injection time. The effect of the applied current is next studied. Then the buffer properties of the buffer solutions, including the pH, ionic strength and concentration, are examined. Finally, the effect of the capillary surface charge density as a means to control the electroosmotic flow magnitude is explored.

Figure 4.6 Computer-simulated separation of nucleotides under standard conditions. Solute identification as in Figure 4.5. (a) Electropherogram. (b) Simulated data.

Figure 4.6a

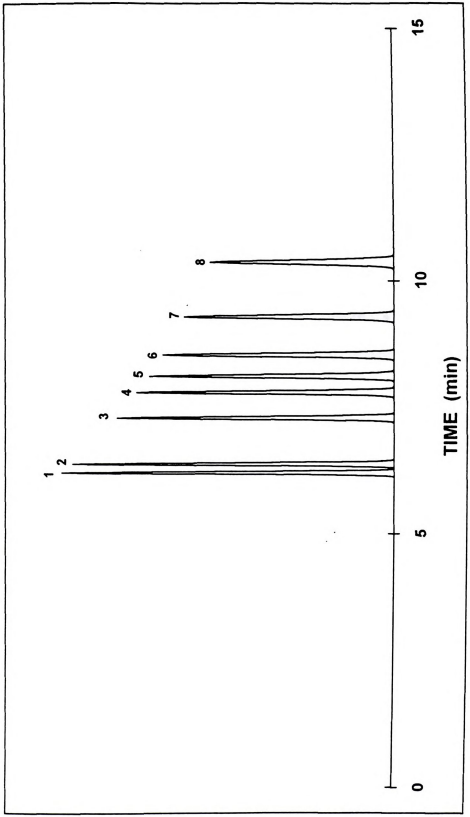

s under standard
Figure 4.5. (a)

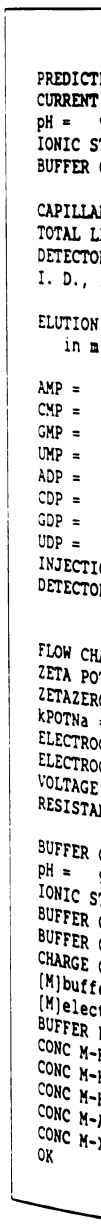
PREDICT
CURRENT
pH =
IONIC S
BUFFER
CAPILLA
TOTAL L
DETECTO
I. D.,
ELUTION
in m
AMP =
CMP =
GMP =
UMP =
ADP =
CDP =
GDP =
UDP =
INJECTI
DETECTO
FLOW CH
ZETA PO
ZETAZER
kPOTNa
ELECTRO
ELECTRO
VOLTAGE
RESISTA
BUFFER
pH =
IONIC S
BUFFER
BUFFER
CHARGE
[M]buff
[M]elec
BUFFER
CONC M-
CONC M-
CONC M-
CONC M-
CONC M-
OK

Figure 4.6b

```
PREDICTED OPTIMUM CONDITIONS FOR THE SEPARATION:
CURRENT, in microamperes =  17.000
pH =   9.800                          Correction Factor, in pH units =   .0000
IONIC STRENGTH, in moles/liter = 1.2500E  -2
BUFFER CONCENTRATION, in moles/liter = 2.5000E  -3

CAPILLARY DIMENSIONS:                 TYPE OF INJECTION: HYDRODYNAMIC
TOTAL LENGTH, in cm =  100.00         HEIGHT DIFFERENCE, in cm =    2.00
DETECTOR LENGTH, in cm =   50.00      INJECTION TIME, in sec =   60.00
I. D., in micrometers =   75.00       HYDRODYNAMIC VELOCITY, in cm/s = 3.93E  -3

ELUTION TIME   WIDTH      EFFECTIVE       DIFFUSION    EFFICIENCY    RESOLUTION
   in min      in min     MOBILITY        VARIANCE
                          in cm2/Vs        in cm2
AMP =   6.20     .090     -.3185E  -3     7.44E  -3    7.56E   4        1.88
CMP =   6.37     .093     -.3300E  -3     7.64E  -3    7.52E   4        9.06
GMP =   7.28     .108     -.3816E  -3     8.73E  -3    7.28E   4        4.48
UMP =   7.78     .116     -.4049E  -3     9.34E  -3    7.15E   4        2.69
ADP =   8.10     .122     -.4183E  -3     9.72E  -3    7.07E   4        3.31
CDP =   8.52     .129     -.4341E  -3     1.02E  -2    6.97E   4        5.61
GDP =   9.28     .142     -.4594E  -3     1.11E  -2    6.80E   4        7.22
UDP =  10.37     .162     -.4895E  -3     1.24E  -2    6.56E   4    CRS =    2.67_
INJECTION ZONE,  in cm =     .24         INJ VARIANCE, in cm2 = 4.63E  -3
DETECTOR WINDOW, in cm =     .50         DET VARIANCE, in cm2 = 2.08E  -2


FLOW CHARACTERISTICS:
ZETA POTENTIAL, in mV =  -93.54
ZETAZERO, in mV =   26.44
kPOTNa = 2.2347E  -1
ELECTROOSMOTIC MOBILITY, in cm2/Vs = 7.4300E  -4
ELECTROOSMOTIC VELOCITY, in cm/s =   .2349
VOLTAGE, in kV =  31.610
RESISTANCE, in ohm = 1.8594E   9

BUFFER CHARACTERISTICS (conc in moles/liter):
pH =   9.800
IONIC STRENGTH = 1.2500E  -2
BUFFER CONCENTRATION = 2.5000E  -3
BUFFER CAPACITY = 2.0380E  -4
CHARGE CONC = 1.9956E  -2
[M]buffer = 5.0796E  -3
[M]electr = 4.8985E  -3
BUFFER FORMULATION:
CONC M-H3A = 0.0000E  -1
CONC M-H2A = 0.0000E  -1
CONC M-HA = 2.4204E  -3
CONC M-A = 7.9567E  -5
CONC M-X = 4.8985E  -3
OK
```

In F
quality is
conditions
increases
differences
conductan
capillary su
this work,
approxima
the surface
thus, is r
simulated
significantl
its initial va

Figu
nucleotides
constant, t
compared
analysis ti
the mixture
are also ap
time due t
capillaries
diameter c
the solution

In c
resolution.

In Figure 4.7, the effect of the capillary total length on the separation quality is studied by comparison with the results obtained for the standard conditions of Figure 4.6. Under constant-current conditions, the resistance increases linearly with the capillary length and so does the voltage. The minor differences observed in migration time result from the overestimation of surface conductance in the shorter capillaries. Surface conductance is a function of the capillary surface area, which is the capillary perimeter multiplied by its length. In this work, surface conductance was characterized for a 75 μm diameter, approximately 100 cm long capillary. The model developed voltage considers the surface conductance as a function of the characteristics of the solution and thus, is restricted to the above cited capillary dimensions. However, the simulated data suggest that the surface conductance may not be affected significantly by the capillary length. By decreasing the capillary lenght to half of its initial value, the calculated voltage is higher than expected by only 1%.

Figure 4.8 presents the effect of the capillary diameter in the separation of nucleotides. In spite of the fact that the applied current and capillary length are constant, there is a much higher field strength in the 75 μm capillary (316 V/cm) compared to the 125 μm (124 V/cm). As a result, an appreciable gain in analysis time and efficiency is achieved without compromise of the resolution of the mixture. The restrictions discussed above regarding surface conductance are also applicable here. However, the ultimate error introduced in the migration time due to false estimation of surface conductance may be critical only when capillaries with diameters much smaller than 75 μm are considered. For wider diameter capillaries, the surface conductance becomes negligible compared to the solution conductance which varies inversely with the square of the radius.

In capillary zone electrophoresis, there is a spatial dependence on resolution. Therefore, the placement of the detector along the capillary length

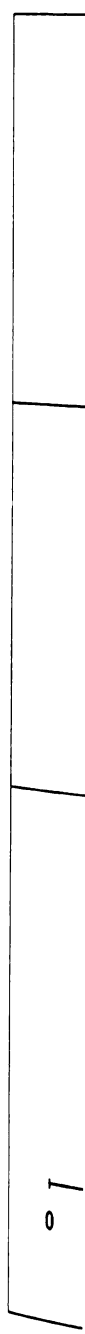

Figure 4.7 Effect of the capillary length (L_{tot}) on the separation of nucleotides. Solute identification and standard conditions as given in Figure 4.6. (a) Computer-simulated electropherograms for 50, 75, and 100 cm capillary length. (b) Separation characteristics for 50 cm capillary length. (c) Separation characteristics for 75 cm capillary length.

Figure 4.7a

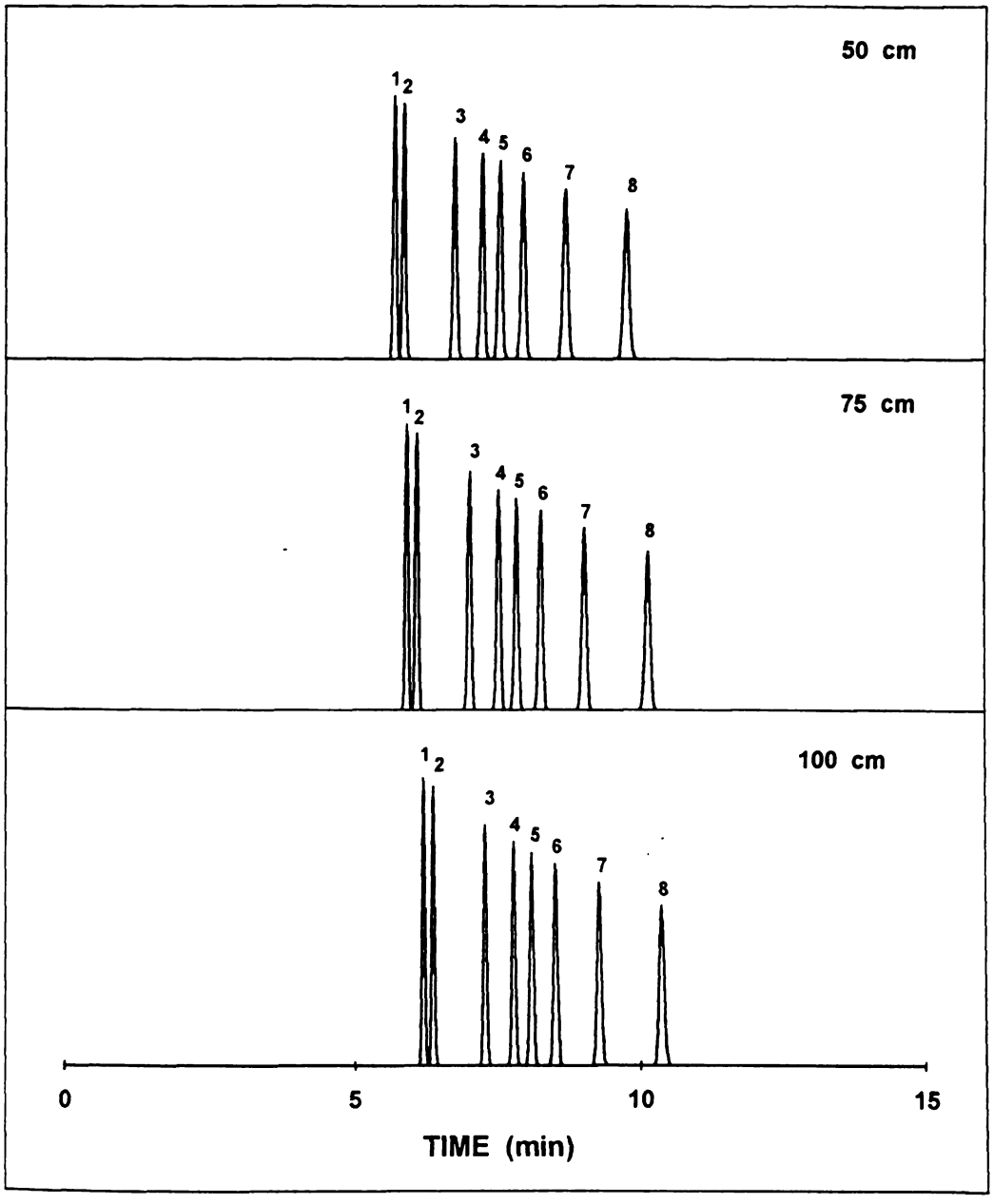

on of nucleotides.
s given in Figure
s for 50, 75, and
eristics for 50 cm
or 75 cm capillary

Figure 4.7b

```
PREDICTED OPTIMUM CONDITIONS FOR THE SEPARATION:
CURRENT, in microamperes =  17.000
pH =   9.800                        Correction Factor, in pH units =   .0000
IONIC STRENGTH, in moles/liter = 1.2500E  -2
BUFFER CONCENTRATION, in moles/liter = 2.5000E  -3

CAPILLARY DIMENSIONS:               TYPE OF INJECTION: HYDRODYNAMIC
TOTAL LENGTH, in cm =   50.00       HEIGHT DIFFERENCE, in cm =    2.00
DETECTOR LENGTH, in cm =   50.00    INJECTION TIME, in sec =   60.00
I. D., in micrometers =   75.00     HYDRODYNAMIC VELOCITY, in cm/s = 7.85E  -3

ELUTION TIME   WIDTH      EFFECTIVE       DIFFUSION    EFFICIENCY    RESOLUTION
   in min      in min     MOBILITY        VARIANCE
                          in cm2/Vs        in cm2
AMP =   5.77     .100     -.3185E  -3     6.92E  -3   5.35E   4        1.58
CMP =   5.93     .103     -.3300E  -3     7.12E  -3   5.33E   4        7.65
GMP =   6.78     .119     -.3816E  -3     8.13E  -3   5.22E   4        3.80
UMP =   7.24     .128     -.4049E  -3     8.69E  -3   5.16E   4        2.28
ADP =   7.54     .133     -.4183E  -3     9.05E  -3   5.12E   4        2.82
CDP =   7.93     .141     -.4341E  -3     9.52E  -3   5.07E   4        4.79
GDP =   8.64     .155     -.4594E  -3     1.04E  -2   4.98E   4        6.20
UDP =   9.66     .175     -.4895E  -3     1.16E  -2   4.86E   4    CRS =    2.43_
INJECTION ZONE,  in cm =    .47         INJ VARIANCE, in cm2 = 1.85E  -2
DETECTOR WINDOW, in cm =    .50         DET VARIANCE, in cm2 = 2.08E  -2


FLOW CHARACTERISTICS:
ZETA POTENTIAL, in mV =  -93.54
ZETAZERO, in mV =   26.44
kPOTNa = 2.2347E  -1
ELECTROOSMOTIC MOBILITY, in cm2/Vs = 7.4300E  -4
ELECTROOSMOTIC VELOCITY, in cm/s =   .2516
VOLTAGE, in kV =  16.932
RESISTANCE, in ohm = 9.9603E   8

BUFFER CHARACTERISTICS (conc in moles/liter):
pH =   9.800
IONIC STRENGTH = 1.2500E  -2
BUFFER CONCENTRATION = 2.5000E  -3
BUFFER CAPACITY = 2.0380E  -4
CHARGE CONC = 1.9956E  -2
[M]buffer = 5.0796E  -3
[M]electr = 4.8985E  -3
BUFFER FORMULATION:
CONC M-HJA = 0.0000E  -1
CONC M-H2A = 0.0000E  -1
CONC M-HA = 2.4204E  -3
CONC M-A = 7.9567E  -5
CONC M-X = 4.8985E  -3
OK
```

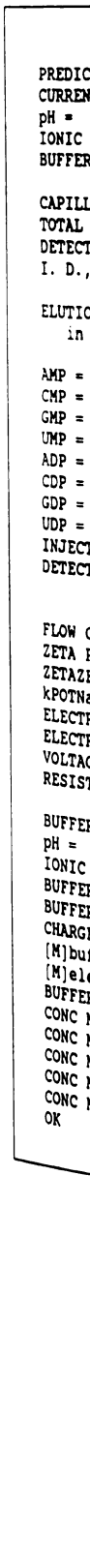
PREDIC
CURREN
pH =
IONIC
BUFFER
CAPILL
TOTAL
DETECT
I. D.,
ELUTIO
in
AMP =
CMP =
GMP =
UMP =
ADP =
CDP =
GDP =
UDP =
INJECT
DETECT
FLOW
ZETA
ZETAZE
kPOTNa
ELECTR
ELECTR
VOLTAG
RESIST
BUFFER
pH =
IONIC
BUFFER
BUFFER
CHARGE
[M]buf
[M]ele
BUFFER
CONC
CONC
CONC
CONC
CONC
OK

Figure 4.7c

```
PREDICTED OPTIMUM CONDITIONS FOR THE SEPARATION:
CURRENT, in microamperes =  17.000
pH =   9.800                          Correction Factor, in pH units =   .0000
IONIC STRENGTH, in moles/liter = 1.2500E  -2
BUFFER CONCENTRATION, in moles/liter = 2.5000E  -3

CAPILLARY DIMENSIONS:                 TYPE OF INJECTION: HYDRODYNAMIC
TOTAL LENGTH, in cm =   75.00         HEIGHT DIFFERENCE, in cm =    2.00
DETECTOR LENGTH, in cm =   50.00      INJECTION TIME, in sec =   60.00
I. D., in micrometers =   75.00       HYDRODYNAMIC VELOCITY, in cm/s = 5.24E  -3

ELUTION TIME   WIDTH      EFFECTIVE        DIFFUSION    EFFICIENCY    RESOLUTION
   in min      in min     MOBILITY         VARIANCE
                         in cm2/Vs         in cm2
AMP =   5.98     .091     -.3185E  -3      7.18E  -3    6.86E   4        1.79
CMP =   6.15     .094     -.3300E  -3      7.38E  -3    6.82E   4        8.64
GMP =   7.03     .109     -.3816E  -3      8.44E  -3    6.63E   4        4.28
UMP =   7.52     .118     -.4049E  -3      9.02E  -3    6.52E   4        2.57
ADP =   7.82     .123     -.4183E  -3      9.39E  -3    6.46E   4        3.16
CDP =   8.23     .130     -.4341E  -3      9.87E  -3    6.38E   4        5.37
GDP =   8.96     .143     -.4594E  -3      1.08E  -2    6.24E   4        6.93
UDP =  10.02     .163     -.4895E  -3      1.20E  -2    6.05E   4    CRS =    2.56_
INJECTION ZONE,  in cm =    .31           INJ VARIANCE, in cm2 = 8.22E  -3
DETECTOR WINDOW, in cm =    .50           DET VARIANCE, in cm2 = 2.08E  -2


FLOW CHARACTERISTICS:
ZETA POTENTIAL, in mV =  -93.54
ZETAZERO, in mV =   26.44
kPOTNa = 2.2347E  -1
ELECTROOSMOTIC MOBILITY, in cm2/Vs = 7.4300E  -4
ELECTROOSMOTIC VELOCITY, in cm/s =   .2429
VOLTAGE, in kV =  24.524
RESISTANCE, in ohm = 1.4426E   9

BUFFER CHARACTERISTICS (conc in moles/liter):
pH =   9.800
IONIC STRENGTH = 1.2500E  -2
BUFFER CONCENTRATION = 2.5000E  -3
BUFFER CAPACITY = 2.0380E  -4
CHARGE CONC = 1.9956E  -2
[M]buffer = 5.0796E  -3
[M]electr = 4.8985E  -3
BUFFER FORMULATION:
CONC M-H3A = 0.0000E  -1
CONC M-H2A = 0.0000E  -1
CONC M-HA = 2.4204E  -3
CONC M-A = 7.9567E  -5
CONC M-X = 4.8985E  -3
OK
```

Figure 4.8 Effect of the capillary diameter on the separation of nucleotides. Solute identification and standard conditions as given in Figure 4.6. (a) Computer-simulated electropherograms for 75, 100, and 125 μm capillary diameter. (b) Separation characteristics for 100 μm capillary diameter. (c) Separation characteristics for 125 μm capillary diameter.

Figure 4.8a

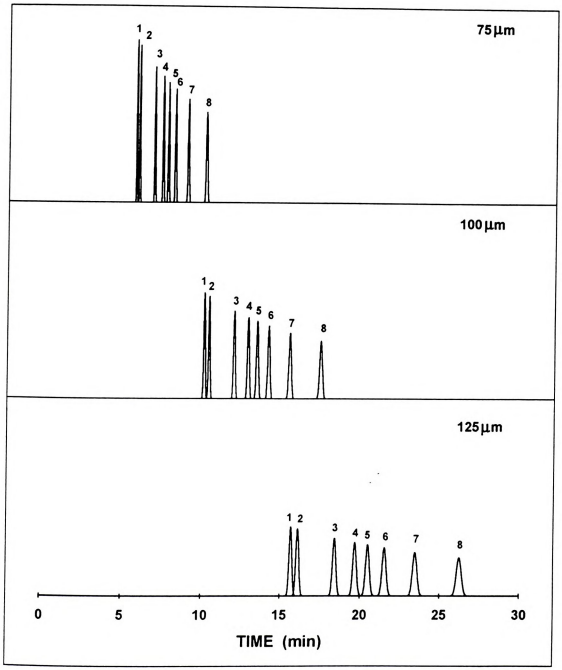

on of nucleotides.
s given in Figure
s for 75, 100, and
characteristics for
characteristics for

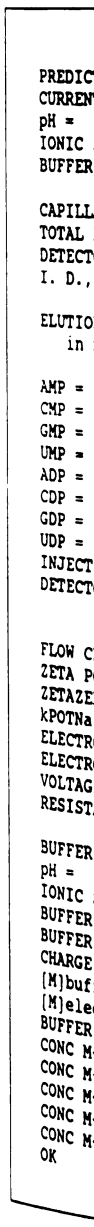
PREDIC
CURREN
pH =
IONIC
BUFFER
CAPILL
TOTAL
DETECT
I. D.,
ELUTIO
in
AMP =
CMP =
GMP =
UMP =
ADP =
CDP =
GDP =
UDP =
INJECT
DETECT
FLOW C
ZETA P
ZETAZE
kPOTNa
ELECTR
ELECTR
VOLTAG
RESIST
BUFFER
pH =
IONIC
BUFFER
BUFFER
CHARGE
[M]buf
[M]ele
BUFFER
CONC M
CONC M
CONC M
CONC M
CONC M
OK

Figure 4.8b

```
PREDICTED OPTIMUM CONDITIONS FOR THE SEPARATION:
CURRENT, in microamperes =  17.000
pH =   9.800                        Correction Factor, in pH units =    .0000
IONIC STRENGTH, in moles/liter = 1.2500E  -2
BUFFER CONCENTRATION, in moles/liter = 2.5000E  -3

CAPILLARY DIMENSIONS:               TYPE OF INJECTION: HYDRODYNAMIC
TOTAL LENGTH, in cm =  100.00       HEIGHT DIFFERENCE, in cm =    2.00
DETECTOR LENGTH, in cm =   50.00    INJECTION TIME, in sec =   60.00
I. D., in micrometers =  100.00     HYDRODYNAMIC VELOCITY, in cm/s = 6.98E  -3

ELUTION TIME   WIDTH     EFFECTIVE       DIFFUSION    EFFICIENCY    RESOLUTION
   in min      in min    MOBILITY        VARIANCE
                        in cm2/Vs         in cm2
AMP =  10.35    .182     -.3185E  -3     1.24E  -2    5.18E   4        1.55
CMP =  10.64    .188     -.3300E  -3     1.28E  -2    5.14E   4        7.48
GMP =  12.16    .219     -.3816E  -3     1.46E  -2    4.95E   4        3.70
UMP =  13.00    .236     -.4049E  -3     1.56E  -2    4.86E   4        2.21
ADP =  13.54    .247     -.4183E  -3     1.62E  -2    4.80E   4        2.72
CDP =  14.23    .262     -.4341E  -3     1.71E  -2    4.72E   4        4.61
GDP =  15.50    .290     -.4594E  -3     1.86E  -2    4.59E   4        5.93
UDP =  17.34    .330     -.4895E  -3     2.08E  -2    4.41E   4    CRS =    4.36_
INJECTION ZONE,  in cm =    .42         INJ VARIANCE, in cm2 = 1.46E  -2
DETECTOR WINDOW, in cm =    .50         DET VARIANCE, in cm2 = 2.08E  -2


FLOW CHARACTERISTICS:
ZETA POTENTIAL, in mV =  -93.54
ZETAZERO, in mV =   26.44
kPOTNa = 2.2347E  -1
ELECTROOSMOTIC MOBILITY, in cm2/Vs = 7.4300E  -4
ELECTROOSMOTIC VELOCITY, in cm/s =   .1403
VOLTAGE, in kV =  18.881
RESISTANCE, in ohm = 1.1106E   9

BUFFER CHARACTERISTICS (conc in moles/liter):
pH =   9.800
IONIC STRENGTH = 1.2500E  -2
BUFFER CONCENTRATION = 2.5000E  -3
BUFFER CAPACITY = 2.0380E  -4
CHARGE CONC = 1.9956E  -2
[M]buffer = 5.0796E  -3
[M]electr = 4.8985E  -3
BUFFER FORMULATION:
CONC M-H3A = 0.0000E  -1
CONC M-H2A = 0.0000E  -1
CONC M-HA = 2.4204E  -3
CONC M-A = 7.9567E  -5
CONC M-X = 4.8985E  -3
OK
```

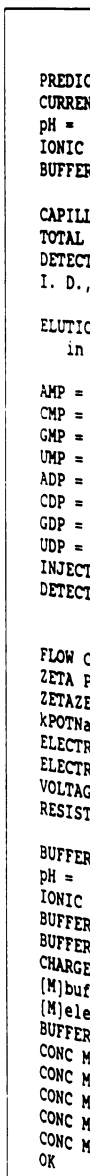
PREDIC
CURREN
pH =
IONIC
BUFFER
CAPILL
TOTAL
DETECT
I. D.,
ELUTIC
in
AMP =
CMP =
GMP =
UMP =
ADP =
CDP =
GDP =
UDP =
INJECT
DETECT
FLOW C
ZETA P
ZETAZE
kPOTNa
ELECTR
ELECTR
VOLTAG
RESIST
BUFFER
pH =
IONIC
BUFFER
BUFFER
CHARGE
[M]buf
[M]ele
BUFFER
CONC M
CONC M
CONC M
CONC M
CONC M
OK

Figure 4.8c

```
PREDICTED OPTIMUM CONDITIONS FOR THE SEPARATION:
CURRENT, in microamperes =  17.000
pH =   9.800                    Correction Factor, in pH units =   .0000
IONIC STRENGTH, in moles/liter = 1.2500E  -2
BUFFER CONCENTRATION, in moles/liter = 2.5000E  -3

CAPILLARY DIMENSIONS:           TYPE OF INJECTION: HYDRODYNAMIC
TOTAL LENGTH, in cm =  100.00   HEIGHT DIFFERENCE, in cm =    2.00
DETECTOR LENGTH, in cm =   50.00  INJECTION TIME, in sec =   60.00
I. D., in micrometers =  125.00  HYDRODYNAMIC VELOCITY, in cm/s = 1.09E  -2

ELUTION TIME   WIDTH     EFFECTIVE      DIFFUSION    EFFICIENCY   RESOLUTION
   in min      in min    MOBILITY       VARIANCE
                        in cm2/Vs       in cm2
AMP =  15.68    .347    -.3185E  -3    1.88E  -2   3.28E   4       1.24
CMP =  16.11    .357    -.3300E  -3    1.93E  -2   3.25E   4       5.95
GMP =  18.41    .416    -.3816E  -3    2.21E  -2   3.14E   4       2.94
UMP =  19.69    .449    -.4049E  -3    2.36E  -2   3.08E   4       1.76
ADP =  20.50    .470    -.4183E  -3    2.46E  -2   3.04E   4       2.17
CDP =  21.55    .498    -.4341E  -3    2.59E  -2   3.00E   4       3.67
GDP =  23.47    .550    -.4594E  -3    2.82E  -2   2.91E   4       4.72
UDP =  26.25    .627    -.4895E  -3    3.15E  -2   2.80E   4    CRS =    7.16_
INJECTION ZONE,  in cm =    .65       INJ VARIANCE, in cm2 = 3.57E  -2
DETECTOR WINDOW, in cm =    .50       DET VARIANCE, in cm2 = 2.08E  -2


FLOW CHARACTERISTICS:
ZETA POTENTIAL, in mV =  -93.54
ZETAZERO, in mV =   26.44
kPOTNa = 2.2347E  -1
ELECTROOSMOTIC MOBILITY, in cm2/Vs = 7.4300E  -4
ELECTROOSMOTIC VELOCITY, in cm/s =   .0924
VOLTAGE, in kV =  12.440
RESISTANCE, in ohm = 7.3176E   8

BUFFER CHARACTERISTICS (conc in moles/liter):
pH =   9.800
IONIC STRENGTH = 1.2500E  -2
BUFFER CONCENTRATION = 2.5000E  -3
BUFFER CAPACITY = 2.0380E  -4
CHARGE CONC = 1.9956E  -2
[M]buffer = 5.0796E  -3
[M]electr = 4.8985E  -3
BUFFER FORMULATION:
CONC M-H3A = 0.0000E  -1
CONC M-H2A = 0.0000E  -1
CONC M-HA = 2.4204E  -3
CONC M-A = 7.9567E  -5
CONC M-X = 4.8985E  -3
OK
```

can affec
several d
from the
sample h
unnecess
time. If t
further av
separatio
capillary
might aga

As
tranducer
Figure 4
character
migration
observed

Th
technique
Hydrodyn
injection
Figure 4.
reservoir
The effec
that resul

Un
presents
Figure 4.

can affect substantially the separation characteristics. In Figure 4.9, the effect of several detector positions is examined. With the detector positioned at 50 cm from the inlet end of the capillary, complete resolution of the components in the sample has already been achieved. Therefore, by increasing this distance, an unnecessary increase in resolution is obtained at the expense of the analysis time. If the resolution of the mixture is of concern, the position of the detector further away from the inlet may be beneficial because it allows more time for the separation to occur. However, as the residence time of the solutes in the capillary increases, diffusional broadening also increases and the resolution might again be compromised.

As discussed in section 4.2, the length of capillary exposed to the tranducer has a direct influence on the observed profile of the solute zone. In Figure 4.10, the effect of the detector window length on the separation characteristics is inspected. By increasing the detector window length, the migration time of each zone is unaffected. However, a substantial broadening is observed with a concomitant deterioration of the overall resolution.

The initial length of the solute zone, which is dependent on the injection technique, is another parameter of the system that can affect the zone profile. Hydrodynamic injection is based strictly on volume transfer and depends on the injection time, capillary dimensions, buffer viscosity, and pressure gradient. In Figure 4.11, the effect of the height difference between the inlet and outlet liquid reservoir is demonstrated, when the sample is introduced by siphoning action. The effect of injection time is presented by Figure 4.12. The loss of of efficiency that results from larger injection volumes is evident.

Under constant-current conditions, the magnitude of the applied current presents a marked effect on the separation characteristics as illustrated by Figure 4.13. A larger current, which imposes an increase in the electroosmotic

Figure 4.9 Effect of the detector position (L_{det}) on the separation of nucleotides. Solute identification and standard conditions as given in Figure 4.6. (a) Computer-simulated electropherograms for 50, 75, and 100 cm detector position. (b) Separation characteristics for 75 cm detector position. (c) Separation characteristics for 100 cm detector position.

Figure 4.9a

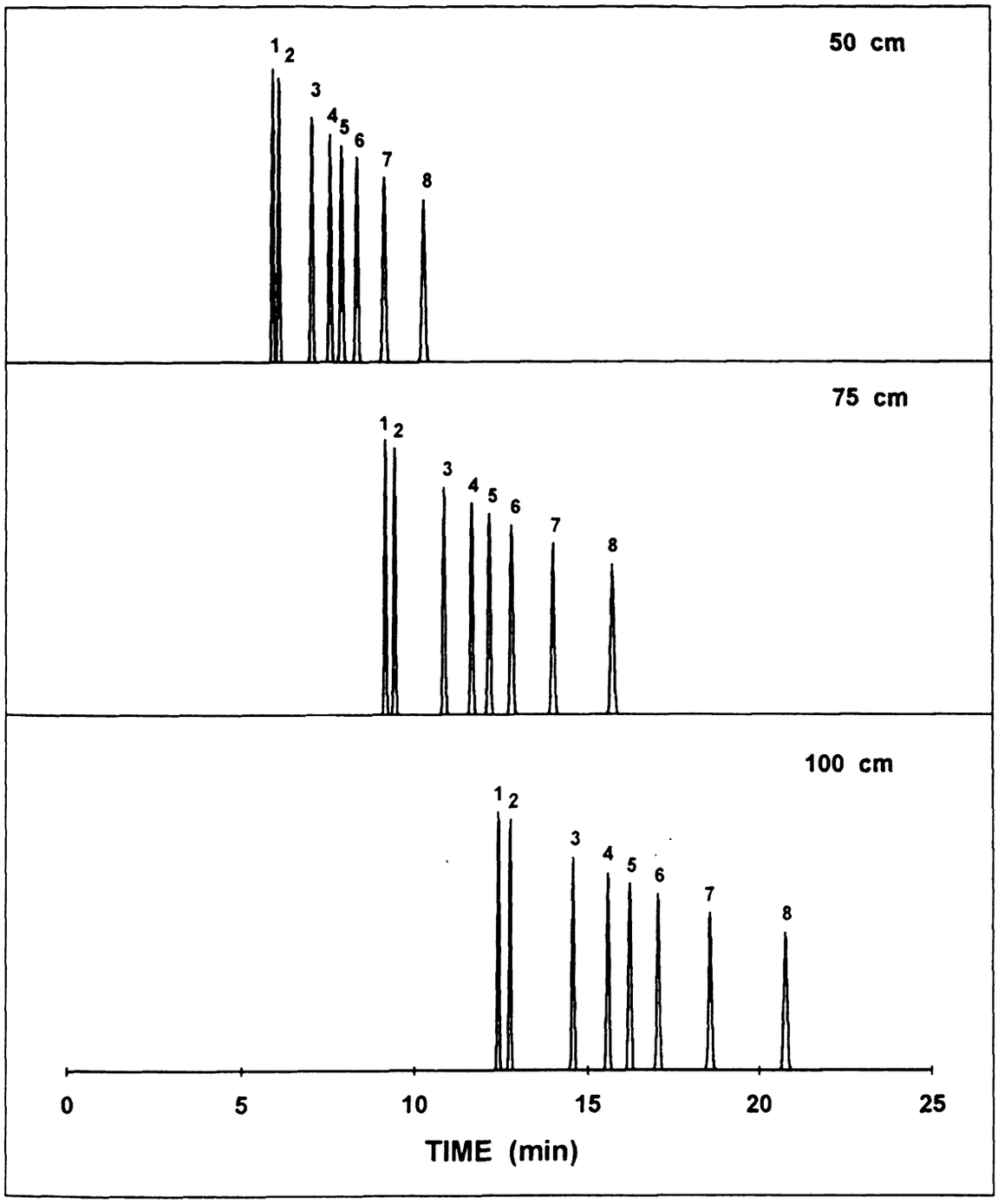
50 cm
1 2
3
4 5
6
7
8
75 cm
1 2
3
4 5
6
7
8
100 cm
1 2
3
4
5
6
7
8
0
5
10
15
20
25
TIME (min)

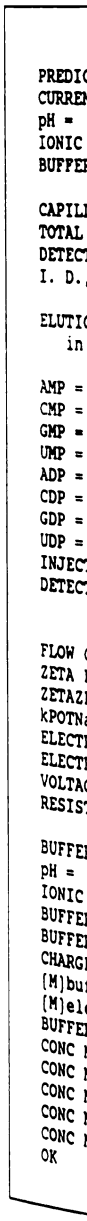
PREDIC
CURREN
pH =
IONIC
BUFFE
CAPILL
TOTAL
DETECT
I. D.,
ELUTIO
in
AMP =
CMP =
GMP =
UMP =
ADP =
CDP =
GDP =
UDP =
INJECT
DETECT
FLOW
ZETA
ZETAZE
kPOTNa
ELECTR
ELECTR
VOLTAG
RESIST
BUFFE
pH =
IONIC
BUFFE
BUFFE
CHARGE
[M]bu
[M]el
BUFFE
CONC
CONC
CONC
CONC
CONC
OK

Figure 4.9b

```
PREDICTED OPTIMUM CONDITIONS FOR THE SEPARATION:
CURRENT, in microamperes =  17.000
pH =   9.800                          Correction Factor, in pH units =   .0000
IONIC STRENGTH, in moles/liter = 1.2500E  -2
BUFFER CONCENTRATION, in moles/liter = 2.5000E  -3

CAPILLARY DIMENSIONS:                 TYPE OF INJECTION: HYDRODYNAMIC
TOTAL LENGTH, in cm =  100.00         HEIGHT DIFFERENCE, in cm =    2.00
DETECTOR LENGTH, in cm =   75.00      INJECTION TIME, in sec =   60.00
I. D., in micrometers =   75.00       HYDRODYNAMIC VELOCITY, in cm/s = 3.93E  -3

ELUTION TIME   WIDTH     EFFECTIVE       DIFFUSION    EFFICIENCY    RESOLUTION
   in min      in min    MOBILITY        VARIANCE
                        in cm2/Vs        in cm2
AMP =   9.30    .095    -.3185E  -3    1.12E  -2   1.53E   5        2.67
CMP =   9.56    .098    -.3300E  -3    1.15E  -2   1.52E   5       12.84
GMP =  10.92    .115    -.3816E  -3    1.31E  -2   1.45E   5        6.33
UMP =  11.68    .124    -.4049E  -3    1.40E  -2   1.42E   5        3.79
ADP =  12.16    .130    -.4183E  -3    1.46E  -2   1.40E   5        4.65
CDP =  12.78    .138    -.4341E  -3    1.53E  -2   1.37E   5        7.86
GDP =  13.92    .153    -.4594E  -3    1.67E  -2   1.33E   5       10.07
UDP =  15.57    .175    -.4895E  -3    1.87E  -2   1.27E   5    CRS =    3.97_
INJECTION ZONE,  in cm =     .24       INJ VARIANCE, in cm2 = 4.63E  -3
DETECTOR WINDOW, in cm =     .50       DET VARIANCE, in cm2 = 2.08E  -2


FLOW CHARACTERISTICS:
ZETA POTENTIAL, in mV =  -93.54
ZETAZERO, in mV =   26.44
kPOTNa = 2.2347E  -1
ELECTROOSMOTIC MOBILITY, in cm2/Vs = 7.4300E  -4
ELECTROOSMOTIC VELOCITY, in cm/s =   .2349
VOLTAGE, in kV =  31.610
RESISTANCE, in ohm = 1.8594E   9

BUFFER CHARACTERISTICS (conc in moles/liter):
pH =   9.800
IONIC STRENGTH = 1.2500E  -2
BUFFER CONCENTRATION = 2.5000E  -3
BUFFER CAPACITY = 2.0380E  -4
CHARGE CONC = 1.9956E   -2
[M]buffer = 5.0796E  -3
[M]electr = 4.8985E  -3
BUFFER FORMULATION:
CONC M-H3A = 0.0000E  -1
CONC M-H2A = 0.0000E  -1
CONC M-HA = 2.4204E  -3
CONC M-A = 7.9567E  -5
CONC M-X = 4.8985E  -3
OK
```

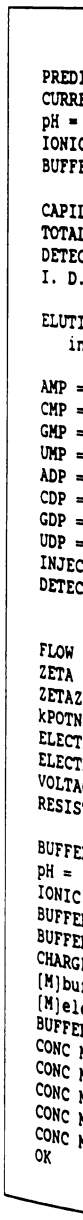
PREDI
CURRE
pH =
IONIC
BUFFE
CAPIL
TOTAL
DETEC
I. D.
ELUTI
in
AMP =
CMP =
GMP =
UMP =
ADP =
CDP =
GDP =
UDP =
INJEC
DETEC
FLOW
ZETA
ZETAZ
kPOTN
ELECT
ELECT
VOLTA
RESIS
BUFFE
pH =
IONIC
BUFFE
BUFFE
CHARG
[M]bu
[M]el
BUFFE
CONC
CONC
CONC
CONC
CONC
OK

Figure 4.9c

```
PREDICTED OPTIMUM CONDITIONS FOR THE SEPARATION:
CURRENT, in microamperes =  17.000
pH =   9.800                        Correction Factor, in pH units =   .0000
IONIC STRENGTH, in moles/liter = 1.2500E  -2
BUFFER CONCENTRATION, in moles/liter = 2.5000E  -3

CAPILLARY DIMENSIONS:               TYPE OF INJECTION: HYDRODYNAMIC
TOTAL LENGTH, in cm =  100.00       HEIGHT DIFFERENCE, in cm =    2.00
DETECTOR LENGTH, in cm =  100.00    INJECTION TIME, in sec =   60.00
I. D., in micrometers =   75.00     HYDRODYNAMIC VELOCITY, in cm/s = 3.93E  -3

ELUTION TIME   WIDTH     EFFECTIVE       DIFFUSION    EFFICIENCY    RESOLUTION
   in min      in min    MOBILITY        VARIANCE
                        in cm2/Vs        in cm2
AMP =  12.41    .100     -.3185E  -3     1.49E  -2    2.47E   5       3.39
CMP =  12.75    .103     -.3300E  -3     1.53E  -2    2.45E   5      16.26
GMP =  14.57    .121     -.3816E  -3     1.75E  -2    2.32E   5       7.99
UMP =  15.58    .131     -.4049E  -3     1.87E  -2    2.26E   5       4.77
ADP =  16.22    .138     -.4183E  -3     1.95E  -2    2.22E   5       5.85
CDP =  17.05    .146     -.4341E  -3     2.05E  -2    2.17E   5       9.86
GDP =  18.57    .163     -.4594E  -3     2.23E  -2    2.09E   5      12.60
UDP =  20.77    .187     -.4895E  -3     2.49E  -2    1.98E   5    CRS =    5.10_
INJECTION ZONE,  in cm =    .24         INJ VARIANCE, in cm2 = 4.63E  -3
DETECTOR WINDOW, in cm =    .50         DET VARIANCE, in cm2 = 2.08E  -2


FLOW CHARACTERISTICS:
ZETA POTENTIAL, in mV =  -93.54
ZETAZERO, in mV =   26.44
kPOTNa = 2.2347E  -1
ELECTROOSMOTIC MOBILITY, in cm2/Vs = 7.4300E  -4
ELECTROOSMOTIC VELOCITY, in cm/s =   .2349
VOLTAGE, in kV =  31.610
RESISTANCE, in ohm = 1.8594E   9

BUFFER CHARACTERISTICS (conc in moles/liter):
pH =   9.800
IONIC STRENGTH = 1.2500E  -2
BUFFER CONCENTRATION = 2.5000E  -3
BUFFER CAPACITY = 2.0380E  -4
CHARGE CONC = 1.9956E  -2
[M]buffer = 5.0796E  -3
[M]electr = 4.8985E  -3
BUFFER FORMULATION:
CONC M-H3A = 0.0000E  -1
CONC M-H2A = 0.0000E  -1
CONC M-HA = 2.4204E  -3
CONC M-A = 7.9567E  -5
CONC M-X = 4.8985E  -3
OK
```

Figure 4.10 Effect of the detector window length (ℓ_{det}) on the separation of nucleotides. Solute identification and standard conditions as given in Figure 4.6. (a) Computer-simulated electropherograms for 0.50, 0.75, and 1.0 cm detector window length. (b) Separation characteristics for 0.75 cm detector window length. (c) Separation characteristics for 1.0 cm detector window length.

Figure 4.10a

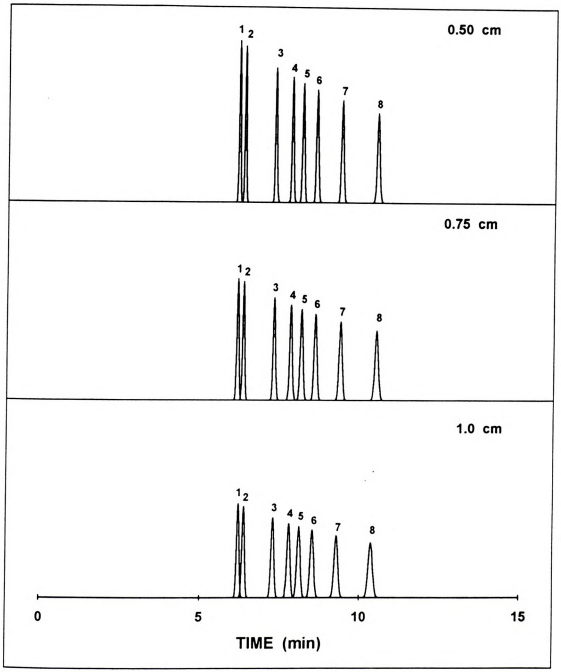

Figure 4.10b

```
PREDICTED OPTIMUM CONDITIONS FOR THE SEPARATION:
CURRENT, in microamperes =  17.000
pH =   9.800                          Correction Factor, in pH units =    .0000
IONIC STRENGTH, in moles/liter = 1.2500E  -2
BUFFER CONCENTRATION, in moles/liter = 2.5000E  -3

CAPILLARY DIMENSIONS:                 TYPE OF INJECTION: HYDRODYNAMIC
TOTAL LENGTH, in cm =  100.00         HEIGHT DIFFERENCE, in cm =    2.00
DETECTOR LENGTH, in cm =   50.00      INJECTION TIME, in sec =   60.00
I. D., in micrometers =   75.00       HYDRODYNAMIC VELOCITY, in cm/s = 3.93E  -3

ELUTION TIME   WIDTH     EFFECTIVE        DIFFUSION    EFFICIENCY    RESOLUTION
   in min      in min    MOBILITY         VARIANCE
                         in cm2/Vs         in cm2
AMP =   6.20     .121     -.3185E  -3     7.44E  -3    4.22E   4        1.40
CMP =   6.37     .124     -.3300E  -3     7.64E  -3    4.21E   4        6.80
GMP =   7.28     .143     -.3816E  -3     8.73E  -3    4.13E   4        3.38
UMP =   7.78     .154     -.4049E  -3     9.34E  -3    4.09E   4        2.04
ADP =   8.10     .161     -.4183E  -3     9.72E  -3    4.06E   4        2.51
CDP =   8.52     .170     -.4341E  -3     1.02E  -2    4.03E   4        4.28
GDP =   9.28     .186     -.4594E  -3     1.11E  -2    3.97E   4        5.54
UDP =  10.37     .210     -.4895E  -3     1.24E  -2    3.89E   4    CRS =    2.60_
INJECTION ZONE,  in cm =     .24         INJ VARIANCE, in cm2 = 4.63E  -3
DETECTOR WINDOW, in cm =     .75         DET VARIANCE, in cm2 = 4.69E  -2


FLOW CHARACTERISTICS:
ZETA POTENTIAL, in mV =  -93.54
ZETAZERO, in mV =   26.44
kPOTNa = 2.2347E   -1
ELECTROOSMOTIC MOBILITY, in cm2/Vs = 7.4300E  -4
ELECTROOSMOTIC VELOCITY, in cm/s =   .2349
VOLTAGE, in kV =  31.610
RESISTANCE, in ohm = 1.8594E   9

BUFFER CHARACTERISTICS (conc in moles/liter):
pH =   9.800
IONIC STRENGTH = 1.2500E  -2
BUFFER CONCENTRATION = 2.5000E  -3
BUFFER CAPACITY = 2.0380E  -4
CHARGE CONC = 1.9956E  -2
[M]buffer = 5.0796E  -3
[M]electr = 4.8985E  -3
BUFFER FORMULATION:
CONC M-H3A = 0.0000E  -1
CONC M-H2A = 0.0000E  -1
CONC M-HA = 2.4204E  -3
CONC M-A = 7.9567E  -5
CONC M-X = 4.8985E  -3
OK
```


PRE
CUR
pH
ION
BUF
CAP
TOT
DET
I.
ELU
AMP
CMP
GMP
UMP
ADP
CDP
GDP
UDP
INJ
DET
FLOW
ZETA
ZETA
kPOT
ELEC
ELEC
VOLT
RESI
BUFF
pH =
IONI
BUFF
BUFF
CHAR
[M]b
[M]e
BUFF
CONC
CONC
CONC
CONC
CONC
OK

Figure 4.10c

```
PREDICTED OPTIMUM CONDITIONS FOR THE SEPARATION:
CURRENT, in microamperes =  17.000
pH =   9.800                          Correction Factor, in pH units =    .0000
IONIC STRENGTH, in moles/liter = 1.2500E  -2
BUFFER CONCENTRATION, in moles/liter = 2.5000E  -3

CAPILLARY DIMENSIONS:                 TYPE OF INJECTION: HYDRODYNAMIC
TOTAL LENGTH, in cm =  100.00         HEIGHT DIFFERENCE, in cm =    2.00
DETECTOR LENGTH, in cm =   50.00      INJECTION TIME, in sec =   60.00
I. D., in micrometers =    75.00      HYDRODYNAMIC VELOCITY, in cm/s = 3.93E  -3

ELUTION TIME   WIDTH     EFFECTIVE       DIFFUSION    EFFICIENCY    RESOLUTION
   in min      in min    MOBILITY        VARIANCE
                        in cm2/Vs        in cm2
AMP =   6.20     .153    -.3185E  -3     7.44E  -3   2.61E   4        1.10
CMP =   6.37     .158    -.3300E  -3     7.64E  -3   2.60E   4        5.36
GMP =   7.28     .181    -.3816E  -3     8.73E  -3   2.57E   4        2.67
UMP =   7.78     .195    -.4049E  -3     9.34E  -3   2.56E   4        1.61
ADP =   8.10     .203    -.4183E  -3     9.72E  -3   2.55E   4        1.99
CDP =   8.52     .214    -.4341E  -3     1.02E  -2   2.53E   4        3.39
GDP =   9.28     .234    -.4594E  -3     1.11E  -2   2.51E   4        4.42
UDP =  10.37     .264    -.4895E  -3     1.24E  -2   2.48E   4    CRS =    3.93
INJECTION ZONE,  in cm =     .24        INJ VARIANCE, in cm2 = 4.63E  -3
DETECTOR WINDOW, in cm =    1.00        DET VARIANCE, in cm2 = 8.33E  -2


FLOW CHARACTERISTICS:
ZETA POTENTIAL, in mV =  -93.54
ZETAZERO, in mV =   26.44
kPOTNa = 2.2347E  -1
ELECTROOSMOTIC MOBILITY, in cm2/Vs = 7.4300E  -4
ELECTROOSMOTIC VELOCITY, in cm/s =   .2349
VOLTAGE, in kV =  31.610
RESISTANCE, in ohm = 1.8594E   9

BUFFER CHARACTERISTICS (conc in moles/liter):
pH =   9.800
IONIC STRENGTH = 1.2500E  -2
BUFFER CONCENTRATION = 2.5000E  -3
BUFFER CAPACITY = 2.0380E  -4
CHARGE CONC = 1.9956E  -2
[M]buffer = 5.0796E  -3
[M]electr = 4.8985E  -3
BUFFER FORMULATION:
CONC M-H3A = 0.0000E  -1
CONC M-H2A = 0.0000E  -1
CONC M-HA = 2.4204E  -3
CONC M-A = 7.9567E  -5
CONC M-X = 4.8985E  -3
OK
```

Figure 4.11 Effect of the height difference (ΔH) of hydrodynamic injection with siphoning action on the separation of nucleotides. Solute identification and standard conditions as given in Figure 4.6. (a) Computer-simulated electropherograms for 1, 2, and 5 cm height difference. (b) Separation characteristics for 1cm height difference. (c) Separation characteristics for 5 cm height difference.

Figure 4.11a

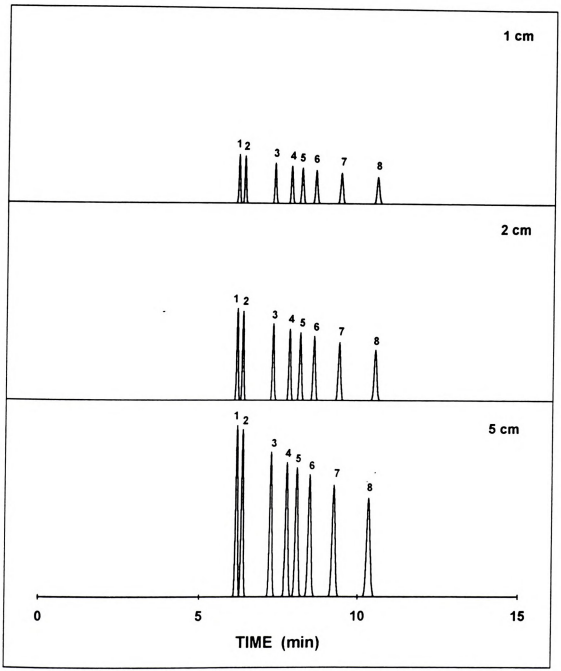

PRI
CUI
pH
ION
BUI

CAI
TOX
DET
I.

ELU

AMI
CMI
GMI
UMI
ADI
CDI
GDI
UDI
INO
DET

FLA
ZET
ZET
kPO
ELI
ELI
VOI
RES

BUF
pH
ION
BUF
BUF
CHA
[M]
[M]
BUF
CON
CON
CON
CON
CON
OK

Figure 4.11b

```
PREDICTED OPTIMUM CONDITIONS FOR THE SEPARATION:
CURRENT, in microamperes =  17.000
pH =   9.800                          Correction Factor, in pH units =    .0000
IONIC STRENGTH, in moles/liter = 1.2500E  -2
BUFFER CONCENTRATION, in moles/liter = 2.5000E  -3

CAPILLARY DIMENSIONS:                 TYPE OF INJECTION: HYDRODYNAMIC
TOTAL LENGTH, in cm =  100.00         HEIGHT DIFFERENCE, in cm =    1.00
DETECTOR LENGTH, in cm =   50.00      INJECTION TIME, in sec =   60.00
I. D., in micrometers =   75.00       HYDRODYNAMIC VELOCITY, in cm/s = 1.96E  -3

ELUTION TIME   WIDTH      EFFECTIVE       DIFFUSION     EFFICIENCY    RESOLUTION
   in min      in min     MOBILITY        VARIANCE
                         in cm2/Vs        in cm2
AMP =   6.20     .085     -.3185E  -3     7.44E  -3     8.47E   4        1.99
CMP =   6.38     .088     -.3300E  -3     7.65E  -3     8.41E   4        9.57
GMP =   7.29     .102     -.3816E  -3     8.74E  -3     8.12E   4        4.73
UMP =   7.79     .110     -.4049E  -3     9.35E  -3     7.96E   4        2.83
ADP =   8.11     .116     -.4183E  -3     9.73E  -3     7.86E   4        3.49
CDP =   8.53     .123     -.4341E  -3     1.02E  -2     7.74E   4        5.90
GDP =   9.29     .135     -.4594E  -3     1.11E  -2     7.53E   4        7.59
UDP =  10.39     .154     -.4895E  -3     1.25E  -2     7.24E   4    CRS =    2.68
INJECTION ZONE,   in cm =     .12        INJ VARIANCE, in cm2 = 1.16E  -3
DETECTOR WINDOW, in cm =      .50        DET VARIANCE, in cm2 = 2.08E  -2


FLOW CHARACTERISTICS:
ZETA POTENTIAL, in mV =  -93.54
ZETAZERO, in mV =   26.44
kPOTNa = 2.2347E  -1
ELECTROOSMOTIC MOBILITY, in cm2/Vs = 7.4300E  -4
ELECTROOSMOTIC VELOCITY, in cm/s =   .2349
VOLTAGE, in kV =  31.610
RESISTANCE, in ohm = 1.8594E   9

BUFFER CHARACTERISTICS (conc in moles/liter):
pH =   9.800
IONIC STRENGTH = 1.2500E  -2
BUFFER CONCENTRATION = 2.5000E  -3
BUFFER CAPACITY = 2.0380E  -4
CHARGE CONC = 1.9956E  -2
[M]buffer = 5.0796E  -3
[M]electr = 4.8985E  -3
BUFFER FORMULATION:
CONC M-H3A = 0.0000E  -1
CONC M-H2A = 0.0000E  -1
CONC M-HA = 2.4204E  -3
CONC M-A = 7.9567E  -5
CONC M-X = 4.8985E  -3
OK
```

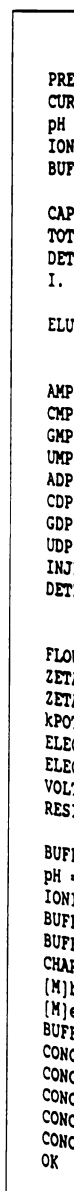

Figure 4.11c

```
PREDICTED OPTIMUM CONDITIONS FOR THE SEPARATION:
CURRENT, in microamperes =  17.000
pH =   9.800                    Correction Factor, in pH units =    .0000
IONIC STRENGTH, in moles/liter = 1.2500E  -2
BUFFER CONCENTRATION, in moles/liter = 2.5000E  -3

CAPILLARY DIMENSIONS:                TYPE OF INJECTION: HYDRODYNAMIC
TOTAL LENGTH, in cm =  100.00        HEIGHT DIFFERENCE, in cm =    5.00
DETECTOR LENGTH, in cm =   50.00     INJECTION TIME, in sec =   60.00
I. D., in micrometers =    75.00     HYDRODYNAMIC VELOCITY, in cm/s = 9.82E  -3

ELUTION TIME   WIDTH     EFFECTIVE       DIFFUSION    EFFICIENCY    RESOLUTION
   in min      in min    MOBILITY        VARIANCE
                        in cm2/Vs        in cm2
AMP =   6.17    .119     -.3185E  -3     7.41E  -3   4.32E   4        1.42
CMP =   6.35    .122     -.3300E  -3     7.61E  -3   4.31E   4        6.88
GMP =   7.25    .141     -.3816E  -3     8.70E  -3   4.23E   4        3.42
UMP =   7.75    .152     -.4049E  -3     9.30E  -3   4.18E   4        2.06
ADP =   8.07    .158     -.4183E  -3     9.69E  -3   4.16E   4        2.54
CDP =   8.48    .167     -.4341E  -3     1.02E  -2   4.12E   4        4.32
GDP =   9.24    .183     -.4594E  -3     1.11E  -2   4.06E   4        5.60
UDP =  10.34    .207     -.4895E  -3     1.24E  -2   3.98E   4    CRS =    2.59_
INJECTION ZONE,  in cm =     .59         INJ VARIANCE, in cm2 = 2.89E  -2
DETECTOR WINDOW, in cm =     .50         DET VARIANCE, in cm2 = 2.08E  -2


FLOW CHARACTERISTICS:
ZETA POTENTIAL, in mV =  -93.54
ZETAZERO, in mV =   26.44
kPOTNa = 2.2347E  -1
ELECTROOSMOTIC MOBILITY, in cm2/Vs = 7.4300E  -4
ELECTROOSMOTIC VELOCITY, in cm/s =   .2349
VOLTAGE, in kV =  31.610
RESISTANCE, in ohm = 1.8594E   9

BUFFER CHARACTERISTICS (conc in moles/liter):
pH =   9.800
IONIC STRENGTH = 1.2500E  -2
BUFFER CONCENTRATION = 2.5000E  -3
BUFFER CAPACITY = 2.0380E  -4
CHARGE CONC = 1.9956E  -2
[M]buffer = 5.0796E  -3
[M]electr = 4.8985E  -3
BUFFER FORMULATION:
CONC M-H3A = 0.0000E  -1
CONC M-H2A = 0.0000E  -1
CONC M-HA = 2.4204E  -3
CONC M-A = 7.9567E  -5
CONC M-X = 4.8985E  -3
OK
```

Figure 4.12 Effect of the hydrodynamic injection time (t_{inj}) on the separation of nucleotides. Solute identification and standard conditions as given in Figure 4.6. (a) Computer-simulated electropherograms for 60, 90, and 120 s injection time. (b) Separation characteristics for 90 s injection time. (c) Separation characteristics for 120 s injection time.

Figure 4.12a

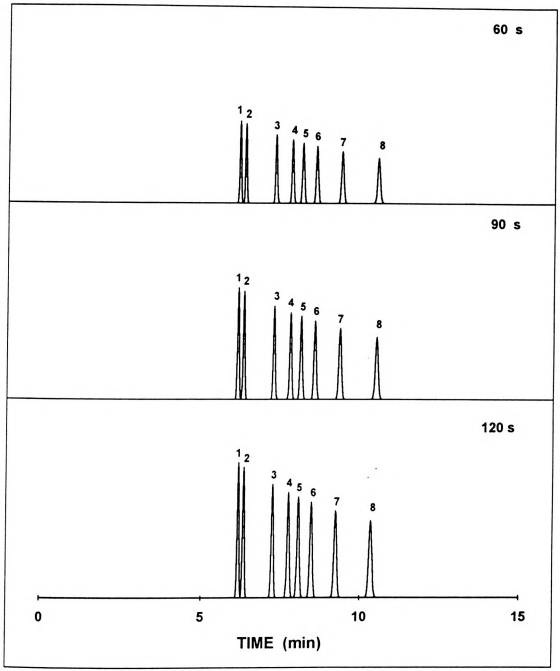

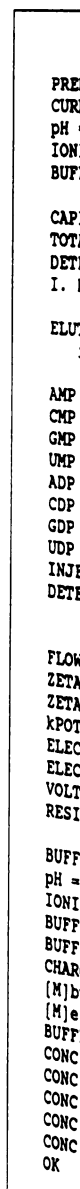

Figure 4.12b

```
PREDICTED OPTIMUM CONDITIONS FOR THE SEPARATION:
CURRENT, in microamperes =  17.000
pH =   9.800                          Correction Factor, in pH units =    .0000
IONIC STRENGTH, in moles/liter = 1.2500E  -2
BUFFER CONCENTRATION, in moles/liter = 2.5000E  -3

CAPILLARY DIMENSIONS:                 TYPE OF INJECTION: HYDRODYNAMIC
TOTAL LENGTH, in cm =  100.00         HEIGHT DIFFERENCE, in cm =    2.00
DETECTOR LENGTH, in cm =   50.00      INJECTION TIME, in sec =   90.00
I. D., in micrometers =   75.00       HYDRODYNAMIC VELOCITY, in cm/s = 3.93E  -3

ELUTION TIME    WIDTH      EFFECTIVE        DIFFUSION     EFFICIENCY    RESOLUTION
   in min       in min     MOBILITY         VARIANCE
                           in cm2/Vs         in cm2
AMP =   6.19     .098     -.3185E  -3     7.43E  -3   6.42E   4          1.73
CMP =   6.36     .101     -.3300E  -3     7.63E  -3   6.39E   4          8.36
GMP =   7.27     .117     -.3816E  -3     8.72E  -3   6.21E   4          4.14
UMP =   7.77     .126     -.4049E  -3     9.32E  -3   6.12E   4          2.49
ADP =   8.09     .131     -.4183E  -3     9.71E  -3   6.06E   4          3.07
CDP =   8.51     .139     -.4341E  -3     1.02E  -2   5.99E   4          5.20
GDP =   9.26     .153     -.4594E  -3     1.11E  -2   5.86E   4          6.71
UDP =  10.36     .174     -.4895E  -3     1.24E  -2   5.68E   4     CRS =      2.64_
INJECTION ZONE,  in cm =      .35        INJ VARIANCE, in cm2 = 1.04E  -2
DETECTOR WINDOW, in cm =      .50        DET VARIANCE, in cm2 = 2.08E  -2


FLOW CHARACTERISTICS:
ZETA POTENTIAL, in mV =  -93.54
ZETAZERO, in mV =   26.44
kPOTNa = 2.2347E  -1
ELECTROOSMOTIC MOBILITY, in cm2/Vs = 7.4300E  -4
ELECTROOSMOTIC VELOCITY, in cm/s =   .2349
VOLTAGE, in kV =  31.610
RESISTANCE, in ohm = 1.8594E   9

BUFFER CHARACTERISTICS (conc in moles/liter):
pH =   9.800
IONIC STRENGTH = 1.2500E  -2
BUFFER CONCENTRATION = 2.5000E  -3
BUFFER CAPACITY = 2.0380E  -4
CHARGE CONC = 1.9956E  -2
[M]buffer = 5.0796E  -3
[M]electr = 4.8985E  -3
BUFFER FORMULATION:
CONC M-H3A = 0.0000E  -1
CONC M-H2A = 0.0000E  -1
CONC M-HA = 2.4204E  -3
CONC M-A = 7.9567E  -5
CONC M-X = 4.8985E  -3
OK
```

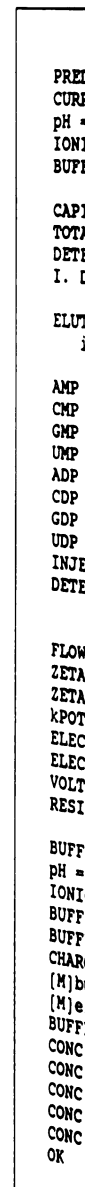
PREI
CURI
pH =
IONI
BUFI
CAPI
TOTA
DETI
I. D
ELUT
i
AMP
CMP
GMP
UMP
ADP
CDP
GDP
UDP
INJE
DETE
FLOW
ZETA
ZETA
kPOT
ELEC
ELEC
VOLT
RESI
BUFF
pH =
IONI
BUFF
BUFF
CHAR
[M]b
[M]e
BUFF
CONC
CONC
CONC
CONC
CONC
OK

Figure 4.12c

```
PREDICTED OPTIMUM CONDITIONS FOR THE SEPARATION:
CURRENT, in microamperes =  17.000
pH =   9.800                          Correction Factor, in pH units =   .0000
IONIC STRENGTH, in moles/liter = 1.2500E  -2
BUFFER CONCENTRATION, in moles/liter = 2.5000E  -3

CAPILLARY DIMENSIONS:                 TYPE OF INJECTION: HYDRODYNAMIC
TOTAL LENGTH, in cm =  100.00         HEIGHT DIFFERENCE, in cm =    2.00
DETECTOR LENGTH, in cm =   50.00      INJECTION TIME, in sec =  120.00
I. D., in micrometers =   75.00       HYDRODYNAMIC VELOCITY, in cm/s = 3.93E  -3

ELUTION TIME   WIDTH     EFFECTIVE       DIFFUSION    EFFICIENCY    RESOLUTION
   in min      in min    MOBILITY        VARIANCE
                        in cm2/Vs        in cm2
AMP =   6.18    .107     -.3185E  -3     7.42E  -3    5.30E   4        1.57
CMP =   6.35    .111     -.3300E  -3     7.62E  -3    5.27E   4        7.61
GMP =   7.26    .128     -.3816E  -3     8.71E  -3    5.15E   4        3.78
UMP =   7.76    .138     -.4049E  -3     9.31E  -3    5.09E   4        2.27
ADP =   8.08    .144     -.4183E  -3     9.70E  -3    5.05E   4        2.80
CDP =   8.49    .152     -.4341E  -3     1.02E  -2    5.00E   4        4.76
GDP =   9.25    .167     -.4594E  -3     1.11E  -2    4.91E   4        6.15
UDP =  10.35    .189     -.4895E  -3     1.24E  -2    4.79E   4    CRS =    2.60_
INJECTION ZONE,  in cm =    .47         INJ VARIANCE, in cm2 = 1.85E  -2
DETECTOR WINDOW, in cm =    .50         DET VARIANCE, in cm2 = 2.08E  -2


FLOW CHARACTERISTICS:
ZETA POTENTIAL, in mV =  -93.54
ZETAZERO, in mV =   26.44
kPOTNa = 2.2347E  -1
ELECTROOSMOTIC MOBILITY, in cm2/Vs = 7.4300E  -4
ELECTROOSMOTIC VELOCITY, in cm/s =   .2349
VOLTAGE, in kV =  31.610
RESISTANCE, in ohm = 1.8594E   9

BUFFER CHARACTERISTICS (conc in moles/liter):
pH =   9.800
IONIC STRENGTH = 1.2500E  -2
BUFFER CONCENTRATION = 2.5000E  -3
BUFFER CAPACITY = 2.0380E  -4
CHARGE CONC = 1.9956E  -2
[M]buffer = 5.0796E  -3
[M]electr = 4.8985E  -3
BUFFER FORMULATION:
CONC M-H3A = 0.0000E  -1
CONC M-H2A = 0.0000E  -1
CONC M-HA = 2.4204E  -3
CONC M-A = 7.9567E  -5
CONC M-X = 4.8985E  -3
OK
```

Figure 4.13 Effect of the applied current (I) on the separation of nucleotides. Solute identification and standard conditions as given in Figure 4.6. (a) Computer-simulated electropherograms for constant-current conditions of 10, 15, and 17 μA. (b) Separation characteristics for constant-current of 10 μA. (c) Separation characteristics for constant-current of 15 μA.

Figure 4.13a

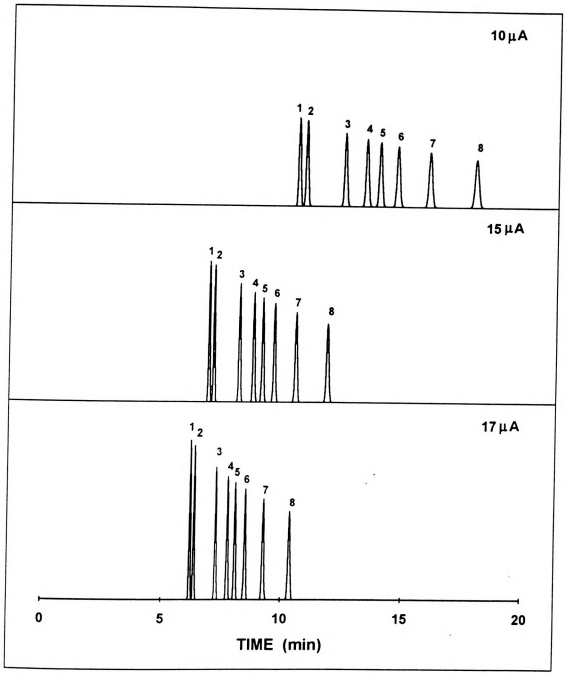
10 µA
1
2
3
4
5
6
7
8
15 µA
1
2
3
4
5
6
7
8
17 µA
1
2
3
4
5
6
7
8
0
5
10
15
20
TIME (min)

Figure 4.13b

```
PREDICTED OPTIMUM CONDITIONS FOR THE SEPARATION:
CURRENT, in microamperes =  10.000
pH =   9.800                        Correction Factor, in pH units =   .0000
IONIC STRENGTH, in moles/liter = 1.2500E  -2
BUFFER CONCENTRATION, in moles/liter = 2.5000E  -3

CAPILLARY DIMENSIONS:               TYPE OF INJECTION: HYDRODYNAMIC
TOTAL LENGTH, in cm =  100.00       HEIGHT DIFFERENCE, in cm =    2.00
DETECTOR LENGTH, in cm =   50.00    INJECTION TIME, in sec =   60.00
I. D., in micrometers =   75.00     HYDRODYNAMIC VELOCITY, in cm/s = 3.93E  -3

ELUTION TIME   WIDTH     EFFECTIVE       DIFFUSION    EFFICIENCY   RESOLUTION
   in min      in min    MOBILITY        VARIANCE
                        in cm2/Vs        in cm2
AMP =  10.53    .165    -.3185E  -3     1.26E  -2    6.53E   4       1.74
CMP =  10.83    .170    -.3300E  -3     1.30E  -2    6.47E   4       8.37
GMP =  12.37    .199    -.3816E  -3     1.48E  -2    6.17E   4       4.12
UMP =  13.23    .216    -.4049E  -3     1.59E  -2    6.02E   4       2.46
ADP =  13.77    .226    -.4183E  -3     1.65E  -2    5.93E   4       3.02
CDP =  14.48    .240    -.4341E  -3     1.74E  -2    5.81E   4       5.10
GDP =  15.77    .266    -.4594E  -3     1.89E  -2    5.61E   4       6.54
UDP =  17.64    .305    -.4895E  -3     2.12E  -2    5.34E   4    CRS =    4.51_
INJECTION ZONE,  in cm =    .24        INJ VARIANCE, in cm2 = 4.63E  -3
DETECTOR WINDOW, in cm =    .50        DET VARIANCE, in cm2 = 2.08E  -2


FLOW CHARACTERISTICS:
ZETA POTENTIAL, in mV =  -93.54
ZETAZERO, in mV =   26.44
kPOTNa = 2.2347E  -1
ELECTROOSMOTIC MOBILITY, in cm2/Vs = 7.4300E  -4
ELECTROOSMOTIC VELOCITY, in cm/s =   .1382
VOLTAGE, in kV =  18.594
RESISTANCE, in ohm = 1.8594E   9

BUFFER CHARACTERISTICS (conc in moles/liter):
pH =   9.800
IONIC STRENGTH = 1.2500E  -2
BUFFER CONCENTRATION = 2.5000E  -3
BUFFER CAPACITY = 2.0380E  -4
CHARGE CONC = 1.9956E  -2
[M]buffer = 5.0796E  -3
[M]electr = 4.8985E  -3
BUFFER FORMULATION:
CONC M-H3A = 0.0000E  -1
CONC M-H2A = 0.0000E  -1
CONC M-HA = 2.4204E  -3
CONC M-A = 7.9567E  -5
CONC M-X = 4.8985E  -3
OK
```

Figure 4.13c

```
PREDICTED OPTIMUM CONDITIONS FOR THE SEPARATION:
CURRENT, in microamperes =  15.000
pH =   9.800                        Correction Factor, in pH units =   .0000
IONIC STRENGTH, in moles/liter = 1.2500E  -2
BUFFER CONCENTRATION, in moles/liter = 2.5000E  -3

CAPILLARY DIMENSIONS:               TYPE OF INJECTION: HYDRODYNAMIC
TOTAL LENGTH, in cm =  100.00       HEIGHT DIFFERENCE, in cm =    2.00
DETECTOR LENGTH, in cm =   50.00    INJECTION TIME, in sec =   60.00
I. D., in micrometers =   75.00     HYDRODYNAMIC VELOCITY, in cm/s = 3.93E  -3

ELUTION TIME   WIDTH     EFFECTIVE       DIFFUSION    EFFICIENCY   RESOLUTION
   in min      in min    MOBILITY        VARIANCE
                        in cm2/Vs        in cm2
AMP =   7.02    .104    -.3185E  -3     8.43E  -3    7.34E   4       1.85
CMP =   7.22    .107    -.3300E  -3     8.66E  -3    7.29E   4       8.91
GMP =   8.25    .124    -.3816E  -3     9.90E  -3    7.04E   4       4.41
UMP =   8.82    .134    -.4049E  -3     1.06E  -2    6.90E   4       2.64
ADP =   9.18    .141    -.4183E  -3     1.10E  -2    6.82E   4       3.25
CDP =   9.65    .149    -.4341E  -3     1.16E  -2    6.72E   4       5.50
GDP =  10.51    .164    -.4594E  -3     1.26E  -2    6.54E   4       7.08
UDP =  11.76    .188    -.4895E  -3     1.41E  -2    6.29E   4    CRS =    3.02_
INJECTION ZONE,  in cm =    .24         INJ VARIANCE, in cm2 = 4.63E  -3
DETECTOR WINDOW, in cm =    .50         DET VARIANCE, in cm2 = 2.08E  -2


FLOW CHARACTERISTICS:
ZETA POTENTIAL, in mV =  -93.54
ZETAZERO, in mV =   26.44
kPOTNa = 2.2347E  -1
ELECTROOSMOTIC MOBILITY, in cm2/Vs = 7.4300E  -4
ELECTROOSMOTIC VELOCITY, in cm/s =   .2072
VOLTAGE, in kV =  27.891
RESISTANCE, in ohm = 1.8594E   9

BUFFER CHARACTERISTICS (conc in moles/liter):
pH =   9.800
IONIC STRENGTH = 1.2500E  -2
BUFFER CONCENTRATION = 2.5000E  -3
BUFFER CAPACITY = 2.0380E  -4
CHARGE CONC = 1.9956E  -2
[M]buffer = 5.0796E  -3
[M]electr = 4.8985E  -3
BUFFER FORMULATION:
CONC M-H3A = 0.0000E  -1
CONC M-H2A = 0.0000E  -1
CONC M-HA = 2.4204E  -3
CONC M-A = 7.9567E  -5
CONC M-X = 4.8985E  -3
OK
```

flow ve

decreas

P

separati

marked

as well

silanol s

ionic st

electrop

migratio

flow by

Chapter

strength

not seem

is evider

overall e

is capabl

also can

Th

Interestin

analysis t

are formu

concentra

charged

sodium c

increased

V/cm with

flow velocity, can decrease substantially the analysis time with a resulting decrease in diffusional variance.

Perhaps the most effective means to influence an electrophoretic separation is by altering the buffer properties. The buffer pH (Figure 4.14) has a marked effect on the effective mobility and dissociation equilibrium of the solutes as well as on the electroosmotic flow characteristics through protonation of silanol sites at the capillary surface (Equations [4.14] and [4.11]). Likewise, the ionic strength of the buffer solution (Figure 4.15) influences the solute electrophoretic behavior by decreasing the solute mobility and retarding its migration (Equation [4.16]). The ionic strength also alters the electroosmotic flow by compression of the double layer structure at the silica surface (*vide* Chapter 3). In traditional paper and slab gel electrophoresis, the effect of ionic strength is to contribute to the sharpening of the band boundaries. That does not seem to be the case in capillary zone electrophoresis. The loss of efficiency is evident as the ionic strength of the solution increases. In conclusion, the overall effect of pH is more dramatic than that of the ionic strength because pH is capable of altering not only the order of solute elution and analysis time but also can cause a distinct change in the resolution pattern.

The effect of the buffer concentration is presented in Figure 4.16. Interestingly, the increase in concentration of the buffer contributes to shorter analysis time. This is a consequence of the manner in which the buffer solutions are formulated. For a constant ionic strength and high pH, an increase in buffer concentration is achieved by an increase in the amount of the doubly and triply charged phosphate species and a corresponding decrease in the amount of sodium chloride. As a result, the resistance of the solution is substantially increased, and so the voltage. The field strength varied from 275 V/cm to 372 V/cm with a small increase in the buffer concentration from 1.5 to 3.5 mM.

Figure 4.14 Effect of the buffer pH on the separation of nucleotides. Solute identification and standard conditions as given in Figure 4.6. (a) Computer-simulated electropherograms for pH 6, 7, and 9.8. (b) Separation characteristics for pH 6. (c) Separation characteristics for pH 7.

Figure 4.14a

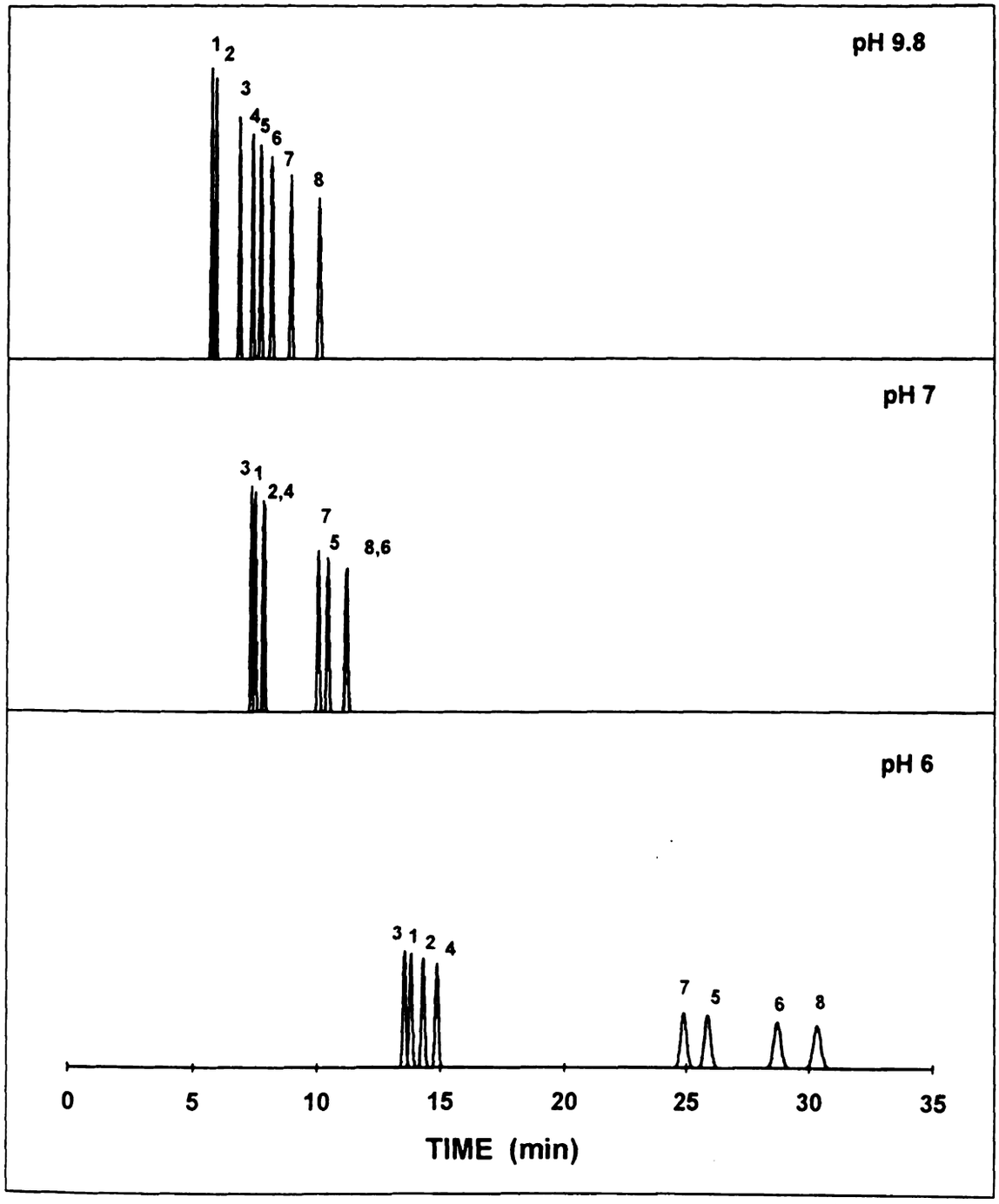
pH 9.8
1 2
3
4 5 6
7
8
pH 7
3 1
2,4
7
5
8,6
pH 6
3 1 2 4
7 5
6 8
0 5 10 15 20 25 30 35
TIME (min)

Figure 4.14b

```
PREDICTED OPTIMUM CONDITIONS FOR THE SEPARATION:
CURRENT, in microamperes =  17.000
pH =   7.000                        Correction Factor, in pH units =   .0000
IONIC STRENGTH, in moles/liter = 1.2500E  -2
BUFFER CONCENTRATION, in moles/liter = 2.5000E  -3

CAPILLARY DIMENSIONS:               TYPE OF INJECTION: HYDRODYNAMIC
TOTAL LENGTH, in cm =  100.00       HEIGHT DIFFERENCE, in cm =    2.00
DETECTOR LENGTH, in cm =   50.00    INJECTION TIME, in sec =   60.00
I. D., in micrometers =   75.00     HYDRODYNAMIC VELOCITY, in cm/s = 3.93E  -3

ELUTION TIME   WIDTH     EFFECTIVE       DIFFUSION    EFFICIENCY   RESOLUTION
   in min      in min    MOBILITY        VARIANCE
                        in cm2/Vs        in cm2
GMP =   7.76    .116    -.2921E  -3     9.31E  -3    7.16E   4       1.30
AMP =   7.91    .119    -.2994E  -3     9.50E  -3    7.12E   4       2.60
CMP =   8.23    .124    -.3137E  -3     9.88E  -3    7.04E   4        .22
UMP =   8.26    .125    -.3149E  -3     9.91E  -3    7.04E   4      14.69
GDP =  10.36    .162    -.3872E  -3     1.24E  -2    6.57E   4       2.26
ADP =  10.73    .169    -.3971E  -3     1.29E  -2    6.49E   4       4.02
UDP =  11.44    .182    -.4139E  -3     1.37E  -2    6.35E   4        .11
CDP =  11.46    .182    -.4144E  -3     1.37E  -2    6.35E   4    CRS =  105.31_
INJECTION ZONE,  in cm =    .24         INJ VARIANCE, in cm2 = 4.63E  -3
DETECTOR WINDOW, in cm =    .50         DET VARIANCE, in cm2 = 2.08E  -2


FLOW CHARACTERISTICS:
ZETA POTENTIAL, in mV =  -84.50
ZETAZERO, in mV =   33.02
kPOTNa = 2.2347E  -1
ELECTROOSMOTIC MOBILITY, in cm2/Vs = 6.7121E  -4
ELECTROOSMOTIC VELOCITY, in cm/s =   .1896
VOLTAGE, in kV =  28.251
RESISTANCE, in ohm = 1.6618E   9

BUFFER CHARACTERISTICS (conc in moles/liter):
pH =   7.000
IONIC STRENGTH = 1.2500E  -2
BUFFER CONCENTRATION = 2.5000E  -3
BUFFER CAPACITY = 1.4340E  -3
CHARGE CONC = 2.2662E  -2
[M]buffer = 3.6691E  -3
[M]electr = 7.6617E  -3
BUFFER FORMULATION:
CONC M-H3A = 0.0000E  -1
CONC M-H2A = 1.3309E  -3
CONC M-HA = 1.1691E  -3
CONC M-A = 0.0000E  -1
CONC M-X = 7.6617E  -3
OK
```

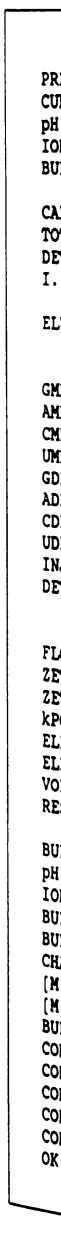

Figure 4.14c

```
PREDICTED OPTIMUM CONDITIONS FOR THE SEPARATION:
CURRENT, in microamperes =  17.000
pH =   6.000                          Correction Factor, in pH units =   .0000
IONIC STRENGTH, in moles/liter = 1.2500E  -2
BUFFER CONCENTRATION, in moles/liter = 2.5000E  -3

CAPILLARY DIMENSIONS:                 TYPE OF INJECTION: HYDRODYNAMIC
TOTAL LENGTH, in cm =  100.00         HEIGHT DIFFERENCE, in cm =    2.00
DETECTOR LENGTH, in cm =   50.00      INJECTION TIME, in sec =   60.00
I. D., in micrometers =   75.00       HYDRODYNAMIC VELOCITY, in cm/s = 3.93E  -3

ELUTION TIME   WIDTH     EFFECTIVE       DIFFUSION    EFFICIENCY   RESOLUTION
   in min      in min    MOBILITY        VARIANCE
                        in cm2/Vs        in cm2
GMP =  13.55     .222    -.2370E  -3     1.63E  -2   5.96E   4       1.17
AMP =  13.81     .227    -.2413E  -3     1.66E  -2   5.92E   4       2.17
CMP =  14.31     .237    -.2490E  -3     1.72E  -2   5.84E   4       2.26
UMP =  14.86     .248    -.2569E  -3     1.78E  -2   5.75E   4      27.96
GDP =  24.89     .470    -.3395E  -3     2.99E  -2   4.50E   4       2.03
ADP =  25.87     .493    -.3441E  -3     3.10E  -2   4.40E   4       5.40
CDP =  28.72     .564    -.3558E  -3     3.45E  -2   4.15E   4       2.77
UDP =  30.34     .605    -.3614E  -3     3.64E  -2   4.02E   4     CRS =   15.88_
INJECTION ZONE,  in cm =    .24         INJ VARIANCE, in cm2 = 4.63E  -3
DETECTOR WINDOW, in cm =    .50         DET VARIANCE, in cm2 = 2.08E  -2


FLOW CHARACTERISTICS:
ZETA POTENTIAL, in mV =  -58.14
ZETAZERO, in mV =   57.80
kPOTNa = 2.2347E  -1
ELECTROOSMOTIC MOBILITY, in cm2/Vs = 4.6179E  -4
ELECTROOSMOTIC VELOCITY, in cm/s =   .1261
VOLTAGE, in kV =  27.307
RESISTANCE, in ohm = 1.6063E   9

BUFFER CHARACTERISTICS (conc in moles/liter):
pH =   6.000
IONIC STRENGTH = 1.2500E  -2
BUFFER CONCENTRATION = 2.5000E  -3
BUFFER CAPACITY = 4.3072E  -4
CHARGE CONC = 2.4596E  -2
[M]buffer = 2.7004E  -3
[M]electr = 9.5966E  -3
BUFFER FORMULATION:
CONC M-H3A = 0.0000E  -1
CONC M-H2A = 2.2996E  -3
CONC M-HA = 2.0044E  -4
CONC M-A = 0.0000E  -1
CONC M-X = 9.5966E  -3
OK
```

Figure 4.15 Effect of the buffer ionic strength (I) on the separation of nucleotides. Solute identification and standard conditions as given in Figure 4.6. (a) Computer-simulated electropherograms for 10, 15, and 20 mM ionic strength. (b) Separation characteristics for 15 mM ionic strength. (c) Separation characteristics for 20 mM ionic strength.

Figure 4.15a

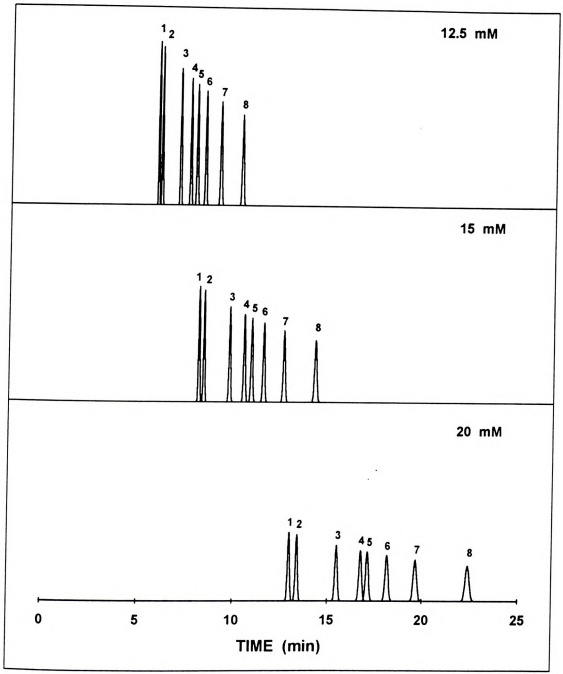
12.5 mM
1 2
3
4 5
6
7
8
15 mM
1 2
3
4 5
6
7
8
20 mM
1 2
3
4 5
6
7
8
0
5
10
15
20
25
TIME (min)

Figure 4.15b

```
PREDICTED OPTIMUM CONDITIONS FOR THE SEPARATION:
CURRENT, in microamperes =  17.000
pH =   9.800                          Correction Factor, in pH units =    .0000
IONIC STRENGTH, in moles/liter = 1.5000E  -2
BUFFER CONCENTRATION, in moles/liter = 2.5000E  -3

CAPILLARY DIMENSIONS:                 TYPE OF INJECTION: HYDRODYNAMIC
TOTAL LENGTH, in cm =  100.00         HEIGHT DIFFERENCE, in cm =    2.00
DETECTOR LENGTH, in cm =   50.00      INJECTION TIME, in sec =   60.00
I. D., in micrometers =   75.00       HYDRODYNAMIC VELOCITY, in cm/s = 3.93E  -3

ELUTION TIME    WIDTH      EFFECTIVE        DIFFUSION     EFFICIENCY    RESOLUTION
   in min       in min     MOBILITY         VARIANCE
                           in cm2/Vs         in cm2
AMP =   8.33     .126      -.3116E  -3     1.00E  -2   7.02E   4          1.92
CMP =   8.58     .130      -.3230E  -3     1.03E  -2   6.96E   4          9.05
GMP =   9.86     .153      -.3732E  -3     1.18E  -2   6.67E   4          4.59
UMP =  10.59     .166      -.3965E  -3     1.27E  -2   6.52E   4          2.17
ADP =  10.96     .173      -.4070E  -3     1.31E  -2   6.44E   4          3.36
CDP =  11.56     .184      -.4227E  -3     1.39E  -2   6.33E   4          5.29
GDP =  12.58     .203      -.4461E  -3     1.51E  -2   6.14E   4          7.28
UDP =  14.17     .234      -.4758E  -3     1.70E  -2   5.86E   4     CRS =    3.63_
INJECTION ZONE,  in cm =     .24          INJ VARIANCE, in cm2 = 4.63E  -3
DETECTOR WINDOW, in cm =     .50          DET VARIANCE, in cm2 = 2.08E  -2


FLOW CHARACTERISTICS:
ZETA POTENTIAL, in mV =  -89.42
ZETAZERO, in mV =   26.44
kPOTNa = 2.2347E  -1
ELECTROOSMOTIC MOBILITY, in cm2/Vs = 7.1024E  -4
ELECTROOSMOTIC VELOCITY, in cm/s =   .1777
VOLTAGE, in kV =   25.022
RESISTANCE, in ohm = 1.4719E   9

BUFFER CHARACTERISTICS (conc in moles/liter):
pH =   9.800
IONIC STRENGTH = 1.5000E  -2
BUFFER CONCENTRATION = 2.5000E  -3
BUFFER CAPACITY = 2.0655E  -4
CHARGE CONC = 2.4953E  -2
[M]buffer = 5.0810E  -3
[M]electr = 7.3956E  -3
BUFFER FORMULATION:
CONC M-H3A = 0.0000E  -1
CONC M-H2A = 0.0000E  -1
CONC M-HA = 2.4190E  -3
CONC M-A = 8.1022E  -5
CONC M-X = 7.3956E  -3
OK
```

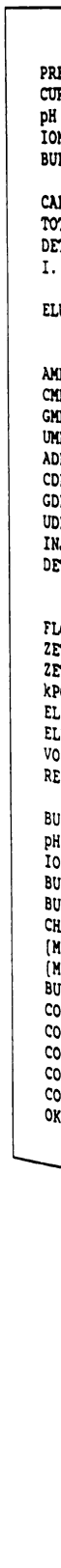

Figure 4.15c

```
PREDICTED OPTIMUM CONDITIONS FOR THE SEPARATION:
CURRENT, in microamperes =  17.000
pH =   9.800                          Correction Factor, in pH units =   .0000
IONIC STRENGTH, in moles/liter = 2.0000E  -2
BUFFER CONCENTRATION, in moles/liter = 2.5000E  -3

CAPILLARY DIMENSIONS:                 TYPE OF INJECTION: HYDRODYNAMIC
TOTAL LENGTH, in cm =  100.00         HEIGHT DIFFERENCE, in cm =    2.00
DETECTOR LENGTH, in cm =   50.00      INJECTION TIME, in sec =   60.00
I. D., in micrometers =   75.00       HYDRODYNAMIC VELOCITY, in cm/s = 3.93E  -3

ELUTION TIME   WIDTH     EFFECTIVE       DIFFUSION    EFFICIENCY   RESOLUTION
   in min      in min    MOBILITY        VARIANCE
                        in cm2/Vs        in cm2
AMP =  12.97    .211     -.2996E  -3     1.56E  -2    6.07E   4        1.95
CMP =  13.39    .219     -.3109E  -3     1.61E  -2    5.99E   4        8.78
GMP =  15.49    .261     -.3585E  -3     1.86E  -2    5.65E   4        4.68
UMP =  16.77    .287     -.3816E  -3     2.01E  -2    5.46E   4        1.24
ADP =  17.13    .295     -.3875E  -3     2.06E  -2    5.41E   4        3.38
CDP =  18.17    .317     -.4031E  -3     2.18E  -2    5.27E   4        4.49
GDP =  19.66    .349     -.4227E  -3     2.36E  -2    5.07E   4        7.18
UDP =  22.39    .411     -.4518E  -3     2.69E  -2    4.76E   4    CRS =    6.29_
INJECTION ZONE,  in cm =    .24         INJ VARIANCE, in cm2 = 4.63E  -3
DETECTOR WINDOW, in cm =    .50         DET VARIANCE, in cm2 = 2.08E  -2


FLOW CHARACTERISTICS:
ZETA POTENTIAL, in mV =  -83.24
ZETAZERO, in mV =   26.44
kPOTNa = 2.2347E  -1
ELECTROOSMOTIC MOBILITY, in cm2/Vs = 6.6116E  -4
ELECTROOSMOTIC VELOCITY, in cm/s =   .1172
VOLTAGE, in kV =  17.732
RESISTANCE, in ohm = 1.0430E   9

BUFFER CHARACTERISTICS (conc in moles/liter):
pH =   9.800
IONIC STRENGTH = 2.0000E  -2
BUFFER CONCENTRATION = 2.5000E  -3
BUFFER CAPACITY = 2.1149E  -4
CHARGE CONC = 3.4948E  -2
[M]buffer = 5.0836E  -3
[M]electr = 1.2390E  -2
BUFFER FORMULATION:
CONC M-H3A = 0.0000E  -1
CONC M-H2A = 0.0000E  -1
CONC M-HA = 2.4164E  -3
CONC M-A = 8.3602E  -5
CONC M-X = 1.2390E  -2
OK
```

Figure 4.16 Effect of the buffer concentration (CT) on the separation of nucleotides. Solute identification and standard conditions as given in Figure 4.6. (a) Computer-simulated electropherograms for 1.5, 2.5, and 3.5 mM buffer concentration. (b) Separation characteristics for 1.5 mM buffer concentration. (c) Separation characteristics for 3.5 mM buffer concentration.

Figure 4.16a

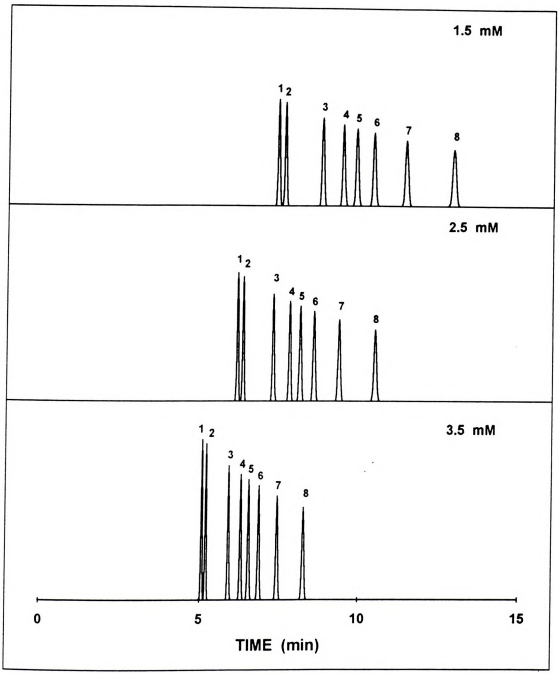

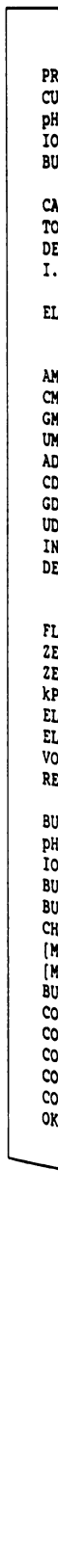

Figure 4.16b

```
PREDICTED OPTIMUM CONDITIONS FOR THE SEPARATION:
CURRENT, in microamperes =  17.000
pH =   9.800                        Correction Factor, in pH units =   .0000
IONIC STRENGTH, in moles/liter = 1.2500E  -2
BUFFER CONCENTRATION, in moles/liter = 1.5000E  -3

CAPILLARY DIMENSIONS:               TYPE OF INJECTION: HYDRODYNAMIC
TOTAL LENGTH, in cm =  100.00       HEIGHT DIFFERENCE, in cm =    2.00
DETECTOR LENGTH, in cm =   50.00    INJECTION TIME, in sec =   60.00
I. D., in micrometers =   75.00     HYDRODYNAMIC VELOCITY, in cm/s = 3.93E  -3

ELUTION TIME   WIDTH     EFFECTIVE       DIFFUSION    EFFICIENCY    RESOLUTION
   in min      in min    MOBILITY        VARIANCE
                        in cm2/Vs        in cm2
AMP =   7.39    .110    -.3185E  -3     8.87E  -3    7.25E   4        1.90
CMP =   7.60    .113    -.3300E  -3     9.12E  -3    7.20E   4        9.20
GMP =   8.73    .133    -.3816E  -3     1.05E  -2    6.92E   4        4.56
UMP =   9.36    .144    -.4049E  -3     1.12E  -2    6.78E   4        2.74
ADP =   9.77    .151    -.4183E  -3     1.17E  -2    6.69E   4        3.37
CDP =  10.29    .160    -.4341E  -3     1.23E  -2    6.58E   4        5.73
GDP =  11.26    .178    -.4594E  -3     1.35E  -2    6.38E   4        7.39
UDP =  12.68    .205    -.4895E  -3     1.52E  -2    6.12E   4    CRS =    3.26
INJECTION ZONE,  in cm =    .24         INJ VARIANCE, in cm2 = 4.63E  -3
DETECTOR WINDOW, in cm =    .50         DET VARIANCE, in cm2 = 2.08E  -2


FLOW CHARACTERISTICS:
ZETA POTENTIAL, in mV =  -91.68
ZETAZERO, in mV =   26.44
kPOTNa = 2.2347E  -1
ELECTROOSMOTIC MOBILITY, in cm2/Vs = 7.2825E  -4
ELECTROOSMOTIC VELOCITY, in cm/s =   .2000
VOLTAGE, in kV =  27.466
RESISTANCE, in ohm = 1.6156E   9

BUFFER CHARACTERISTICS (conc in moles/liter):
pH =   9.800
IONIC STRENGTH = 1.2500E  -2
BUFFER CONCENTRATION = 1.5000E  -3
BUFFER CAPACITY = 1.8753E  -4
CHARGE CONC = 2.1974E  -2
[M]buffer = 3.0761E  -3
[M]electr = 7.9108E  -3
BUFFER FORMULATION:
CONC M-H3A = 0.0000E  -1
CONC M-H2A = 0.0000E  -1
CONC M-HA = 1.4239E  -3
CONC M-A = 7.6073E  -5
CONC M-X = 7.9108E  -3
OK
```

Figure 4.16c

```
PREDICTED OPTIMUM CONDITIONS FOR THE SEPARATION:
CURRENT, in microamperes =  17.000
pH =   9.800                        Correction Factor, in pH units =    .0000
IONIC STRENGTH, in moles/liter = 1.2500E  -2
BUFFER CONCENTRATION, in moles/liter = 3.5000E  -3

CAPILLARY DIMENSIONS:               TYPE OF INJECTION: HYDRODYNAMIC
TOTAL LENGTH, in cm =  100.00       HEIGHT DIFFERENCE, in cm =    2.00
DETECTOR LENGTH, in cm =   50.00    INJECTION TIME, in sec =   60.00
I. D., in micrometers =   75.00     HYDRODYNAMIC VELOCITY, in cm/s = 3.93E  -3

ELUTION TIME   WIDTH     EFFECTIVE       DIFFUSION    EFFICIENCY    RESOLUTION
   in min      in min    MOBILITY        VARIANCE
                        in cm2/Vs        in cm2
AMP =   5.07    .072    -.3185E  -3     6.08E  -3    7.89E   4        1.85
CMP =   5.20    .074    -.3300E  -3     6.24E  -3    7.85E   4        8.90
GMP =   5.91    .086    -.3816E  -3     7.09E  -3    7.64E   4        4.39
UMP =   6.30    .092    -.4049E  -3     7.56E  -3    7.54E   4        2.63
ADP =   6.55    .096    -.4183E  -3     7.86E  -3    7.47E   4        3.24
CDP =   6.87    .101    -.4341E  -3     8.24E  -3    7.38E   4        5.48
GDP =   7.45    .111    -.4594E  -3     8.94E  -3    7.23E   4        7.04
UDP =   8.28    .125    -.4895E  -3     9.93E  -3    7.03E   4    CRS =    2.13_
INJECTION ZONE,  in cm =    .24         INJ VARIANCE, in cm2 = 4.63E  -3
DETECTOR WINDOW, in cm =    .50         DET VARIANCE, in cm2 = 2.08E  -2


FLOW CHARACTERISTICS:
ZETA POTENTIAL, in mV =  -95.60
ZETAZERO, in mV =   26.44
kPOTNa = 2.2347E  -1
ELECTROOSMOTIC MOBILITY, in cm2/Vs = 7.5932E  -4
ELECTROOSMOTIC VELOCITY, in cm/s =   .2827
VOLTAGE, in kV =  37.227
RESISTANCE, in ohm = 2.1898E   9

BUFFER CHARACTERISTICS (conc in moles/liter):
pH =   9.800
IONIC STRENGTH = 1.2500E  -2
BUFFER CONCENTRATION = 3.5000E  -3
BUFFER CAPACITY = 2.2007E  -4
CHARGE CONC = 1.7939E  -2
[M]buffer = 7.0831E  -3
[M]electr = 1.8862E  -3
BUFFER FORMULATION:
CONC M-H3A = 0.0000E  -1
CONC M-H2A = 0.0000E  -1
CONC M-HA = 3.4169E  -3
CONC M-A = 8.3060E  -5
CONC M-X = 1.8862E  -3
OK
```

solutio

the re

Capill

The p

flow a

chara

on the

achie

same

time c

may c

4.4 C

appro

base

enco

detec

appli

diam

Also,

cons

instr

and

The double-layer structure at the capillary surface can be affected by the solution characteristics and the surface charge density (Chapter 3). In any case, the result is a change in the electroosmotic flow magnitude and even direction. Capillary coating is a versatile means to manipulate the surface charge density. The program can simulate this effect by accepting values of the electroosmotic flow as an input parameter rather than by calculating the flow from the buffer characteristics. Figure 4.17 illustrates the effect of the electroosmotic mobility on the separation characteristics. The electroosmotic flow does not contribute to achieve any separation, because it affects the migration of all solutes to the same extent. However, since the electroosmotic flow influences the residence time of the solutes in the capillary, a dramatic change in efficiency and resolution may occur.

4.4 Conclusions

The computer routine developed in this work constitutes a resourceful approach to the optimization of electrophoretic separations. The program is based on theoretical models for zone migration and dispersion and encompasses versatile features, such as the choice of different injection and detection conditions as well as a particular power-supply operation mode. The applicability of the program model for voltage is restricted to capillaries of 75 μm diameter and approximately 100 cm long because of the surface conductance. Also, in this program, temperature effects that result from Joule heating are not considered. Possible consequences of the temperature increase during instrument operation are changes in the electrophoretic mobility of the solutes, and changes in the viscosity of the buffer solution, which directly alter the

Figure 4.17 Effect of the electroosmotic mobility (μ_{osm}) on the separation of nucleotides. Solute identification and standard conditions as given in Figure 4.6. (a) Computer-simulated electropherograms for 0.200, 0.235, and 0.260 $cm^2\ V^{-1}\ s^{-1}$. (b) Separation characteristics for 0.200 $cm^2\ V^{-1}\ s^{-1}$. (c) Separation characteristics for 0.260 $cm^2\ V^{-1}\ s^{-1}$.

Figure 4.17a

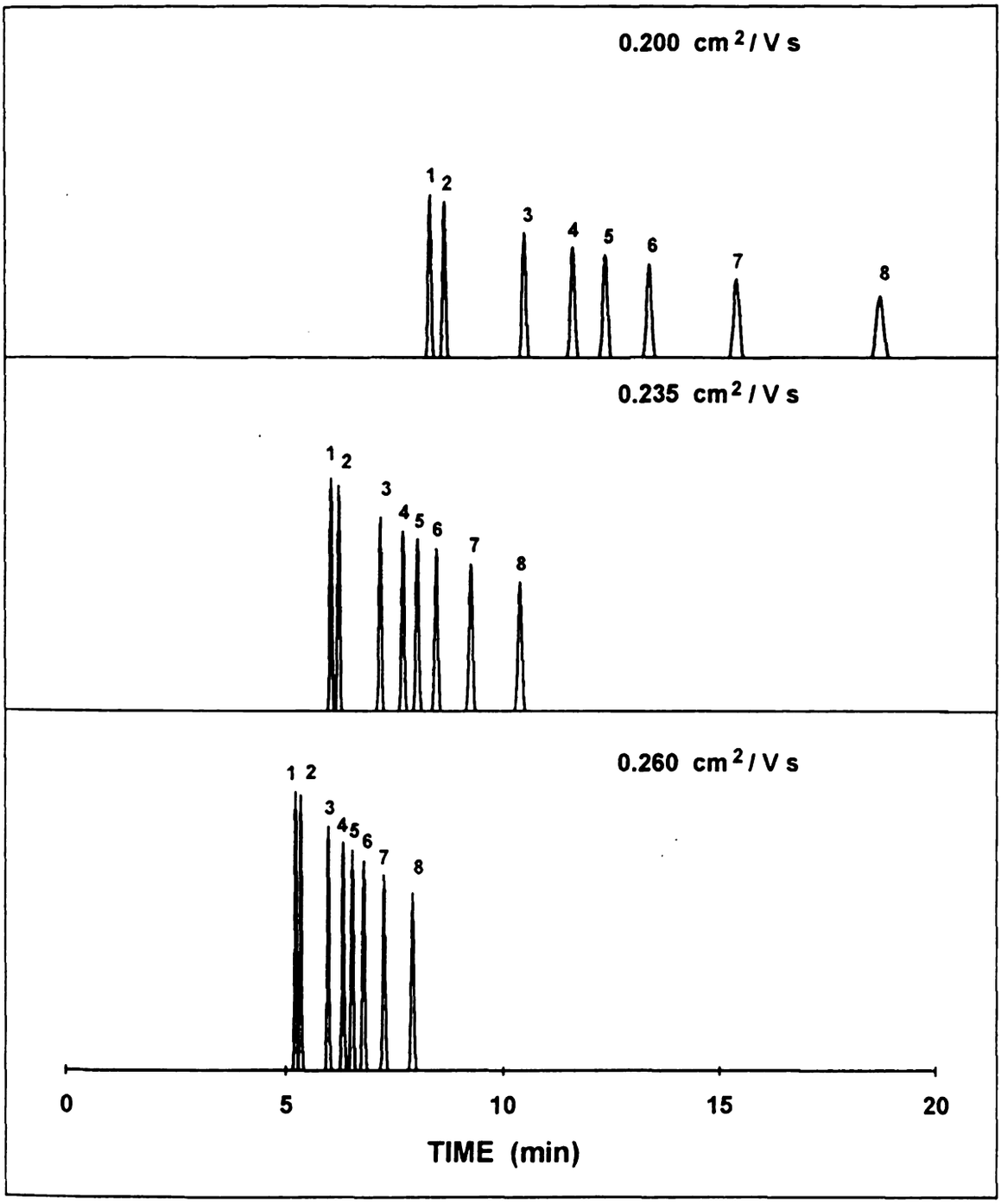
0.200 cm 2 / V s
1 2
3
4
5
6
7
8
0.235 cm 2 / V s
1 2
3
4 5 6
7
8
0.260 cm 2 / V s
1 2
3
4 5 6
7
8
0
5
10
15
20
TIME (min)

Figure 4.17b

```
PREDICTED OPTIMUM CONDITIONS FOR THE SEPARATION:
CURRENT, in microamperes =  17.000
pH =   9.800                          Correction Factor, in pH units =    .0000
IONIC STRENGTH, in moles/liter = 1.2500E  -2
BUFFER CONCENTRATION, in moles/liter = 2.5000E  -3

CAPILLARY DIMENSIONS:                 TYPE OF INJECTION: HYDRODYNAMIC
TOTAL LENGTH, in cm =  100.00         HEIGHT DIFFERENCE, in cm =    2.00
DETECTOR LENGTH, in cm =   50.00      INJECTION TIME, in sec =   60.00
I. D., in micrometers =   75.00       HYDRODYNAMIC VELOCITY, in cm/s = 3.93E  -3

ELUTION TIME   WIDTH     EFFECTIVE        DIFFUSION     EFFICIENCY    RESOLUTION
   in min      in min    MOBILITY         VARIANCE
                        in cm2/Vs         in cm2
AMP =   8.37     .126    -.3185E  -3     1.00E  -2   7.01E   4        2.45
CMP =   8.69     .132    -.3300E  -3     1.04E  -2   6.93E   4       12.08
GMP =  10.47     .164    -.3816E  -3     1.26E  -2   6.54E   4        6.18
UMP =  11.55     .184    -.4049E  -3     1.39E  -2   6.33E   4        3.78
ADP =  12.27     .197    -.4183E  -3     1.47E  -2   6.19E   4        4.73
CDP =  13.24     .216    -.4341E  -3     1.59E  -2   6.02E   4        8.23
GDP =  15.18     .254    -.4594E  -3     1.82E  -2   5.70E   4       11.07
UDP =  18.36     .321    -.4895E  -3     2.20E  -2   5.24E   4     CRS =    4.65_
INJECTION ZONE,  in cm =     .24         INJ VARIANCE, in cm2 = 4.63E  -3
DETECTOR WINDOW, in cm =     .50         DET VARIANCE, in cm2 = 2.08E  -2


FLOW CHARACTERISTICS (experimental values):
ELECTROOSMOTIC MOBILITY, in cm2/Vs = 6.3271E  -4
ELECTROOSMOTIC VELOCITY, in cm/s =   .2000
VOLTAGE, in kV =  31.610
RESISTANCE, in ohm = 1.8594E   9

BUFFER CHARACTERISTICS (conc in moles/liter):
pH =   9.800
IONIC STRENGTH = 1.2500E  -2
BUFFER CONCENTRATION = 2.5000E  -3
BUFFER CAPACITY = 2.0380E  -4
CHARGE CONC = 1.9956E  -2
[M]buffer = 5.0796E  -3
[M]electr = 4.8985E  -3
BUFFER FORMULATION:
CONC M-H3A = 0.0000E  -1
CONC M-H2A = 0.0000E  -1
CONC M-HA = 2.4204E  -3
CONC M-A = 7.9567E  -5
CONC M-X = 4.8985E  -3
OK
```

Figure 4.17c

```
PREDICTED OPTIMUM CONDITIONS FOR THE SEPARATION:
CURRENT, in microamperes =  17.000
pH =   9.800                          Correction Factor, in pH units =   .0000
IONIC STRENGTH, in moles/liter = 1.2500E  -2
BUFFER CONCENTRATION, in moles/liter = 2.5000E  -3

CAPILLARY DIMENSIONS:                 TYPE OF INJECTION: HYDRODYNAMIC
TOTAL LENGTH, in cm =  100.00         HEIGHT DIFFERENCE, in cm =    2.00
DETECTOR LENGTH, in cm =   50.00      INJECTION TIME, in sec =   60.00
I. D., in micrometers =   75.00       HYDRODYNAMIC VELOCITY, in cm/s = 3.93E  -3

ELUTION TIME   WIDTH     EFFECTIVE       DIFFUSION    EFFICIENCY   RESOLUTION
   in min      in min    MOBILITY        VARIANCE
                        in cm2/Vs        in cm2
AMP =   5.22    .075     -.3185E  -3     6.26E  -3    7.84E   4       1.61
CMP =   5.34    .076     -.3300E  -3     6.41E  -3    7.81E   4       7.68
GMP =   5.96    .086     -.3816E  -3     7.16E  -3    7.63E   4       3.75
UMP =   6.30    .092     -.4049E  -3     7.56E  -3    7.54E   4       2.23
ADP =   6.51    .095     -.4183E  -3     7.81E  -3    7.48E   4       2.72
CDP =   6.77    .100     -.4341E  -3     8.13E  -3    7.41E   4       4.57
GDP =   7.24    .107     -.4594E  -3     8.69E  -3    7.29E   4       5.79
UDP =   7.90    .118     -.4895E  -3     9.48E  -3    7.12E   4    CRS =    1.99_
INJECTION ZONE,  in cm =    .24         INJ VARIANCE, in cm2 = 4.63E  -3
DETECTOR WINDOW, in cm =    .50         DET VARIANCE, in cm2 = 2.08E  -2


FLOW CHARACTERISTICS (experimental values):
ELECTROOSMOTIC MOBILITY, in cm2/Vs = 8.2252E  -4
ELECTROOSMOTIC VELOCITY, in cm/s =   .2600
VOLTAGE, in kV =  31.610
RESISTANCE, in ohm = 1.8594E   9

BUFFER CHARACTERISTICS (conc in moles/liter):
pH =   9.800
IONIC STRENGTH = 1.2500E  -2
BUFFER CONCENTRATION = 2.5000E  -3
BUFFER CAPACITY = 2.0380E  -4
CHARGE CONC = 1.9956E  -2
[M]buffer = 5.0796E  -3
[M]electr = 4.8985E  -3
BUFFER FORMULATION:
CONC M-H3A = 0.0000E  -1
CONC M-H2A = 0.0000E  -1
CONC M-HA = 2.4204E  -3
CONC M-A = 7.9567E  -5
CONC M-X = 4.8985E  -3
OK
```

electroomotic flow. Moreover, temperature gradients in the capillary cause convective flow which may be detrimental to the separation performance. Experimentally, temperature effects can be minimized by limiting the field strength of the system to less than 350 V/cm. Another aspect that is neglected by the program is the differences in conductivity between the sample zone and the buffer solution, which can cause either fronting or tailing of the zone profile. This effect can also be controlled experimentally, by the judicious choice of the solute concentration in the buffer solution. This program can be used advantageously as a pedagogical tool to examine the effect of buffer composition and instrumental parameters on the separation performance. Furthermore, this optimization routine can be easily implemented on personal computers.

4.5 References

1. Kuhr, W. G.; Monnig, C. A. *Anal. Chem.* **1992**, *64*, 389R-407R.

2. Grossman, P. D.; Colburn, J. C., Eds.; *Capillary Electrophoresis - Theory and Practice*; Academic Press Inc.: San Diego, CA, 1992.

3. Massart, D. L.; Dijkstra, A.; Kaufman, L. *Evaluation and Optimization of Laboratory Methods and Analytical Procedures;* Elsevier: New York, 1978.

4. Massart, D. L.; Vandeginste, B. G. M.; Deming, S. N.; Michotte, Y.; Kaufman, L. *Chemometrics: a textbook*; Elsevier: New York, 1988.

5. Kuhr, W. G.; Yeung, E. S. *Anal. Chem.* **1988**, *60*, 2642-2646.

6. Vindevogel, J.; Sandra, P. *Anal. Chem.* **1991**, *63*, 1530-1536.

7. Khaledi, M. G.; Smith, S. C.; Strasters, J. K. *Anal. Chem.* **1991**, *63*, 1820-1830.

8. Smith, S. C.; Khaledi, M. G. *Anal. Chem.* **1993**, *65*, 193-198.

9. Friedl, W.; Kenndler, E. *Anal. Chem.* **1993**, *65*, 2003-2009.

10. Ng, C. L.; Ong, C. P.; Lee, H. K.; Li, S. F. Y. *J. Microcol. Sep.* **1993**, *5*, 191-197.

11. Bier, M., Ed.; *Electrophoresis - Theory, Methods and Applications;* Academic Press Inc.: New York, 1959.

12. Bier, M.; Palusinski, O. A.; Mosher, R. A.; Saville, D. A. *Science* **1983**, *219*, 1281-1287.

13. Gas, B.; Vacik, J.; Zelensky, I. *J. Chromatogr.* **1991**, *545*, 225-237.

14. Dose, E. V.; Guiochon, G. A. *Anal. Chem.* **1991**, *63*, 1063-1072.

15. Giannovario, J. A.; Griffin, R. N.; Gray, E. L. *J. Chromatogr.* **1978**, *153*, 329-352.

16. Mosher, R. A.; Dewey, D.; Thormann, W.; Saville, D. A.; Bier, M. *Anal. Chem.* **1989**, *61*, 362-366.

17. Mikkers, F. E. P.; Everaerts, F. M.; Verheggen, Th. P. E. M. *J. Chromatogr.* **1979**, *169*, 1-10.

18. Ermakov, S. V.; Mazhorova, O. S.; Zhukov, M. Y. *Electrophoresis* **1991**, *13*, 838-848.

19. Jones, H. K.; Nguyen, N. T.; Smith, R. D. *J. Chromatogr.* **1990**, *504*, 1-19.

20. Huang, X.; Coleman, W. F.; Zare, R. N. *J. Chromatogr.* **1989**, *480*, 95-110.

21. Roberts, G. O.; Rhodes, P. H.; Snyder, R. S. *J. Chromatogr.* **1989**, 480, 35-67.

22. Schlabach, T. D.; Excoffier, J. L. *J. Chromatogr.* **1988**, *439*, 173-184.

23. Giddings, J. C. *Unified Separation Science;* Wiley-Interscience Pulication: New York, 1991.

24. Bard, A. J.; Faulkner, L. R. *Electrochemical Methods - Fundamentals and Applications*; John Wiley & Sons: New York, 1980.

25. Robinson, R. A.; Stokes, R. H. *Electrolyte Solutions - The Measurement and Interpretation of Conductance, Chemical Potential and Diffusion in Solutions of Simple Electrolytes*; Butterworths Scientific Publications: London, 1959.

26. Hiemenz, P. C. *Principles of Colloid and Surface Chemistry, 2nd ed.*; Marcel Dekker: New York, 1986.

27. Hayes, M. A.; Kheterpal, I.; Ewing, A. G. *Anal. Chem.* **1993**, *65*, 2010-2013.

28. Spanier,J.; Oldham, K. *An Atlas of Functions*; Hemisphere Pub. Corp.: Washington, DC, 1987.

29. Lyklema, J. *J. Electroanal. Chem.* **1968**, *18*, 341-348.

30. Butler, J. N. *Ionic Equilibrium - A Mathematical Approach*; Addison-Wesley Publishing Company, Inc: Massachusetts, 1964.

31. Rossotti, F. J. C.; Rossotti, H. *The Determination of Stability Constants and other Equilibrium Constants in Solution*; McGraw Hill Book Company, Inc.: New York, 1961.

32. Rossotti, H. *The Study of Ionic Equilibria - An Introduction*; Longman: New York, 1978.

33. Hirokawa, T.; Kobayashi, S.; Kiso, Y. *J. Chromatogr.* **1985**, *318*, 195-210.

34. Beckers, J. L.; Everaerts, F. M.; Ackermans, M. T. *J. Chromatogr.* **1991**, *537*, 407-428.

35. Cai, J.; Smith, J. T.; El Rassi, Z. *J. High. Resol. Chromatogr.* **1992**, *15*, 30-32.

36. Lambert, W. J. *J. Chem. Ed.* **1990**, *67*, 150-153.

37. Sternberg, J. C. in *Advances in Chromatography,* Vol. 2, pp. 205-270; Giddings, J. C.; Keller, R. A., Eds.; Marcel Dekker, Inc.: New York, 1966.

38. Glajch, J. L.; Snyder, L. R., Eds.; *Computer-Assisted Method Development for High-Performance Liquid Chromatography*; Elsevier Science Publishing Company Inc: New York, 1990.

39. Schoenmakers, P. J. *Optimization of Chromatographic Selectivity - a guide to method development, J. Chromatogr. Lib.*, Vol. 35; Elsevier Science Publishing Company Inc: New York, 1986.

40. Berridge, J. C. *Techniques for the Automated Optimization Of HPLC Separations*, John Wiley and Sons: New York, 1986.

CHAPTER 5

EXPERIMENTAL VALIDATION OF THE OPTIMIZATION PROGRAM WITH NUCLEOTIDE MIXTURES

5.1 Introduction

In order to validate experimentally the computer optimization program described in Chapter 4, the nucleotides 5'-mono- and di-phosphates were chosen as model solutes. Nucleotides constitute an important class of biomolecules that function as intermediates in nearly all biochemical processes.[1] As building blocks, they are the precursors of nucleic acids (DNA and RNA) and the components of three major coenzymes (NAD^+, FAD and CoA). Nucleotides act as metabolic regulators, mediating the action of many hormones and as storage of chemical energy for biological reactions. Inhibitors of the nucleotide biosynthesis[2] (methotrexate and fluorouracil) have been employed in cancer chemotherapy, and the metabolism of nucleotide analogs[3] (azidothymidine, AZT) has been exploited in the treatment of acquired immune deficiency syndrome (AIDS).

Nucleotides contain characteristic structural features:[4-6] a nitrogenous heterocyclic base, which is a derivative of either pyrimidine or purine, and a pentose sugar ring, esterified by phosphoric acid at the 5' position. The structures and ionization patterns of the nucleotides studied in this work are displayed in Figure 5.1. The base and the sugar rings are nearly planar and in the most stable conformation, they are positioned almost at right angles to each other. Although the heterocyclic bases can exist in several tautomeric forms, the

Figure 5.1 Chemical structures and ionization pattern of nucleotides.

Figure 5.1

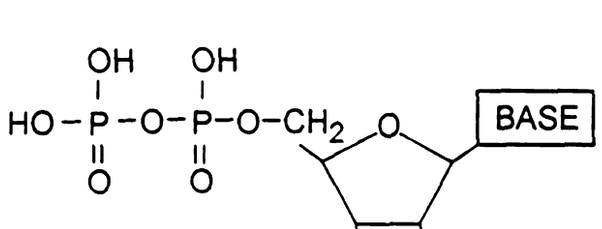

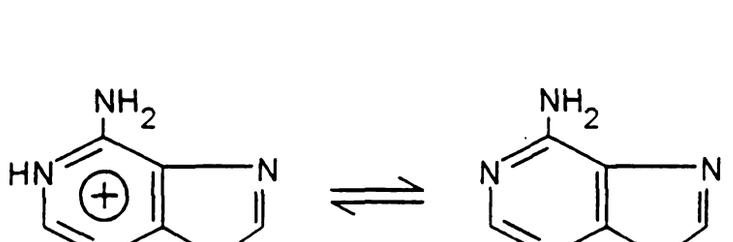

ADENOSINE

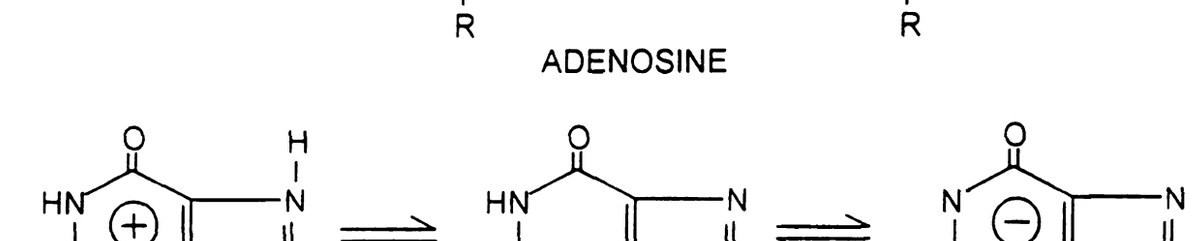

GUANOSINE

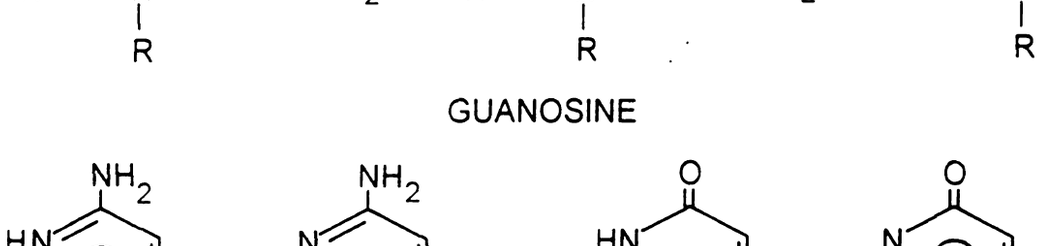

CYTIDINE URIDINE

enol-imino structure is usually regarded as a minor form. Thus, for uridine the corresponding base occurs predominantly as the diketo tautomer. The keto-amino tautomeric forms prevail in cytidine and guanosine, and the amino form prevails in adenosine. The phosphate chain is acidic in character, but the heterocyclic bases can actually have properties of weak acids, bases or both.[5,7-9]

The presence of multiple ionization sites makes the nucleotides suitable molecules for electrophoretic analysis. Nucleotides have been chosen as model compounds in a variety of applications,[3,10] to demonstrate different modes of electrophoretic methods,[9,11-13] detection schemes,[14-18] and optimization strategies.[9,14] In this work, the electrophoretic behavior of nucleotides in phosphate buffer solutions is characterized. The computational method developed in section 4.2 (Chapter 4) to determine dissociation constants and individual electrophoretic mobility is applied here. A new set of dissociation constants and individual electrophoretic mobility of nucleotide molecules is derived, which complements the available literature data.[7-9] The characteristics of the separation of these compounds are then thoroughly examined in the pH range from 6 to 11, and contrasted with those predicted by the computer optimization routine.

5.2 Results and Discussion

Study of the Electrophoretic Behavior of Nucleotides. The model for effective mobility and the computational method developed to determine dissociation constants and electrophoretic mobilities (section 4.2) were applied to evaluate the electrophoretic behavior of nucleotides in phosphate buffer

solutions. The experimental determination of the effective electrophoretic mobility is based on measurements of migration time and electroosmotic velocity (Equation [4.3]), under a variety of pH conditions. The experimental curve of effective mobility versus pH of each nucleotide is then analyzed by numerical procedures, where the plateaus and inflection points serve as initial estimates of the individual mobilities and dissociation constants (pK_a), respectively (Equation [4.14]). The best values for these parameters are determined by the least-squares method.[19] The experimentally measured effective mobility of guanosine 5'-monophosphate and the curve calculated from the procedure described above are shown in Figure 5.2 as a function of pH. Additionally, Figure 5.2 shows the curve derived from dissociation constants and electrophoretic mobilities corrected to the condition of infinite dilution (Equations [4.15] and [4.16]).[20] The decrease in mobility, imposed by the ionic strength of the medium, is a phenomenon known as the retardation effect.[21]

The experimentally determined pK_a and individual electrophoretic mobilities of the nucleotides studied in this work are given in Table 5.1. All constants and mobilities were corrected to the condition of infinite dilution.[20] In the table, the marked values were obtained from determinations of pK_a and mobility performed in other buffer systems.[7,9] These parameters could not be evaluated in phosphate buffer solutions because, the region below pH 5 is experimentally inaccessible for both nucleotide mono- and di-phosphates, concomitantly. This is clear from inspection of Figure 5.3, where the electroosmotic mobility curve of the phosphate buffer is superimposed to the effective mobility curves of the nucleotides. In fused-silica capillaries, the electroosmotic flow is directed towards the cathode.[21] Thus, according with the convention adopted in this work, the electroosmotic mobility has a positive sign. Conversely, above pH 4, all nucleotides are negatively charged and thus, their

Figure 5.2 Effective mobility of guanosine 5'-monophosphate as a function of pH in phosphate buffer solutions formulated to contain a total concentration of sodium of 10 mM. (Bottom) Experimental values and calculated curve. (Top) Calculated curve under conditions of infinite dilution.

Figure 5.2

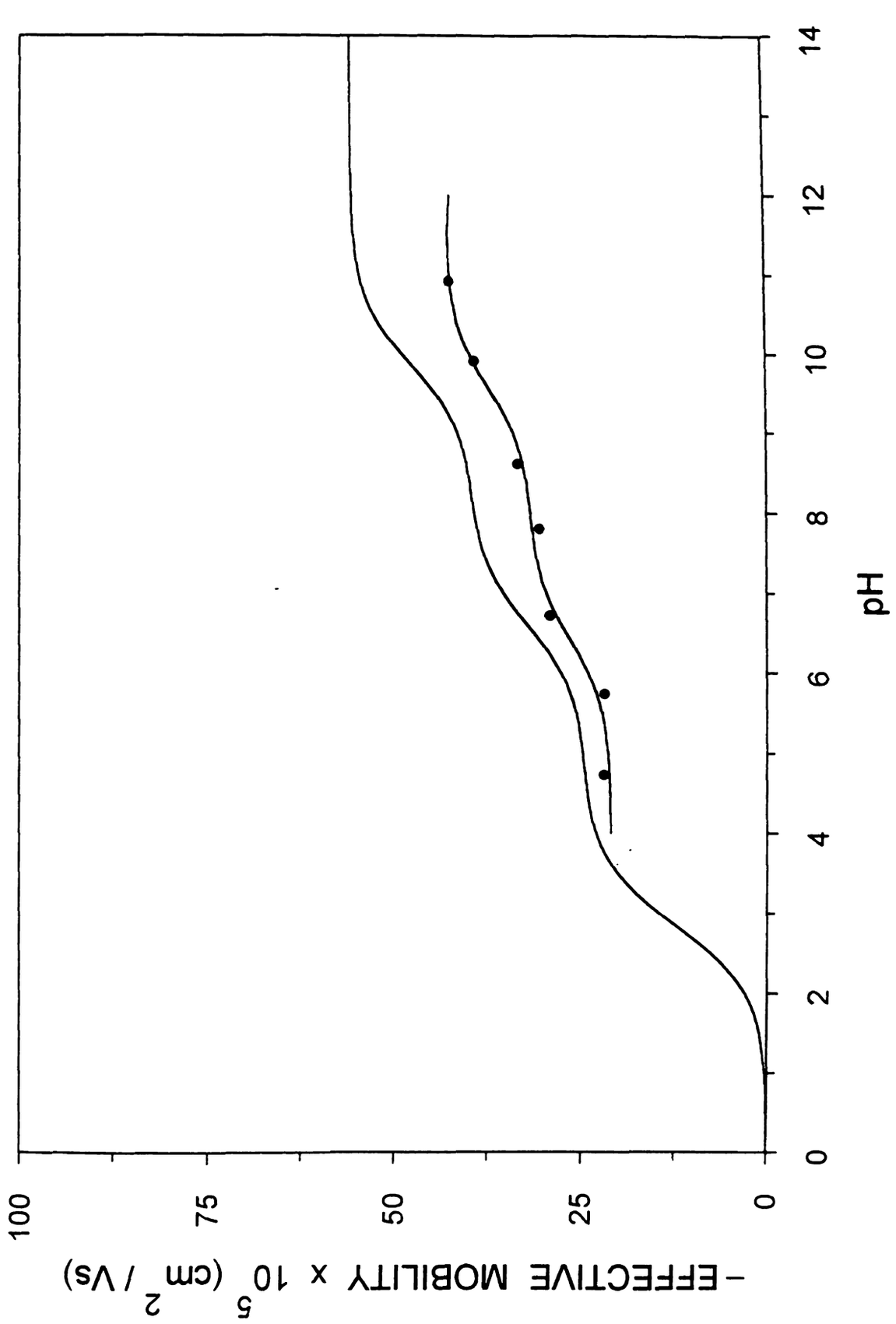

Table 5.1 Dissociation contants and electrophoretic mobilities of nucleotides at 25° C and infinite dilution (the subscript b denotes the constants associated with the nucleotide base).

SOLUTE	DISSOCIATION CONSTANT					ELECTROPHORETIC MOBILITY ($\times 10^5$ cm^2 V^{-1} s^{-1})			
	pK_{a1}	pK_{a2}	pK_{a3}	pK_{a4}	pK_{a5}	μ_1	μ_2	μ_3	μ_4
AMP	0.9**	3.981_b*	6.444			−23.96	−40.0		
ADP	<1	1+	4.101_b*	6.673		−19.2*	−39.8	−55.1	
GMP	0.7**	2.845_b*	6.591	9.871_b		−24.6	−39.6	−55.9	
GDP	<1	1+	2.958_b*	6.678	9.845_b	−18.7*	−39.6	−53.8	−67.4
CMP	0.8**	4.468_b*	6.255			−22.2	−41.2		
CDP	<1	1+	4.782_b*	6.570		−19.5*	−40.1	−56.8	
UMP	1.0** 2.499*	6.511	9.873_b			−26.0	−41.8	−58.6	
UDP	1+	2.5+	6.568	9.790_b		−20+	−41.0	−56.5	−70.6

* from reference 9
** from reference 7
\+ value attributed by the computational method

Figure 5.3 Effective mobility curve of the nucleotides superimposed to the electroosmotic mobility of phosphate buffer solutions.

Figure 5.3

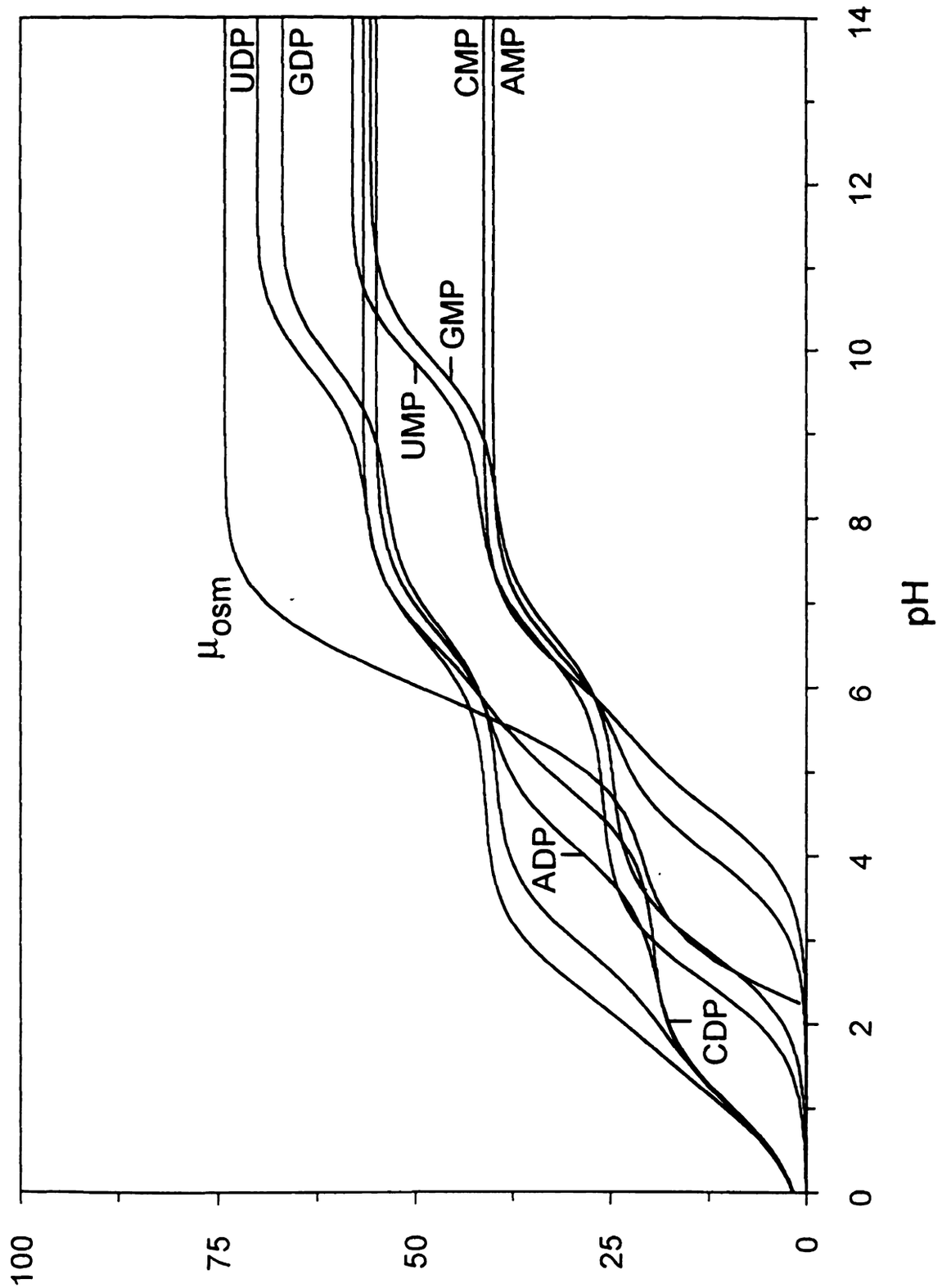
UDP
GDP
CMP
AMP
GMP
UMP
ADP
CDP
μ_{osm}
pH
0
2
4
6
8
10
12
14
0
25
50
75
100
-EFFECTIVE MOBILITY x 10^5 (cm^2 / Vs)

mobility is negative in sign. When the magnitude of the electroosmotic flow is larger compared to the electrophoretic migration, all nucleotides are directed towards the cathode. However, near pH 5, the electroosmotic mobility has decreased to a value in between the electrophoretic mobility of the nucleotide mono- and di-phosphates. Therefore, at this pH condition, only the monophosphates are able to migrate towards the cathode, and the analysis of both groups of solutes in the same mixture is no longer possible.

The effective mobility as a function of pH curve constitutes a valuable tool for the preliminary assessment of an electrophoretic separation. As Figure 5.3 illustrates, in phosphate buffers, it would be very difficult to accomplish the separation of nucleotides in the range of pH between 5 and 9, due to the similarities in electrophoretic behavior. The region above pH 9 is promising. However, the differences in the magnitude of the electrophoretic mobility are small, and operational conditions must be optimized to enhance efficiency.

Nucleotides as Model Solutes for the Optimization Program. In order to utilize the optimization program described in Chapter 4 to the separation of nucleotides, appropriate boundary conditions must be established. Some of these boundary conditions are necessary to define the domains of the input parameters and, hence, are chosen explicitly by the user for a specific application. Minimum and maximum values together with a suitable interval must be chosen for the applied current or voltage as well as the buffer pH, concentration, and ionic strength. Other boundary conditions are invoked implicitly by the program whenever the specified input parameters lead to an undesirable situation. For example, high voltage may cause temperature effects that are not considered in the program models. Therefore, combinations of the experimental parameters that lead to a predicted voltage in excess of 35 kV are

rejected. Other constraints considered by the program are related to the buffer formulation. Not all combinations of the buffer pH, concentration, and ionic strength are experimentally feasible. In addition, when solutes possess an effective mobility that is opposite in sign and larger in magnitude than the electroosmotic mobility, they will not migrate toward the cathode. Appropriate constraints have been incorporated in the program to avoid these unacceptable conditions.

By methodically varying the input parameters within the defined boundary conditions and evaluating the CRS response function, the computer program can predict the experimental conditions required for optimal separation of the solutes. This simulation has been applied to assess the separation of the nucleotide mono- and di-phosphates in phosphate buffer solutions, under constant-current conditions. Figures 5.4 and 5.5 present surface maps and contour plots, which allow for visual inspection of the CRS response function within the defined range of parameters. This system is characterized by the presence of multiple minima.

Appropriate sets of conditions were chosen, including the vicinity of the optimum conditions (pH 10, ionic strength 12.5 mM, buffer concentration 2.4 mM, current 12.5 μA), to study the separation of nucleotides. The resulting electropherograms are shown in Figures 5.6 to 5.10 together with those predicted by the program, followed by outputs of the simulated conditions. The program predicts the correct elution order for all nucleotides, and provides a reasonable estimate of the peak width and resolution. However, the predicted migration times are considerably longer than those observed experimentally. In order to understand this discrepancy, the errors associated with each constituent model of the program must be examined separately. As shown in Table 5.2, the voltage and electrophoretic mobility are predicted with average relative errors of

Figure 5.4 Surface maps representing the separation of nucleotide mono- and di-phosphates. (a) CRS as a function of pH and applied current with constant ionic strength of 12.5 mM and buffer concentration of 2.5 mM. (b) CRS as a function of pH and ionic strength with constant buffer concentration of 2.5 mM and current of 12.5 μA. (c) CRS as a function of pH and buffer concentration with constant ionic strength of 12.5 mM and current of 12.5 μA.

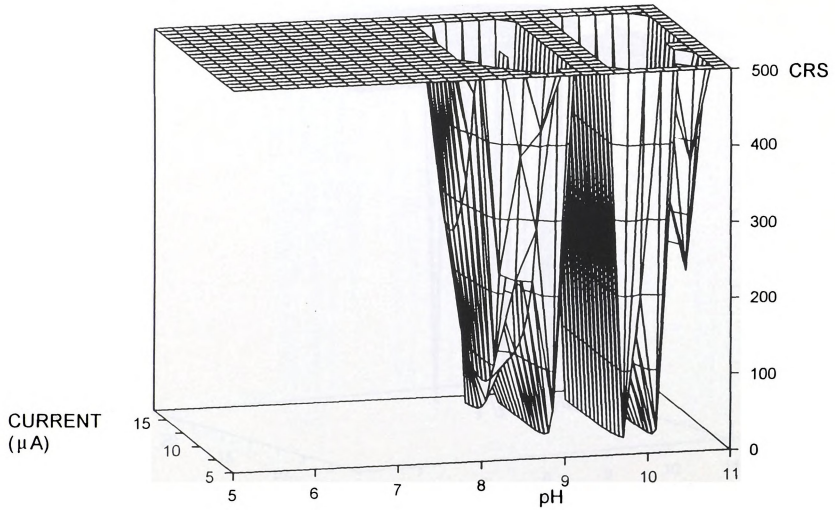

Figure 5.4a

Figure 5.4b

500 CRS
400
300
200
100
0
11
10
9
8
pH
7
6
5
5
10
15
20
IONIC
STRENGTH
(mM)

Figure 5.4c

Figure 5.4c

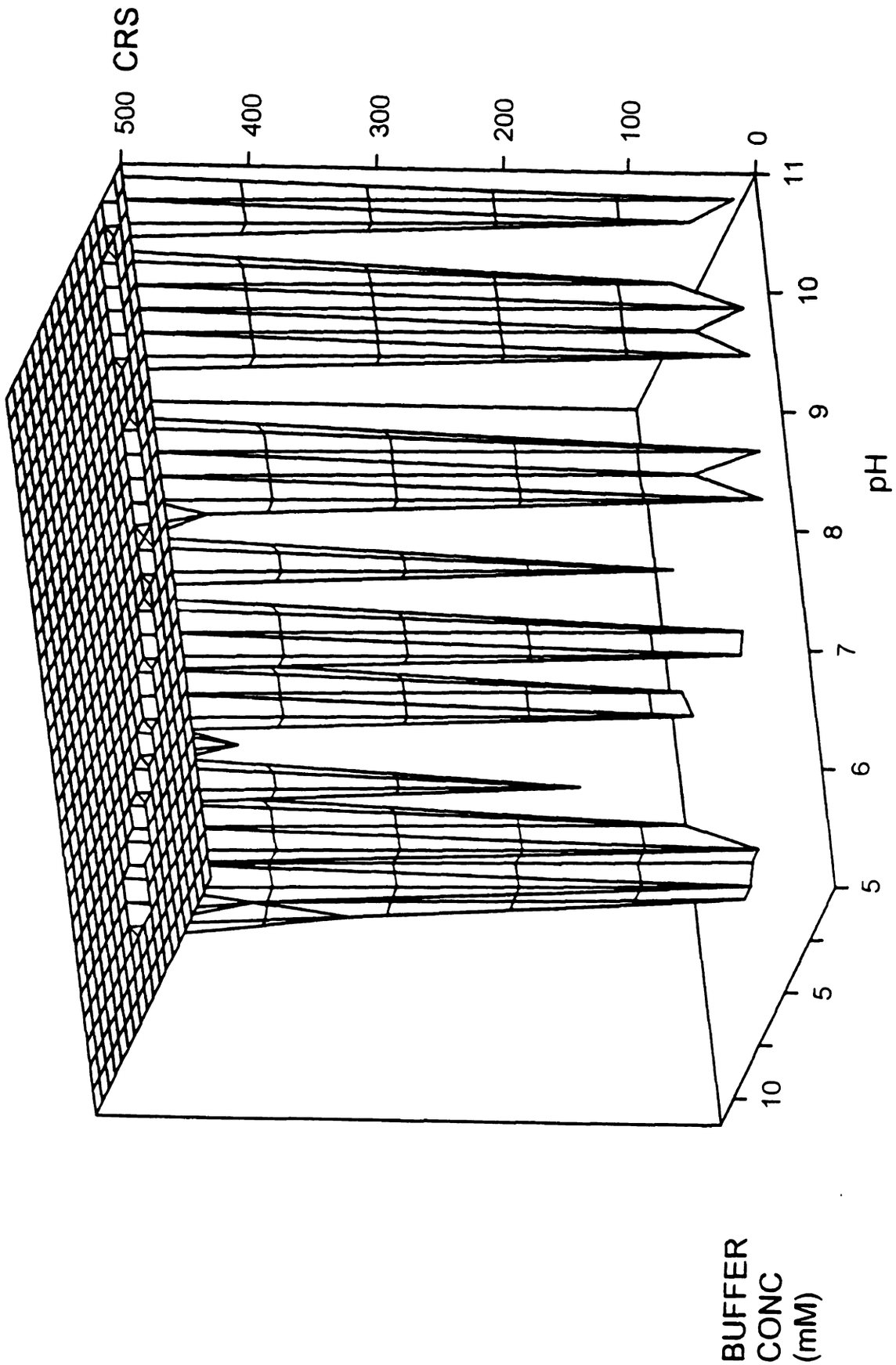

Figure 5.5 Contour maps representing the separation of nucleotide mono- and di-phosphates. (a) CRS as a function of pH and applied current with constant ionic strength of 12.5 mM and buffer concentration of 2.5 mM. (a) CRS as a function of pH and ionic strength with constant buffer concentration of 2.5 mM and current of 12.5 μA. (c) CRS as a function of pH and buffer concentration with constant ionic strength of 12.5 mM and current of 12.5 μA.

200

Figure 5.5a

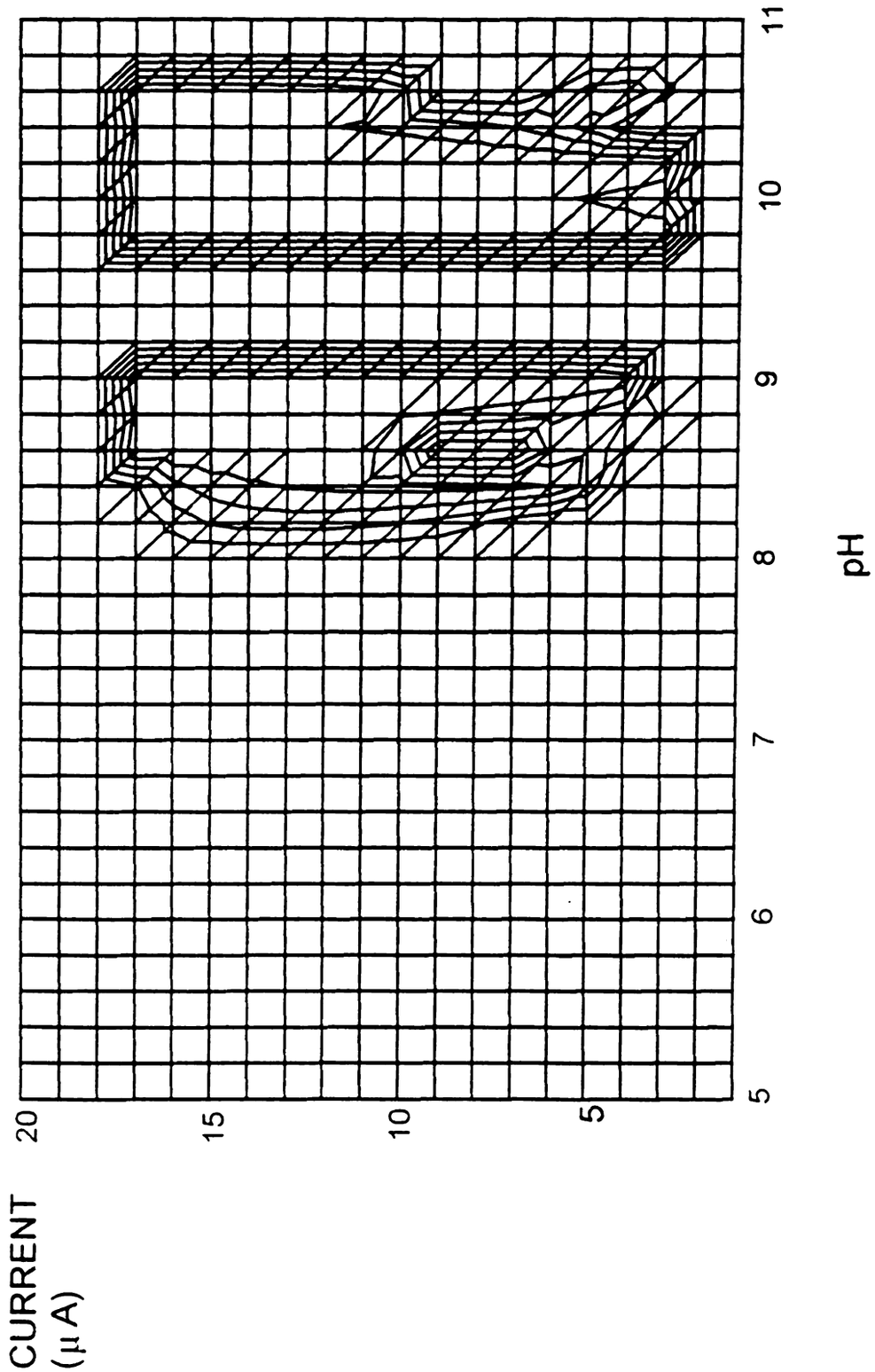

Figure 5.5b

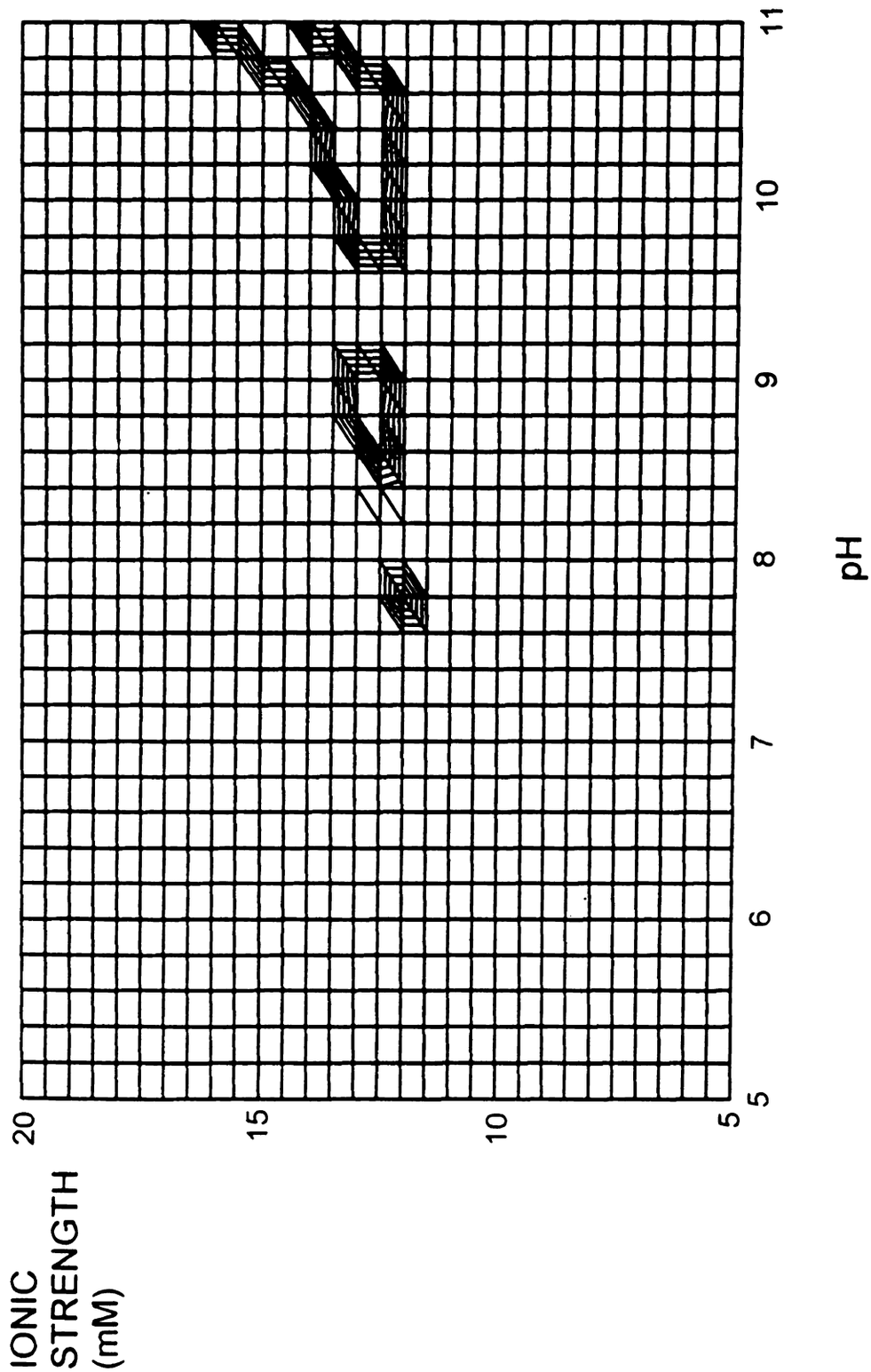

Figure 5.5c

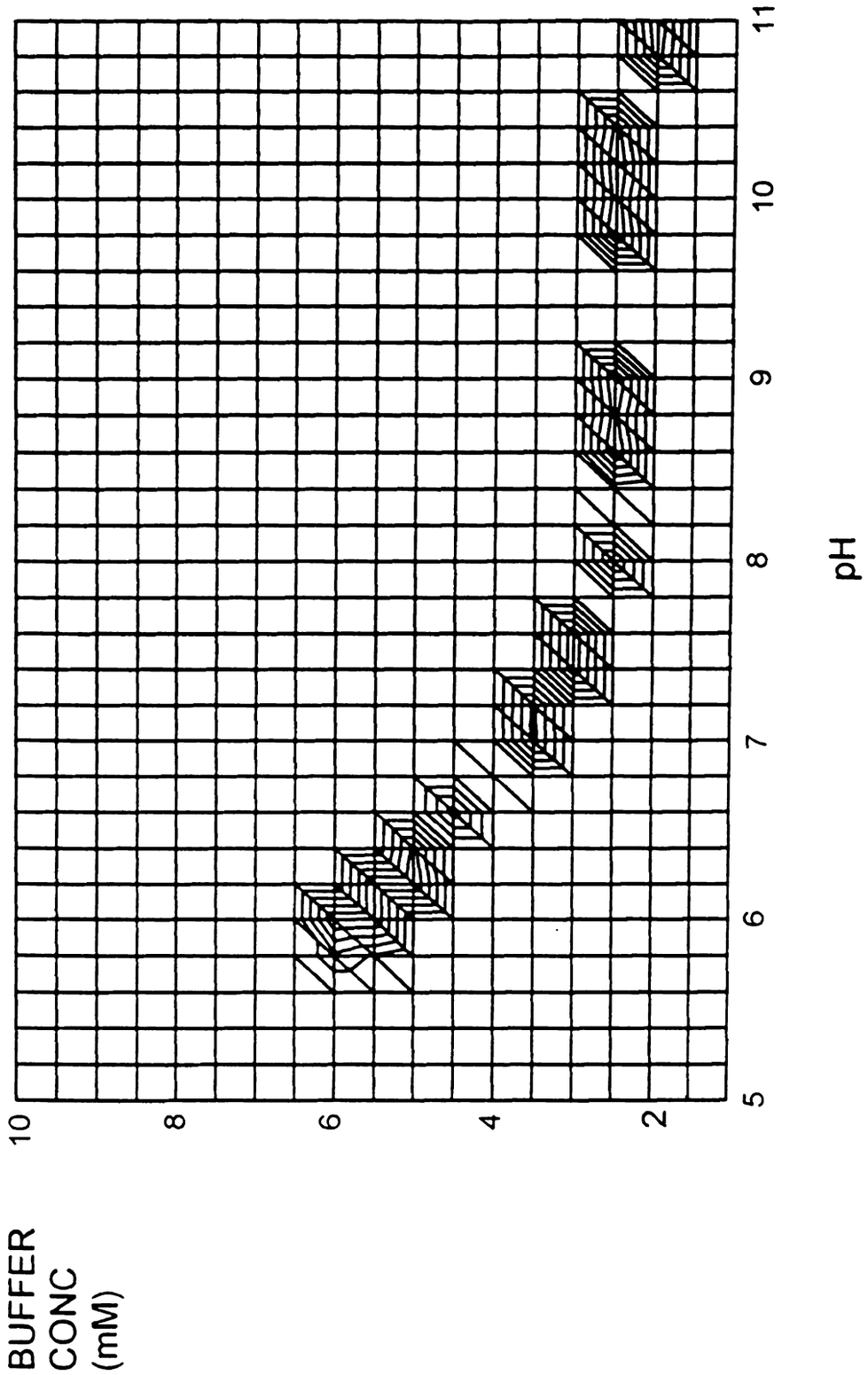

Figure 5.6 Separation of the nucleotides (1) AMP, (2) CMP, (3) GMP, (4) UMP, (5) ADP, (6) CDP, (7) GDP, and (8) UDP in phosphate buffer solution at pH 6, and 10 mM sodium concentration, under constant-current conditions of 12.5 μA. (a) Experimental electropherogram (top), computer-simulated electropherogram (middle), computer-simulated electropherogram with experimentally measured value of electroosmotic mobility and voltage (bottom). (b) Separation characteristics under the predicted conditions. (c) Separation characteristics under the predicted conditions, after input of the experimentally determined value of electroosmotic mobility and voltage.

Figure 5.6a

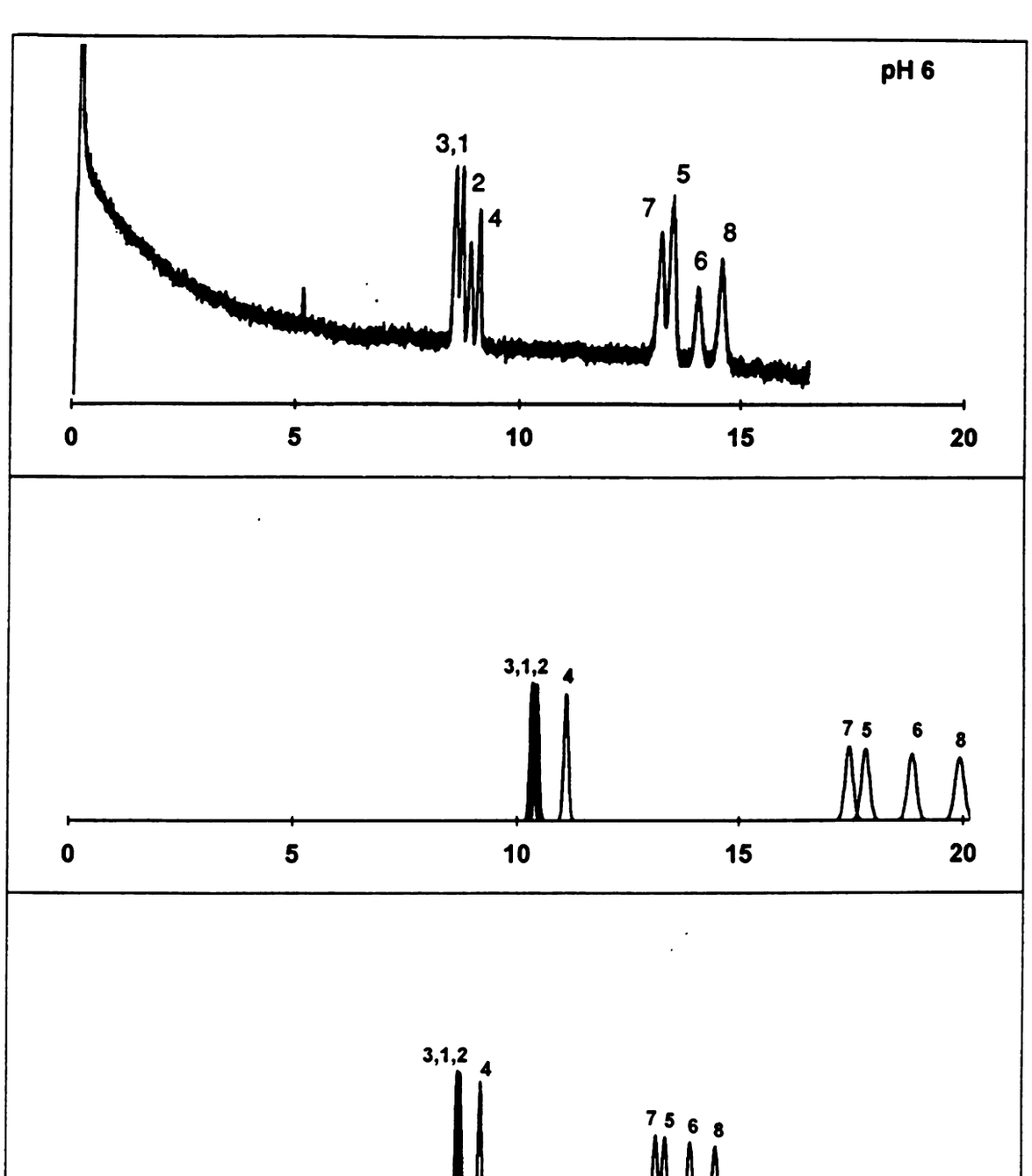
pH 6
3,1
2
4
7
5
6
8
0
5
10
15
20
3,1,2
4
7 5
6
8
0
5
10
15
20
3,1,2
4
7 5
6
8
0
5
10
15
20
TIME (min)

Figure 5.6b

```
PREDICTED OPTIMUM CONDITIONS FOR THE SEPARATION:
CURRENT, in microamperes =  12.500
pH =   6.000                        Correction Factor, in pH units =   .2550
IONIC STRENGTH, in moles/liter = 1.0366E  -2
BUFFER CONCENTRATION, in moles/liter = 4.6367E  -3

CAPILLARY DIMENSIONS:               TYPE OF INJECTION: HYDRODYNAMIC
TOTAL LENGTH, in cm =  112.15       HEIGHT DIFFERENCE, in cm =    2.00
DETECTOR LENGTH, in cm =   43.40    INJECTION TIME, in sec =   60.00
I. D., in micrometers =   75.50     HYDRODYNAMIC VELOCITY, in cm/s = 3.55E  -3

ELUTION TIME   WIDTH     EFFECTIVE       DIFFUSION    EFFICIENCY   RESOLUTION
   in min      in min    MOBILITY        VARIANCE
                        in cm2/Vs        in cm2
GMP =  10.33    .184    -.2298E  -3     1.24E  -2    5.06E   4        .24
AMP =  10.38    .185    -.2309E  -3     1.25E  -2    5.06E   4        .36
CMP =  10.44    .186    -.2326E  -3     1.25E  -2    5.05E   4       3.38
UMP =  11.10    .200    -.2479E  -3     1.33E  -2    4.94E   4      23.37
GDP =  17.45    .344    -.3368E  -3     2.09E  -2    4.11E   4       1.05
ADP =  17.82    .353    -.3400E  -3     2.14E  -2    4.08E   4       2.85
CDP =  18.86    .379    -.3484E  -3     2.26E  -2    3.97E   4       2.72
UDP =  19.93    .406    -.3561E  -3     2.39E  -2    3.86E   4    CRS =  137.58_
INJECTION ZONE,  in cm =    .21        INJ VARIANCE, in cm2 = 3.78E  -3
DETECTOR WINDOW, in cm =    .50        DET VARIANCE, in cm2 = 2.08E  -2


FLOW CHARACTERISTICS:
ZETA POTENTIAL, in mV =  -61.95
ZETAZERO, in mV =   57.80
kPOTNa = 2.2347E  -1
ELECTROOSMOTIC MOBILITY, in cm2/Vs = 4.9204E  -4
ELECTROOSMOTIC VELOCITY, in cm/s =   .1310
VOLTAGE, in kV =  29.863
RESISTANCE, in ohm = 2.3891E   9

BUFFER CHARACTERISTICS (conc in moles/liter):
pH =   6.000
IONIC STRENGTH = 1.0366E  -2
BUFFER CONCENTRATION = 4.6367E  -3
BUFFER CAPACITY = 7.7847E  -4
CHARGE CONC = 2.0002E  -2
[M]buffer = 5.0000E  -3
[M]electr = 4.9999E  -3
BUFFER FORMULATION:
CONC M-H3A = 0.0000E  -1
CONC M-H2A = 4.2734E  -3
CONC M-HA = 3.6333E  -4
CONC M-A = 0.0000E  -1
CONC M-X = 4.9999E  -3
OK
```

Figure 5.6c

```
PREDICTED OPTIMUM CONDITIONS FOR THE SEPARATION:
CURRENT, in microamperes =  12.500
pH =   6.000                          Correction Factor, in pH units =   .2550
IONIC STRENGTH, in moles/liter = 1.0366E  -2
BUFFER CONCENTRATION, in moles/liter = 4.6367E  -3

CAPILLARY DIMENSIONS:                 TYPE OF INJECTION: HYDRODYNAMIC
TOTAL LENGTH, in cm =  112.15         HEIGHT DIFFERENCE, in cm =    2.00
DETECTOR LENGTH, in cm =   43.40      INJECTION TIME, in sec =   60.00
I. D., in micrometers =   75.50       HYDRODYNAMIC VELOCITY, in cm/s = 3.55E  -3

ELUTION TIME   WIDTH      EFFECTIVE       DIFFUSION    EFFICIENCY    RESOLUTION
   in min      in min     MOBILITY        VARIANCE
                         in cm2/Vs        in cm2
GMP =   8.69    .150     -.2298E  -3     1.04E  -2    5.35E   4         .21
AMP =   8.72    .151     -.2309E  -3     1.05E  -2    5.34E   4         .31
CMP =   8.76    .152     -.2326E  -3     1.05E  -2    5.34E   4        2.89
UMP =   9.21    .161     -.2479E  -3     1.11E  -2    5.26E   4       19.49
GDP =  13.16    .244     -.3368E  -3     1.58E  -2    4.64E   4         .83
ADP =  13.37    .249     -.3400E  -3     1.60E  -2    4.61E   4        2.25
CDP =  13.94    .262     -.3484E  -3     1.67E  -2    4.53E   4        2.13
UDP =  14.51    .275     -.3561E  -3     1.74E  -2    4.46E   4    CRS =  243.18_
INJECTION ZONE,  in cm =    .21         INJ VARIANCE, in cm2 = 3.78E  -3
DETECTOR WINDOW, in cm =    .50         DET VARIANCE, in cm2 = 2.08E  -2


FLOW CHARACTERISTICS (experimental values):
ELECTROOSMOTIC MOBILITY, in cm2/Vs = 5.4421E  -4
ELECTROOSMOTIC VELOCITY, in cm/s =   .1438
VOLTAGE, in kV =  29.634
RESISTANCE, in ohm = 2.3707E   9

BUFFER CHARACTERISTICS (conc in moles/liter):
pH =   6.000
IONIC STRENGTH = 1.0366E  -2
BUFFER CONCENTRATION = 4.6367E  -3
BUFFER CAPACITY = 7.7847E  -4
CHARGE CONC = 2.0002E  -2
[M]buffer = 5.0000E  -3
[M]electr = 4.9999E  -3
BUFFER FORMULATION:
CONC M-H3A = 0.0000E  -1
CONC M-H2A = 4.2734E  -3
CONC M-HA = 3.6333E  -4
CONC M-A = 0.0000E  -1
CONC M-X = 4.9999E  -3
OK
```

Figure 5.7 Separation of nucleotides in pH 7 phosphate buffer solution. Solute identification and conditions as given in Figure 5.6.

Figure 5.7a

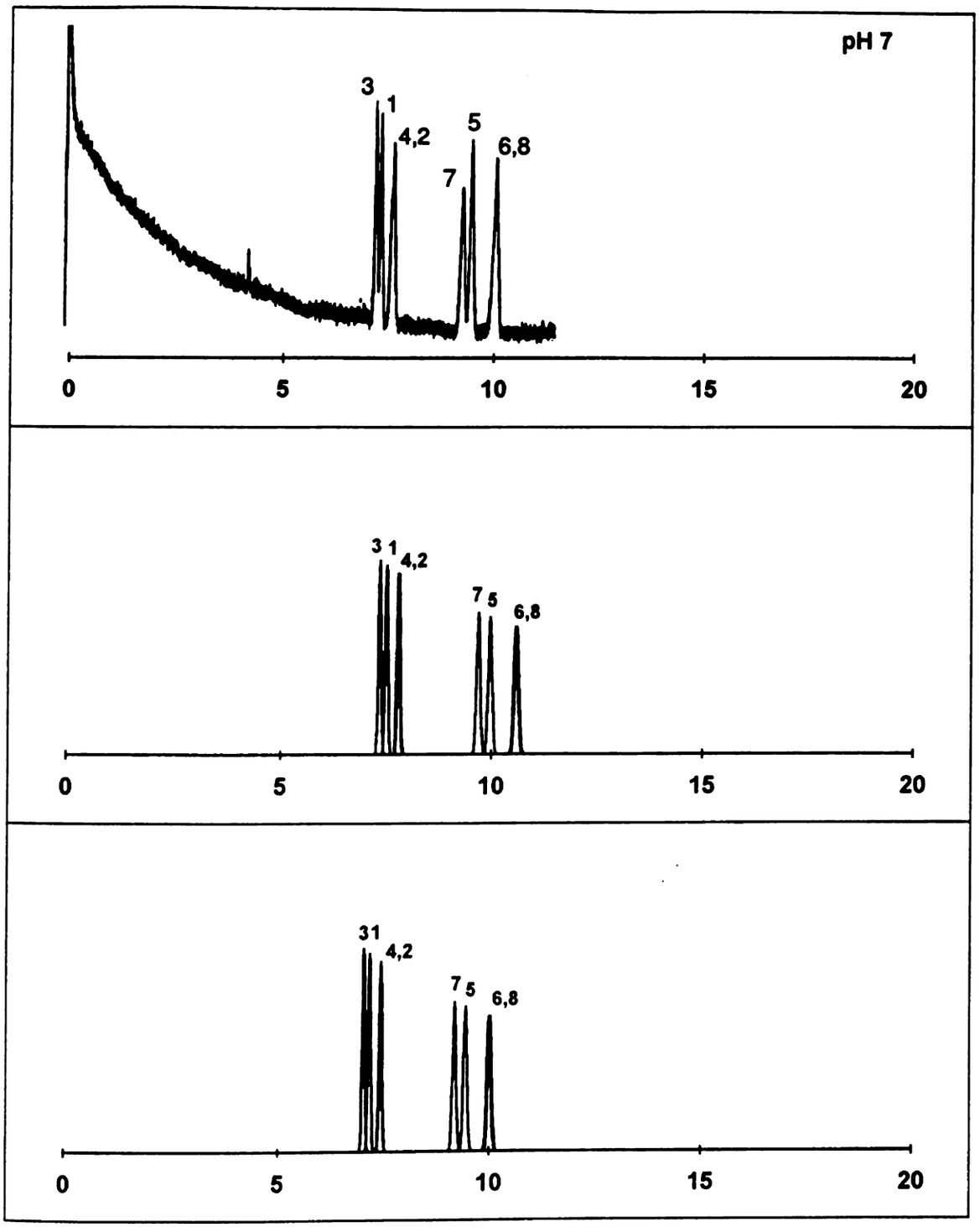
pH 7
3
1
4,2
5
6,8
7
0
5
10
15
20
3 1
4,2
7 5
6,8
0
5
10
15
20
31
4,2
7 5
6,8
0
5
10
15
20
TIME (min)

Figure 5.7b

```
PREDICTED OPTIMUM CONDITIONS FOR THE SEPARATION:
CURRENT, in microamperes =  12.500
pH =   7.000                          Correction Factor, in pH units =   .2800
IONIC STRENGTH, in moles/liter = 1.1587E  -2
BUFFER CONCENTRATION, in moles/liter = 3.4135E  -3

CAPILLARY DIMENSIONS:                 TYPE OF INJECTION: HYDRODYNAMIC
TOTAL LENGTH, in cm =  112.15         HEIGHT DIFFERENCE, in cm =    2.00
DETECTOR LENGTH, in cm =   43.40      INJECTION TIME, in sec =   60.00
I. D., in micrometers =   75.50       HYDRODYNAMIC VELOCITY, in cm/s = 3.55E  -3

ELUTION TIME   WIDTH     EFFECTIVE       DIFFUSION    EFFICIENCY   RESOLUTION
   in min      in min    MOBILITY        VARIANCE
                        in cm2/Vs        in cm2
GMP =   7.35    .124    -.2803E  -3     8.82E  -3    5.61E   4       1.24
AMP =   7.51    .127    -.2889E  -3     9.01E  -3    5.57E   4       2.18
UMP =   7.79    .133    -.3035E  -3     9.35E  -3    5.52E   4        .08
CMP =   7.81    .133    -.3040E  -3     9.37E  -3    5.52E   4      12.41
GDP =   9.69    .170    -.3789E  -3     1.16E  -2    5.17E   4       1.62
ADP =   9.97    .176    -.3877E  -3     1.20E  -2    5.13E   4       3.33
CDP =  10.57    .189    -.4050E  -3     1.27E  -2    5.03E   4        .16
UDP =  10.60    .189    -.4058E  -3     1.27E  -2    5.02E   4    CRS =  121.65_
INJECTION ZONE,  in cm =    .21        INJ VARIANCE, in cm2 = 3.78E  -3
DETECTOR WINDOW, in cm =    .50        DET VARIANCE, in cm2 = 2.08E  -2


FLOW CHARACTERISTICS:
ZETA POTENTIAL, in mV =  -86.84
ZETAZERO, in mV =   33.02
kPOTNa = 2.2347E  -1
ELECTROOSMOTIC MOBILITY, in cm2/Vs = 6.8976E  -4
ELECTROOSMOTIC VELOCITY, in cm/s =   .1653
VOLTAGE, in kV =  26.876
RESISTANCE, in ohm = 2.1500E   9

BUFFER CHARACTERISTICS (conc in moles/liter):
pH =   7.000
IONIC STRENGTH = 1.1587E  -2
BUFFER CONCENTRATION = 3.4135E  -3
BUFFER CAPACITY = 1.9563E  -3
CHARGE CONC = 2.0001E  -2
[M]buffer = 5.0001E  -3
[M]electr = 5.0002E  -3
BUFFER FORMULATION:
CONC M-H3A = 0.0000E  -1
CONC M-H2A = 1.8269E  -3
CONC M-HA = 1.5866E  -3
CONC M-A = 0.0000E  -1
CONC M-X = 5.0002E  -3
OK
```

Figure 5.7c

```
PREDICTED OPTIMUM CONDITIONS FOR THE SEPARATION:
CURRENT, in microamperes =  12.500
pH =   7.000                          Correction Factor, in pH units =   .2800
IONIC STRENGTH, in moles/liter = 1.1587E  -2
BUFFER CONCENTRATION, in moles/liter = 3.4135E  -3

CAPILLARY DIMENSIONS:                 TYPE OF INJECTION: HYDRODYNAMIC
TOTAL LENGTH, in cm =  112.15         HEIGHT DIFFERENCE, in cm =    2.00
DETECTOR LENGTH, in cm =   43.40      INJECTION TIME, in sec =   60.00
I. D., in micrometers =   75.50       HYDRODYNAMIC VELOCITY, in cm/s = 3.55E  -3

ELUTION TIME   WIDTH     EFFECTIVE       DIFFUSION    EFFICIENCY    RESOLUTION
   in min      in min    MOBILITY        VARIANCE
                        in cm2/Vs        in cm2
GMP =   7.03    .118    -.2803E  -3     8.43E  -3    5.67E   4        1.22
AMP =   7.17    .121    -.2889E  -3     8.61E  -3    5.64E   4        2.14
UMP =   7.43    .126    -.3035E  -3     8.92E  -3    5.59E   4         .08
CMP =   7.44    .126    -.3040E  -3     8.93E  -3    5.59E   4       12.13
GDP =   9.18    .160    -.3789E  -3     1.10E  -2    5.26E   4        1.58
ADP =   9.44    .165    -.3877E  -3     1.13E  -2    5.22E   4        3.24
CDP =   9.99    .177    -.4050E  -3     1.20E  -2    5.12E   4         .15
UDP =  10.02    .177    -.4058E  -3     1.20E  -2    5.12E   4    CRS =  117.13_
INJECTION ZONE,  in cm =    .21        INJ VARIANCE, in cm2 = 3.78E  -3
DETECTOR WINDOW, in cm =    .50        DET VARIANCE, in cm2 = 2.08E  -2


FLOW CHARACTERISTICS (experimental values):
ELECTROOSMOTIC MOBILITY, in cm2/Vs = 7.0066E  -4
ELECTROOSMOTIC VELOCITY, in cm/s =   .1712
VOLTAGE, in kV =  27.403
RESISTANCE, in ohm = 2.1922E   9

BUFFER CHARACTERISTICS (conc in moles/liter):
pH =   7.000
IONIC STRENGTH = 1.1587E  -2
BUFFER CONCENTRATION = 3.4135E  -3
BUFFER CAPACITY = 1.9563E  -3
CHARGE CONC = 2.0001E  -2
[M]buffer = 5.0001E  -3
[M]electr = 5.0002E  -3
BUFFER FORMULATION:
CONC M-H3A = 0.0000E  -1
CONC M-H2A = 1.8269E  -3
CONC M-HA = 1.5866E  -3
CONC M-A = 0.0000E  -1
CONC M-X = 5.0002E  -3
OK
```

Figure 5.8 Separation of nucleotides in pH 8 phosphate buffer solution. Solute identification and conditions as given in Figure 5.6.

Figure 5.8a

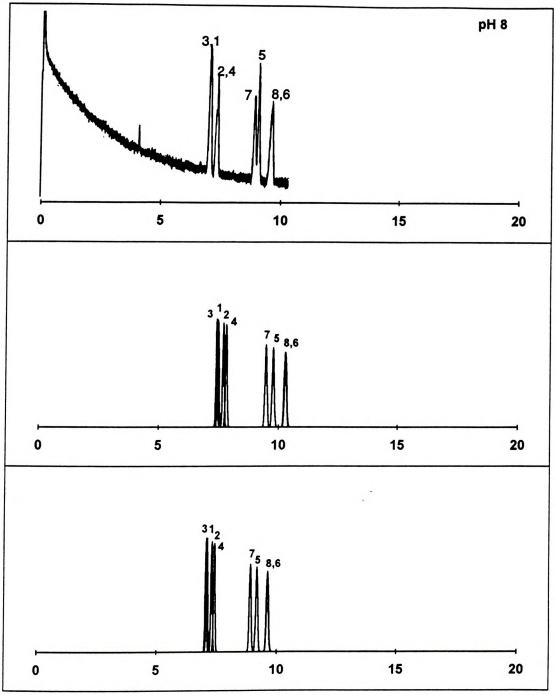
pH 8
3,1
2,4
5
7
8,6
0
5
10
15
20
3
1
2
4
7
5
8,6
0
5
10
15
20
3
1
2
4
7
5
8,6
0
5
10
15
20
TIME (min)

Figure 5.8b

```
PREDICTED OPTIMUM CONDITIONS FOR THE SEPARATION:
CURRENT, in microamperes =  12.500
pH =   8.000                          Correction Factor, in pH units =    .2000
IONIC STRENGTH, in moles/liter = 1.2365E  -2
BUFFER CONCENTRATION, in moles/liter = 2.6342E  -3

CAPILLARY DIMENSIONS:                 TYPE OF INJECTION: HYDRODYNAMIC
TOTAL LENGTH, in cm =  112.15         HEIGHT DIFFERENCE, in cm =    2.00
DETECTOR LENGTH, in cm =   43.40      INJECTION TIME, in sec =   60.00
I. D., in micrometers =   75.50       HYDRODYNAMIC VELOCITY, in cm/s = 3.55E  -3

ELUTION TIME   WIDTH     EFFECTIVE       DIFFUSION    EFFICIENCY    RESOLUTION
   in min      in min    MOBILITY        VARIANCE
                         in cm2/Vs        in cm2
GMP =   7.42     .126    -.3123E  -3     8.91E  -3    5.59E   4        .43
AMP =   7.48     .127    -.3154E  -3     8.97E  -3    5.58E   4       1.71
CMP =   7.70     .131    -.3275E  -3     9.24E  -3    5.54E   4        .91
UMP =   7.82     .133    -.3338E  -3     9.38E  -3    5.51E   4      11.07
GDP =   9.47     .166    -.4047E  -3     1.14E  -2    5.21E   4       1.75
ADP =   9.77     .172    -.4149E  -3     1.17E  -2    5.16E   4       2.81
UDP =  10.27     .182    -.4306E  -3     1.23E  -2    5.08E   4        .10
CDP =  10.29     .183    -.4311E  -3     1.23E  -2    5.07E   4    CRS =  118.83_
INJECTION ZONE,  in cm =     .21        INJ VARIANCE, in cm2 = 3.78E  -3
DETECTOR WINDOW, in cm =     .50        DET VARIANCE, in cm2 = 2.08E  -2


FLOW CHARACTERISTICS:
ZETA POTENTIAL, in mV =  -93.08
ZETAZERO, in mV =   26.85
kPOTNa = 2.2347E  -1
ELECTROOSMOTIC MOBILITY, in cm2/Vs = 7.3933E  -4
ELECTROOSMOTIC VELOCITY, in cm/s =   .1683
VOLTAGE, in kV =  25.528
RESISTANCE, in ohm = 2.0423E   9

BUFFER CHARACTERISTICS (conc in moles/liter):
pH =   8.000
IONIC STRENGTH = 1.2365E  -2
BUFFER CONCENTRATION = 2.6342E  -3
BUFFER CAPACITY = 5.6053E  -4
CHARGE CONC = 2.0000E  -2
[M]buffer = 5.0001E  -3
[M]electr = 4.9999E  -3
BUFFER FORMULATION:
CONC M-HJA = 0.0000E  -1
CONC M-H2A = 2.6831E  -4
CONC M-HA = 2.3659E  -3
CONC M-A = 0.0000E  -1
CONC M-X = 4.9999E  -3
OK
```

Figure 5.8c

```
PREDICTED OPTIMUM CONDITIONS FOR THE SEPARATION:
CURRENT, in microamperes =  12.500
pH =   8.000                    Correction Factor, in pH units =    .2000
IONIC STRENGTH, in moles/liter = 1.2365E  -2
BUFFER CONCENTRATION, in moles/liter = 2.6342E  -3

CAPILLARY DIMENSIONS:                TYPE OF INJECTION: HYDRODYNAMIC
TOTAL LENGTH, in cm =  112.15        HEIGHT DIFFERENCE, in cm =     2.00
DETECTOR LENGTH, in cm =   43.40     INJECTION TIME, in sec =    60.00
I. D., in micrometers =   75.50      HYDRODYNAMIC VELOCITY, in cm/s = 3.55E  -3

ELUTION TIME   WIDTH     EFFECTIVE       DIFFUSION    EFFICIENCY    RESOLUTION
   in min      in min    MOBILITY        VARIANCE
                        in cm2/Vs        in cm2
GMP =   7.06    .119    -.3123E  -3     8.47E  -3    5.67E   4         .41
AMP =   7.10    .119    -.3154E  -3     8.53E  -3    5.66E   4        1.65
CMP =   7.30    .121    -.3275E  -3     8.77E  -3    5.62E   4         .88
UMP =   7.41    .125    -.3338E  -3     8.90E  -3    5.59E   4       10.64
GDP =   8.90    .155    -.4047E  -3     1.07E  -2    5.31E   4        1.68
ADP =   9.17    .160    -.4149E  -3     1.10E  -2    5.26E   4        2.68
UDP =   9.61    .169    -.4306E  -3     1.15E  -2    5.19E   4         .09
CDP =   9.62    .169    -.4311E  -3     1.15E  -2    5.18E   4    CRS =  128.28_
INJECTION ZONE,  in cm =    .21         INJ VARIANCE, in cm2 = 3.78E  -3
DETECTOR WINDOW, in cm =    .50         DET VARIANCE, in cm2 = 2.08E  -2


FLOW CHARACTERISTICS (experimental values):
ELECTROOSMOTIC MOBILITY, in cm2/Vs = 7.5768E  -4
ELECTROOSMOTIC VELOCITY, in cm/s =   .1740
VOLTAGE, in kV =  25.755
RESISTANCE, in ohm = 2.0604E   9

BUFFER CHARACTERISTICS (conc in moles/liter):
pH =   8.000
IONIC STRENGTH = 1.2365E  -2
BUFFER CONCENTRATION = 2.6342E  -3
BUFFER CAPACITY = 5.6053E  -4
CHARGE CONC = 2.0000E  -2
[M]buffer = 5.0001E  -3
[M]electr = 4.9999E  -3
BUFFER FORMULATION:
CONC M-H3A = 0.0000E  -1
CONC M-H2A = 2.6831E  -4
CONC M-HA = 2.3659E  -3
CONC M-A = 0.0000E  -1
CONC M-X = 4.9999E  -3
OK
```

Figure 5.9 Separation of nucleotides in pH 9 phosphate buffer solution. Solute identification and conditions as given in Figure 5.6.

Figure 5.9a

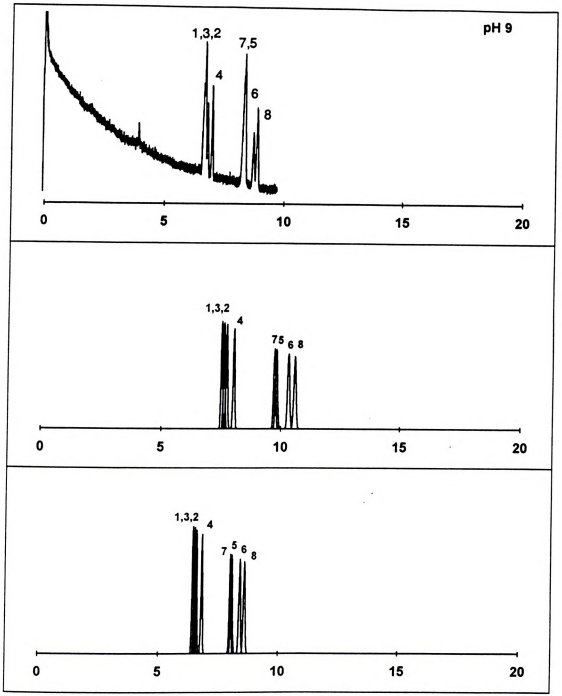
pH 9
1,3,2
4
7,5
6
8
0
5
10
15
20
1,3,2
4
7
5
6
8
0
5
10
15
20
1,3,2
4
7
5
6
8
0
5
10
15
20
TIME (min)

Figure 5.9b

```
PREDICTED OPTIMUM CONDITIONS FOR THE SEPARATION:
CURRENT, in microamperes =  12.500
pH =   9.000                        Correction Factor, in pH units =   .3900
IONIC STRENGTH, in moles/liter = 1.2484E  -2
BUFFER CONCENTRATION, in moles/liter = 2.5075E  -3

CAPILLARY DIMENSIONS:               TYPE OF INJECTION: HYDRODYNAMIC
TOTAL LENGTH, in cm =  112.15       HEIGHT DIFFERENCE, in cm =    2.00
DETECTOR LENGTH, in cm =   43.40    INJECTION TIME, in sec =   60.00
I. D., in micrometers =   75.50     HYDRODYNAMIC VELOCITY, in cm/s = 3.55E  -3

ELUTION TIME   WIDTH     EFFECTIVE       DIFFUSION    EFFICIENCY    RESOLUTION
   in min      in min    MOBILITY        VARIANCE
                        in cm2/Vs        in cm2
AMP =   7.51    .127    -.3180E  -3     9.01E  -3    5.58E   4         .83
GMP =   7.61    .129    -.3240E  -3     9.14E  -3    5.55E   4         .80
CMP =   7.72    .131    -.3296E  -3     9.26E  -3    5.53E   4        2.28
UMP =   8.02    .137    -.3453E  -3     9.63E  -3    5.47E   4       11.05
GDP =   9.73    .171    -.4149E  -3     1.17E  -2    5.17E   4         .49
ADP =   9.81    .173    -.4178E  -3     1.18E  -2    5.15E   4        2.83
CDP =  10.32    .183    -.4337E  -3     1.24E  -2    5.07E   4        1.49
UDP =  10.59    .189    -.4417E  -3     1.27E  -2    5.02E   4    CRS =  531.98_
INJECTION ZONE,  in cm =    .21         INJ VARIANCE, in cm2 = 3.78E  -3
DETECTOR WINDOW, in cm =    .50         DET VARIANCE, in cm2 = 2.08E  -2


FLOW CHARACTERISTICS:
ZETA POTENTIAL, in mV =  -93.49
ZETAZERO, in mV =   26.44
kPOTNa = 2.2347E  -1
ELECTROOSMOTIC MOBILITY, in cm2/Vs = 7.4259E  -4
ELECTROOSMOTIC VELOCITY, in cm/s =   .1681
VOLTAGE, in kV =  25.390
RESISTANCE, in ohm = 2.0312E   9

BUFFER CHARACTERISTICS (conc in moles/liter):
pH =   9.000
IONIC STRENGTH = 1.2484E  -2
BUFFER CONCENTRATION = 2.5075E  -3
BUFFER CAPACITY = 9.5000E  -5
CHARGE CONC = 2.0001E  -2
[M]buffer = 5.0001E  -3
[M]electr = 5.0004E  -3
BUFFER FORMULATION:
CONC M-H3A = 0.0000E  -1
CONC M-H2A = 1.4893E  -5
CONC M-HA = 2.4926E  -3
CONC M-A = 0.0000E  -1
CONC M-X = 5.0004E  -3
OK
```

Figure 5.9c

```
PREDICTED OPTIMUM CONDITIONS FOR THE SEPARATION:
CURRENT, in microamperes =  12.500
pH =   9.000                        Correction Factor, in pH units =   .3900
IONIC STRENGTH, in moles/liter = 1.2484E  -2
BUFFER CONCENTRATION, in moles/liter = 2.5075E  -3

CAPILLARY DIMENSIONS:               TYPE OF INJECTION: HYDRODYNAMIC
TOTAL LENGTH, in cm =  112.15       HEIGHT DIFFERENCE, in cm =    2.00
DETECTOR LENGTH, in cm =   43.40    INJECTION TIME, in sec =   60.00
I. D., in micrometers =   75.50     HYDRODYNAMIC VELOCITY, in cm/s = 3.55E  -3

ELUTION TIME   WIDTH     EFFECTIVE       DIFFUSION    EFFICIENCY    RESOLUTION
   in min      in min    MOBILITY        VARIANCE
                        in cm2/Vs        in cm2
AMP =   6.42    .107    -.3180E  -3     7.70E  -3    5.80E   4         .73
GMP =   6.50    .108    -.3240E  -3     7.80E  -3    5.78E   4         .70
CMP =   6.57    .110    -.3296E  -3     7.89E  -3    5.77E   4        2.00
UMP =   6.80    .114    -.3453E  -3     8.16E  -3    5.72E   4        9.56
GDP =   7.99    .137    -.4149E  -3     9.59E  -3    5.48E   4         .42
ADP =   8.05    .138    -.4178E  -3     9.66E  -3    5.47E   4        2.41
CDP =   8.39    .144    -.4337E  -3     1.01E  -2    5.40E   4        1.26
UDP =   8.58    .148    -.4417E  -3     1.03E  -2    5.37E   4    CRS = 2318.49_
INJECTION ZONE,  in cm =    .21         INJ VARIANCE, in cm2 = 3.78E  -3
DETECTOR WINDOW, in cm =    .50         DET VARIANCE, in cm2 = 2.08E  -2


FLOW CHARACTERISTICS (experimental values):
ELECTROOSMOTIC MOBILITY, in cm2/Vs = 8.1027E  -4
ELECTROOSMOTIC VELOCITY, in cm/s =   .1850
VOLTAGE, in kV =  25.606
RESISTANCE, in ohm = 2.0485E   9

BUFFER CHARACTERISTICS (conc in moles/liter):
pH =   9.000
IONIC STRENGTH = 1.2484E  -2
BUFFER CONCENTRATION = 2.5075E  -3
BUFFER CAPACITY = 9.5000E  -5
CHARGE CONC = 2.0001E  -2
[M]buffer = 5.0001E  -3
[M]electr = 5.0004E  -3
BUFFER FORMULATION:
CONC M-H3A = 0.0000E  -1
CONC M-H2A = 1.4893E  -5
CONC M-HA = 2.4926E  -3
CONC M-A = 0.0000E  -1
CONC M-X = 5.0004E  -3
OK
```

Figure 5.10 Separation of nucleotides in the vicinity of the optimum conditions: pH 10, ionic strength of 12.5 mM, buffer concentration of 2.4 mM, and constant-current conditions of 12.5 μA. Solute identification and electropherogram specification as given in Figure 5.6.

Figure 5.10a

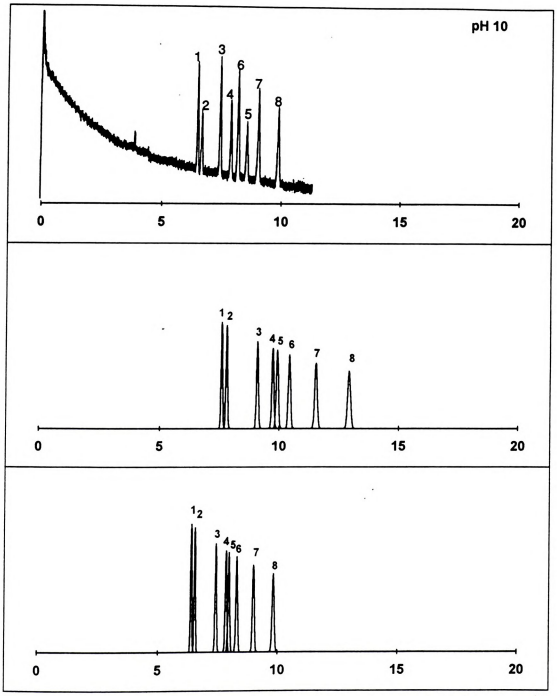

Figure 5.10b

```
PREDICTED OPTIMUM CONDITIONS FOR THE SEPARATION:
CURRENT, in microamperes =  12.500
pH =  10.000                          Correction Factor, in pH units =    .0850
IONIC STRENGTH, in moles/liter = 1.2475E  -2
BUFFER CONCENTRATION, in moles/liter = 2.4355E  -3

CAPILLARY DIMENSIONS:                 TYPE OF INJECTION: HYDRODYNAMIC
TOTAL LENGTH, in cm =  112.15         HEIGHT DIFFERENCE, in cm =    2.00
DETECTOR LENGTH, in cm =   43.40      INJECTION TIME, in sec =   60.00
I. D., in micrometers =   75.50       HYDRODYNAMIC VELOCITY, in cm/s = 3.55E  -3

ELUTION TIME   WIDTH      EFFECTIVE        DIFFUSION     EFFICIENCY    RESOLUTION
   in min      in min     MOBILITY         VARIANCE
                         in cm2/Vs         in cm2
AMP =   7.58     .129     -.3186E  -3      9.10E  -3     5.56E   4        1.61
CMP =   7.79     .133     -.3300E  -3      9.35E  -3     5.52E   4        8.85
GMP =   9.08     .158     -.3885E  -3      1.09E  -2     5.28E   4        3.94
UMP =   9.73     .171     -.4121E  -3      1.17E  -2     5.17E   4        1.09
ADP =   9.92     .175     -.4184E  -3      1.19E  -2     5.13E   4        2.82
CDP =  10.43     .186     -.4343E  -3      1.25E  -2     5.05E   4        5.65
GDP =  11.54     .209     -.4640E  -3      1.38E  -2     4.87E   4        6.21
UDP =  12.93     .239     -.4940E  -3      1.55E  -2     4.67E   4    CRS =    5.31_
INJECTION ZONE,  in cm =     .21          INJ VARIANCE, in cm2 = 3.78E  -3
DETECTOR WINDOW, in cm =     .50          DET VARIANCE, in cm2 = 2.08E  -2


FLOW CHARACTERISTICS:
ZETA POTENTIAL, in mV =  -93.49
ZETAZERO, in mV =   26.44
kPOTNa = 2.2347E  -1
ELECTROOSMOTIC MOBILITY, in cm2/Vs = 7.4262E  -4
ELECTROOSMOTIC VELOCITY, in cm/s =   .1667
VOLTAGE, in kV =  25.170
RESISTANCE, in ohm = 2.0136E   9

BUFFER CHARACTERISTICS (conc in moles/liter):
pH =  10.000
IONIC STRENGTH = 1.2475E  -2
BUFFER CONCENTRATION = 2.4355E  -3
BUFFER CAPACITY = 3.1139E  -4
CHARGE CONC = 2.0001E  -2
[M]buffer = 5.0008E  -3
[M]electr = 5.0007E  -3
BUFFER FORMULATION:
CONC M-HJA = 0.0000E  -1
CONC M-H2A = 0.0000E  -1
CONC M-HA = 2.3057E  -3
CONC M-A = 1.2984E  -4
CONC M-X = 5.0007E  -3
OK
```

Figure 5.10c

```
PREDICTED OPTIMUM CONDITIONS FOR THE SEPARATION:
CURRENT, in microamperes =  12.500
pH =  10.000                          Correction Factor, in pH units =   .0850
IONIC STRENGTH, in moles/liter = 1.2475E  -2
BUFFER CONCENTRATION, in moles/liter = 2.4355E  -3

CAPILLARY DIMENSIONS:                 TYPE OF INJECTION: HYDRODYNAMIC
TOTAL LENGTH, in cm =  112.15         HEIGHT DIFFERENCE, in cm =    2.00
DETECTOR LENGTH, in cm =   43.40      INJECTION TIME, in sec =   60.00
I. D., in micrometers =   75.50       HYDRODYNAMIC VELOCITY, in cm/s = 3.55E  -3

ELUTION TIME   WIDTH     EFFECTIVE       DIFFUSION    EFFICIENCY   RESOLUTION
   in min      in min    MOBILITY        VARIANCE
                        in cm2/Vs        in cm2
AMP =   6.38    .106    -.3186E  -3     7.65E  -3    5.81E   4       1.39
CMP =   6.53    .109    -.3300E  -3     7.83E  -3    5.78E   4       7.57
GMP =   7.41    .125    -.3885E  -3     8.89E  -3    5.59E   4       3.32
UMP =   7.84    .134    -.4121E  -3     9.41E  -3    5.51E   4        .91
ADP =   7.96    .136    -.4184E  -3     9.56E  -3    5.49E   4       2.35
CDP =   8.29    .142    -.4343E  -3     9.95E  -3    5.42E   4       4.65
GDP =   8.99    .156    -.4640E  -3     1.08E  -2    5.30E   4       5.03
UDP =   9.82    .173    -.4940E  -3     1.18E  -2    5.15E   4    CRS =   19.52_
INJECTION ZONE,  in cm =    .21        INJ VARIANCE, in cm2 = 3.78E  -3
DETECTOR WINDOW, in cm =    .50        DET VARIANCE, in cm2 = 2.08E  -2


FLOW CHARACTERISTICS (experimental values):
ELECTROOSMOTIC MOBILITY, in cm2/Vs = 8.1954E  -4
ELECTROOSMOTIC VELOCITY, in cm/s =   .1851
VOLTAGE, in kV =  25.330
RESISTANCE, in ohm = 2.0264E   9

BUFFER CHARACTERISTICS (conc in moles/liter):
pH =  10.000
IONIC STRENGTH = 1.2475E  -2
BUFFER CONCENTRATION = 2.4355E  -3
BUFFER CAPACITY = 3.1139E  -4
CHARGE CONC = 2.0003E  -2
[M]buffer = 5.0008E  -3
[M]electr = 5.0007E  -3
BUFFER FORMULATION:
CONC M-H3A = 0.0000E  -1
CONC M-H2A = 0.0000E  -1
CONC M-HA = 2.3057E  -3
CONC M-A = 1.2984E  -4
CONC M-X = 5.0007E  -3
OK
```

Figure 5.11 Separation of nucleotides in pH 11 phosphate buffer solution. Solute identification and conditions as given in Figure 5.6.

Figure 5.11a

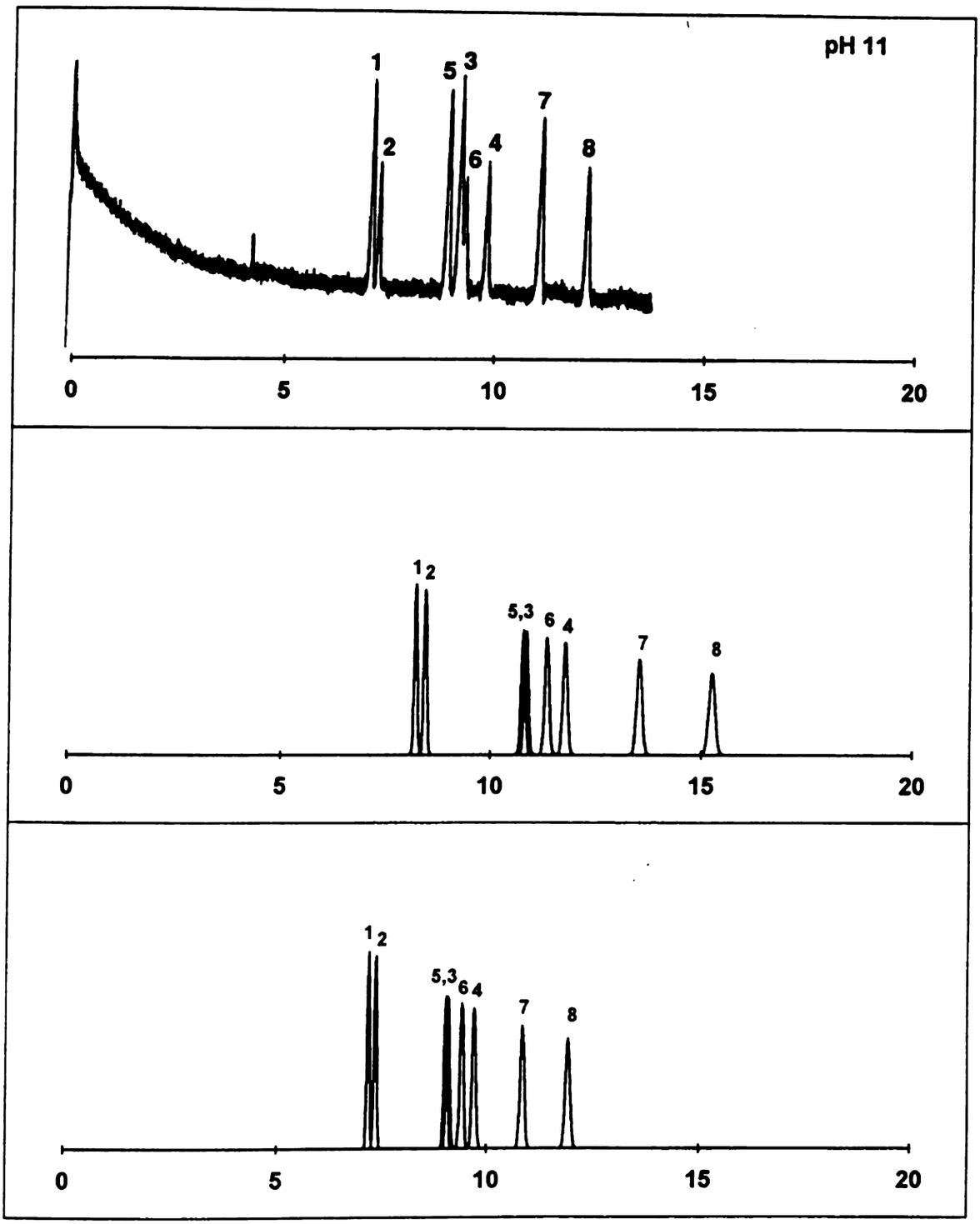
pH 11
1
2
5
3
6
4
7
8
0
5
10
15
20
1
2
5,3
6
4
7
8
0
5
10
15
20
1
2
5,3
6
4
7
8
0
5
10
15
20
TIME (min)

Figure 5.11b

```
PREDICTED OPTIMUM CONDITIONS FOR THE SEPARATION:
CURRENT, in microamperes =  12.500
pH =  11.000                          Correction Factor, in pH units =   .0775
IONIC STRENGTH, in moles/liter = 1.2156E  -2
BUFFER CONCENTRATION, in moles/liter = 1.8674E  -3

CAPILLARY DIMENSIONS:                 TYPE OF INJECTION: HYDRODYNAMIC
TOTAL LENGTH, in cm =  112.15         HEIGHT DIFFERENCE, in cm =    2.00
DETECTOR LENGTH, in cm =   43.40      INJECTION TIME, in sec =   60.00
I. D., in micrometers =   75.50       HYDRODYNAMIC VELOCITY, in cm/s = 3.55E  -3

ELUTION TIME   WIDTH     EFFECTIVE       DIFFUSION    EFFICIENCY    RESOLUTION
   in min      in min    MOBILITY        VARIANCE
                         in cm2/Vs        in cm2
AMP =   8.22     .141    -.3196E  -3    9.87E  -3   5.44E   4        1.60
CMP =   8.45     .146    -.3310E  -3    1.01E  -2   5.39E   4       13.77
ADP =  10.78     .193    -.4200E  -3    1.29E  -2   4.99E   4         .37
GMP =  10.85     .195    -.4221E  -3    1.30E  -2   4.98E   4        2.43
CDP =  11.34     .205    -.4358E  -3    1.36E  -2   4.90E   4        2.05
UMP =  11.77     .214    -.4470E  -3    1.41E  -2   4.84E   4        7.48
GDP =  13.52     .252    -.4852E  -3    1.62E  -2   4.59E   4        6.38
UDP =  15.25     .292    -.5145E  -3    1.83E  -2   4.37E   4    CRS =   49.90_
INJECTION ZONE,  in cm =     .21        INJ VARIANCE, in cm2 = 3.78E  -3
DETECTOR WINDOW, in cm =     .50        DET VARIANCE, in cm2 = 2.08E  -2


FLOW CHARACTERISTICS:
ZETA POTENTIAL, in mV =  -93.47
ZETAZERO, in mV =   26.44
kPOTNa = 2.2347E  -1
ELECTROOSMOTIC MOBILITY, in cm2/Vs = 7.4244E  -4
ELECTROOSMOTIC VELOCITY, in cm/s =   .1541
VOLTAGE, in kV =  23.273
RESISTANCE, in ohm = 1.8618E   9

BUFFER CHARACTERISTICS (conc in moles/liter):
pH =  11.000
IONIC STRENGTH = 1.2156E  -2
BUFFER CONCENTRATION = 1.8674E  -3
BUFFER CAPACITY = 2.8890E  -3
CHARGE CONC = 2.0000E  -2
[M]buffer = 5.0000E  -3
[M]electr = 5.0002E  -3
BUFFER FORMULATION:
CONC M-H3A = 0.0000E  -1
CONC M-H2A = 0.0000E  -1
CONC M-HA = 6.0224E  -4
CONC M-A = 1.2652E  -3
CONC M-X = 5.0002E  -3
OK
```

Figure 5.11c

```
PREDICTED OPTIMUM CONDITIONS FOR THE SEPARATION:
CURRENT, in microamperes =  12.500
pH =  11.000                          Correction Factor, in pH units =   .0775
IONIC STRENGTH, in moles/liter = 1.2156E  -2
BUFFER CONCENTRATION, in moles/liter = 1.8674E  -3

CAPILLARY DIMENSIONS:                 TYPE OF INJECTION: HYDRODYNAMIC
TOTAL LENGTH, in cm =  112.15         HEIGHT DIFFERENCE, in cm =    2.00
DETECTOR LENGTH, in cm =   43.40      INJECTION TIME, in sec =   60.00
I. D., in micrometers =   75.50       HYDRODYNAMIC VELOCITY, in cm/s = 3.55E  -3

ELUTION TIME   WIDTH     EFFECTIVE       DIFFUSION    EFFICIENCY    RESOLUTION
   in min      in min    MOBILITY        VARIANCE
                        in cm2/Vs        in cm2
AMP =   7.18    .121    -.3196E  -3     8.62E  -3    5.64E   4       1.40
CMP =   7.35    .124    -.3310E  -3     8.82E  -3    5.61E   4      11.90
ADP =   9.03    .157    -.4200E  -3     1.08E  -2    5.29E   4        .31
GMP =   9.08    .158    -.4221E  -3     1.09E  -2    5.28E   4       2.06
CDP =   9.41    .165    -.4358E  -3     1.13E  -2    5.22E   4       1.73
UMP =   9.70    .171    -.4470E  -3     1.16E  -2    5.17E   4       6.23
GDP =  10.83    .194    -.4852E  -3     1.30E  -2    4.98E   4       5.21
UDP =  11.91    .217    -.5145E  -3     1.43E  -2    4.82E   4    CRS =   38.49_
INJECTION ZONE,  in cm =    .21        INJ VARIANCE, in cm2 = 3.78E  -3
DETECTOR WINDOW, in cm =    .50        DET VARIANCE, in cm2 = 2.08E  -2

FLOW CHARACTERISTICS (experimental values):
ELECTROOSMOTIC MOBILITY, in cm2/Vs = 8.1089E  -4
ELECTROOSMOTIC VELOCITY, in cm/s =   .1658
VOLTAGE, in kV =  22.931
RESISTANCE, in ohm = 1.8345E   9

BUFFER CHARACTERISTICS (conç in moles/liter):
pH =  11.000
IONIC STRENGTH = 1.2156E  -2
BUFFER CONCENTRATION = 1.8674E  -3
BUFFER CAPACITY = 2.8890E  -3
CHARGE CONC = 2.0000E  -2
[M]buffer = 5.0000E  -3
[M]electr = 5.0002E  -3
BUFFER FORMULATION:
CONC M-H3A = 0.0000E  -1
CONC M-H2A = 0.0000E  -1
CONC M-HA = 6.0224E  -4
CONC M-A = 1.2652E  -3
CONC M-X = 5.0002E  -3
OK
```

Table 5.2 Prediction of voltage, electroosmotic mobility, effective mobility, and zone variance for nucleotide mono- and di-phosphates in phosphate buffer solution, in the vicinity of the optimum conditions (pH 10, ionic strength of 12.5 mM, buffer concentration of 2.4 mM, and constant-current conditions of 12.5 μA).

SOLUTE	VOLTAGE (kV)			ELECTROOSMOTIC MOBILITY ($\times 10^5$ $cm^2 V^{-1} s^{-1}$)			EFFECTIVE MOBILITY ($\times 10^5$ $cm^2 V^{-1} s^{-1}$)			ZONE VARIANCE (cm^2)		
	EXP	CALC	%ERROR*	EXP	CALC	%ERROR*	EXP	CALC	%ERROR*	EXP	CALC	%ERROR*
AMP	25.3	25.2	−0.63	82.0	74.3	−9.4	−32.7	−31.9	−2.6	0.0292	0.0325	11
CMP							−34.0	−33.0	−2.9	0.0308	0.0328	6.5
GMP							−39.2	−38.9	−0.89	0.0287	0.0335	17
UMP							−41.7	−41.2	−1.1	0.0269	0.0344	28
ADP							−42.9	−41.8	−2.5	0.0298	0.0344	15
CDP							−44.5	−43.4	−2.5	0.0324	0.0345	6.5
GDP							−46.6	−46.4	−0.47	0.0337	0.0355	5.3
UDP							−49.7	−49.4	−0.52	0.0242	0.0365	51

* % ERROR = (CALC − EXP) x 100 / EXP

0.6 and 1.7 %, respectively, which are comparable to those obtained previously in the validation studies (Chapter 4, Tables 4.1 to 4.4). Although the zone variance is less accurately predicted, it has no influence on the migration time. The electroosmotic mobility, which affects the migration time of all solutes in a similar manner (Equation [4.3]), is significantly lower than the experimentally measured value (9.4%). Changes in the electroosmotic flow may arise from alteration in either the buffer composition or the capillary surface. If the prepared buffer differed appreciably from the recommended formulation, the resulting solution conductance would also differ and a larger discrepancy in the predicted voltage would be expected. Therefore, it seems more likely that the capillary surface has been altered, possibly due to the wash with alkaline solution over an extended period of time (*vide* Chapter 3). However, the error introduced by changes in the electroosmotic mobility is not sufficiently large to compromise the search for the optimum conditions. When the experimentally measured value of the electroosmotic mobility is used as an input parameter, the predicted electropherogram is in very good agreement with the experimental results in all respects (Figures 5.6 to 5.11, bottom).

5.3 Conclusions

The electrophoretic behavior of 5'-mono and diphosphate nucleotides was characterized in phosphate buffer solutions, in the range of pH from 5 to 11. A new set of dissociation constants and individual electrophoretic mobilites, complementary to the literature data, was generated based on a computer methodology developed in Chapter 4. The separation of nucleotide mixtures was studied as a means to validate the computer routine developed to optimize

separations in capillary zone electrophoresis. The program provided accurate predictions of the separation characteristics in the entire pH range studied, from 6 to 11 as well as a good estimate of the optimum conditions.

5.4 References

1. Lehninger, A. L. *Principles of Biochemistry;* Worth Publishers, Inc.: New York, 1993.

2. De, B. E. A.; Pattyn, G.; David, F.; Sandra, P. *J. High Resolut.Chromatogr.* **1991**, *14*, 627-629.

3. Ng, M.; Blaschke, T. F.; Arias, A. A.; Zare, R. N. *Anal. Chem.* **1992**, *64* 1682-1684.

4. Saenger, W. *Principles of Nucleic Acid Structure;* Springer-Verlag: New York, 1984.

5. Bloomfield, V. A.; Crothers, D. M.; Tinoco, I., Jr. *Physical Chemistry of Nucleic Acids;* Harper & Row: New York, 1974.

6. Towsend, L. B. *Chemistry of Nucleosides and Nucleotides;* Plenum Press: New York, 1988.

7. Chargaff, E.; Davidson, J. N. *The Nucleic Acids - Chemistry and Biology;* Academic Press Inc., Publishers: New York, 1955.

8 Dawson, R. M. C.; Elliott, D. C.; Elliott, W. H.; Jones, K. M. *Data for Biochemical Research;* Clarendon Press: Oxford, 1986.

9. Hirokawa, T.; Kobayashi, S.; Kiso, Y. *J. Chromatogr.* **1985**, *318*, 195-210.

10. Swerdlow, H.; Wu, S.; Harke, H.; Dovichi, N. J. *J. Chromatogr.* **1990**, *516* 61-67.

11. Tsuda, T.; Nakagawa, G.; Sato, M.; Yagi, K. *J. Appl. Biochem.* **1983**, *5,* 330-336.

12. Cohen, A. S.; Terabe, S.; Smith, J. A.; Karger, B. L. *Anal. Chem.* **1987**, *59*, 1021-1027.

13. Row, K. H.; Griest, W. H.; Maskarinec, M. P. *J. Chromatogr.* **1987**, *409*, 193-203.

14. Kuhr, W. G.; Yeung, E. S. *Anal. Chem.* **1988**, *60*, 2642-2646.

15. Gross, L.; Yeung, E. S. *J. Chromatogr.* **1989**, *480*, 169-178.

16. Pentoney, S. L.; Zare, R. N.; Quint, J. F. *Anal. Chem.* **1989**, *61*, 1642-1647.

17. Wang, T.; Hartwick, R. A.; Champlin, J. *J. Chromatogr.* **1989**, *462*, 147-154.

18. Milofsky, R. E.; Yeung, E. S. *Anal. Chem.* **1993**, *65*, 153-157.

19. Devore, J. L. *Probability and Statistics for Engineering and the Sciences*; Brooks/Cole Publishing Company: Monterey, CA, 1987.

20. Robinson, R. A.; Stokes, R. H. *Electrolyte Solutions - The Measurement and Interpretation of Conductance, Chemical Potential and Diffusion in Solutions of Simple Electrolytes*, Butterworths Scientific Publications: London, 1959.

21. Bier, M., Ed.; *Electrophoresis - Theory, Methods and Applications*; Academic Press Inc.: New York, 1959.

CHAPTER 6

APPLICATION OF THE OPTIMIZATION PROGRAM TO THE SEPARATION OF TETRACYCLINE ANTIBIOTICS

6.1 Introduction

Tetracyclines are a group of clinically important natural products and semi-synthetic derivatives, characterized by a broad-spectrum activity against pathogenic microorganisms.[1,2] In addition to their extensive therapeutical use, these drugs have found application in the preservation of harvested fruits and vegetables, extermination of insect pests, and as animal feed supplement.[3-5]

All members of the group possess closely related chemical structures, derived from a common hydronaphthacene nucleus containing four fused rings,[1,5] as shown schematically in Figure 6.1. The presence of multiple functional groups with acid-base properties confers an amphoteric character to the tetracyclines, most of which exhibit an isoelectric point between 4 and 6.[5] The same structural features account for their appreciably high solubility in polar organic solvents and water, which is enhanced at low pH. These compounds undergo complex formation and precipitation reactions with a variety of metallic cations, among which the complexes with calcium, magnesium, and aluminum have been particularly well characterized.[5]

Commercially available tetracycline and tetracycline derivatives may contain significant amounts of degradation products.[6-8] These contaminants are often isomers with only minor structural differences from the original precursor. The most important impurities of tetracycline (TC) are the products of

Figure 6.1 Chemical structures of common tetracycline antibiotics.

Figure 6.1

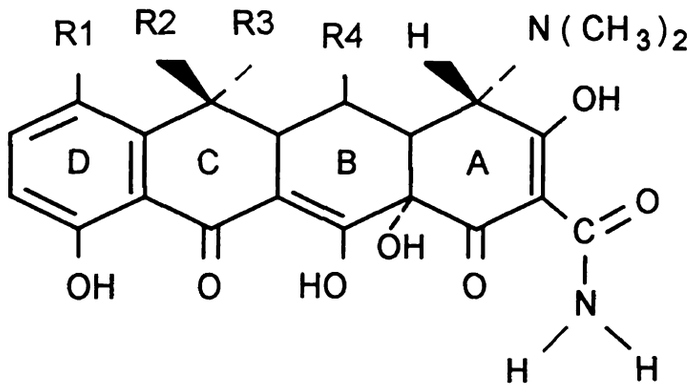

NAME	SYMBOL	R1	R2	R3	R4
TETRACYCLINE	TC	H	OH	CH_3	H
CHLORTETRACYCLINE	CTC	Cl	OH	CH_3	H
DEMECLOCYCLINE	DMCC	Cl	OH	H	H
OXYTETRACYCLINE	OTC	H	OH	CH_3	OH
DOXYCYCLINE	DOC	H	H	CH_3	OH
METHACYCLINE	MTC	H	$= CH_2$		OH
MINOCYCLINE	MNC	$N(CH_3)_2$	H	H	H

epimerization (epiTC), dehydration (anhydroTC), and combined epimerization-dehydration (epianhydroTC) reactions, as shown schematically in Figure 6.2. EpianhydroTC has been implicated in several toxic manifestations such as renal dysfunction caused by ingestion of degraded tetracycline products.[1]

The analytical methodology applied to tetracyclines has supported microbiological production, synthetic and pharmacological studies, and clinical practice. Several techniques have been employed,[2,5,9] including microbiological assays,[5] spectrophotometry,[10-12] phosphorimetry,[13] chemiluminescence,[14] as well as flow injection methods.[15] Many of these methods do not provide a precise and accurate means to determine the tetracycline content in the presence of known degradation products. In particular, the microbiological methods lack specificity, since the total drug activity is estimated without correlation to the chemical structure. Also, the presence of metabolites with no antimicrobial activity is disregarded. Among the chromatographic techniques, thin-layer, paper, and column chromatography followed by UV spectrometric assay have been used extensively.[16-22] However, even these methods have proven to be laborious, often requiring extensive sample pretreatment, and generally exhibit poor sensitivity and precision. Gas chromatographic methods, although fast and specific, require derivatization of the polar functional groups under carefully controlled conditions. This limits its application to antibiotics which are termally stable after derivatization. Liquid chromatography, specially the reversed-phase and ion-exchange modes, has been the method of choice for tetracyclines.[6-8,23-30] Some of these procedures, however, use solvent systems at relatively low pH at which the tetracyclines are known to epimerize and many silica-based stationary phases are unstable. Other methods employ mobile phases containing high salt concentration which, in combination with the low pH, can be deleterious to the life of the column. Moreover, because of the structural

Figure 6.2 Epimerization and dehydration pathways for the decomposition of tetracycline.

Figure 6.2

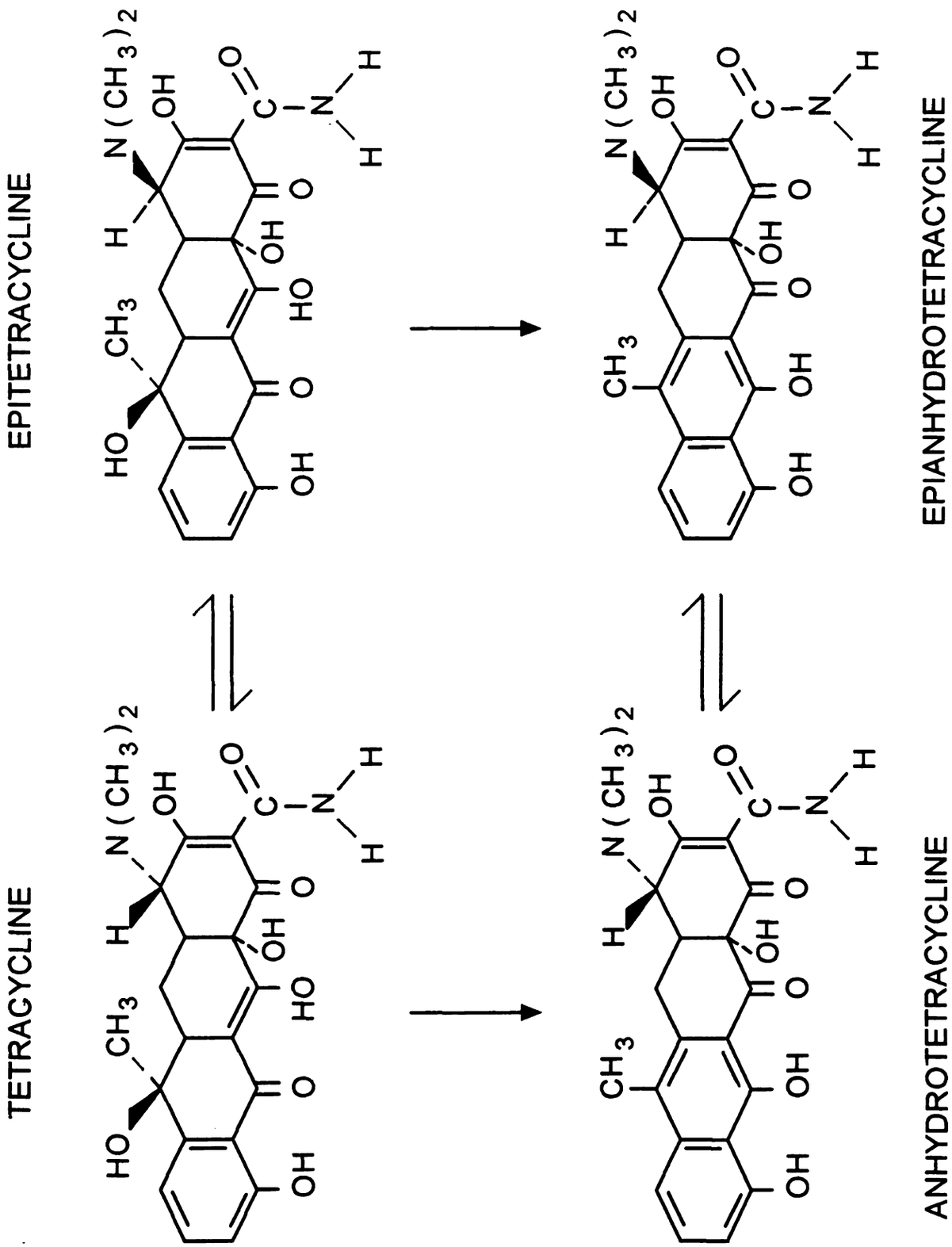
EPITETRACYCLINE
EPIANHYDROTETRACYCLINE
TETRACYCLINE
ANHYDROTETRACYCLINE

similarities of the tetracyclines and their potential contaminants, complete resolution of the compounds is not usually achieved.

The physicochemical properties of tetracyclines, particularly their ionic nature, multiple ionization sites and water solubility, make them suitable for electrophoretic analysis. Capillary zone electrophoresis (CZE) has gained increased acceptance for the analysis of pharmaceuticals,[9,31-33] as a result of relevant features such as high efficiency, high speed, full automation, and compatibility with a variety of detection schemes. This chapter explores CZE as an attractive alternative to the available analytical methodologies for tetracyclines. The computer optimization routine developed in Chapter 4 is used here to assess the separation of seven naturally occuring and synthetically produced tetracyclines. Based on this program, an optimized analytical procedure is developed and applied to the quantitation of tetracyclines in comercially available pharmaceutical drugs.

6.2 Results and Discussion

Characterization of the Electrophoretic Behavior of Tetracyclines. In order to characterize the electrophoretic behavior of tetracyclines knowledge of the dissociation constants and individual species electrophoretic mobility is required. Dissociation constants of very few tetracyclines are available in the literature.[5] After an initial misassigment,[34] the attribution of pK_a values to specific functional groups in the molecule was reevaluated[35] and is now generally accepted. The most acidic group of tetracycline, with a typical pK_a value of about 3.3, corresponds to the tricarbonyl system in ring A (Figure 6.1). The second dissociation constant, with a pK_a value of about 7.6, is assigned to the

dicarbonyl system between rings B and C. The third constant, with a pK_a value of about 9.7, is attributed to the dimethylamino functionality in ring A. The highest dissociation constant, with a pK_a of 10.7, was recently related to the phenolic group in ring D.[35]

The electrophoretic determination of dissociation constants and electrophoretic mobilities is based on experimental measurements of migration time as a function of pH, as described in section 4.2. Table 6.1 presents the constants corrected to the condition of infinite dilution, for seven members of the tetracycline group. The agreement between these values and those previously reported in the literature (*vide supra*) is very good. The data of Table 6.1 were used to calculate the effective mobility as a function of pH (Equation [4.14]), which is displayed in Figure 6.3, for selected mixtures of tetracyclines containing four, five, and seven compounds. An effective mobility curve *versus* pH is a valuable tool for the preliminary assessment of a separation, because it can indicate regions of pH where the mobilities differ and the separation is likely to be achieved. As observed from Figure 6.3, the electrophoretic behavior of tetracyclines is quite similar in the entire pH range studied and the separation appears to be very difficult. Even for the selected mixtures containing fewer tetracyclines, differences in effective mobility occur at very narrow pH regions and a procedure able to optimize the conditions for the separation is highly desirable.

Optimization of the Separation of Tetracyclines. The separation of tetracyclines was approached by the computer optimization routine described in Chapter 4. The separation was optimized under constant-current conditions, with hydrodynamic injection, for a capillary of fixed dimensions, and the detector positioned at a known distance from the capillary inlet. In the search of optimum

Table 6.1 Dissociation constants and electrophoretic mobilities of tetracyclines at 25° C, corrected to the conditions of infinite dilution.

SOLUTE	DISSOCIATION CONSTANT				ELECTROPHORETIC MOBILITY (x 10^5 cm^2 V^{-1} s^{-1})				
	pK_{a1}	pK_{a2}	pK_{a3}	pK_{a4}	μ_{+1}	μ_0	μ_{-1}	μ_{-2}	μ_{-3}
TC	3.46	7.39	9.59	12.1	15.4	1.30	–15.2	–33.6	–64.7
CTC	3.60	7.52	9.88	10.4	19.5	–1.75	–19.1	–30.5	–43.8
DMCC	3.64	6.81	9.43	12.1	14.4	–0.045	–13.3	–36.8	–44.6
OTC	3.57	7.49	9.44	10.5	16.4	–0.60	–15.8	–34.7	–42.3
DOC	3.56	7.48	9.36	12.1	13.3	0.41	–12.5	–35.9	–57.7
MTC	3.56	7.29	9.46	12.0	14.3	0.015	–14.2	–34.4	–66.1
MNC	4.22*	6.86	9.32	11.9	32.5**	3.62	–7.75	–31.5	–53.7

* average pK_a corresponding to the dissociation of the protonated amino group of rings A and D (Figure 6.1)

** doubly charged species

Figure 6.3 Effective mobility curves as a function of pH for selected mixtures of tetracyclines at 25° C and infinite dilution. (a) CTC, DMCC, DOC, and OTC. (b) CTC, DMCC, MNC, MTC, and TC. (c) CTC, DMCC, DOC, MNC, MTC, OTC, and TC.

Figure 6.3a

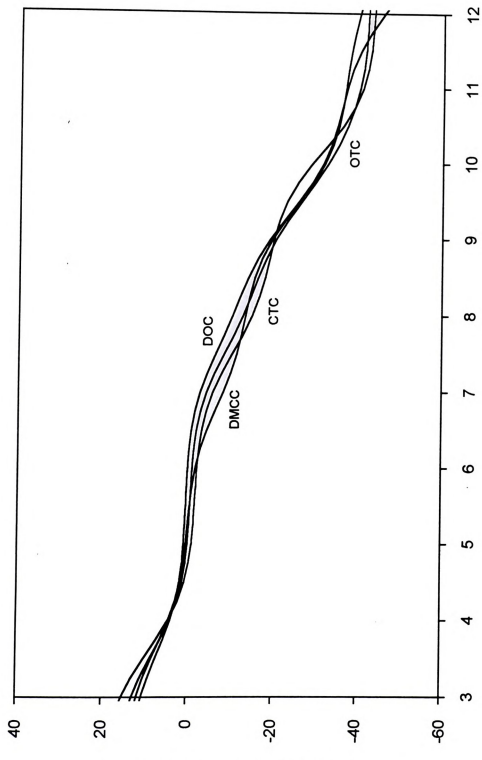
EFFECTIVE MOBILITY x 10^5 cm^2 V^{-1} s^{-1}
40
20
0
-20
-40
-60
3
4
5
6
7
8
9
10
11
12
pH
DOC
DMCC
CTC
OTC

Figure 6.3b

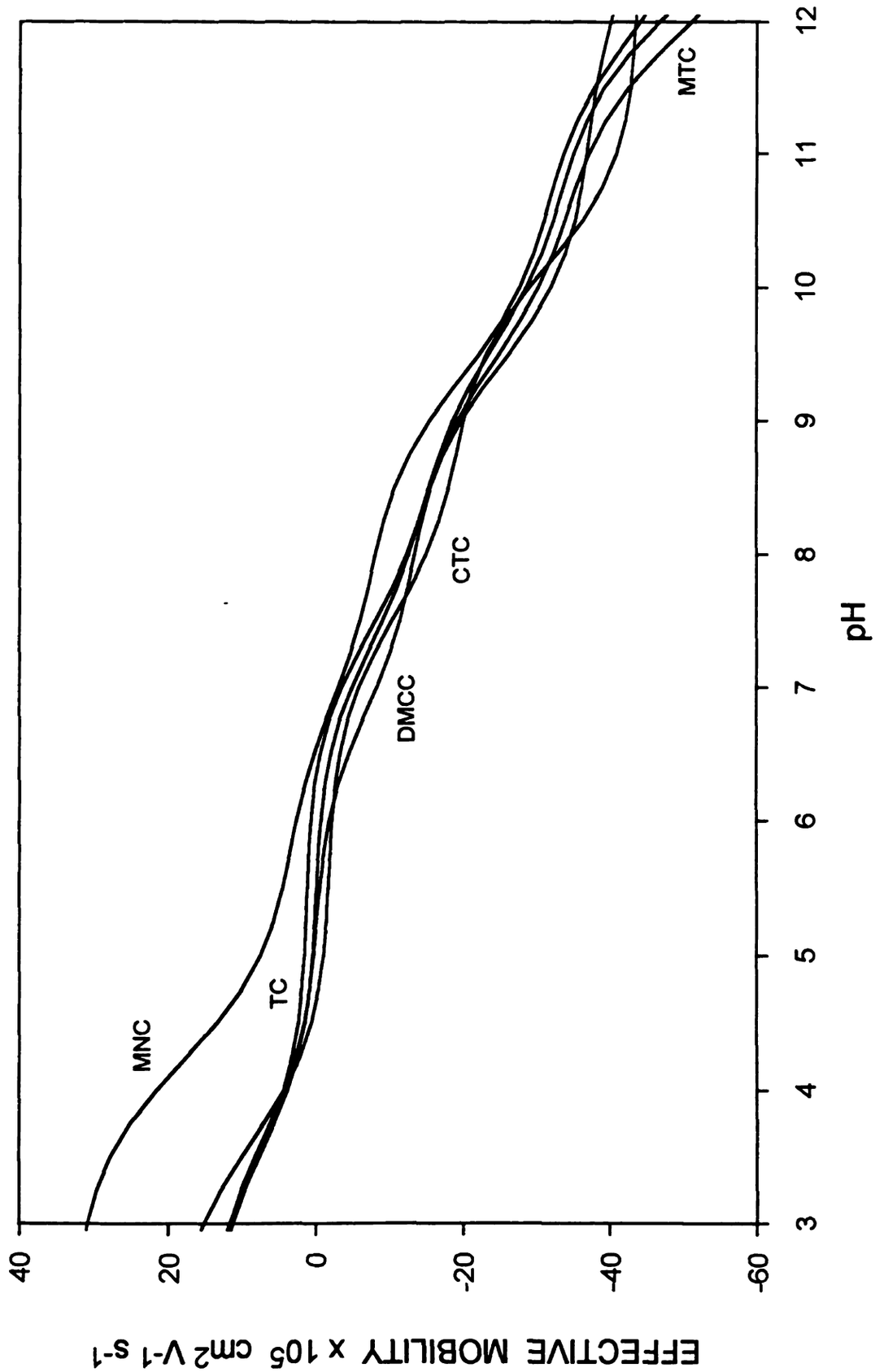
EFFECTIVE MOBILITY x 10⁵ cm² V⁻¹ s⁻¹
40
20
0
-20
-40
-60
3
4
5
6
7
8
9
10
11
12
pH
MNC
TC
DMCC
CTC
MTC

Figure 6.3c

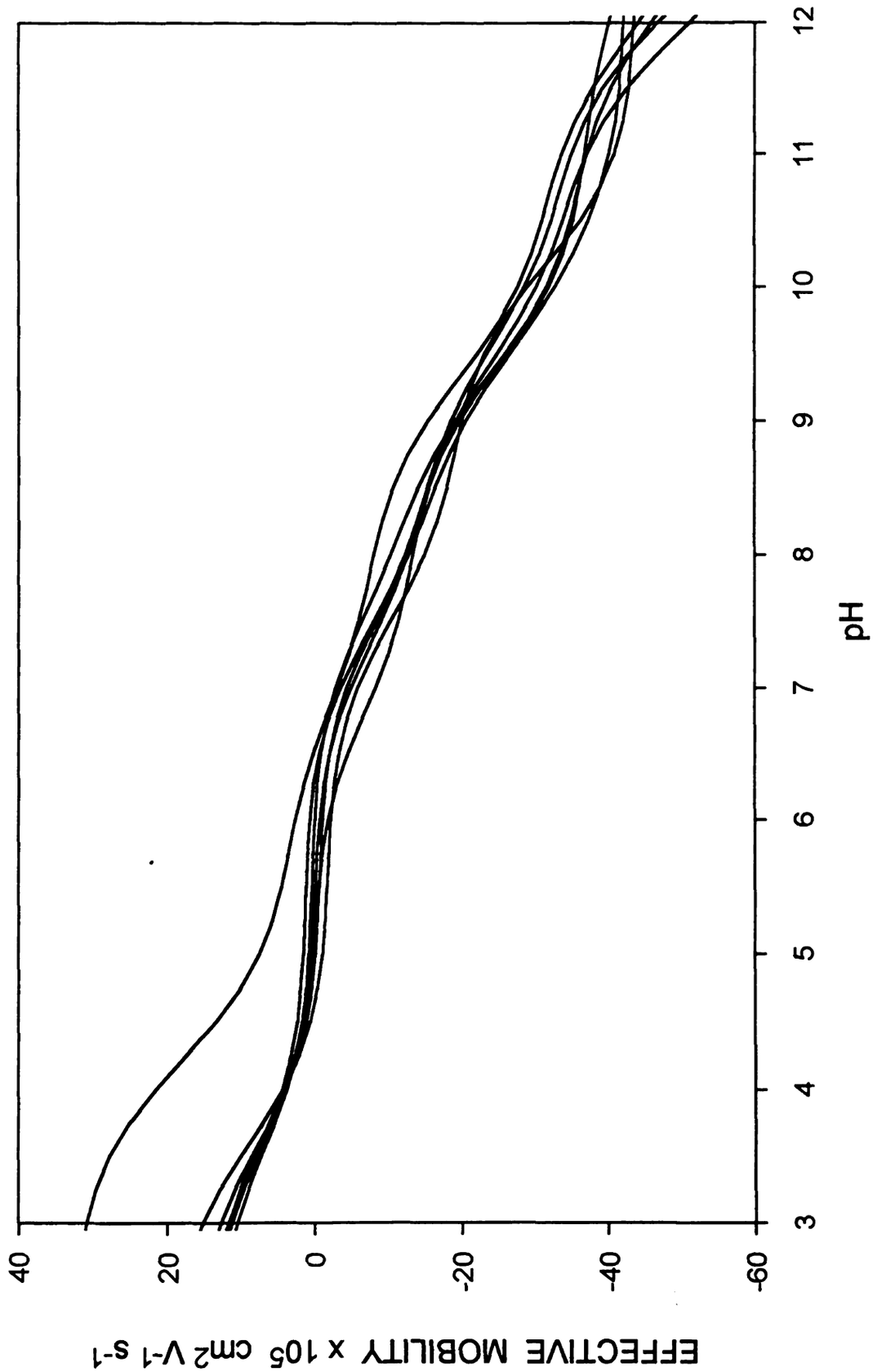
EFFECTIVE MOBILITY x 10⁵ cm² V⁻¹ s⁻¹
40
20
0
-20
-40
-60
3
4
5
6
7
8
9
10
11
12
pH

conditions, the current was varied from 5.00 to 22.50 μA with 0.25 increments, the pH was varied from 4.0 to 11.0 with increments of 0.10, the ionic strength from 5.00 to 22.50 mM with 0.25 mM increments, and the buffer concentration from 0.50 to 11.00 mM with 0.15 mM increments. The surface maps and correspondent contour plots presented in Figures 6.4 and 6.5 allow the visual inspection of the CRS response function within the defined range of parameters. A minimum value of CRS occurs between pH 7 and 8. In this region, the CRS function decreases rapidly as the current approaches 20 μA. The function behaves similarly when the buffer concentration approaches 4 mM. In contrast, the ionic strength surface map is composed of several very sharp minima in the region between 15 and 20 mM, which indicates that this variable must be controlled carefully.

The separation of seven tetracyclines in the vicinity of the optimal conditions, is demonstrated in Figure 6.6. Even though it is possible to identify unequivocally all components of the mixture, complete separation of the seven tetracyclines is not accomplished. For comparison, other mixtures containing fewer tetracyclines are also presented in Figure 6.6. Regardless of the partial resolution of these mixtures, the analysis of tetracyclines by capillary electrophoresis represents an improvement over the available methodology for tetracycline, since there is a gain in efficiency (about 3×10^4 theoretical plates per meter) and analysis time (analysis is performed in less than 6 min). Reversed-phase liquid chromatographic methods, which are among the most commonly employed methods for tetracyclines, provide efficiencies in the order of thousands of plates and analysis time as long as 30 min for typical mixtures.[2]

The program predicts the correct elution order for all tetracyclines, and provides a reasonable estimate of migration time and peak width. The agreement between predicted and experimental values for migration time and

Figure 6.4 Surface maps representing the separation of tetracyclines. (a) CRS as a function of pH and applied current with constant ionic strength of 18 mM and buffer concentration of 4.5 mM. (b) CRS as a function of pH and ionic strength with constant buffer concentration of 4.5 mM and current of 20 μA. (c) CRS as a function of pH and buffer concentration with constant ionic strength of 18 mM and current of 20 μA.

Figure 6.4a

Figure 6.4b

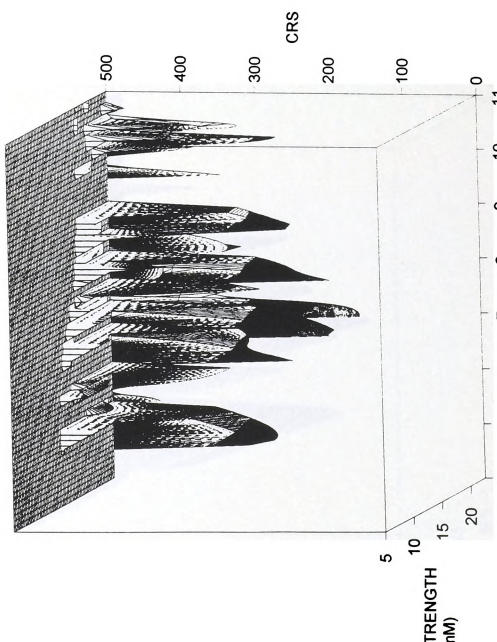
CRS
500
400
300
200
100
0
11
10
9
8
7
6
5
4
pH
5
10
15
20
IONIC STRENGTH
(mM)

Figure 6.4c

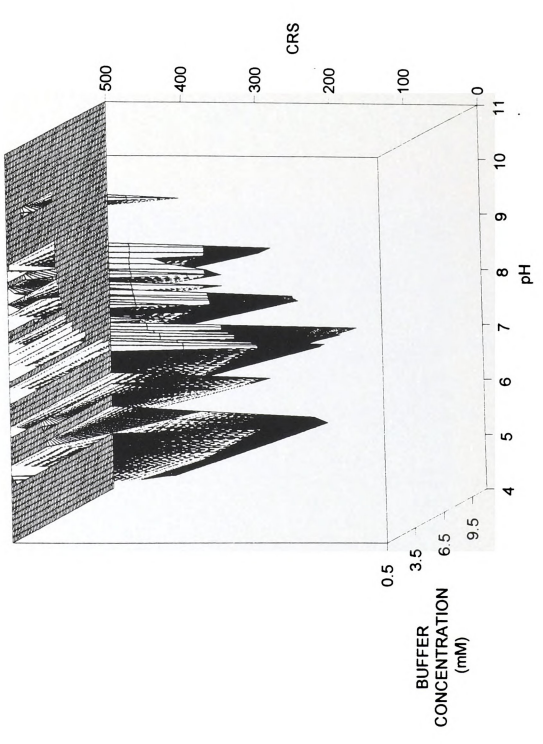
CRS
500
400
300
200
100
0
11
10
9
8
7
6
5
4
pH
9.5
6.5
3.5
0.5
BUFFER
CONCENTRATION
(mM)

Figure 6.5 Contour maps representing the separation of tetracyclines. (a) CRS as a function of pH and applied current with constant ionic strength of 18 mM and buffer concentration of 4.5 mM. (B) CRS as a function of pH and ionic strength with constant buffer concentration of 4.5 mM and current of 20 μA. (C) CRS as a function of pH and buffer concentration with constant ionic strength of 18 mM and current of 20 μA.

Figure 6.5a

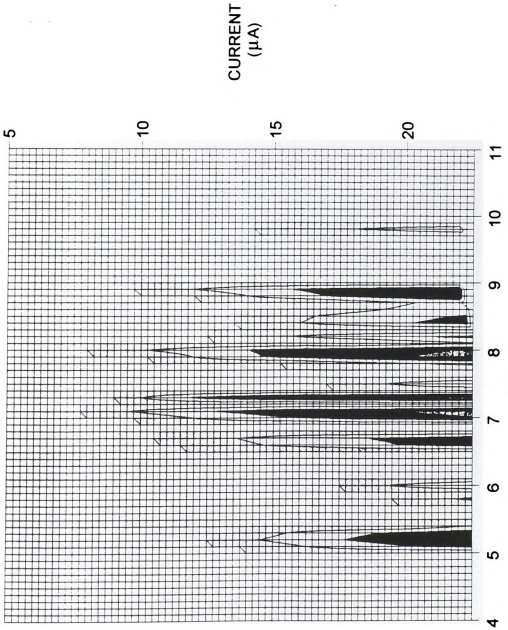

Figure 6.5b

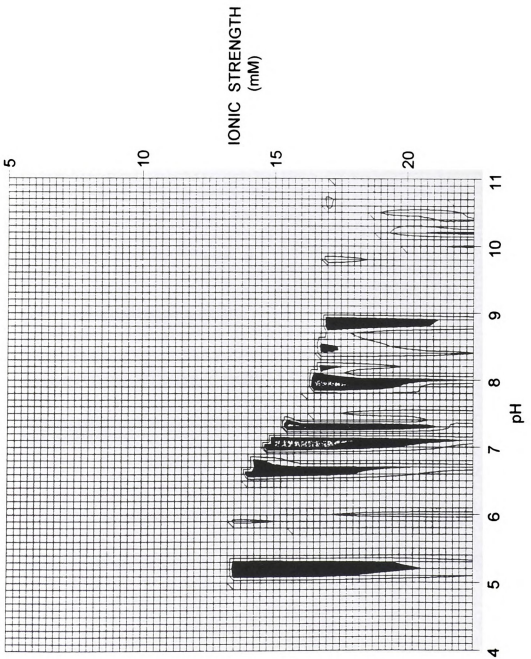

Figure 6.5c

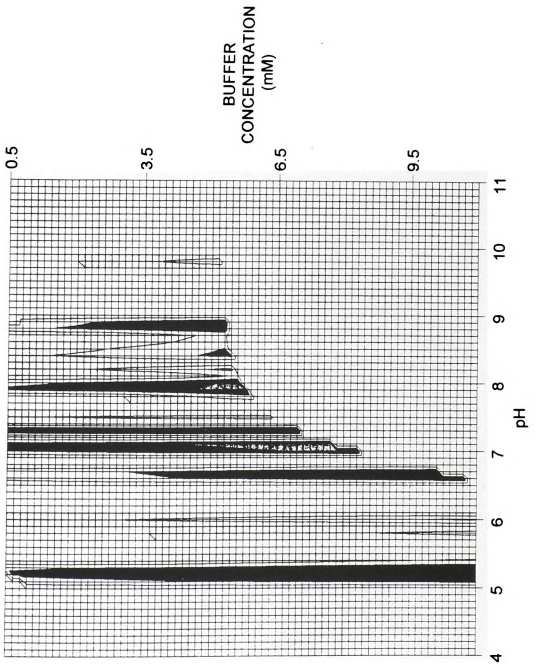

Figure 6.6 Separation of mixtures of tetracyclines in the vicinity of the optimum conditions (pH 7.5, with 15 mM total sodium concentration, ionic strength of 18.2 mM, buffer concentration of 4.3 mM, and applied current of 20 μA.

Figure 6.6

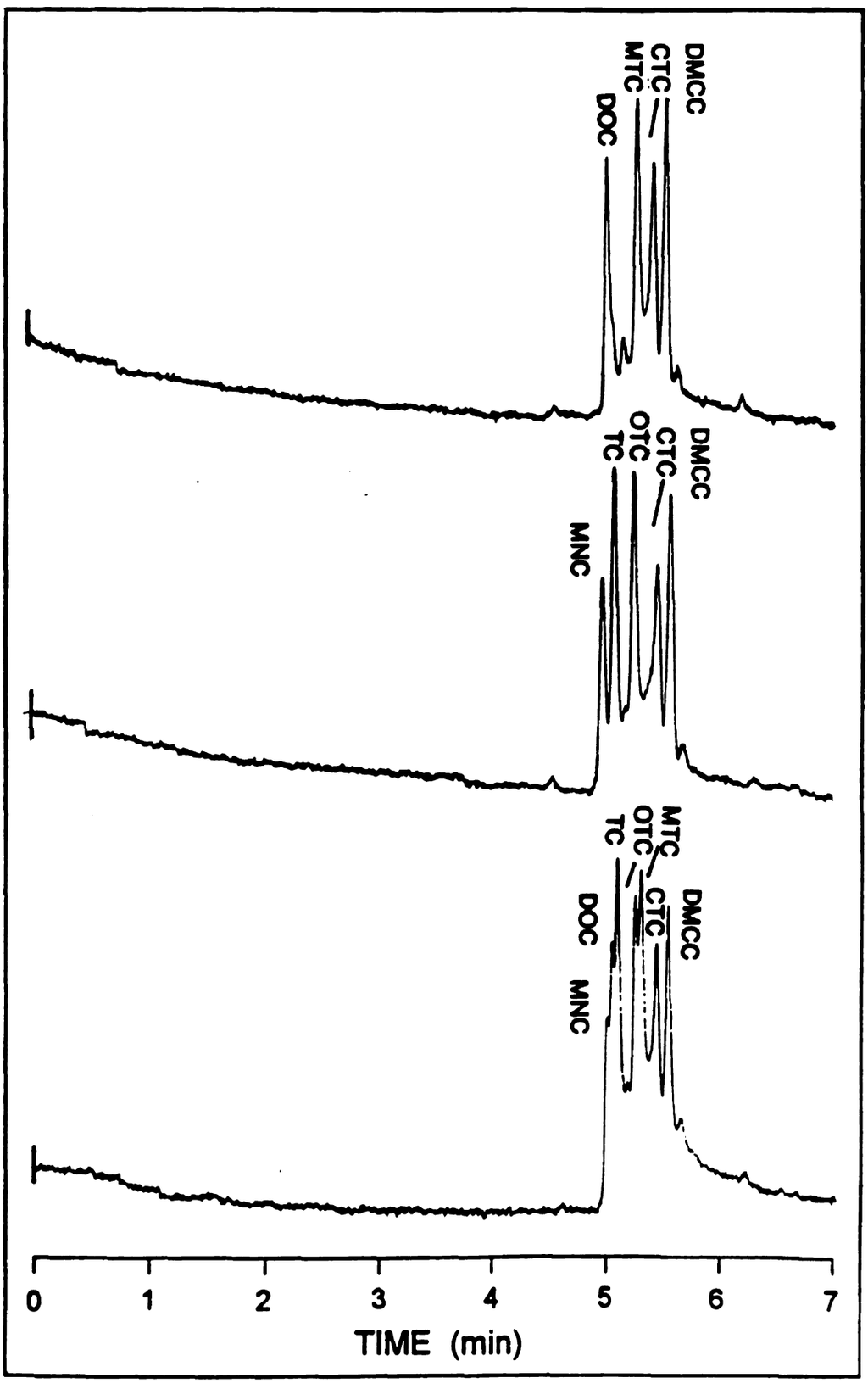
DOC
MTC
CTC
DMCC
MNC
TC
OTC
CTC
DMCC
MTC
OTC
TC
DOC
MNC
CTC
DMCC
0
1
2
3
4
5
6
7
TIME (min)

peak width is typically 1.7 % and 23 %, respectively, as demonstrated in Table 6.2.

Decomposition of Tetracyclines. A common concern in the manufacture industry of tetracycline antibiotics is the control of impurities. Tetracyclines can degrade through at least four different pathways (epimerization, dehydration, hydrolysis and oxidation), where epimerization and dehydration are the most important processes.[5] The epimerization of the dimethylamine group in ring A of tetracycline produces the inactive and non-toxic epitetracycline (Figure 6.2). Dehydration followed by aromatization of the C-ring give anhydrotetracycline, which is also inactive and nontoxic. Both epimerization of the anhydrotetracycline and dehydration of the epitetracycline lead to the formation of the inactive, but rather toxic epianhydrotetracycline. The kinetics of the epimerization and dehydration reactions have been extensively studied,[5,36-37] indicating that these processes can be accelerated at very low pH and under thermal conditions. In Figure 6.7, the electropherogram of a tetracycline sample, which was previously decomposed by heating under acidic conditions, is displayed together with the intact standard. The presence of new zones is clearly visualized in the electropherogram of the decomposed sample, suggesting the formation of the dehydration and epimerization products. However, the unequivocal identification of these zones was not possible due to unavailability of standards. The analysis of a commercially available formulation of tetracycline is also illustrated in Figure 6.7, for comparison purposes. The electropherograms indicate the presence of the epitetracycline in the pharmaceutical formulation, and of anhydrotetracycline in the tetracycline standard.

Table 6.2. Comparison of experimentally determined migration time and base width of tetracyclines with computer-simulated values in the vicinity of the optimum conditions (pH 7.5, ionic strength of 18.2 mM, buffer concentration of 4.3 mM, and constant-current conditions of 20 μA).

SOLUTE	MIGRATION TIME (min)			WIDTH (min)		
	EXP	CALC*	% ERROR+	EXP	CALC	% ERROR+
MNC	5.05	5.03	0.40	0.085	0.098	–15
DOC	5.16	5.14	0.39	0.0679	0.100	–47
TC	5.25	5.24	0.19	0.0807	0.102	–26
OTC	5.41	5.30	2.0	0.0807	0.104	–29
MTC	5.48	5.32	2.9	0.0849	0.104	–22
CTC	5.59	5.46	2.3	0.115	0.107	+7.0
DMCC	5.71	5.49	3.9	0.123	0.108	+12

* calculated from Equation [1] with an experimentally determined electroosmotic mobility of 6.40×10^{-4} cm^2 V^{-1} s^{-1}.

\+ % ERROR = 100 (EXP – CALC) / EXP

Figure 6.7 Identification of tetracycline decomposition products under the optimized conditions given in Figre 6.6. (Top) Tetracycline standard. (Middle) Tetracycline standard previously treated with hydrochloric acid at pH 2, and submitted to 70° C during 1 h. (Bottom) Hard filled capsule of tetracycline 250 mg (Warner-Chillcott®).

Figure 6.7

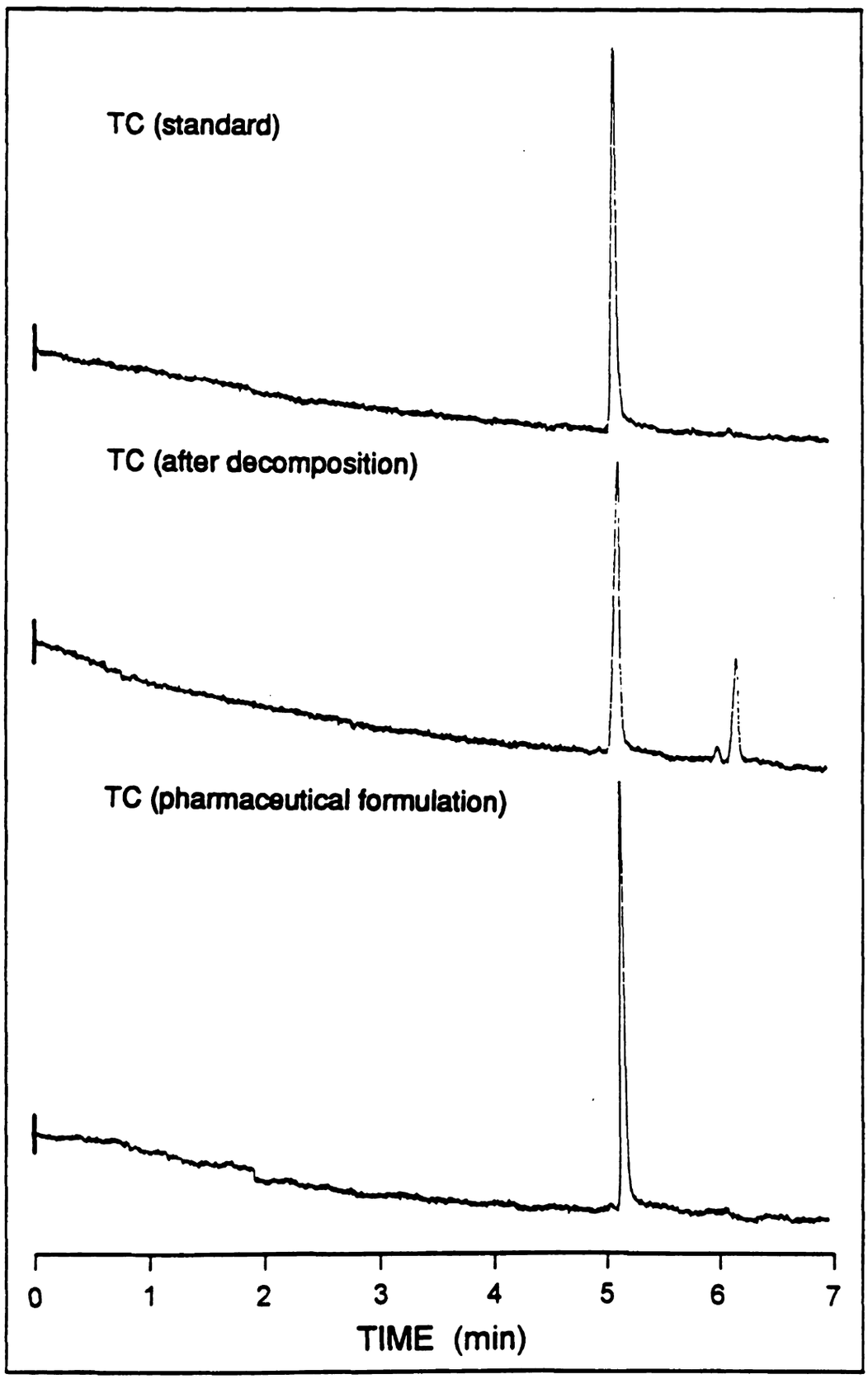
TC (standard)
TC (after decomposition)
TC (pharmaceutical formulation)
0
1
2
3
4
5
6
7
TIME (min)

Analysis of Tetracyclines. The analysis of hard filled capsules of tetracycline was performed with a minimum of 95% recovery in the dissolution process. A calibration curve of peak height *versus* concentration with slope of 6.15×10^{-4} cm M^{-1}, intercept of -1.18×10^{-5} and coefficient of determination equal to 0.9989. A linear range of two orders of magnitude, with a detection limit of 10^{-5} M at a signal-to-noise ratio[38] of approximately 3 were obtained. In addition to tetracycline, other commercially available pharmaceutical counter drugs were examined, such as minocycline and doxycycline (expired lot), presenting comparable degrees of purity.

Among all tetracyclines characterized in this work, chlortetracycline exhibited the most unusual electrophoretic behavior, as demonstrated in Figure 6.8. The chlortetracycline zone exhibits a marked asymmetry towards a minor zone which possesses a migration time coincident with that of tetracycline. Chlortetracycline is known to decompose to tetracycline under mild conditions.[39-41] However, the behavior of chlortetracycline upon the influence of the electric field suggests that the convertion of chlortetracycline to tetracycline may be enhanced during the electrophoretic migration. These results indicate that the use of capillary zone electrophoresis may be impaired as a means to detect the presence of tetracycline in chlortetracycline pharmaceutical formulations as well as to monitor the decomposition of chlortetracycline during storage. It is interesting to observe from the electropherograms of Figure 6.6 that a shift in the baseline occurred during the passage of the solute zones through the detector. This phenomenon, which deteriorated the resolution of all solutes to certain extent, can be associated to the presence of chlortetracycline in these mixtures.

Figure 6.8 Electrophoretic behavior of chlortetracycline under the optimized conditions of Figure 6.6.

Figure 6.8

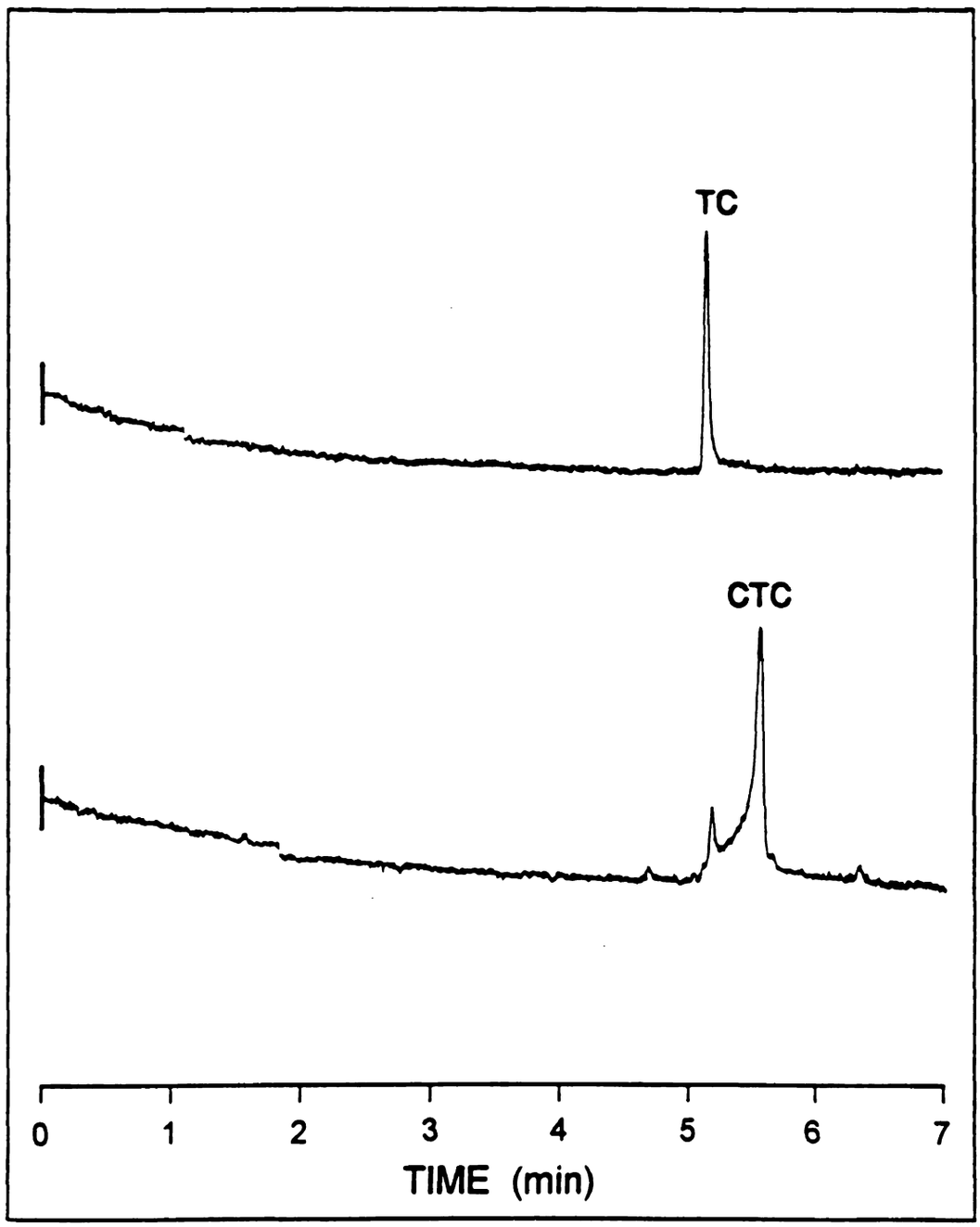

6.3 Conclusions

This work characterized CZE as a very resourceful alternative method for the separation and quantitative analysis of tetracycline, its analogs and common impurities originated from decomposition. The electrophoretic behavior of seven members of the group was studied and a complete set of dissociation constants and individual electrophoretic mobilities derived. The separation of all seven antibiotics was approached by a computer optimization program which indicated that the separation can be performed satisfactorily under mild conditions. The analysis of tetracycline in commercially available pharmaceutical counter drugs gave a linear range of two orders of magnitude, with a detection limit of 10^{-5} M (UV detection) and a signal-to-noise ratio of approximately 3.

6.4 References

1. Lambert, H. P.; O'Grady, F. W. *Antibiotic and Chemotherapy*, 6th edition; Churchill Livingstone: London, 1992.

2. Aszalos, A. *Modern Analysis of Antibiotics, Drugs and the Pharmaceutical Sciences*, Vol. 27; Marcel Dekker: New York, 1986.

3. De Leenheer, A. P.; Nelis, H. J. C. F. *J. Pharm. Sci.* **1979**, *68*, 999-1002.

4. Sharma, J. P.; Perkins, E. G.; Bevill, R. F. *J. Chromatogr.* **1977**, *134*, 441-450.

5. Mitscher, L. A. *The Chemistry of the Tetracycline Antibiotics, Medicinal Research Series*, Vol. 9; Marcel Dekker: New York, 1978.

6. Hermansson, J.; Andersson, M. *J. Pharm. Sci.* **1982**, *71*, 222-229.

7. Mack, G. D.; Ashworth, R. B. *J. Chromatogr. Sci.* **1978**, *16*, 93-101.

8. Tsuji, K.; Robertson, J. H. *J. Pharm. Sci.* **1976**, *65*, 400-404.

9. Gilpin, R. K.; Pachla, L. A. *Anal. Chem.* **1993**, *65*, 117R-132R.

10. Ping-Kay, H.; Wai-Kwong, F. *Analyst* **1991**, *116*, 751-752.

11. Emara, K. M.; Askal, H. F.; Saleh, G. A. *Talanta* **1991**, *38*, 1219-1221.

12. Saha, U.; Sen, A. K.; Das, T. K.; Bhowal, S. K. *Talanta* **1990**, *37*, 1193-1196.

13. Duggan, J. X. *J. Liq. Chromatogr.* **1991**, *14*, 2499-2525.

14. Syropoulos, A. B.; Calokerinos, A. C. *Anal. Chim. Acta* **1991**, *255*, 403-411.

15. Alwarthan, A. A.; Al-Tamrah, S. A.; Sultan, S. M. *Analyst* **1991**, *116*, 183-186.

16. Naidong, W.; Hua, S.; Roets, E.; Hoogmartens, J. *J. Planar Chromatogr. - Mod. TLC* **1992**, *5*, 92-98.

17. Naidong, W.; Hauglustaine, C.; Roets, E.; Hoogmartens, J. *J. Planar Chromatogr. - Mod. TLC* **1991**, *4*, 63-68.

18. Naidong, W.; Hua, S.; Verresen, K.; Roets, E.; Hoogmartens, J. *J. Pharm. Biomed. Anal.* **1991**, *9*, 717-723.

19. Kovács-Hadady, K. J. *J. Planar Chromatogr. - Mod. TLC* **1991**, *4*, 456-459.

20. Naidong, W.; Geelen, S.; Roets, E.; Hoogmartens, J. *J. Pharm. Biomed. Anal.* **1990**, *8*, 891-898.

21. Naidong, W.; Cachet, T.; Roets, E.; Hoogmartens, J. *J. Planar Chromatogr. - Mod. TLC* **1989**, *2*, 424-429.

22. Kang, J. S.; Ebel, S. J. *J. Planar Chromatogr. - Mod. TLC* **1989**, *2*, 434-437.

23. Khan, N. H.; Wera, P.; Roets, E.; Hoogmartens, J. *J. Liq. Chromatogr.* **1990**, *13*, 1351-1374.

24. Naidong, W.; Roets, E.; Hoogmartens, J. *J. Pharm. Biomed. Anal.* **1989**, 7, 1691-1703.

25. Aszalos, A.; Haneke, C.; Hayden, M. J.; Crawford, J. *Chromatographia* **1982**, *15*, 367-373.

26. Knox, J. H.; Jurand, J. *J. Chromatogr.* **1979**, *186*, 763-782.

27. De Leenheer, A. P.; Nelis, H. J. C. F. *J. Chromatogr.* **1977**, *140*, 293-299.

28. Knox, J. H.; Jurand, J. *J. Chromatogr.* **1975**, *110*, 103-115.

29. White, E. R.; Carrol, M. A.; Zarembo, J. E.; Bender, A. D. *J. Antibiotics* **1975**, *28*, 205-214.

30. Butterfield, A. G.; Hughes, D. W.; Pound, N. J.; Wilson, W. L. *Antimicrob. Ag. Chemother.* **1973**, *4*, 11-15.

31. Grossman, P. D.; Colburn, J. C., Ed.; *Capillary Electrophoresis - Theory and Practice;* Academic Press Inc.: San Diego, CA, 1992.

32. Ackermans, M. T.; Beckers, J. L.; Everaerts, F. M.; Seelen, I. G. J. A. *J. Chromatogr.* **1992**, 590, 341-353.

33. Lookabaugh, M.; Biswas, M.; Krull, I. S. *J. Chromatogr.* **1991**, *549*, 357-366.

34. Leeson, L. J.; Krueger, J. E.; Nash, R. A. *Tetrahedron Letters* **1963**, *18*, 1155-1160.

35. Rigler, N. E.; Bag, S. P.; Leyden, D. E.; Sudmeier, J. L.; Reilley, C. N. *Anal. Chem.* **1965**, *37*, 872-875.

36. Schlecht, K. D.; Frank, C. W. *J. Pharm. Sci.* **1975**, 64, 352-354.

37. Hoener, B. A.; Sokoloski, T. D.; Mitscher, L. A.; Malspeis, L. *J. Pharm. Sci.* **1974**, *63*, 1901-1904.

38. St. John, P. A.; McCathy, W. J.; Winefordner, J. D. *Anal. Chem.* **1967**, *39*, 1495-1497.

39. Naidong, W.; Roets, E.; Busson, R.; Hoogmartens, J. *J. Pharm. Biomed. Anal.* **1990**, *8*, 881-889.

40. Sokolic, M.; Filipovic, B.; Pokorny, M. *J. Chromatogr.* **1990**, *509*, 189-193.

41. Naidong, W.; Roets, E.; Hoogmartens, J. *Chromatographia* **1990**, *30*, 105-109.

CHAPTER 7

SUMMARY AND FUTURE WORK

7.1 Summary

In this work, a systematic approach to the optimization of capillary zone electrophoresis separations has been devised with the development, experimental validation, and application of a computer routine. This optimization program is structured on theoretical models for both electroosmotic and electrophoretic migration and incorporates a simple rationale for zone dispersion. The program is able to accommodate different injection methods and can be used to optimize separations under constant-current or constant-voltage conditions. In addition to the solute characteristics, variables related to the buffer composition (pH, ionic strength and concentration), capillary dimensions (diameter and length) and instrumental parameters (applied voltage or current) are also utilized by the program. For any given set of conditions, the solute zone is characterized by its migration time and temporal width. The migration time of each solute zone is derived from the sum of the solute effective mobility and the electroosmotic mobility. The temporal width is derived from contributions to variance resulting from longitudinal diffusion and finite injection and detection volumes. Resolution between adjacent zones is then estimated and the overall quality of the separation is assessed by means of an appropriate response function, such as the chromatographic resolution statistic.[1] By methodically varying the input parameters and evaluating the quality of the resulting separation, this computer program can be used to predict the

experimental conditions required for optimal separation of the solutes.

The mathematical model for electroosmotic migration (Chapter 3) was developed by taking into consideration the ion-selective properties of silica surfaces. A study of electroosmotic flow characteristics in solutions of singly charged, strong electrolytes (NaCl, LiCl, KCl, NaBr, NaI, $NaNO_3$, and $NaClO_4$), as well as the phosphate buffer system, revealed a linear correlation between the zeta potential and the logarithm of the cation activity. These results suggested that the capillary surface behaves as an ion-selective electrode. Consequently, the zeta potential can be calculated as a function of the composition and pH of the solution with the corresponding modified Nernst equation for ion-selective electrodes.[2] If the viscosity and dielectric constant of the solution are known, the electroosmotic velocity can then be accurately predicted by means of the Helmholtz-Smoluchowski equation.[3] The proposed model for electroosmotic flow has been succcessfully applied to phosphate buffer solutions in the pH range from 4 to 10, containing sodium chloride from 5 to 15 mM, resulting in approximately 5 % error in the prediction of the zeta potential. The model for the electrophoretic migration (Chapter 4) is based on classical equilibrium calculations and requires the knowledge of the dissociation constants and electrophoretic mobilities of the solutes under investigation. When these constants are not available, a numerical evaluation of pK_a and electrophoretic mobilities may be attempted. The conceptual basis of this procedure was presented in Chapter 4 and verified in Chapters 5 and 6 for the determination of constants for nucleotides and tetracyclines, respectively.

The overall optimization routine has been experimentally validated with a mixture of nucleotides in phosphate buffer solutions (Chapter 5). In preliminary studies, the electrophoretic behavior of the nucleotides adenosine, guanosine, cytidine and uridine 5'-mono- and di-phosphates was studied in the pH range

from 5 to 11. In final studies, the separation of mixtures of nucleotides was characterized by the program and contrasted with experimental results. A good agreement between migration time, order of elution, zone profile and resolution pattern was obtained for the entire pH range studied.

The optimization program was then applied to study the separation of tetracycline antibiotics (Chapter 6). The electrophoretic behavior of tetracycline, chlortetracycline, demeclocycline, oxytetracycline, doxycycline, methacycline, and minocycline was characterized by measurements of migration time in phosphate buffer solutions, in the range of pH from 4 to 11. A complete set of dissociation constants and individual electrophoretic mobilities was derived numerically for the optimization program. The computer routine was then employed to determine the experimental conditions for the optimal separation of all seven antibiotics. In the vicinity of the optimum, baseline resolution was not achieved for separation of all solutes, however, the separation can be performed satisfactorily under the following experimental conditions: pH 7.5 phosphate buffer solution, with 18.2 mM ionic strength, and 4.3 mM concentration, under constant-current conditions of 20 μA. A common concern in the manufacture of tetracyclines is the control of impurities resulting from decomposition. The treatment of a tetracycline standard solution, under acidic conditions and prolonged heating, generated dehydration and epimerization products, which were easily distinguished from the standard zone. The analysis of tetracycline, minocycline, and doxycycline was performed in commercially available pharmaceutical drugs with a minimum of 95 % recovery. A calibration curve of peak height *versus* concentration with slope of 6.15×10^{-4} M/cm, intercept of -1.18×10^{-5} M, and coefficient of determination equal to 0.9989 gave a linear range of two orders of magnitude for tetracycline, with a detection limit of 10^{-5} M (UV detection at 260 nm) and a signal-to-noise ratio of approximately 3. Among

all the antibiotics studied, chlortetracycline presented the most unusual behavior. The asymmetry of the zone suggested its conversion to tetracycline during the electrophoretic measurement. This result may impair the identification of tetracycline as an impurity in chlortetracycline formulations.

The computer optimization routine has proven to be a valuable tool to study the separation of complex mixtures. It represents a simple but reliable approach to electrophoretic separations, based on physically meaningful models and thorough consideration of the variables that influence the migration processes. Furthermore, this optimization routine is easily implemented on personal computers and is instructive from a pedagogical point of view.

7.2 Future Work

According to Braun and Nagydiosi-Rozsa,[4] who evaluated the growth of capillary electrophoresis from the *Science Citation Index*® database, the technique seems to have reached a stage of maturity. Yet, a rich variety of separation mechanisms and detection schemes have presently been under development.[5-7] Capillary zone electrophoresis differs from the other modes of electrophoresis (*vide* Chapter 1) in an important respect: there is no secondary mechanism, such as partition into micelles or sieving through a gel framework, contributing to the separation selectivity. Indeed, selectivity in capillary zone electrophoresis separations relies exclusively on intrinsic differences in the solute mobility. Perhaps the only means to manipulate the solute mobility, without introducing a secondary phase to the separation, is to alter the chemical and physical properties of the solution. In this context, changes in the buffer pH, concentration, and ionic strength,[8,9] type and concentration of an inert

electrolyte or organic additive,[10-13] as well as changes in temperature[7,14] have all been demonstrated to affect direct or indirectly the solute mobility.

An alternative approach to influence the solute mobility is by complexation with an appropriate chelating agent. By incorporating a chelating agent in the buffer solution, not only the solute mobility can be altered but also the detectability may be enhanced due to the fact that many of these complexes are chromophores. Many solutes of biomedical importance are known to form stable complexes with a variety of metallic cations. The very analytes used in this work can serve as examples: magnesium-nucleotide complexes[15] and calcium-tetracycline complexes[16] are well characterized in the literature. In fact, the separation of nucleotides in the presence of magnesium salts has been attempted.[17] However, this approach was based on trial-and-error experimentation and resulted in a complicated procedure for the separation. Therefore, a systematic approach to the electrophoretic separation of solutes that include complexation equilibrium in parallel to the acid-base equilibrium could find many applications in biotechnology.

With this purpose, minor modifications of the computer optimization program developed in this work would be required. The electrophoretic mobility subroutine must be expanded to include the new equilibrium stages. Preliminary evaluation of the solute equilibria is required with the determination of both dissociation and complexation constants. Then, the electrophoretic behavior of the analyte in buffer solutions containing the chelating agent must be characterized as a means to determine the solute individual mobility. The number of species to be analysed may increase considerably, depending on the number of protonation sites of the solute and the number of complexes formed with the chelating agent. With knowledge of the dissociation constants, complex-formation constants, and the electrophoretic mobility of individual

species, the effective mobility of the solute can then be calculated. The content of chelating agent in the buffer solution is now an additional variable that can be optimized.

Another complement of this work would be a more thorough understanding of the surface conductance phenomenon. In the past few years, the tendency towards performing separations in small-diameter capillaries (5 – 10 μm has increased significantly as a means to enhance separation efficiency and to accommodate sample availability.[5-7] Surface conductance may be critical in such small-diameter capillaries.[3] In this work, surface conductance has been evaluated for 75 μm capillaries, 100 cm long and the corrections to the prediction of voltage resulting from this study are restricted to capillaries of these dimensions. Therefore, with the characterization of the surface conductance in other bore capillaries, the capillary diameter and lengthcould be used as variables for optimization purposes.

Temperature is another interesting parameter to study because of its effect on electrophoretic separations. The detrimental effect of temperature gradients arising from Joule heating on the separation efficiency is well characterized.[5-7] The description of the intracapillary temperature profile is also relatively well stated.[5] However, in spite of previous efforts,[7,14] the effect of temperature on the solute mobility and how resolution, efficiency, and analysis time can benefit from this effect is a subject that needs better understanding.

In conclusion, the optimization program developed in this work is a valuable tool for the assessment of electrophoretic separations and clearly can be expanded to serve many applications based on free solution as well as gel and micellar capillary electrophoresis.

7.3 References

1. Schlabach, T. D.; Excoffier, J. L. *J. Chromatogr.* **1988**, *439*, 173-184.

2. Bard, A. J.; Faulkner, L. R. *Electrochemical Methods - Fundamentals and Applications*; John Wiley & Sons: New York, 1980.

3. Hiemenz, P. C. *Principles of Colloid and Surface Chemistry*, 2nd ed.; Marcel Dekker: New York, 1986.

4. Braun, T.; Nagydiósi-Rózsa, S. *Trends Anal. Chem.* **1991**, *9*, 266-268.

5. Grossman, P. D.; Colburn, J. C., Ed.; *Capillary Electrophoresis - Theory and Practice*; Academic Press Inc.: San Diego, CA, 1992.

6. Kuhr, W. G.; Monnig, C. A. *Anal. Chem.* **1992**, *64*, 389R-407R.

7. McLaughlin, G. M.; Nolan, J. A.; Lindahl, J. L.; Palmieri, R. H.; Anderson, K. W.; Morris, S. C.; Morrison, J. A.; Bronzert, T. J. *J. Liq. Chromatogr.* **1992**, *15*, 961-1021.

8. Vindevogel, J.; Sandra, P. *J. Chromatogr.* **1991**, *541*, 483-488.

9. VanOrman, B. B.; Liversidge, G. G.; McIntire, G. L.; Olefirowicz, T. M.; Ewing, A. G. *J. Microcol. Sep.* **1990**, 2, 176-180.

10. Atamna, I. Z.; Metral, C. J.; Muschik, G. M.; Issaq, H. J. *J. Liq. Chromatogr.* **1990**, *13*, 2517-2527.

11. Atamna, I. Z.; Metral, C. J.; Muschik, G. M.; Issaq, H. J. *J. Liq. Chromatogr.* **1990**, *13*, 3201-3210.

12. Green J. S.; Jorgenson, J. W. *J. Chromatogr.* **1989**, *478*, 63-70.

13. Fujiwara, S.; Honda, S. *Anal. Chem.* **1987**, *59*, 487-490.

14. Kurosu, Y.; Hibi, K.; Sasaki, T.; Saito, M. *J. High Resol. Chromatogr.* **1991**, *14*, 200-203.

15. Lehninger, A. L. *Principles of Biochemistry;* Worth Publishers, Inc.: New York, 1993.

16. Mitscher, L. A. *The Chemistry of the Tetracycline Antibiotics, Medicinal Research Series*, Vol. 9; Marcel Dekker: New York, 1978.

17. Nukatsuka, I.; Yoshida, H. *J. Chromatogr.* **1982**, *237*, 506.

APPENDIX 1

COMPUTER PROGRAM FOR BUFFER PREPARATION

In this appendix, the mathematical basis of the program used for buffer preparation is discussed. The program BUFFER.PRP, whose copy is attached, was written in the Forth-based programming language Asyst (version 2.1, Keithley Asyst, Rochester, NY) to be executed on a 80-286 microprocessor-based computer. This program performs the calculations required to prepare buffers at a specified pH given the thermodynamic dissociation constants and the ionic charge of the individual buffer species. Options are available to prepare buffers under conditions of constant ionic strength, constant buffer concentration, and/or constant buffer capacity. This program is based on classical equilibrium calculations,[1-3] with no simplifying assumptions regarding the relative magnitude of the equilibrium concentration of the buffer species. The following equilibria define the thermodynamic formation constants (K^f), in successive steps, for a triprotic weak acid system. The numerical values correspond to the phosphate buffer system.[4] Charges are omitted for simplification.

$$H + A \leftrightarrow HA, \quad K_1^f = \frac{1}{K_{a3}} = \frac{[HA]\,\gamma_{HA}}{[A]\,[H]\,\gamma_A\,\gamma_H} = 2.11 \times 10^{12} \qquad [A1.1]$$

$$H + HA \leftrightarrow H_2A, \quad K_2^f = \frac{1}{K_{a2}} = \frac{[H_2A]\,\gamma_{H2A}}{[HA]\,[H]\,\gamma_{HA}\,\gamma_H} = 1.61 \times 10^{7} \qquad [A1.2]$$

$$H + H_2A \leftrightarrow H_3A, \quad K_3^f = \frac{1}{K_{a1}} = \frac{[H_3A]\,\gamma_{H3A}}{[H_2A]\,[H]\,\gamma_{H2A}\,\gamma_H} = 1.45 \times 10^{2} \qquad [A1.3]$$

where K_a are the dissociation constants and γ_i are the activity coefficients of individual species. The overall formation constants (β^f) can be written as:

$$H + A \leftrightarrow HA, \qquad \beta_1^f = K_1^f = 2.11 \times 10^{12} \qquad [A1.4]$$

$$2H + A \leftrightarrow H_2A, \qquad \beta_2^f = K_1^f \times K_2^f = 3.40 \times 10^{19} \qquad [A1.5]$$

$$3H + A \leftrightarrow H_3A, \qquad \beta_3^f = K_1^f \times K_2^f \times K_3^f = 4.93 \times 10^{21} \qquad [A1.6]$$

The activity coefficients are determined by means of the Davies equation, which incorporates ionic strength corrections valid up to 0.5 M:[1-3]

$$-\log \gamma_i = 0.509\ Z_i^2 \left[\frac{\sqrt{I}}{1 + \sqrt{I}} - 0.15\ I \right] \qquad [A1.7]$$

where Z_i is the species charge, and I is the ionic strength. The distribution function (α_i) of each species is defined as:

$$\alpha_0 = \frac{[A]}{CT} \left(1 + \beta_1^f [H] + \beta_2^f [H]^2 + \beta_3^f [H]^3 \right)^{-1} \qquad [A1.8]$$

$$\alpha_1 = \frac{[HA]}{CT} \beta_1^f [H]\ \alpha_0 \qquad [A1.9]$$

$$\alpha_2 = \frac{[H_2A]}{CT} \beta_2^f [H]^2\ \alpha_0 \qquad [A1.10]$$

$$\alpha_3 = \frac{[H_3A]}{CT} \beta_3^f [H]^3\ \alpha_0 \qquad [A1.11]$$

where CT is the sum of the equilibrium concentrations of all the species of the buffer system:

$$CT = [A] + [HA] + [H_2A] + [H_3A] \qquad [A1.12]$$

The buffer capacity (BUFCAP) can be calculated by:[2,3]

$$BUFCAP = 2.303 \left[\frac{CT\ [H]\ KAPPA}{(K_{a1}\ K_{a2}\ K_{a3} + [H]\ K_{a1}\ K_{a2} + [H]^2\ K_{a1} + [H]^3)^2} + [H] + [OH] \right] \quad [A1.13]$$

where KAPPA is a cluster of constants given by the term:

$$KAPPA = K_{a1}^2\ K_{a2}^2\ K_{a3} + 4\ [H]\ K_{a1}^2\ K_{a2}\ K_{a3} + 9\ [H]^2\ K_{a1}\ K_{a2}\ K_{a3} + [H]^2\ K_{a1}^2\ K_{a2} + 4\ [H]^3\ K_{a1}\ K_{a2} + [H]^4\ K_{a1} \quad [A1.14]$$

Equations [A1.1] to [A1.14] convene the basic concepts for the calculation of buffer formulations. Depending on the pH region and the pK_a of the buffer system, a different combination of the buffer salts must be used to prepare the buffer solution, such as H_3A/H_2A, H_2A/HA or HA/A. Once the pH is chosen, BUFFER.PRP solves an appropriate system of equations based on the user specification of ionic strength, buffer concentration, and/or buffer capacity. This system of equations is comprised of three out of four distribution functions (Equations [A1.8] to [A1.11]), a mass balance equation, an equation for the hydrogen ion concentration, and an equation for the ionic strength. The sections that follow define in more detail these equations for any given pH region. A schematic diagram of the main program (defined as BUF.PREP), and the three most important subroutines of BUFFER.PRP is shown in Figures A1.1 to A1.4. The subroutine BUF.PLOT is designed to output graphically the distribution functions, buffer concentration, buffer capacity, and cation concentration (as p[M]) as a function of pH. The subroutine BUF.LIB is a library of pK_a and pK_b values for the most commonly used buffer systems.

Figure A1.1 Schematic representation of the BUFFER.PRP main program.

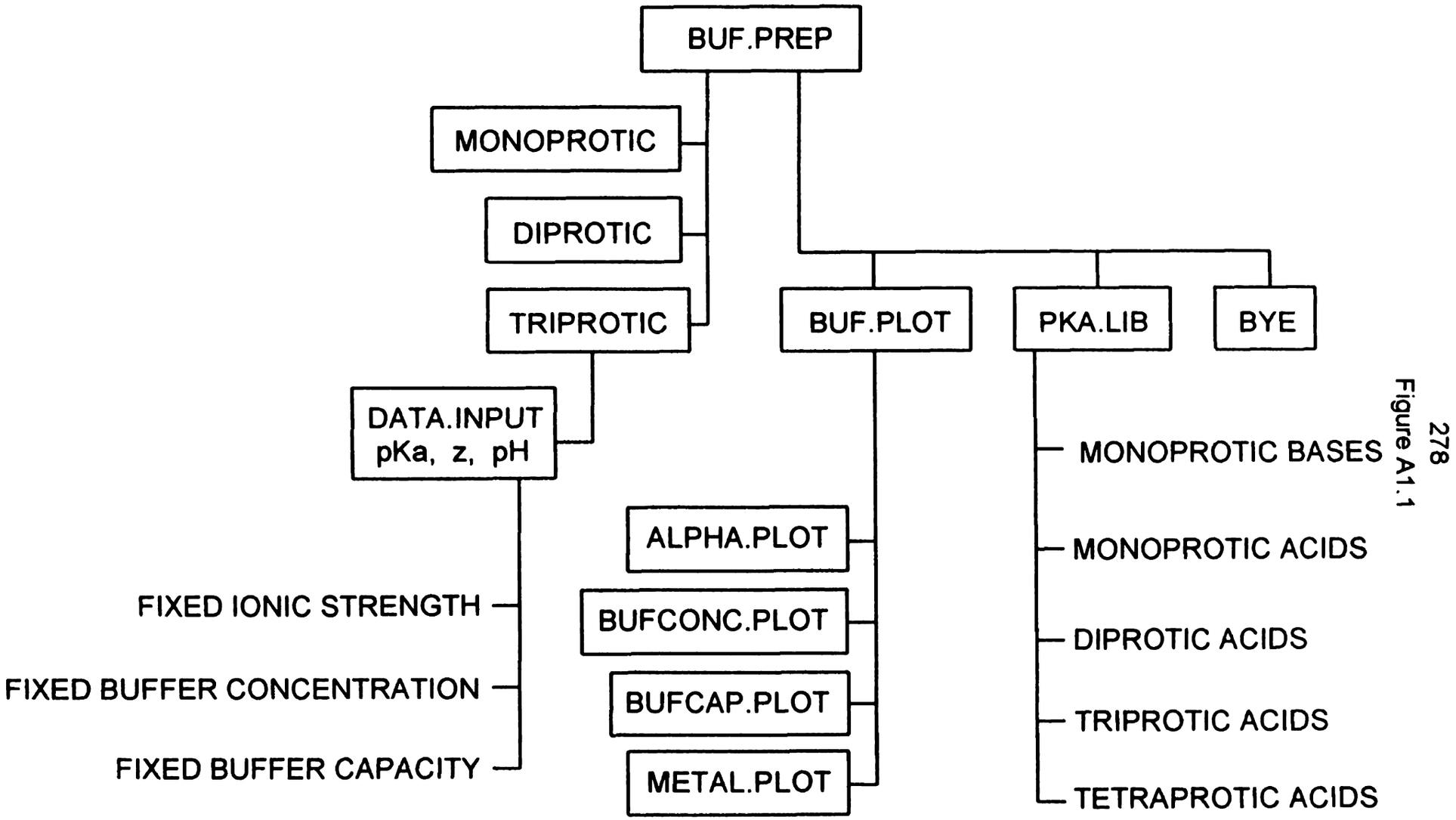
BUF.PREP
MONOPROTIC
DIPROTIC
TRIPROTIC
BUF.PLOT
PKA.LIB
BYE
DATA.INPUT
pKa, z, pH
FIXED IONIC STRENGTH
FIXED BUFFER CONCENTRATION
FIXED BUFFER CAPACITY
ALPHA.PLOT
BUFCONC.PLOT
BUFCAP.PLOT
METAL.PLOT
MONOPROTIC BASES
MONOPROTIC ACIDS
DIPROTIC ACIDS
TRIPROTIC ACIDS
TETRAPROTIC ACIDS

Figure A1.1

Figure A1.2 Schematic representation of the BUFFER.PRP subroutine for constant ionic strength buffer formulations.

Figure A1.2

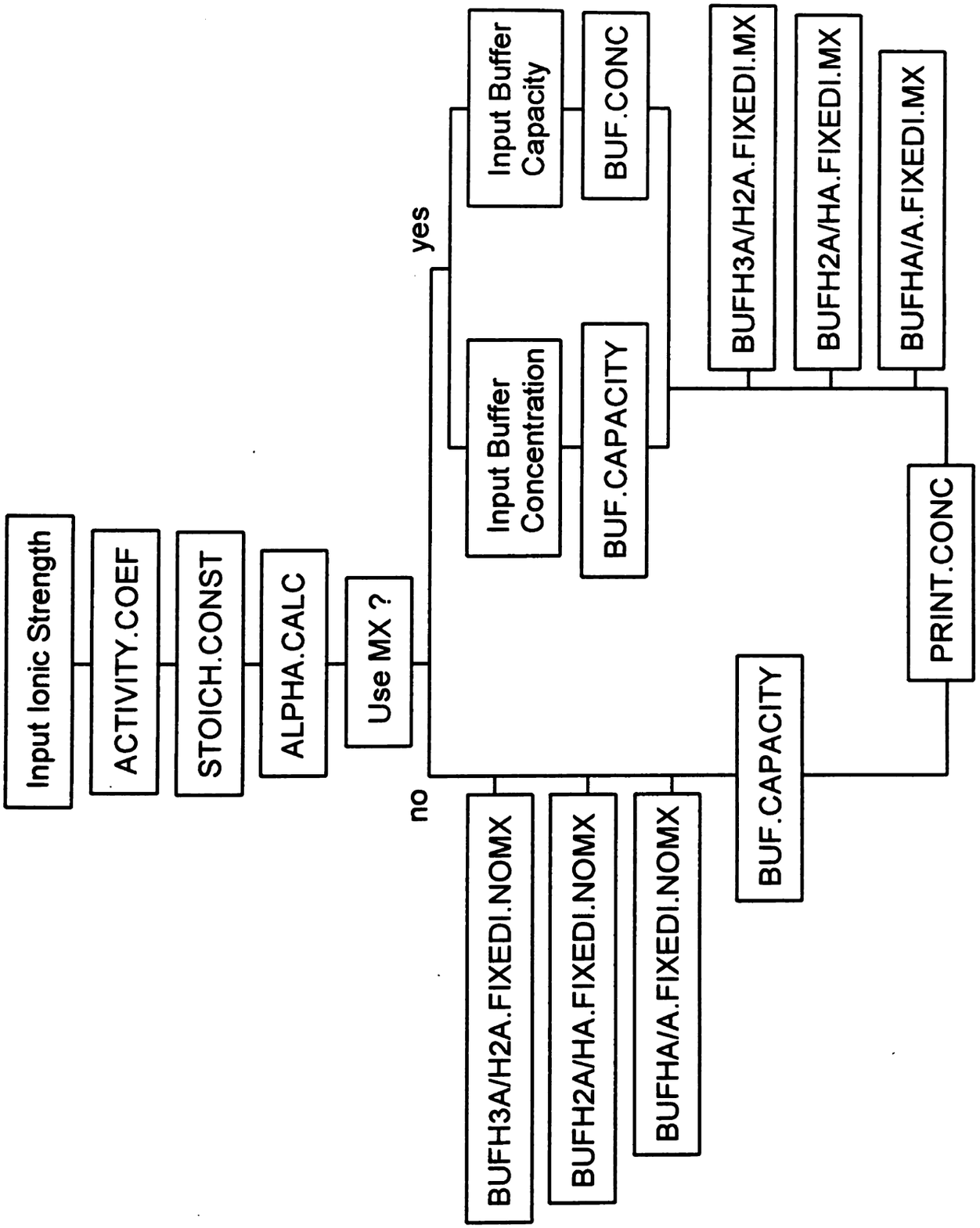
Input Ionic Strength
ACTIVITY.COEF
STOICH.CONST
ALPHA.CALC
Use MX ?
yes
Input Buffer Concentration
Input Buffer Capacity
BUF.CAPACITY
BUF.CONC
BUFH3A/H2A.FIXEDI.MX
BUFH2A/HA.FIXEDI.MX
BUFHA/A.FIXEDI.MX
PRINT.CONC
no
BUFH3A/H2A.FIXEDI.NOMX
BUFH2A/HA.FIXEDI.NOMX
BUFHA/A.FIXEDI.NOMX
BUF.CAPACITY

Figure A1.3 Schematic representation of the BUFFER.PRP subroutine for constant buffer concentration formulations.

Figure A1.3

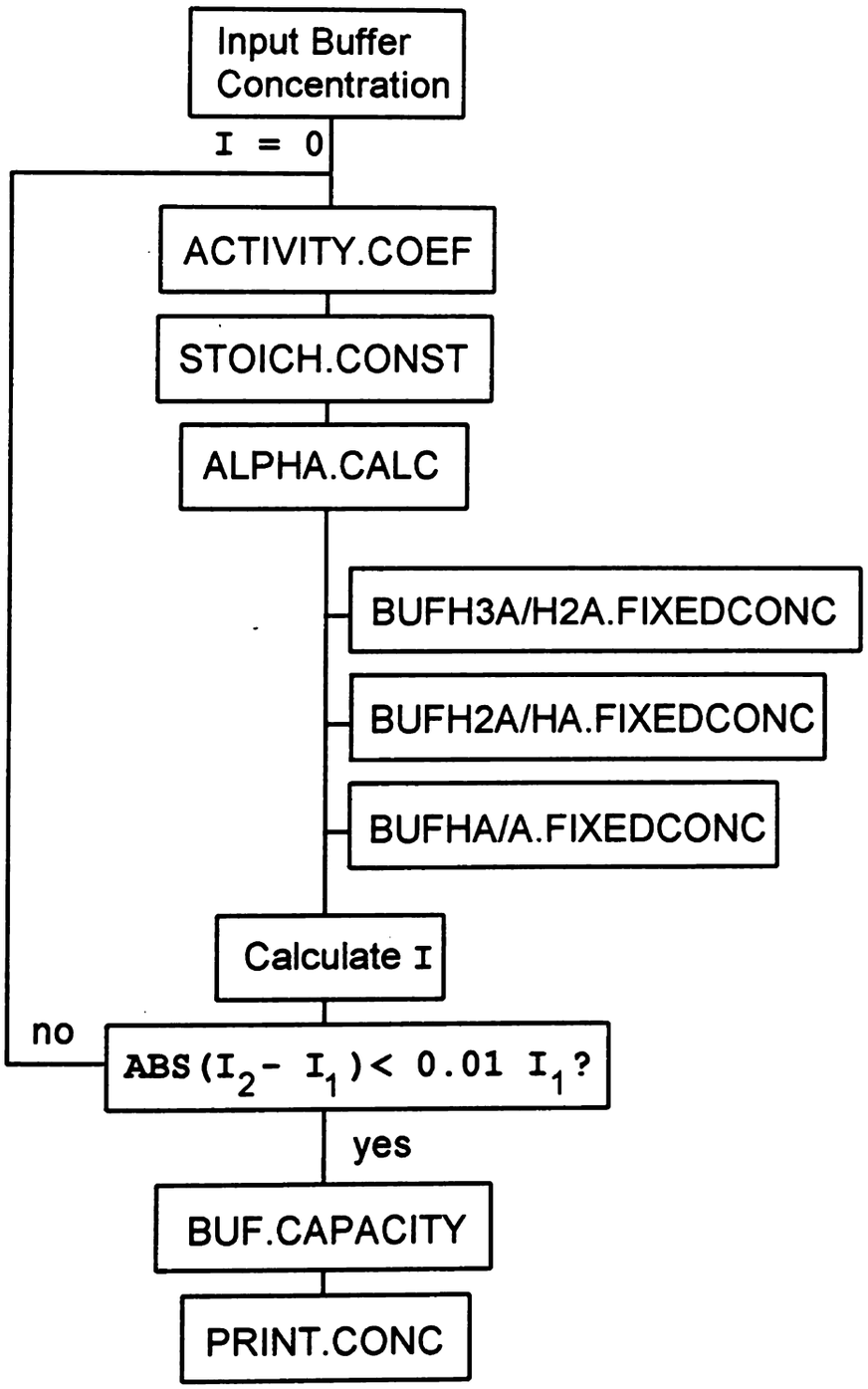
Input Buffer Concentration
I = 0
ACTIVITY.COEF
STOICH.CONST
ALPHA.CALC
BUFH3A/H2A.FIXEDCONC
BUFH2A/HA.FIXEDCONC
BUFHA/A.FIXEDCONC
Calculate I
no
ABS(I2- I1)< 0.01 I1?
yes
BUF.CAPACITY
PRINT.CONC

Figure A1.4 Schematic representation of the BUFFER.PRP subroutine for constant buffer capacity formulations.

Figure A1.4

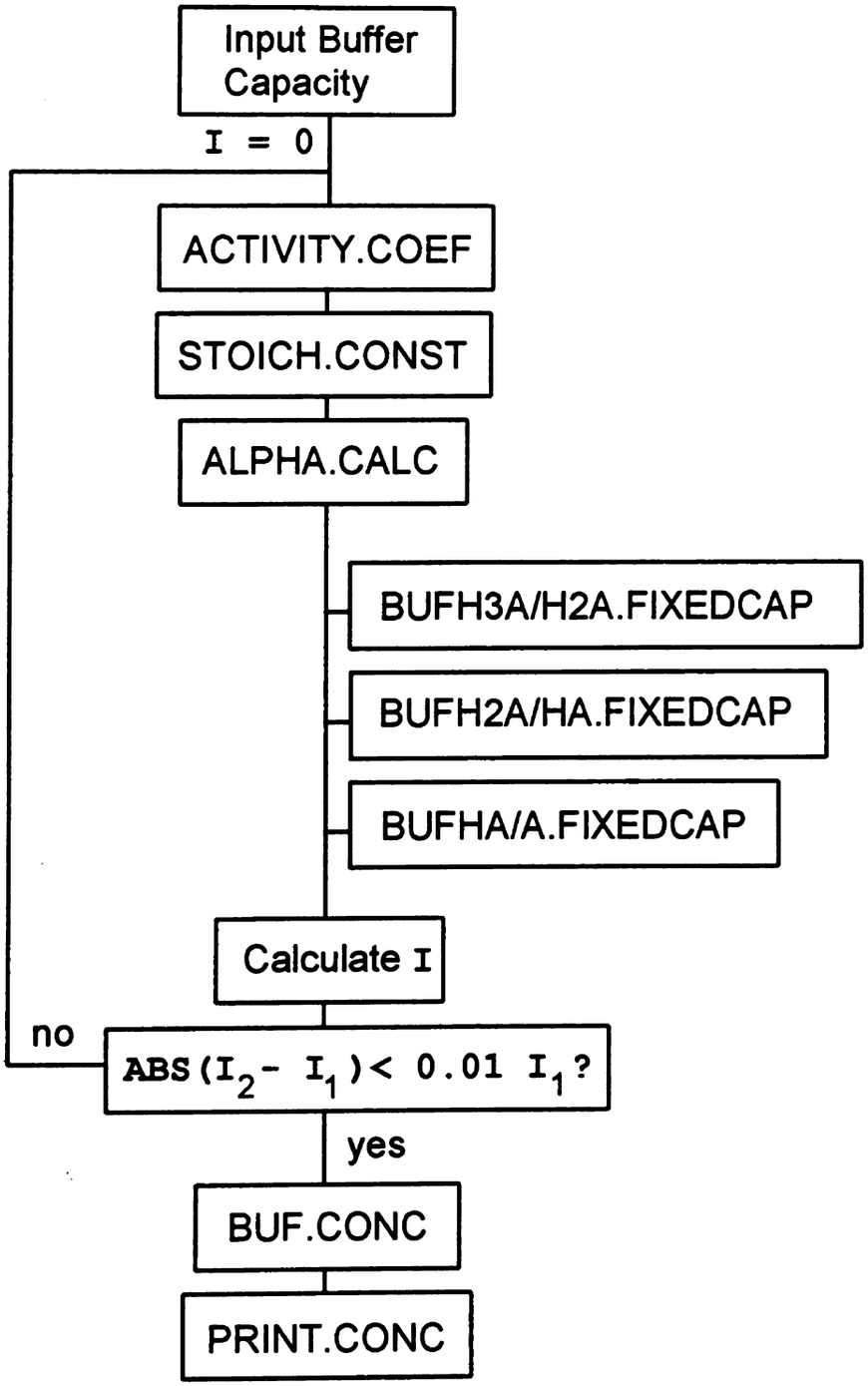
Input Buffer Capacity
I = 0
ACTIVITY.COEF
STOICH.CONST
ALPHA.CALC
BUFH3A/H2A.FIXEDCAP
BUFH2A/HA.FIXEDCAP
BUFHA/A.FIXEDCAP
Calculate I
no
ABS(I2- I1)< 0.01 I1?
yes
BUF.CONC
PRINT.CONC

Buffer H_3A / H_2A. Valid approximately for pH 0 – 4.5 for the phosphate buffer system. C_i represents the analytical concentration of the buffer species; MX represents sodium chloride; N represents sodium from the buffer salts; the subscripts 0 to 3 refers to the buffer species charge.

EQUILIBRIA:

$$\begin{array}{ccccc} H_3A & \leftrightarrow & H_2A & + & H \\ -x & & x & & x \end{array}$$

$$\begin{array}{ccccc} H_2A & \leftrightarrow & HA & + & H \\ -y & & y & & y \end{array}$$

$$\begin{array}{ccccc} HA & \leftrightarrow & A & + & H \\ -z & & z & & z \end{array}$$

$$\begin{array}{ccccc} H_2O & \leftrightarrow & OH & + & H \\ -w & & w & & w \end{array}$$

EQUILIBRIUM CONCENTRATIONS:

$$[H_3A] = C_{H3A} |Z_N| - x$$

$$[H_2A] = C_{H2A} |Z_N| + x - y$$

$$[HA] = y - z$$

$$[A] = z$$

$$[H] = x + y + z + w$$

$$[OH] = w = K_w / [H]$$

$$[N] = CH_3A |Z_3| + C_{H2A} |Z_2|$$

$$[M] = C_{MX} |Z_X|$$

$$[X] = C_{MX} |Z_M|$$

MASS BALANCE:

$$CT = C_{H3A} |Z_N| + C_{H2A} |Z_N|$$

$$\begin{aligned} I = \; & 1/2 \, [H + OH + (C_{H3A} |Z_3| + C_{H2A} |Z_2|) Z_N^2 + \\ & (C_{MX} |Z_X|) Z_M^2 + (C_{MX} |Z_M|) Z_X^2 + \\ & (Z_3^2 \alpha_3 + Z_2^2 \alpha_2 + Z_1^2 \alpha_1 + Z_0^2 \alpha_0) \, CT] \end{aligned}$$

Buffer H_2A / HA. Valid approximately for pH 4.5 – 9.5 for the phosphate buffer system.

EQUILIBRIA:

$$\underset{-y}{H_2A} \leftrightarrow \underset{y}{HA} + \underset{y}{H}$$

$$\underset{-z}{HA} \leftrightarrow \underset{z}{A} + \underset{z}{H}$$

$$\underset{-x}{H_2A} + \underset{-x}{H} \leftrightarrow \underset{x}{H_3A}$$

$$\underset{-w}{H_2O} \leftrightarrow \underset{w}{OH} + \underset{w}{H}$$

EQUILIBRIUM CONCENTRATIONS:

$$[H_3A] = x$$

$$[H_2A] = C_{H2A} |Z_N| - x - y$$

$$[HA] = C_{HA} |Z_N| + y - z$$

$$[A] = z$$

$$[H] = -x + y + z + w$$

$$[OH] = w = K_w / [H]$$

$$[N] = C_{H2A} |Z_2| + C_{HA} |Z_1|$$

$$[M] = C_{MX} |Z_X|$$

$$[X] = C_{MX} |Z_M|$$

MASS BALANCE:

$$CT = C_{H2A} |Z_N| + C_{HA} |Z_N|$$

$$I = 1/2 \, [H + OH + (C_{H2A} |Z_2| + C_{HA} |Z_1|) Z_N^2 + (C_{MX} |Z_X|) Z_M^2 + (C_{MX} |Z_M|) Z_X^2 + (Z_3^2 \alpha_3 + Z_2^2 \alpha_2 + Z_1^2 \alpha_1 + Z_0^2 \alpha_0) CT]$$

Buffer HA / A. Valid approximately for pH 9.5 – 14 for the phosphate buffer system.

EQUILIBRIA:

$$\underset{z}{HA} \leftrightarrow \underset{-z}{A} + \underset{-z}{H}$$

$$\underset{-y}{HA} + \underset{-y}{H} \leftrightarrow \underset{y}{H_2A}$$

$$\underset{-x}{H_2A} + \underset{-x}{H} \leftrightarrow \underset{x}{H_3A}$$

$$\underset{-w}{H_2O} \leftrightarrow \underset{w}{OH} + \underset{w}{H}$$

EQUILIBRIUM CONCENTRATIONS:

$[H_3A] = x$

$[H_2A] = -x + y$

$[HA] = C_{HA} |Z_N| - y + z$

$[A] = C_A |Z_N| - z$

$[H] = -x - y - z + w$

$[OH] = w = K_w / H$

$[N] = C_{HA} |Z_1| + C_A |Z_0|$

$[M] = C_{MX} |Z_X|$

$[X] = C_{MX} |Z_M|$

MASS BALANCE:

$$CT = C_{HA} |Z_N| + C_A |Z_N|$$

$$I = 1/2 [H + OH + (C_{HA} |Z_1| + C_A |Z_0|) Z_N^2 + (C_{MX} |Z_X|) Z_M^2 + (C_{MX} |Z_M|) Z_X^2 + (Z_3^2 \alpha_3 + Z_2^2 \alpha_2 + Z_1^2 \alpha_1 + Z_0^2 \alpha_0) CT]$$

A1.2 References

1. Butler, J. N.; *Ionic Equilibrium - A Mathematical Approach*; Addison-Wesley Publishing Company, Inc: Massachusetts, 1964.

2. Lambert, W. J. *J. Chem. Ed.* **1990**, *67*, 150-153.

3. Rilbe, H. *Electrophoresis* **1992**, *13*, 811-816.

4. Hirokawa, S. Kobayashi and Y. Kiso, *J. Chromatogr.* **1985**, *318*, 195-210.

A1.3 BUFFER.PRP Program

A typical buffer formulation provided by the program BUFFER.PRP is attached. A copy of the program is available upon request.

```
CONDITIONS
paH = 7.5000E   0
pcH = 7.4409E   0
IONIC STRENGTH =
1.8207E  -2
BUFFER CONCENTRATION =
4.2927E  -3
BUFFER CAPACITY =
1.8693E  -3

THERMODYNAMIC CONSTANTS
pKa1 = 2.1610E   0
pKa2 = 7.2070E   0
pKa3 = 1.2325E   1
Kw = 1.0000E -14

ACTIVITY COEFFICIENTS
actcoef H3A = 1.0000E   0
actcoef H2A = 8.7272E  -1
actcoef HA = 5.8009E  -1
actcoef A = 2.9368E  -1
actcoef H = 8.7272E  -1

STOICHIOMETRIC CONSTANTS
Ka1 = 9.0626E  -3
Ka2 = 1.0703E  -7
Ka3 = 1.0709E -12
Kw = 1.3130E -14

DISTRIBUTION FUNCTIONS
ALPHA 0 = 2.2079E  -5
ALPHA 1 = 7.4706E  -1
ALPHA 2 = 2.5292E  -1
ALPHA 3 = 1.0112E  -6

ANALYTICAL CONCENTRATIONS
CONC M-H3A = 0.0000E  -1
CONC M-H2A = 1.0853E  -3
CONC M-HA = 3.2074E  -3
CONC M-A = 0.0000E  -1
CONC M-X = 7.4997E  -3

EQUILIBRIUM CONCENTRATIONS
[H3A] = 4.3409E  -9
[H2A] = 1.0857E  -3
[HA] = 3.2069E  -3
[A] = 9.4779E  -8
[H] = 3.6235E  -8
[OH] = 3.6235E  -7
[M]buffer = 7.5001E  -3
[M]electr = 7.4997E  -3
[X]electr = 7.4997E  -3

CHARGE CONC = 3.0000E  -2
```

APPENDIX 2

COMPUTER OPTIMIZATION PROGRAM

A2.1 Introduction

In this appendix, the computer program developed to optimize electrophoretic separations is discussed. The mathematical rationale of the program has been described previously in Chapter 4. The program TETRA.OPT, whose copy is attached, was written in the Forth-based programming language Asyst (version 2.1, Keithley Asyst, Rochester, NY) to be executed on a 80-286 microprocessor-based computer. A schematic representation of the main program and most relevant subroutines are given in Figure A2.1. The program is based on four nested loops, in which all possible combinations of the variables pH, applied current, ionic strength and buffer concentration are evaluated. The quality of the separation obtained with each set of conditions is analysed according to the response function CRS (Equation 4.1, Chapter 4). The resulting CRS is then compared with the value obtained from the previous set of conditions. The set of conditions that leads to the separation with the minimum value of CRS is saved along with other important parameters of the system, such as illustrated by a typical output of the program (Figure A2.2). The non-optimal sets of conditions, or user-selected sets of conditions, can either be stored in a file (version 2.0, Lotus Development Corporation, Cambridge, Massachussets) for further graphic manipulation or disregarded.

Figure A2.1 Schematic representation of the computer optimization main program.

Figure A2.1

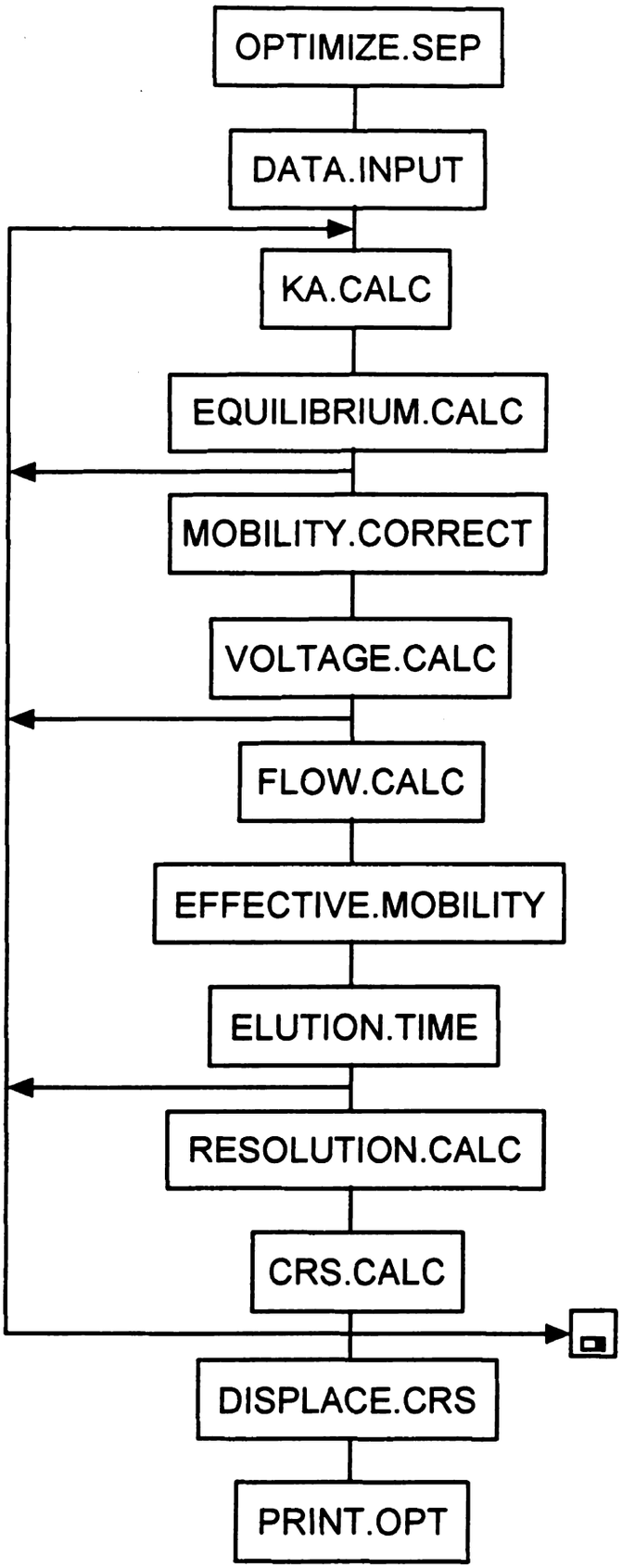
OPTIMIZE.SEP
DATA.INPUT
KA.CALC
EQUILIBRIUM.CALC
MOBILITY.CORRECT
VOLTAGE.CALC
FLOW.CALC
EFFECTIVE.MOBILITY
ELUTION.TIME
RESOLUTION.CALC
CRS.CALC
DISPLACE.CRS
PRINT.OPT

Figure A2.2 Typical output of the computer optimization program representing a separation of (a) nucleotides, and (b) tetracyclines.

Figure A2.2a

```
PREDICTED OPTIMUM CONDITIONS FOR THE SEPARATION:
CURRENT, in microamperes =  12.500
pH =  10.000                          Correction Factor, in pH units =   .0850
IONIC STRENGTH, in moles/liter = 1.2475E -2
BUFFER CONCENTRATION, in moles/liter = 2.4355E -3

CAPILLARY DIMENSIONS:                 TYPE OF INJECTION: HYDRODYNAMIC
TOTAL LENGTH, in cm =  112.15         HEIGHT DIFFERENCE, in cm =    2.00
DETECTOR LENGTH, in cm =   43.40      INJECTION TIME, in sec =   60.00
I. D., in micrometers =   75.50       HYDRODYNAMIC VELOCITY, in cm/s = 3.55E -3

ELUTION TIME   WIDTH     EFFECTIVE       DIFFUSION    EFFICIENCY   RESOLUTION
   in min      in min    MOBILITY        VARIANCE
                        in cm2/Vs        in cm2
AMP =   7.58    .129    -.3186E -3     9.10E -3   5.56E   4        1.61
CMP =   7.79    .133    -.3300E -3     9.35E -3   5.52E   4        8.85
GMP =   9.08    .158    -.3885E -3     1.09E -2   5.28E   4        3.94
UMP =   9.73    .171    -.4121E -3     1.17E -2   5.17E   4        1.09
ADP =   9.92    .175    -.4184E -3     1.19E -2   5.13E   4        2.82
CDP =  10.43    .186    -.4343E -3     1.25E -2   5.05E   4        5.65
GDP =  11.54    .209    -.4640E -3     1.38E -2   4.87E   4        6.21
UDP =  12.93    .239    -.4940E -3     1.55E -2   4.67E   4    CRS =    5.31_
INJECTION ZONE,  in cm =    .21        INJ VARIANCE, in cm2 = 3.78E -3
DETECTOR WINDOW, in cm =    .50        DET VARIANCE, in cm2 = 2.08E -2


FLOW CHARACTERISTICS:
ZETA POTENTIAL, in mV =  -93.49
ZETAZERO, in mV =   26.44
kPOTNa = 2.2347E -1
ELECTROOSMOTIC MOBILITY, in cm2/Vs = 7.4262E -4
ELECTROOSMOTIC VELOCITY, in cm/s =   .1667
VOLTAGE, in kV =  25.170
RESISTANCE, in ohm = 2.0136E  9

BUFFER CHARACTERISTICS (conc in moles/liter):
pH =  10.000
IONIC STRENGTH = 1.2475E -2
BUFFER CONCENTRATION = 2.4355E -3
BUFFER CAPACITY = 3.1139E -4
CHARGE CONC = 2.0003E -2
[M]buffer = 5.0008E -3
[M]electr = 5.0007E -3
BUFFER FORMULATION:
CONC M-H3A = 0.0000E -1
CONC M-H2A = 0.0000E -1
CONC M-HA = 2.3057E -3
CONC M-A = 1.2984E -4
CONC M-X = 5.0007E -3
OK
```

Figure A2.2b

```
PREDICTED OPTIMUM CONDITIONS FOR THE SEPARATION:
CURRENT, in microamperes =  20.000
pH =   7.500                          Correction Factor, in pH units =   .2000
IONIC STRENGTH, in moles/liter = 1.8207E  -2
BUFFER CONCENTRATION, in moles/liter = 4.2927E  -3

CAPILLARY DIMENSIONS:                 TYPE OF INJECTION: HYDRODYNAMIC
TOTAL LENGTH, in cm =  111.90         HEIGHT DIFFERENCE, in cm =    2.00
DETECTOR LENGTH, in cm =   43.40      INJECTION TIME, in sec =   30.00
I. D., in micrometers =   75.50       HYDRODYNAMIC VELOCITY, in cm/s = 3.56E  -3

SOLUTE   ELUTION  WIDTH    EFFECTIVE     DIFFUSION    EFFICIENCY   RESOLUTION
          TIME    in min   MOBILITY      VARIANCE
         in min             in cm2/Vs      in cm2
 MNC      4.45    .086    -.2231E  -4    5.34E  -3    4.28E   4       1.02
 DOC      4.54    .088    -.3492E  -4    5.44E  -3    4.26E   4        .99
 TC       4.62    .090    -.4690E  -4    5.55E  -3    4.25E   4        .57
 OTC      4.67    .091    -.5370E  -4    5.61E  -3    4.25E   4        .17
 MTC      4.69    .091    -.5573E  -4    5.63E  -3    4.25E   4       1.34
 CTC      4.81    .094    -.7143E  -4    5.78E  -3    4.23E   4        .23
 DMCC     4.83    .094    -.7408E  -4    5.80E  -3    4.23E   4    CRS =  366.18
                                                                    RMIN =     .50_
INJECTION ZONE,  in cm =    .11         INJ VARIANCE, in cm2 = 1.78E  -2
DETECTOR WINDOW, in cm =    .50         DET VARIANCE, in cm2 = 2.08E  -2


FLOW CHARACTERISTICS:
ZETA POTENTIAL, in mV =  -84.14
ZETAZERO, in mV =   28.37
kPOTNa = 2.2347E  -1
ELECTROOSMOTIC MOBILITY, in cm2/Vs = 6.6836E  -4
ELECTROOSMOTIC VELOCITY, in cm/s =   .1681
VOLTAGE, in kV =  28.139
RESISTANCE, in ohm = 1.4070E   9

BUFFER CHARACTERISTICS (conc in moles/liter):
pH =   7.500
IONIC STRENGTH = 1.8207E  -2
BUFFER CONCENTRATION = 4.2927E  -3
BUFFER CAPACITY = 1.8693E  -3
CHARGE CONC = 3.0000E  -2
[M]buffer = 7.5001E  -3
[M]electr = 7.4997E  -3
BUFFER FORMULATION:
CONC M-H3A = 0.0000E  -1
CONC M-H2A = 1.0853E  -3
CONC M-HA = 3.2074E  -3
CONC M-A = 0.0000E  -1
CONC M-X = 7.4997E  -3
OK
```

The first block of the program is reserved for data input. In this block, the capillary dimensions, type and conditions of sample injection, detector position and window length are supplied. Additionally, the initial and final values as well as increments of the parameters to be optimized are entered, which are the pH, ionic strength, and concentration of the buffer and the applied current. The thermodynamic dissociation constants, as pKa values, in addition to the electrophoretic mobilities of the buffer species and the solutes under investigation are permanently stored during the program loading.

The next block of the program performs the calculations to correct the dissociation constants and mobilities for ionic strength effects and to find the equilibrium concentrations and distribution functions of all species. If a combination of variables indicates a buffer formulation with negative values for any species concentration, that set of conditions is disregarded and an arbitrary value of 510 is assigned to CRS. Moreover, the program imposes that the concentration of sodium chloride always surpasses the concentration of sodium originated from the buffer salts. In case this restriction is not obeyed, a value of 520 is assigned to CRS. A value of 515 is assigned to CRS when both restrictions, feasible buffer formulation and sodium chloride concentration larger than sodium concentration from buffer salts, are not met.

In the next block of the program, the overall electrical resistance of the system is calculated and the voltage is predicted. If the voltage value falls ouside the range between 5 kV and 35 kV, that particular set of conditions is disregarded and a value of 530 is assigned to CRS.

The program follows with the prediction of the electroosmotic flow, effective mobility of the solutes and migration time. A negative value of migration time results if the electroosmotic velocity is smaller in magnitude and opposite in sign than the electrophoretic velocity. In this particular case, the

solute do not migrate towards the cathode under the influence of the applied electric field. Therefore, the correspondent set of conditions is disregarded and a value of 540 is assigned to CRS.

Once the migration time of the solutes is available, the resolution between all adjacent pairs is calculated and the CRS is detemined. If the CRS value exceeds 500, a value of 500 is assigned to CRS, which indicates that that particular set of conditions is further from the system optimum. The minimum value that the CRS function can achieve is 1.0, however the obtainable CRS value depends on the system of solutes under examination. Generally, CRS values of less than 3.0 are indicative of good separation characteristics.

A2.2 NUCLEO.OPT and TETRA.OPT Programs

A copy of the programs for the optimization of the separation of nucleotides (NUCLEO.OPT) and tetracyclines (TETRA.OPT) is available upon request.